



THE UNIVERSITY OF  
**WAIKATO**  
*Te Whare Wānanga o Waikato*

Research Commons

<http://waikato.researchgateway.ac.nz/>

## Research Commons at the University of Waikato

### Copyright Statement:

The digital copy of this thesis is protected by the Copyright Act 1994 (New Zealand).

The thesis may be consulted by you, provided you comply with the provisions of the Act and the following conditions of use:

- Any use you make of these documents or images must be for research or private study purposes only, and you may not make them available to any other person.
- Authors control the copyright of their thesis. You will recognise the author's right to be identified as the author of the thesis, and due acknowledgement will be made to the author where appropriate.
- You will obtain the author's permission before publishing any material from the thesis.

# ELECTROLYTIC PURIFICATION OF WATER

A thesis  
submitted in partial fulfilment  
of the requirements for the degree  
of  
**Doctor of Philosophy**  
**in both Chemistry *and* Materials and Process Engineering**  
at  
**The University of Waikato**  
by  
**Grant Alexander Mathieson**



THE UNIVERSITY OF  
**WAIKATO**  
*Te Whare Wānanga o Waikato*

The University of Waikato

2006



## Abstract

This thesis develops the concept of an *in situ* electrolytic processor, a machine with electrochemical functions that purifies aqueous fluids at the point of production, whether from a bore water supply or effluent from a tannery. Where the contaminants in an effluent are useful they are separated in a specialised electrolyser for re-use in the process that produced the original effluent. The value in doing this exceeds the cost of electrolytic processing for tannery effluent. The functions of an electrolytic purifier were resolved into: flotation by bubbles, flocculation by corrosion of aluminium anodes, electrowinning by cathodic plating, disinfection, oxidation-reduction and pH modification. Improved understanding of the control of these functions has led to the ability to design better electrolysers because the functions were combined in a form that was appropriate to the required purification process. A link between extra-faradic corrosion of an aluminium anode and pH modification is postulated.

Electrochemical principles were used as the basis for development of real processor models. These models were tested using bore water, cooling tower fluid, virus contaminated water, laundry water, municipal waste water, landfill leachate and pulp mill effluent.

The most effective model, designed during the course of the project and described as the Flume, incorporated a novel corroding anode composed of thin pieces of aluminium, water flow in a cathodic flume, and a cheap water-porous membrane to separate the electrolyte into anolyte and catholyte. The novel anode was designed to improve clearance of corrosion products by maintaining a fast flow speed in proximity to the zone of anodic corrosion. The Flume model was used in an extensive test at a tannery. Greater than 90% of chromium in tannery effluent was removed by a combination of electroflocculation and electroflotation, at a lower cost than by treatment using standard chemical flocculent, using a side-stream Flume processor at a tannery. A smaller scale Flume model was used to test mechanisms of treatment in the laboratory using synthetic tannery effluent.

When treating alkaline effluent, the separating membrane in the Flume model enabled production of alkali at the cathode and production of acid at the anode.

This was used for pH modification of effluent and, where the majority of the flow was anolyte, was able to produce a catholyte of pH greater than 13 from a wide range of inflow pH. The caustic catholyte is a valuable by-product of the electrolytic processing, especially when the upstream processes require net input of alkali (as is the case at a tannery or kraft pulp mill) and more generally because downstream biological treatment processes benefit from receiving neutralised effluent.

The degree of pH moderation of the whole outflow compared to the inflow was found to be controllable by adjustment of cell voltage. This effect enables treatment of effluent with variable pH.

Optimisation of an electrolyser for energy recovery, by both reduction of electrode over-potentials and electrolyte resistance, was incorporated in the full-scale designs. Based on a feasible cell voltage of 5 V, 20% recovery of the energy input is expected.

## Acknowledgements

### **Dedication**

Thanks Dad; wish you were able to see the finished product. Your influence is evident on every page. Thanks to Tom Hill for letting me start the PhD, Alan Langdon for letting me finish, and Graham Jamieson for everything in-between.

### **Attribution and motivation**

Tom's Uncertainty Principle:

*The more predictable a process is in limited experimentally controlled conditions, the less robust it is in highly variable field conditions. Conversely, the more robustly a process operates in highly variable field conditions, the less amenable it is to examination and discernment in experimentally controlled conditions.*

(Attributed to Thomas A. Hill, raconteur-about-town in Hamilton, New Zealand).

The principle laments the divergence of science from application, the divestment of empirical experience from the exposition of theories and the loss of exuberant discovery of phenomena by experiment. This thesis attempts to shift the balance, and based on the imperatives for a process, determines the point of optimum certainty.

### **Corollary**

In order to move on from the keen insight offered to me by the aforementioned motivator, I found it necessary to ditch any romantic notions of science as a glorious pastime and perform the extreme drudgeries of disciplined experiments, exhaustive computer analysis, followed by more of the same and then repeated for good measure to make a small but certain step forward. Recording results and critically examining initial assumptions became second nature. Even presuming that hoped for effects were guilty as charged artefacts and attacking them from all sides became routine. I hope the applications to follow will benefit from the rigorous examination of the basic principles upon which they are based.

### ***Mathieson's principle of experimental time sharing:***

*A day in the field is well balanced by four in the lab; field work is more intense and lab work is more time consuming.*

*I would like to thank:*

The Chemistry technical staff, particularly Jannine Sims, Wendy Jackson and Annie Barker; MAPE Technical Staff, particularly Paul Ewart and Yuanji Zhang; University of Waikato Administration Staff, particularly Mary Dalbeth, Carol Robinson and John Little; the University MAPE and Chemistry Departments, as well as the NZIC, for both sending me to a conference in Los Angeles and welcoming me back to NZ; the University Library staff who stayed 110% helpful despite the numerous interloan requests and fuss with EndNote - Trisha Kruyff and Cheryl Ward both have the patience of a stone and the flexibility of a rubber band.

Technology New Zealand paid the stipend for the three year TIF fellowship with Works Filter Systems Limited. The Works Filter Systems' crew are an amazing bunch of characters.

Fellow students like Jacob Croal, Dougal Laird and Soriya Em gave me a better perspective of what being a student ought to be like. Brian Ellens set the standard for writing.

The Hamilton City Council and Waste Water Treatment Plant Staff were a great help. To Louis Botha and Marcus Shipton...I am in deep debt to both of you.

WaterCare Services Laboratory's Ted Wnorowski assisted me greatly.

Julian Booker, Sean Meehan and Michael Allen provided field test facilities and Bruce Robertson of Boltac Industries supplied the JarStar tester. A-Line Sheet Metal and Plastic Welders turned my bizarre designs into useable equipment. Hill Laboratories did reliable analytical testing of numerous samples with precision and efficiency.

Family: Mum, Linda, Trevor, Sarah, Richard and the wonderful Hisako.

If I missed you out, sorry. You were probably very helpful.

# Table of Contents

<b>1</b>	<b>General introduction .....</b>	<b>1</b>
1.1	Background .....	1
1.1.1	The global picture .....	1
1.1.2	The local action .....	1
1.1.3	The hydrogen economy .....	3
1.2	Thesis overview .....	3
1.2.1	Structure .....	3
1.2.2	Emphasis .....	4
1.3	Aim and scope of this thesis .....	4
1.3.1	Aim .....	4
1.3.2	Scope .....	4
1.4	Literature review .....	6
1.4.1	Background and history of electrolytic purification .....	6
1.4.2	Review of the state of the art .....	14
1.5	Electrochemical principles .....	15
1.5.1	Components of cell voltage .....	15
1.5.2	Current fraction and current efficiency .....	21
1.5.3	Mass transport limitations .....	21
1.5.4	The effect of pH .....	22
1.6	Electrochemical water treatment processes .....	23
1.6.1	General reactions and conditions .....	23
1.6.2	Electrofloculation by electrolysis of aluminium or iron .....	27
1.6.3	Electroflotation versus dissolved air flotation .....	35
1.6.4	Electrosterilisation and electro-oxidation .....	36
1.6.5	Electrolytic production of hydrogen .....	37
1.6.6	Combined effects and limitation of combinations .....	38
1.7	Hypothesis and research questions .....	39
1.7.1	Electro-flocculants .....	39
1.7.2	Overcoming low conductivity .....	39
1.7.3	Benign anodes .....	39
1.7.4	Recovery of by-products .....	40



1.7.5	Ability to configure function .....	40
1.7.6	Turning waste into a resource at the point of production .....	40
<b>2</b>	<b>Materials and methods .....</b>	<b>41</b>
2.1	Experimental philosophy.....	41
2.1.1	Selection of methods for experiments .....	41
2.1.2	Selection of case studies .....	41
2.1.3	Selection of methods for controlled laboratory conditions .....	41
2.2	The essential parts of an electrolytic water processor.....	41
2.2.1	Electrodes .....	41
2.2.2	Electrolyte and compartments .....	44
2.2.3	Separating membranes.....	44
2.2.4	Electrical components.....	45
2.2.5	Flow control.....	45
2.3	Materials for electrolytic processing .....	45
2.3.1	Using the fluid to be treated as an electrolyte .....	45
2.3.2	Electrode materials .....	47
2.3.3	Separating membranes.....	48
2.3.4	Synthetic fluids .....	48
2.3.5	Catholyte modification .....	49
2.3.6	Chemical flocculants and coagulants for comparison .....	49
2.4	Post-processing.....	50
2.4.1	Acidification .....	50
2.4.2	Settling and stirring .....	50
2.5	General measurement methods and instruments .....	50
2.5.1	Conductivity .....	50
2.5.2	Turbidity .....	51
2.5.3	Trace element analysis.....	51
2.5.4	pH measurement.....	51
2.5.5	Particle sizing .....	51
2.5.6	Electrical measurements .....	51
2.5.7	Automated measurements .....	53
2.5.8	Software for modeling, data recording and presentation.....	53
2.5.9	Microbiological counts .....	53

2.5.10	Dissolved oxygen .....	54
2.5.11	Residual chlorine.....	54
2.6	General equipment and techniques .....	54
2.6.1	Power supplies .....	54
2.6.2	Filters .....	55
2.6.3	Jar stirrer.....	56
2.6.4	Presentation of multiple graphs and traces in a single figure.....	56
<b>3</b>	<b>Development of bipolar stack processors .....</b>	<b>57</b>
3.1	Introduction .....	57
3.2	Stages of development .....	57
3.2.1	Starting point - Model 0: jubilee clips on porous ceramic.....	57
3.2.2	Narrowed gap, increased area, lower voltage .....	58
3.2.3	Optimisation for hydrogen production or sterilisation.....	59
3.2.4	Model 1: stainless steel plates single cell.....	62
3.2.5	Model 2: stainless steel plates in a bipolar stack.....	63
3.2.6	Model 3 (minimum gap) and Model 4 (maximum area).....	64
3.2.7	Model 5: stainless steel plates bipolar stack with forced flow.....	65
3.3	Applications of bipolar stacks .....	66
3.3.1	Treatment of iron laden bore water (iron-water).....	66
3.3.2	Treatment of cooling tower water to prevent legionellosis.....	71
3.3.3	Electrosterilisation of virus-contaminated water .....	76
3.3.4	Electroflotation of laundry water .....	79
3.3.5	Treatment of municipal wastewater .....	83
3.4	Proposed effluent processor .....	86
3.4.1	Emphasis on electroflotation of suspended solids .....	86
<b>4</b>	<b>Development of corroding anode processors .....</b>	<b>91</b>
4.1	Development sequence.....	91
4.1.1	Model 6: corroding anode plates.....	91
4.1.2	Model 7: corroding anode disc.....	91
4.1.3	Model 8: corroding anode made of shavings – the Tower.....	92
4.1.4	Model 9: the Flume processor.....	99
4.2	Treatment of landfill leachate .....	102

4.2.1	Rational for treatment.....	102
4.2.2	Materials and methods.....	103
4.2.3	Results .....	103
4.2.4	Proposed leachate processor.....	103
4.2.5	Discussion and conclusion .....	105
4.3	Pulp mill effluent.....	105
4.3.1	Rationale for treatment.....	105
4.3.2	Materials and methods.....	105
4.3.3	Results .....	105
4.3.4	Discussion.....	106
4.3.5	Conclusion.....	106
4.4	Treatment of tannery effluent.....	107
4.4.1	Introduction .....	107
4.4.2	Trials.....	108
4.4.3	Site and trial conditions .....	108
4.4.4	Materials and methods.....	111
4.4.5	Removal of suspended solids .....	113
4.4.6	Floc removal by flotation .....	114
4.4.7	Treatment of moderate to high pH effluent.....	116
4.4.8	Treatment of near neutral pH effluent .....	123
4.4.9	Cost effectiveness of chromium removal .....	128
4.4.10	The effect of processing on microbes.....	130
4.4.11	Blockage at the top and bottom of the Flume processor .....	130
4.4.12	Release of aluminium fragments.....	132
4.4.13	Discussion and conclusions.....	132
4.4.14	Unresolved issues suggesting further work.....	134

## **5 Further investigation of the Flume in a laboratory. 137**

5.1	Studies in controlled conditions .....	137
5.1.1	Introduction .....	137
5.1.2	Targets of investigation .....	137
5.2	Materials and methods.....	138
5.2.1	Inflow stabilisation tank .....	138
5.2.2	The laboratory Flume .....	140

5.2.3	Electrical equipment.....	140
5.2.4	Sampling systems.....	140
5.2.5	Steady state, ramp and step change experiments .....	141
5.2.6	Contaminants .....	141
5.2.7	Modulation of the power supply .....	142
5.2.8	Analytical tools .....	142
5.3	Aluminium electroflocculation of pH modified saline .....	143
5.3.1	Elimination of complications due to other contaminants.....	143
5.3.2	Long-run trials.....	143
5.3.3	Discussion .....	155
5.4	pH modification by splitting the outflow .....	156
5.4.1	Passage of fluid through the membrane .....	156
5.4.2	Using split flow to achieve lower residual aluminium.....	157
5.4.3	Discussion .....	166
5.5	Chromium removal from saline and saline with protein.....	167
5.5.1	Chromium and protein .....	167
5.5.2	Chromium removal from pH-modified saline.....	167
5.5.3	Chromium removal from protein contaminated saline .....	171
5.6	Modification of pH and effective conductivity by catholyte modification.....	179
5.6.1	The need to improve effective conductivity.....	179
5.6.2	Discussion .....	182
5.7	Pulse modulation of the current or voltage .....	182
5.7.1	Capacitance of the processor.....	182
5.7.2	Pulse modulation of the power.....	183
5.8	Discussion .....	186
5.8.1	Dissolution of hydroxide to form aluminate .....	186
5.8.2	pH modification control by cell voltage .....	186
5.8.3	Crystallinity and co-floc of aluminium and chromium.....	187
5.9	Discussion of Technical Applications.....	187
5.9.1	Trials summary.....	187
5.9.2	Variable pH and salinity of tannery effluent.....	188
5.9.3	Proposed larger scale processing systems.....	190
5.9.4	Sensitivity to electricity and aluminium price increases.....	194

5.10	Conclusions .....	195
5.10.1	Verification in laboratory conditions.....	195
5.10.2	Mechanism of treatment .....	195
5.10.3	Extending operating time.....	196

## **6 Conclusions ..... 197**

6.1	Evolutionary design to address historical problems.....	197
6.2	The Flume - an advance in electrolytic water purification .	197
6.2.1	Structure of the Flume .....	197
6.2.2	Increasing conductance with an inert membrane .....	198
6.2.3	Electro-flocculator .....	198
6.2.4	Turning waste into a resource at the point of production .....	198
6.2.5	Control of flocculation and pH adjustment .....	199
6.2.6	Modification of the pH of either split or whole flows.....	199
6.2.7	Extraction of useable alkali from effluent .....	199
6.2.8	Increasing the effective conductivity of the electrolyte.....	200
6.2.9	Using acidic catholyte and alkaline anolyte .....	200
6.2.10	Continuously replaced corrodible aluminium anode.....	201
6.2.11	Crystalline co-flocculation of aluminium and chromium.....	201
6.3	Bipolar stack structure and functions .....	201
6.3.1	Bipolar stack structure .....	201
6.3.2	Electroflotation .....	202
6.3.3	Rapid electrolytic oxidation and self-flocculation of iron.....	203
6.3.4	Electro-steriliser.....	203
6.4	Combined functions.....	203
6.4.1	The value of combining functions .....	203
6.4.2	Electroflocculation and electroflotation .....	204
6.4.3	Combination with sterilisation .....	204
6.4.4	Combination with electrowinning .....	205
6.4.5	Combination of more than two functions .....	205
6.5	Enhancing or surpassing chemical water treatment .....	206
6.5.1	Electro-flocculants.....	206
6.5.2	Overcoming low conductivity electrolyte .....	206
6.5.3	Benign anodes .....	206

6.5.4	Energy recovery by production of hydrogen .....	207
6.5.5	Flexibility and control .....	208
6.5.6	Feasible scale of operation .....	208
6.6	Suggestions for further work.....	209
6.6.1	Resolve the anodic potential experimentally .....	209
6.6.2	Microscopic observation of anodic corrosion of aluminium .....	209
6.6.3	Application.....	209
6.6.4	Make non-porous Magnéli phase anodes.....	209
6.6.5	Accounting for pH changes.....	209
<b>7</b>	<b>Appendices.....</b>	<b>211</b>
7.1	Appendix A .....	211
7.2	Appendix B.....	213

## List of Figures

Figure 1-1 The DC electrical equivalent of an electrolytic cell.....	17
Figure 1-2 Conductivity of dilute aqueous NaCl solutions at 25 °C (Bryan 2003).....	18
Figure 1-3 How electrolyte voltage drop is lowered to the order of the cathodic over-potential by reducing the gap. Based on an iron cathode and fluid with a conductivity of 0.02 S m <sup>-1</sup> . Result for concentrated electrolyte shown for comparison. ....	19
Figure 1-4 Pourbaix diagram for aluminium. ....	28
Figure 1-5 Saturation concentration of aluminium (mg L <sup>-1</sup> ) for alkaline pH at which Al(OH) <sub>4</sub> <sup>-</sup> precipitates as either amorphous or crystalline forms of Al(OH) <sub>3</sub> . Multiply [Al] by 1.889 to find the [Al <sub>2</sub> O <sub>3</sub> ] equivalent. ....	29
Figure 1-6 The fraction of energy recoverable as hydrogen from electrolysis of water.....	38
Figure 2-1 The four-wire method of voltage measurement as applied to an entire electrochemical cell.....	52
Figure 3-1 Tubular TMGCC as an electrolytic filter (left) and a typical application (right). ....	58
Figure 3-2 Left: Two cells in series on a TMGCC with a central bipolar electrode and two terminal unipolar electrodes (endplates). Right: notation for leakages, series current and total current in a four-cell stack.....	61
Figure 3-3 Modeled 2-series-cell response to changes in gap between the electrodes: how decreasing the gap between stainless steel electrodes in a bipolar stack bathed in dilute electrolyte can reduce leakage current. ....	61
Figure 3-4 Single cell composed of stainless steel plates. External connections were made by either welding a rod to each plate or clamping a wire to each plate using the fasteners. ....	62
Figure 3-5 12 cell plate electrolyser: cross-sections of concept (left) and realisation (right). ....	63
Figure 3-6 Minimum gap-width cell – Model 3. ....	65
Figure 3-7 Maximum area cell – Model 4. ....	65
Figure 3-8 The Breadbox – used for processing Fe-laden bore water. ....	68
Figure 3-9 Complete iron water processing system.....	68
Figure 3-10 Side-stream processing scheme for cooling tower water treatment. ....	75
Figure 3-11 Result of electrolytic processing of cooling tower fluid. ....	75
Figure 3-12 The electrolytic processor designed for the trial at the University of Auckland.....	77
Figure 3-13 The device for laundry water recycling including a 3 cell electrolyser. ....	81
Figure 3-14 Aggregated results of attempted electrosterilisation of terminal effluent. ....	84
Figure 3-15 Down-flow electroflotation clarifier. Algae and other particulates were raised above the inflow point in sturdy foam. Some small bubbles passed down beyond the processor to	

the outflow stream at the bottom. Some of these small bubbles coalesced to form larger bubbles that rose back up through the processor. ....	84
Figure 3-16 Proposed scheme for electroflotation of municipal waste water plant terminal effluent. A truncated cone with down flow ensures lower flow speed toward the bottom so that small bubbles will rise to some level in the tank where a floc-bubble blanket will form, preventing suspended solids from progressing downward. Rotational flow like an inverted teacup will concentrate the bubbles and solids in the centre at the top. ....	87
Figure 3-17 Mesh and membrane bipolar cell stack for large scale electroflotation. While gas is produced mainly at the mesh membrane contact surfaces it is able to depart via the inter-cellular gap which is relatively large. Thus current leakage and gas voidage are eliminated. This form is mass-producible as the only close-tolerance dimension is the intracell gap and this is assured by the membrane. ....	90
Figure 4-1 Perforated cathode and radial flow over a corroding anode. ....	91
Figure 4-2 Aluminium shavings corroder – the Tower. ....	93
Figure 4-3 Immediate turbidity after filtration of outflow from the Tower. ....	98
Figure 4-4 The turbidity of terminal effluent at different stages after processing in the Tower at 35 V (January 26 <sup>th</sup> 2005). ....	99
Figure 4-5 Model 9 system - the Flume processor. ....	101
Figure 4-6 Bi-modal (A and B) and uni-modal (C) treatment schemes. ....	104
Figure 4-7 Flow schematic for tannery effluent trials. ....	111
Figure 4-8 Comparison of electrolytic treatment with PFS dosing for reducing supernatant suspended solids in DAF outflow (inflow to Hides and Skins Pond). One hour settling times were used (March 4 <sup>th</sup> 2005). ....	114
Figure 4-9 Schematic of electrolytic processing, followed by electroflotation then mixing or settling. Sample numbers 1 to 5 are used in Figure 4-10. ....	115
Figure 4-10 The turbidity and metal concentration at the sample points shown in Figure 4-9. This shows the improvement due to removing the electro-floated floc that formed less than five minutes after processing (April 8 <sup>th</sup> 2005). ....	115
Figure 4-11 Effectiveness and cost of electrolytic addition of aluminium versus PACl dosing. (April 15 <sup>th</sup> 2005). ....	118
Figure 4-12 Comparison of electrolytic treatment with PACl dosing (May 12 2005). ....	120
Figure 4-13 The superior turbidity removal of electrolytic treatment compared to dosing with PACl in terms of outflow supernatant turbidity for operating cost (May 12 <sup>th</sup> 2005). ....	121
Figure 4-14 Supernatant aluminium and chromium and total aluminium levels measured by ICP-OES (May 12 <sup>th</sup> 2005). ....	122
Figure 4-15 pH of inflow and processed effluent (May 12 <sup>th</sup> 2005). ....	122



Figure 4-16 Comparison of PACl/PFS dosing and electrolytic processing, based on Al <sub>2</sub> O <sub>3</sub> equivalents, on Pond 6 terminal effluent at the tannery (May 4 <sup>th</sup> 2005).	124
Figure 4-17 Lower current efficiency at near-neutral pH of Pond 6 water shown by measured total aluminium compared with the faradic prediction for treatment (May 4 <sup>th</sup> 2005).	125
Figure 4-18 The poor performance of both electrolytic treatment and PAC23 dosing when treating tannery DAF outflow (inflow to H&S pond) that was relatively low in pH (19 May 2005).	127
Figure 4-19 24 hour turbidity and cost for PAC23 and electrolytic treatment (19 May 2005).	128
Figure 4-20 High levels of supernatant metals at low pH for both electrolytic treatment and flocculent dosing of DAF outflow (19 May 2005).	128
Figure 4-21 Chromium remaining in the supernatant and operating cost for electrolysis of DAF outflow, based on measured aluminium in the outflow. The changes in slope of the cost graph occurred at changes in supply voltage (March 10 <sup>th</sup> 2005).	129
Figure 4-22 The progress over time of bottom end blockage by accumulated corrosion products, shown in cross-section of the Flume. The flow (shown darker where faster) lifts through the body of shavings over time and becomes thicker, lowering the flow speed and accelerating the blockage, eventually overflowing. Because corrosion products are still delivered from higher up the Flume, the blockage continues to develop higher up the Flume even after the onset of overflow.	131
Figure 4-23 Possible means of leveling the flow speed by lowering areas of higher flow resistance to slow or prevent blockage. The walls are electrically insulated to prevent initiation of blockage there and greater bottom area to side wall area ratio is illustrated.	132
Figure 5-1 The Flume, as used in the laboratory (above) and the experimental system it was part of (below).	139
Figure 5-2 The switching circuitry used to modulate the current or voltage of a constant-current (shown) or voltage-source supply. Square wave modulation was used.	142
Figure 5-3 The effect of a prolonged run time on process variables and aluminium levels in the outflow for a continuous 9-hour trial of the lab Flume, using saline as electrolyte.	144
Figure 5-4 The effect of continued use and anode compression during two more days of the trial shown in Figure 5-3.	145
Figure 5-5 The effect of acid rinsing the anode shavings followed by severe compression during continuation of the trial shown in Figure 5-3 and Figure 5-4 for a further day.	146
Figure 5-6 The effect using pH 8.8 inflow on process control variables and outflow aluminium levels for a four day trial.	148
Figure 5-7 The effect of an acid inflow on the process control variables and outflow aluminium levels for a long run trial.	149
Figure 5-8 The effect of increasing the current on processing of acidic inflow.	150

Figure 5-9 The effect of an upward inflow pH ramp from under pH 3 to over pH 10 on process control variables and outflow aluminium levels. ....	152
Figure 5-10 The change in pH from inflow to outflow for the conditions shown in Figure 5-9. ...	152
Figure 5-11 The effect of a down-ramp of inflow pH from around pH 11 to near neutral on process control variables and outflow aluminium levels. ....	153
Figure 5-12 The effect of ramping pH down then back up on process control variables and outflow aluminium levels. ....	154
Figure 5-13 The effect of splitting the anolyte and the catholyte while changing the current in steps on process control variables and outflow aluminium levels. ....	157
Figure 5-14 Process control variables and outflow aluminium levels showing the greater pH moderation in anolyte compared to whole outflow, corroborated by lower dissolved aluminium in the anolyte. ....	159
Figure 5-15 Comparison of predicted and measured aluminium in the both the anolyte and whole outflow. The solubility prediction is a function of pH, but both the 48-hour supernatants and the 0.45 $\mu\text{m}$ filtered samples had lower aluminium levels than predicted. ....	160
Figure 5-16 Comparison of predicted dissolved aluminium levels, for both amorphous and crystalline forms of $\text{Al}(\text{OH})_3$ , with measured levels of aluminium after 0.45 $\mu\text{m}$ filtration. ....	161
Figure 5-17 The effect of split outflow when treating high pH inflow on process control variables and outflow aluminium levels. ....	162
Figure 5-18 Comparison of both whole outflow and anolyte dissolved aluminium with theoretical predictions for solubility of amorphous and crystalline $\text{Al}(\text{OH})_3$ . ....	163
Figure 5-19 Greater extra-faradic corrosion at moderate pH with low conductivity water at a given current than for high pH with high conductivity. ....	164
Figure 5-20 Total outflow aluminium versus cell voltage for two different electrolytes. ....	165
Figure 5-21 Typical XRD spectrum ( $\text{Cu K}\alpha$ ) of aluminium floc after freeze drying showing no well-defined crystalline structure. ....	166
Figure 5-22 chromium removal from high pH and conductivity chromium-laden water by electrolytic treatment. ....	168
Figure 5-23 Comparison of predicted and actual solubility of aluminium when treating chromium contaminated water. ....	169
Figure 5-24 Comparison of presonicated and postsonicated metal levels. Note the log scales. The measured anolyte pH was lower after standing and ultra-sonication, but both the aluminium and chromium residuals were higher. ....	170
Figure 5-25 Particle sizes in processed and sonicated anolyte at three different treatment levels. The order of treatment was 2, 4, and 1 (August 30 <sup>th</sup> 2005). ....	171

Figure 5-26 The effect of loading the inflow with protein at 500 mg L <sup>-1</sup> on chromium removal and residual aluminium. ....	172
Figure 5-27 Comparison of predicted and actual solubility of aluminium before and after protein addition. ....	173
Figure 5-28 The XRD spectrum (Cu K <sub>α</sub> ) of freeze-dried fresh floc containing both chromium and aluminium, analysed on September 16 <sup>th</sup> 2005, showing a crystalline structure that contained some peaks of known crystalline aluminium and chromium species but did not match any substance in the Philips X'Pert Database. Provisionally named Alexandrite. ....	174
Figure 5-29 Particle size analysis below 2 µm. Particles in this size range are very difficult to filter in practice (trial date September 1 <sup>st</sup> 2005). ....	175
Figure 5-30 Particle size analysis below 10 µm. Significant volume fractions are present in this range, which is marginal for capture in a fast coarse filter (trial date September 1 <sup>st</sup> 2005). ....	176
Figure 5-31 Particle size analysis below 100 µm. The upper part of this range could be captured in a fast coarse filter. The inflow would not be easily filterable (trial date September 1 <sup>st</sup> 2005). ....	177
Figure 5-32 A log-scale version of Figure 5-31 – particle size analysis below 100 µm. The peak-shifting is emphasised in this view and reinforces the pattern of 3 A (L min <sup>-1</sup> ) <sup>-1</sup> dosage being adequate when there is no protein in the inflow but that 4 A (L min <sup>-1</sup> ) <sup>-1</sup> dosage can restore the performance (trial date September 1 <sup>st</sup> 2005). ....	178
Figure 5-33 The effect of adding a small concentrated flow to the catholyte. The first and last samples are inflows (October 5 <sup>th</sup> 2005). ....	180
Figure 5-34 Electrolytic treatment of very low conductivity neutral pH water by modification of the catholyte. ....	181
Figure 5-35 The current decay (Channel 1) for a 25 kHz square wave input voltage. ....	183
Figure 5-36 A time-expanded view of the (inverted) current decay with 400 µs time constant. ....	183
Figure 5-37 The effect of varying frequency and duty cycle at constant RMS current on the electrolytic processing. The actual waveforms used are shown in Figure 5-38. ....	184
Figure 5-38 Waveforms used for results shown in Figure 5-37. ....	185
Figure 5-39 Basic scheme for treatment of 10% of the tannery effluent, making use of the existing DAF to collect the organic sludge. ....	190
Figure 5-40 Proposed scheme for processing the entire tannery effluent flow. Chromium could be recycled at 10 kg day <sup>-1</sup> . Recycling of aluminium coagulant is also shown. ....	191
Figure 5-41 A longitudinal section of a flume system that could be used for continuous treatment of tannery effluent. ....	192
Figure 5-42 Idealised Flume cross-section featuring moveable electrical distribution grid (just one cross-member shown) made of aluminium rod fitted to the partitions and able to be picked	

up for clearing floc deposits in the shavings matrix. A flow block warning sensor is placed below the level of the distribution grid. The shavings are replaced by gravity. ....	193
Figure 5-43 Proposed use of straight vertical ribbons or punched plates to improve upon curly shavings. The punched holes in the plates will have a rough edge that ensures a gap between the plates. The staggering of holes precludes catching on another hole if different plates corrode at different rates. ....	194
Figure 6-1 Cross section of the Flume. ....	197
Figure 6-2 Proposed alkali recycling scheme for an industrial process requiring net alkali input.	200
Figure 6-3 Proposed bipolar stack structure, showing narrow intracell gap and wide intercell gap that minimises current leakage. ....	202
Figure 7-1 The basic method settings for low aluminium measurement by ICP and low level chromium signal. ....	211
Figure 7-2 The background settings for low chromium measurement by ICP and a low level aluminium signal. ....	212
Figure 7-3 The grating settings for low aluminium measurement and a sample trace. ....	212

## List of Tables

Table 2-1 Percentages of additives in ferrous metals (MatWeb 1996).....	42
Table 2-2 Comparison of some anode material components.....	43
Table 2-3 Conductivity ( $S\ m^{-1}$ ) of electrolytes (italic) and typical fluids for purification.....	44
Table 2-4 Properties for fluids to be treated (see Table 2-3 and Table 4-7).....	46
Table 3-1 Performance of bipolar cell stacks in clarified terminal effluent.....	64
Table 3-2 Conditions in which electrolytic treatment of saline spiked with <i>Legionella pneumophila</i> at 10000 cfu $mL^{-1}$ resulted in complete disinfection - <i>Legionella pneumophila</i> levels below the minimum resolvable amount of 10 cfu $L^{-1}$ (December 3rd 2003).....	73
Table 3-3 $Log_{10}$ reduction of <i>Legionella pneumophila</i> by electrolytic treatment of low conductivity microbe-spiked saline (March 17 <sup>th</sup> 2004).....	74
Table 3-4 Summaries of organisms and electrolyte composition, as well as control voltage and flow rate.....	78
Table 3-5 The $Log_{10}$ microbial reduction rates achieved by electrolytic processing of model wastewater (Em 2003).....	79
Table 3-6 Chlorine production for synthetic laundry water using a single cell electrolyser operated at 17 V.....	82
Table 3-7 Operating parameters of a terminal effluent recycling plant assuming a current density of 25 $A\ m^{-2}$ that would require an electrode gap of 1 mm (see §3.2.5).....	88
Table 3-8 Specifications for a possible electroflotation treatment system for the entire flow of previously up-flow clarified effluent at the Hamilton City Council Waste Water Treatment Plant. The cell voltage and gas dose have been reduced to the point where the power requirement per volume is less than that of the UV system. Subsequent UV disinfection would require less energy input. Overall operating cost savings are possible.....	89
Table 4-1 Impurities in aluminium Alloy EN AW-6060. All in weight % (Matter Project 2001).....	94
Table 4-2 Corrosion product saturation and greater than faradic clearance from the Tower while processing clarified effluent at the Hamilton City Council Wastewater Treatment Plant. Total aluminium analysed by Hill Laboratories (January 18 <sup>th</sup> 2005).....	95
Table 4-3 The effect of high cell voltage on aluminium corrosion. Total aluminium analysed by Hill Laboratories (January 24 <sup>th</sup> 2005).....	97
Table 4-4 Test flume basic parameters.....	101
Table 4-5 Flow characteristics of the Flume with aluminium shavings in place, using salted tap water without electrical power.....	102
Table 4-6 Colloidal precipitate produced by electroflocculation of low-conductivity alkaline pulp mill effluent.....	106

Table 4-7 “H&S pond” (supplied by DAF outflow) analytical data supplied by the tannery company.....	110
Table 4-8 Pond 6 (source of final effluent) composition data - supplied by the tannery company.....	110
Table 4-9 The conditions of electrolysis for results shown in Figure 4-11 (April 15 <sup>th</sup> 2005).....	117
Table 4-10 Conditions and sample details for Figure 4-12 (May 12 <sup>th</sup> 2005).....	119
Table 4-11 Conditions to achieve dose shown as dependent variable in Figure 4-22.....	129
Table 4-12 The positive effect on bacterial growth of chromium removal by flocculation.....	130

# Nomenclature

## 1. The basic parameters that are used to model and monitor the function of an electrolytic water purifier are:

- V<sub>DC</sub>** Direct current supply voltage (V).
- l** Electrode gap (m).
- A** Electrode area (m<sup>2</sup>).
- c** Fluid impurity concentration (mg L<sup>-1</sup>).
- a<sub>i</sub>** Activity of species *i*.
- T** Temperature in °C.
- f** Fluid flow rate (m<sup>3</sup> s<sup>-1</sup> or L min<sup>-1</sup>).
- I** Current (A) and I<sub>d</sub>, current density (A m<sup>-2</sup>). If the current passes through cells in series, multiply the current by the number of cells to calculate Ampere-cells before conversion to Farads.
- IR<sub>Ω</sub>** Voltage drop across an ohmic resistor.
- C** Coulomb – a unit of electrical charge.
- D<sub>I</sub>** Faradic dose in electrical charge transferred per volume. The amount of treatment of a fluid by electrolysis is quantified by the ratio of charge transferred across the fluid to the volume of fluid treated. Hence the units are C m<sup>-3</sup>. An equivalent unit, composed of measurable rates, is electrical current per fluid flow rate, which for example is expressed as A (L min<sup>-1</sup>)<sup>-1</sup>. The conversion factor between the SI unit and the rate unit is 60000 C m<sup>-3</sup> (A (L min<sup>-1</sup>)<sup>-1</sup>)<sup>-1</sup>. For example, at 100% anodic current efficiency for aluminium corrosion and 100% clearance of corrosion products into the fluid, 1 A (L min<sup>-1</sup>)<sup>-1</sup> would result in 5.6 mg L<sup>-1</sup> of aluminium in solution, which is equivalent to 10.6 mg L<sup>-1</sup> of Al<sub>2</sub>O<sub>3</sub>.
- α** Current Fraction (%).
- Δφ** Equilibrium potential.
- E°** Standard redox potentials (V).
- E<sub>TDV</sub>** Minimum theoretical decomposition voltage of the species under consideration.
- ε** Energy efficiency.
- ε<sub>g</sub>** Gas void ratio.
- ε<sub>Δ</sub>** Triangular gas void ratio.
- F** Faraday constant, equal to 96485.309 C mol<sup>-1</sup>.

<b>R</b>	Universal gas constant, equal to $8.314510 \text{ J K}^{-1} \text{ mol}^{-1}$ .
<b>R<sub>x</sub></b>	Resistance of component x in ohms ( $\Omega$ ).
<b><math>\eta</math></b>	Over-voltage also known as over-potential (V).
<b>T</b>	Temperature ( $^{\circ}\text{C}$ ).
<b><math>\rho</math></b>	Resistivity ( $\Omega \text{ m}$ ), the reciprocal of conductivity, see below.
<b><math>\sigma</math></b>	Electrical conductivity ( $\text{S m}^{-1}$ ) is a measure of how easily electric charge passes through a material.
<b>pH</b>	Defined as $-\text{Log}_{10}[\text{H}^{+}]$ , where $[\text{H}^{+}]$ is the activity of protons in aqueous solution.
<b>E</b>	Volumetric energy input also known as energy density ( $\text{kWh m}^{-3}$ ).
<b>U<sub>c</sub></b>	Cell voltage.
<b>V<sub>m</sub></b>	Molar volume of and ideal gas, approximately $0.0224 \text{ m}^3$ or $22.4 \text{ L}$ .
<b>V<sub>x</sub></b>	Voltage across component x.

## 2. Abbreviations

<b>§</b>	Section mark symbol.
<b>CC</b>	Coliform count is an indicative measure of the microbial contamination of water, based a particular flora that exists in mammalian intestinal tracts, measured by the multiple dilution most probable number (MPN) test in units of density of colony forming units as cfu/100 ml.
<b>CFU</b>	Colony forming units, also known as cfu.
<b>COD/BOD</b>	Chemical Oxygen Demand and Biochemical Oxygen Demand are indicators of the amount of oxygen required to oxidise contaminants and maintain the metabolism of living contaminants respectively. The units are $\text{mg L}^{-1}$ .
<b>DAF</b>	Dissolved air flotation.
<b>DSA®</b>	Dimensionally stable anode. Noble metal oxide coated electrode for chlorine production.
<b>FAC</b>	Free available chlorine.
<b>HTE</b>	Hamilton City Council waste water Treatment plant terminal Effluent. Refers to clarified effluent for the trial that were carried out and UV treated clarified effluent for the proposed recycled water plant.
<b>IBC</b>	International bulky container (1000 L chemical container).



- H&S pond** Hides and Skins pond which collects DAF outflow at the tannery (see Appendix B).
- ICP-OES** Inductively coupled plasma optical emission spectroscopy.
- MOSFET** Metal oxide semiconductor field effect transistor. A power electronic switch.
- MPN** Most probable number of coliforms (see coliform count, CC).
- PAC23** A form of polyaluminium chloride, polyaluminium chlorohydrate. (Leitzau 2004a).
- PACI** Polyaluminium chloride that is used as a general purpose flocculent (Leitzau 2004b).
- PFS** Polyferric sulphate, a flocculent that is highly effective over the wide range of pH that is used in wastewater applications (Leitzau 2004c).
- PPP** Point of production processor.
- RMS** Root mean square.
- SMPS** Switch mode power supply.
- TMGCC** Titanomagnetite-glass composite ceramic. Produced by Silicon Industries for Works Filter Systems in Hamilton, New Zealand.
- TMOS** Trench metal oxide semiconductor field effect transistor (see MOSFET).
- TSS** Total suspended solids is a measure of how much undissolved solid is present where undissolved solid is defined as that which cannot pass through a 0.45  $\mu\text{m}$  filter. Units of  $\text{mg L}^{-1}$ .
- XRD** X-ray diffraction.

### 3. Locality

The fieldwork was carried out in the Waikato province of New Zealand.

### 4. Presentation of multiple graphs and traces in a single figure

Multiple graphs in a figure are presented with a common independent variable axis and several dependent axes. Common dependent variable

groupings were flow rate and pH, cell current and cell voltage, and metal concentrations. The different graphs are referred to by graph number from the top of the figure. Individual traces are referred to by trace name from the legend for that graph. For example, the Inflow pH in the top graph would be referred to as the inflow pH trace in graph 1.



# **1 General introduction**

## **1.1 Background**

### **1.1.1 The global picture**

Living organisms are extremely sensitive to nutrients and contaminants in water. While the total volume of water in the world is  $1.4 \times 10^9$  cubic kilometres, only 2.5% of this, or  $3.5 \times 10^7$  cubic kilometres is freshwater, the rest being oceanic saltwater. The total usable freshwater supply for ecosystems and humans is  $2 \times 10^5$  cubic kilometres of water, which is less than 1% of all freshwater resources, and only 0.01% of all the water on Earth (Gleick 1993; Shiklomanov 1999; UNEP 2002). While the average annual global consumption of this available resource is 10%, the fraction is rising, with strain felt especially in arid regions that have high growth of either population or economy (UNESCO 2000). It is prudent to note that planet Earth is a closed water system, with effective but rather slow recycling processes that rely on solar and geothermal energy input to continue.

Electrolysis is a mature technology, in that some particular industrial processes like chlor-alkali are well established (Hine et al. 1977). However, there are many possible applications that have not been developed. This is partly because the value of changing reactants to products does not justify the cost of the electrical energy input, or that lowering the required electrical energy input has an unacceptably high capital cost. Water and wastewater are generally not high conductivity electrolytes and effective electrolytic processing could be expected to have either high energy input or high capital cost. The value of treatment is either, in the case of water, improving the purity and aesthetic quality or, in the case of wastewater, improving the state of the environment and lowering the cost of discharge where there are penalties for causing pollution.

### **1.1.2 The local action**

A point of balance is passed when the water consumption in a catchment region exceeds the rate at which the available resource is replenished naturally. This necessitates re-use or artificial recycling of water. In this scenario, the acceptable standard for wastewater effluent outflow becomes much more stringent, as these

form part of the inflow to pre-consumption purification processes. For example, in Germany, it is common practice to force local authorities to discharge treated municipal wastewater into a river upstream of the drinking water supply intake, so there is an incentive to improve waste-water treatment (Neitzert, T. 2003, pers. comm., April). The ultimate expression of this is demonstrated when wastewater treatment merges with pre-consumption purification.

Local authorities are constrained to produce high-quality effluent outflows and are also responsible for the state of their freshwater resources. They are tending to enforce stricter standards on point-source discharges from domestic and industrial sites, so that particularly harmful contaminants are separated out before they enter the main treatment stream. Treatment systems that are appropriate for municipal and regional scale discharges are able to take advantage of passive processes like settling and flotation with free energy sources like gravity. However, reliance on settling ponds is not appropriate for individual and relatively small-scale effluent producers, especially in a crowded urban setting. Yet these point source discharges are too large, or the contaminants too finely dispersed, to be treated immediately by the sort of in-line filtration that is suitable for final polishing of potable water. Because of the increasingly stringent purity standards set for both potable water and discharge of wastewater, currently available technology cannot meet the demand for water treatment without unacceptably increasing its cost, particularly for installations with a throughput of between 1 and  $10^4 \text{ m}^3 \text{ day}^{-1}$ . Hence, there is a place for medium scale treatment systems that can produce reusable water from wastewater.

Artificial means of increasing the rate of recycling inevitably require energy input and lead to build-up of extracted impurities. These practices are well established in cases such as augmenting natural reservoirs by forming dams and removing suspended solids by settling and filtration. The further step of adding flocculent is considered as a leveraged contaminant that causes itself and other contaminants to be easily separated from the water (Peters et al. 1987).

Physical, chemical and biological changes occur simultaneously during electrolysis of water. The driving forces for change are very strong, as the energy is delivered in quanta that are larger than that required for common ionic and

organic reactions. The reaction-zone is spread over a large surface area. The combination of effects is tailored to suit the required treatment. Electrolytic purification of a wide variety of water types is achieved through appropriate application of a balance of the available functions: flotation by bubbles, flocculation by corrosion of anodes, electrowinning by cathodic plating, disinfection, oxidation-reduction and pH modification.

### **1.1.3 The hydrogen economy**

Electrolysis of water is a well-known means of producing hydrogen, but it requires input of electrical energy so conversion efficiency must be maximised (Barnitz 1920; Kruger 2001; Marceta et al. 2002; Marceta Kaninski et al. 2004; Stojic et al. 2004). Establishing economic means of producing hydrogen is essential to use of hydrogen as an energy carrier in a hydrogen economy. While using hydrogen as a form of energy storage from low electrical tariff periods has been considered, there is another possibility. By achieving another process goal such as water purification simultaneously, electrolysis may become economic.

## **1.2 Thesis overview**

### **1.2.1 Structure**

Chapter 1 defines the area of study, and then examines the literature of electrolytic water purification systems, and the overall technology required to build an electrolytic water purifier. In some cases, like basic materials characterisation, much of the prior research was not in the context of water purification, but may be applied to it.

General materials and methods are described in Chapter 2.

The step-wise development of electrolytic processors and their use in this project is arranged by model number. Chapter 3 covers the development of bipolar stacks, while Chapter 4 describes the development and usage in the field of a novel corroding anode system. During the field trials, a specialised electrolytic processor, known as the Flume, was found to be effective but the composition and

state of the inflow water could not be controlled easily. Hence, controlled experiments were carried out in the laboratory to examine mechanisms of treatment. These are described in Chapter 5.

Chapter 6 covers novel findings of the research, implications for design of large scale electrolytic processors and suggestions for further work.

### **1.2.2 Emphasis**

The best working system that was developed during this research was the Flume. This is reported extensively in Chapters 4 and 5, including the choice of materials and how they were developed, system specifications as designed, performance data and recommendations for improvements.

Because the project had an applications outlook, the field trial results were of paramount importance. In-depth study was only pursued on any track so long as it remained potentially feasible for application. This appears as many starts on different paths that were pursued if they showed promise in real applications. However, even the dead-ends are reported up to the point of termination, along with reasoning for their cessation.

## **1.3 Aim and scope of this thesis**

### **1.3.1 Aim**

The aim was to develop electrolytic water purification principles so that the circumstances in which electrolytic purification is feasible could be defined. Feasibility was considered in terms of cost-effectiveness compared to present methods of treatment.

### **1.3.2 Scope**

The systems to be designed were to be optimised for: effectiveness of purification as determined by meeting or exceeding outflow purity requirements; least energy consumption, either as gross or net energy input; and minimum capital cost.

An electrolyser in this context is a device that contains at least one electrochemical cell with the aqueous fluid that is to be purified as electrolyte. By this means, there is no need to supply or refresh chemicals to maintain the conductivity of the entire electrolyte. This eliminates standard brine electrolyzers, which are highly efficient and effective producers of purification agents, but consume large quantities of salt. The fluid to be purified may be treated as either a batch or a continuous flow. The electrolyte will flow or move in response to convection and gas pumping induced by the electrolysis.

The water to be treated must be electrically conductive. At a current density of  $100 \text{ A m}^{-2}$  through water with low conductivity of  $10^{-2} \text{ S m}^{-1}$ , the voltage drop through an electrolyte gap of  $0.001 \text{ m}$  is  $10 \text{ V}$ . This voltage is an order of magnitude higher than the reversible potentials of most electrochemical reactions, implying poor energy efficiency. Most tap waters are more conductive than this lower limit. For electrolytes more conductive than seawater ( $5 \text{ S m}^{-1}$ ), the equivalent electrolyte voltage drop is  $0.02 \text{ V}$  would not be expected to cause the dominant loss in the system. In order to focus on lowering the ohmic losses for weakly conducting electrolytes, which are potable or dischargeable, the range of conductivities considered was limited from  $10^{-2}$  to  $5 \text{ S m}^{-1}$ .

The achievable current density at cell voltages below  $10 \text{ V}$  for these conductivities is likely to be in the range of  $1 \text{ A m}^{-2}$  to  $100 \text{ A m}^{-2}$ . Given that the effects are mainly dependent upon current and become noticeable at a dose ( $D_I$ ) in the vicinity of  $1 \text{ A (L min}^{-1})^{-1}$ , the energy density of treatment can only be reduced by reducing the cell voltage. The essential challenge therefore appears to be increasing the current density while maintaining a low cell voltage by reducing the cell resistance. As the cell voltage drops to levels comparable to the reversible potential of water-splitting,  $1.23 \text{ V}$ , this has the additional benefit of producing hydrogen at an efficiency that makes energy recovery worthwhile.

The scale of application is limited. For potable water demands below a cubic metre per day, the scale of domestic users, filtration is the best approach. Wastewater from isolated single dwellings at similar flows can be dealt with by septic tanks. The capital cost of an electrolytic system and any associated energy recovery means are not economic at this scale.



Large scale limits are imposed by the maximum size of an electrochemical cell, the number of cells that are combined into an electrochemical module and the increasing complexity of interconnections between combined modules. Furthermore, at flows greater than  $10^4$  cubic metres per day, the economy of scale begins to work in favour of traditional plants that use gravity as the means of purification.

In between, from the smallest economic single cell system to a large factory wastewater processor, there are many possible combinations. The development of optimal maximum size modules is the greatest challenge, leaving only the problem of fluid and electrical interconnection between modules as a barrier to reaching the largest scale possible.

## **1.4 Literature review**

### **1.4.1 Background and history of electrolytic purification**

In 1887 French and British patents for electrolytic purifier were issued to Eugene Hermite (Marson 1965). Electrode electrochemical wastewater treatment, based on these patents, and using chlorine generation for disinfection and deodorising, was first trialed in London England from 1889 to 1899. A similar treatment plant using iron electrodes, and seawater as a chloride source, was built the same year as the London plant in Salford England for treating canal water (Vik et al. 1984). A US patent for purification of wastewater using aluminium and iron corroding electrodes was received by J. T. Harries in 1909 (Vik et al. 1984) and the first installation in the former Soviet Union at Shature Power Station, in 1925, used soluble iron anodes (Strokach 1975), as referred to recently (Matteson et al. 1995). Other early literature on electrolytic wastewater treatment was about treatment of tannery effluent (Fassina 1938) and interest is on-going (Ramirez et al. 1978; Vlyssides et al. 1997; Bellakhal, N. et al. 2004; Murugananthan, Bhaskar Raju et al. 2004; Zaroual et al. 2005). Thus the opportunity to treat tannery effluent *in situ* during this project was considered invaluable.

Electrolytic water purification has been trialled many times since work about Potomac River (Washington DC) water purification was published just after the Second World War (Stuart 1946; Bonilla 1947; Stuart 1947) and recent work has focused on use of microbial fuel cells (Kim et al. 2004; Logan 2004; Tender et al. 2004). Electrolytically induced flotation, flocculation (Maslennikov et al. 1961; Gerasimov et al. 1962; Matov 1967; Archakova 1969; Chebanov et al. 1972; Dorokhina 1976) and sterilisation (Johnsen 1938) are mechanisms that are used to purify water which would otherwise have to be carried out by other means. Other established electrolytic processes, such as the chlor-alkali process (Walde 1937), show the pH-manipulation ability of electrolysis. In favourable conditions electrolytic processing is both more effective and less costly than established methods (Chen et al. 2003; Sasaki 2004; Lin et al. 2005; Nielson et al. 2005; Spagnoletto 2005).

The crucial barrier to extensive use of electrolysis in purification of both potable and waste waters is energy consumption, which is directly related to the low electrical conductivity of relatively pure water. However, even when the cost of treatment is acceptable (Meunier et al. 2004), other difficulties that are well known in industrial and laboratory electrolytic processes are encountered (Pletcher 1984; Pletcher et al. 1990). These include poor electrical connection to electrodes, electrode fouling, anodic dissolution and uneven fluid flow distribution.

While researchers have solved some of these problems in isolation, such as electrode fouling (Rodrigo et al. 2001), a complete workable solution with an acceptable lifetime in real application has been elusive. This is due to the wide ranging technical issues that must be solved, in traditionally separate subject areas ranging from electrical engineering through to electrochemistry and materials fabrication. The rate of anode corrosion is limited in practice by poor clearance of the hydrolysed corrosion products. As these products are intended to be good flocculants it is to be expected that they bind together on the anode surface forming a layer that becomes thicker until the resistance prevents further passage of electrical current. Increasing the flow rate of the fluid to be treated will improve the clearance but cannot maintain adequate treatment in a steady state. A typical end-point for many projects has been to state that the electrodes must be replaced

or cleaned regularly (Plantes et al. 1982; Tetrault 2003) which is an indication of both electrode metal wastage and high maintenance requirements.

In the last few decades, a revitalisation of medium scale application of electrolytic water purification has occurred (Osipenko et al. 1977; Musquere 1983; Musquere et al. 1983; Pensaert et al. 1995; Ordonez 1997; Sakakibara et al. 2001; Sakakibara et al. 2002). Many reviews were also published recently (Abu-Orf et al. 2004; Kraft 2004; Mollah, M. Y. A. et al. 2004; Mouli et al. 2004; Holt et al. 2005; Torem et al. 2005). A recommended review with 300 references was published by Elsevier (Chen 2004). Complementary work in electrode materials science and other fundamental topics has also progressed (Millet et al. 1993; Chen, X et al. 2002; Nagai et al. 2003; Chen 2004; Chen et al. 2005) A further driver is the potential for energy recovery as hydrogen which has wider impact on energy-carrier strategies (Sherif et al. 2003).

The factors that control the efficiency (energy input per volume of water treated) for the various electrolytic water purification systems have been explored over many decades. The literature states that the energy input required to treat various aqueous fluids is in the range  $0.1 \text{ kWh m}^{-3}$  to  $30 \text{ kWh m}^{-3}$  (Bonilla 1947; Stuart 1947; Costaz et al. 1983; Donini et al. 1994; Bayramoglu et al. 2004) and is commonly around  $1 \text{ kWh m}^{-3}$  (Gao et al. 2005). The energy efficiency depends on the cell voltage, with any excess over the equilibrium reaction potential (over-potential) contributing to the losses. The cell voltage required depends largely on the gap between electrodes, electrolyte conductivity, current density and the electrode surface state (Chen, X. et al. 2002). For waters with conductivity of less than  $0.1 \text{ S m}^{-1}$ , simple calculation shows that main source of loss, for all practical current densities, is electrolyte resistance. Hence, the literature reports many instances of attempts to increase the electrolyte conductivity, either by increasing its specific conductivity, most often by adding NaCl (Kobayashi 1985; Ordonez 1997), or by reducing electrode spacing (Nagai et al. 2003). A practical system requires the use of series-cells of similar total area to a single cell system, to lower the required current. There are reports on the use of bipolar series-electrode systems for electrolytic and biological water treatments (Osasa et al. 1993; Osasa et al. 1995; Sakakibara et al. 2001).

Flocculation and coagulation are common techniques in modern water and wastewater treatment, usually achieved by addition of iron or aluminium salts such as polyferric sulphate (PFS) or polyaluminium chloride (PACl), or organic polymers such as polyacrylamide (Pontius 1990). Acidic flocculants are best suited to treating fluids with high alkalinity (Leitzau 2004b). Acidic fluids can be treated with basic polyaluminium flocculants (Hagiya et al. 1974; Tanji et al. 1975). Electroflocculation (also known as electrocoagulation) by electrolysis is a common and well-established process but the mechanisms are poorly understood (Napper 1983; Damien 1992; Debillemont 1996; Kraft 2004). There are extensive and thorough considerations of some aspects like kinetics and electrophoresis (Matteson et al. 1995). There are also numerous examples of trials (Rovel 1975; Vertes et al. 1983; Kaspar et al. 1988; Anon 1995; Muller 2002; Neti et al. 2003; Bellakhal and Brisset 2004; Paschoal et al. 2005), and a  $3 \text{ m}^3 \text{ hour}^{-1}$  prototype has been described (Adin et al. 2002). Full commercialisation seems to have been hindered by the factors mentioned earlier in this section. In particular, insufficient clearance of corrosion products from the anode, leading to anode fouling and greatly increased resistance over time, known euphemistically as passivation, is reported by the most forthright researchers (Donini et al. 1992; Donini et al. 1993; Donini et al. 1994) and there are thorough analyses of the economics of electrocoagulation in the literature (Donini et al. 1994). One fully translated paper from the former Soviet Union describes a system with a radial fluid flow to continuously clear the corrosion products and avoid passivation of the anode (Nikolaev et al. 1982).

The very point of purification, that is separation of impurities from water, leads to the task of dealing with a concentrated stream of impurities. Over-effectiveness in purification, or at least a lack of planning when dealing effectively and economically with large quantities of extracted impurities, has limited many projects. This includes the earliest recorded electrolytic sludge treatment plants, at both Santa Monica and Oklahoma City, USA (Collier 1912), which despite their effectiveness (Miller et al. 1963) were dismantled in 1930 because of the cost of removing and transporting the treated and settled sludge. The lesson is clear – a means of dealing with the sludge produced by electrocoagulation must be established or it becomes a problem of equal magnitude, if less volume, than the original problem of impure water (Hill, T. 2003, pers. comm., January 4<sup>th</sup>).

It has been reported that high pH increases the corrosion rate of anodic aluminium by orders of magnitude and that the electrochemical corrosion rate is faradic (Canizares et al. 2005). The comparison between iron and aluminium anodes is covered well in the literature, from iron specific phenomena like production of magnetite (Mollah, Mohammad Y. A. et al. 2004; Parga et al. 2005) that enable post-processing by magnetic separation (Shin et al. 2004) to direct comparisons of cast iron and aluminium electrodes at the same current density in a fowl slaughterhouse application which indicated that the cast iron electrodes were suitable for removal of soluble sulphides (Marconato et al. 1998).

The well known Dissolved Air Flotation (DAF) process produces bubbles by injection of a water side-stream loaded with dissolved gases under pressure. The gas comes out of solution in the form of very fine bubbles that adhere to impurities in a body of water and float them out (Pontius 1990). In this way, substances with a very similar density to water, that cannot easily be removed by passive settling or flotation, can be lifted out of the water. The volume of gas required per mass of solids to treat a low-solids fluid is higher than for high-solids water – 380 mL g<sup>-1</sup> (air volume per solid mass) for water with 20 mg L<sup>-1</sup> of solids but only 30 mL g<sup>-1</sup> for activated sludge - because of the reduced chance of collision between bubbles and solids in a purer fluid (Maddock 1977).

Electroflotation of solid from water, first proposed in a patent (Elmore 1904), is achieved by buoyant bubbles of hydrogen and oxygen in a manner similar to DAF (Evans 1974; Mraz et al. 1993; Marti et al. 1994; Park et al. 2002; Wu et al. 2002; Stoica et al. 2005). Electrolytic gas evolution is the specialty of at least one researcher (Sides 1981, 1986). It has been reported that the small bubbles made by electrolysis give electroflotation an advantage over other forms of bubble flotation (Mayer et al. 1990; Chen 2004). The gas and solid phases can agglomerate so long as the bubble size is less than 130 µm because the bubbles will rise in laminar (non-turbulent) flow (Turner 1975). Bubbles of air rise in tap water at a rate exponentially dependent on their diameter (Turner 1975); 10 µm bubbles rise at 50 µm s<sup>-1</sup> while 100 µm bubbles rise at 5 mm s<sup>-1</sup>. Hence, downward fluid flow speeds must be limited so that highly effective small bubbles can rise against such a flow.

The bubbles of hydrogen and oxygen produced by electrolysis are likely to have minimum diameters in the range of 10  $\mu\text{m}$  to 100  $\mu\text{m}$ , especially when produced by pulses of current a few milliseconds in duration, but can be larger depending on coalescence (Khosla et al. 1991). Current density also has an effect which depends on other factors (Jiang et al. 2002; Chen 2004). The electrode service life is inversely proportional to approximately the square of the current density (Backhurst et al. 1969). Electrolytically produced bubbles can have a lower diameter than those produced by DAF though with a greater variability of size (Burns et al. 1997). A number of studies have investigated the effect of water conditions on electrolytically derived bubble size (Kolibaba 1970; Glembotskii et al. 1973; Zekel et al. 1975; Matis 1980; Alekseev 1988; Ketkar et al. 1988; Llerena et al. 1997). One study found that oxygen bubbles give better flotation than hydrogen for a given gas evolution rate and that while higher current densities resulted in faster flotation, lower current densities had better gas usage efficiency (Khosla et al. 1995). Another study of gold-ore flotation found that a mixture of hydrogen and oxygen gave the best result (Mamakov et al. 1976). Oxygen bubbles are generally bigger than hydrogen bubbles, especially at high pH as the negative charge on hydrogen bubbles at high pH causes electrostatic repulsion from the cathode. The size of oxygen bubbles generated from platinum anodes decreases with current density (Ketkar et al. 1988). The smallest average hydrogen bubble size (22  $\mu\text{m}$ ) recorded was made using a polished stainless steel cathode (Ketkar et al. 1988).

Electroflotation can be carried out in conjunction with electrocoagulation, using just one anode material (Karpuzcu et al. 2002; Muruganathan, Raju et al. 2004). Older Western European literature suggests that that electroflocculation and electroflotation should be physically and temporally separate processes (Bertay et al. 1981; Christoforetti et al. 1986). Others have reported that simultaneous electroflotation and electrocoagulation are synergistic in that nucleation of bubbles and initiation of flocculation, entrapment of fine bubbles in floc and further coagulation are linked (Muruganathan, Raju et al. 2004; da Rosa et al. 2005). Reports of trials of electroflotation prototypes made thirty years ago, operating at fluid treatment rate of 1  $\text{m}^3 \text{hour}^{-1}$ , described large area electrodes that were claimed to be able to give an even coverage of bubbles in a container and

suggested that nascent gas bubbles assist flocculation (Barrett 1975). Another study of the same era found that combined electroflocculation-flotation was a more effective and rapid treatment method than chemical treatment followed by DAF (Beck et al. 1974). Hence, it is worth considering the increased complexity in a working system that uses separate specialised electrodes (Qu et al. 2002), compared to the performance of multi-functional electrodes (Ge et al. 2004; Hu et al. 2005). In order to achieve an optimisation, the appropriate flow sequences and orientations must be considered as part of the process.

The consensus of the literature is that electrosterilisation is achieved by production of aggressive oxidative species (Costaz et al. 1983; Tao et al. 1999), though it must be noted that the functions of electroflotation (Tsai et al. 2002) and electroflocculation (Adin et al. 2002) are both independently effectual in removing solid and also synergistic with the oxidative species. Pre-removal of solid eases the chemical loading. Anodic production of oxygen and chlorine is well known and predictable in chloride containing waters (Dylewski et al. 1996; Vijayaraghavan et al. 1999; Franz et al. 2002). As for electroflotation, small bubble size is considered an advantage (Lambert et al. 2001). Non-corroding yet conductive anodes with a high oxygen production over-potential (hence, favouring production of other oxidising agents) are formed from monolithic  $\text{TiO}_2$  by partial reduction in a hydrogen atmosphere to the Magnéli series  $\text{Ti}_n\text{O}_{2n-1}$ , particularly  $\text{Ti}_4\text{O}_7$  (Smith et al. 1998).

Before citing work that makes claims about production of other oxidising agents, it is worth noting one unambiguous statement in the literature, to the effect that free available chlorine (FAC) is the primary oxidant resulting from salt brine electrolysis and that chlorine dioxide, ozone and hydrogen peroxide are not detected (Gordon et al. 2001). The same group of authors also explain that FAC can break down ozone (Gordon et al. 1998). In dilute solutions with very high cell voltages, especially where there is no separating membrane between the cathode and the anode, the situation is more complex with a number of reaction pathways competing to produce a range of bio-active intermediates, including radicals. Electrolytic hydrogen peroxide production was reported in the 1930s (Berl 1937, 1939), whereby externally derived oxygen was delivered to a cathode. Though many reactions and species have been identified, the complexity has not been

fully explored. Only in a few cases has specificity been achieved (Osaka et al. 2000; Drogui, Rumeau et al. 2001). Both the identification of two steps of cathodic oxygen reduction, the first to a hydrogen peroxide intermediate and the second to water and the rate limiting of the second step, so that hydrogen peroxide is released, have made residual hydrogen peroxide disinfection feasible (Drogui, Elmaleh et al. 2001). This suggests that there is considerable work to do in targeting preferred reactions and suppressing unwanted ones. For example, choosing to enhance or suppress chlorine production depending on the potential for organochlorine formation, and making some effort to replace the disinfection function of chlorine with hydrogen peroxide. A recent patent shows the increasing technical sophistication of electrolytic hydrogen peroxide production (Ramanathan 2003). Commercially slanted literature suggests that certain electrolytically produced species, such as chlorine dioxide, are more effective than hypochlorite and less apt to produce carcinogenic tri-halomethane (Kimbrough et al. 2002). A thorough review of reactions of pollutants with  $\text{ClO}_2$ , with at least 114 references, has been published (Rav-Acha 1998). Because electrolytic ozone generation has up until now required a high current density and high cell voltage, improvement of the cost effectiveness of ozone production has been an issue for over a century (Targetti 1899; Fischer 1905; Fischer et al. 1907; Mumm 1907; Briner et al. 1937; Briner et al. 1941; Semchenko et al. 1973; Foller et al. 1981; Foller 1982; Rengarajan et al. 1985; Takahashi 1986; Onda et al. 2005). A broad review of electrical discharge purification has been published recently (Malik et al. 2001).

Hence, it is crucial to determine what chemical species are required for treatment, and to direct the electrolytic reactions appropriately using correct materials. Commercial application has already been achieved for applications like swimming pools (Busse et al. 1985; Houghton 1985; Wilson 1995; Rimpler et al. 1997; Gottard 2001; Diegner 2003).

Anodic electro-oxidation (Szpyrkowicz et al. 2000; Xiong et al. 2001; de Lima Leite et al. 2002; Lanza et al. 2002; Leite et al. 2002; Liao et al. 2002; Neti Nageswara et al. 2003; Chen 2004) and cathodic electro-reduction (Barradas et al. 1974; Koga et al. 1993; Kunugi et al. 1993; Pekmez et al. 1993; Lu, C. et al. 1999; Paidar et al. 1999; Huang et al. 2000; Juttner et al. 2000; Lessene et al. 2000;



Koparal et al. 2002; Ahmed et al. 2004; Latuzt et al. 2005) are well represented in the literature. It is interesting to consider whether or not the reported phenomena are the result of direct electrochemical reactions, where electrons are transferred to or from the electrode from or to the species being treated; or rapid reaction with oxidising and reducing agents produced at the electrodes. For the case of cyanide oxidation the direct reaction and specificity of the electrode material has been verified by voltammetry (Lanza et al. 2002), whereas oxidation of sulphides in petroleum refinery wastewater has been achieved by reaction with the OH<sup>-</sup> Radical, Fenton's reagent, electrolytically-derived from Fe<sup>2+</sup> ions and hydrogen peroxide (Tao et al. 1999).

Electrode materials have been widely considered in the literature. In particular, mixtures of non-oxidisable TiO<sub>2</sub>/RuO<sub>2</sub>/SnO<sub>2</sub>/IrO<sub>x</sub>/Sb<sub>2</sub>O<sub>5</sub> coatings for titanium anodes give good performance and lifetime for disinfection and oxidation applications (Pelegri et al. 2001; Chen 2002; Lanza et al. 2002; Chen et al. 2005). For coagulation applications the best results have been obtained with a sacrificial aluminium or iron anode, with stainless steel or graphite cathodes (Tabakov 1982; Tabakov et al. 1982).

#### **1.4.2 Review of the state of the art**

As recently as two decades ago, electrolytic water purification systems with good performance specifications were being proposed without any claim about their energy consumption (Krofta 1984). Subsequent lack of commercial development suggests that such systems were commercially unfeasible because the energy consumption was too high. While recovery of hydrogen has recently been represented as a way of compensating for the high energy consumption of electrolytic treatment (Kobayashi et al. 2004; Nagai et al. 2004; Ichimaru et al. 2005; Yamamoto 2005), the literature lacks any description of industrial examples, suggesting that either the cell voltages were too high for efficient recovery or the benefits of collecting the hydrogen were outweighed by technical difficulties and safety issues.

## 1.5 Electrochemical principles

### 1.5.1 Components of cell voltage

In this section, the components of total cell voltage are considered as losses over a series of three main components: the anodic interface, the electrolyte gap and the cathodic interface.

If the electrochemical reactions are viewed as lyses or breakdown, then the overall cell voltage  $U_c$  has having several distinct components.

*Equation 1-1* 
$$U_c = E_{TDV} + \eta_a + \eta_c + IR_{\Omega}$$

$E_{TDV}$  is the minimum theoretical decomposition voltage of the species under consideration,  $\eta_a$  and  $\eta_c$  are over-potentials at the anode and cathode respectively and  $IR_{\Omega}$  is the sum of ohmic losses (Lu, G. et al. 1999). Metallic or inter-metallic anode surfaces have the thermodynamic potential to oxidise, in preference to producing oxygen from water, or chlorine from chloride. Hence, there are two distinct strategies to follow in choosing anode materials: easily corrodible, where the products of corrosion are useable; non-corrodible, either by forming a poorly conducting but thin oxide at the surface (passivation) or by being composed entirely of a high-conductance oxide that is resistant to further oxidation.

The study of the behaviour of electrochemical interfaces, electrodictics, is based on three central tenets shown in the following equations, which express the same principles from different perspectives (Bockris and Reddy 1970):

*Equation 1-2* 
$$\Delta\phi = \Delta\phi^{\circ} + \frac{RT}{F} \ln a_i$$

Nernst's Law, shown in Equation 1-2, allows prediction of *equilibrium* potentials ( $\Delta\phi$ ) for non-standard conditions from the potential for standard conditions ( $\Delta\phi^o$ ) and the temperature (T) and activity of the reacting species,  $a_i$ .

$$\text{Equation 1-3} \quad \Delta\phi = P + Q \ln i$$

The potentiocentric form of Tafel's Law, shown in Equation 1-3, defines the *non-equilibrium* potential of an electrochemical reaction in terms of two constants, P and Q, as a function of the natural logarithm of the current density. The voltage additional to the equilibrium potential, the over-voltage, is seen as being a disadvantageous consequence of the passage of current.

$$\text{Equation 1-4} \quad i = i_0 \left( e^{\frac{(1-\alpha)nF}{RT}\eta} - e^{-\frac{\alpha nF}{RT}\eta} \right)$$

$$\text{Equation 1-5} \quad i = A e^{B\eta}$$

Equation 1-5 (the current-centric Tafel equation) is an accurate simplification of Equation 1-4 (the Butler-Volmer relation) when  $|\eta| > 118 \text{ mV}$ , where n is the number of electrons transferred by the reaction and  $\eta$  is the over-potential. The current-centric form of Tafel's Law defines the non-equilibrium current density of an electrochemical reaction in terms of two arbitrary constants, A and B, as an exponential function of the over-potential ( $\eta$ ) which is the potential in excess of the equilibrium potential. In this sense, the over-potential is seen as a necessary governor of the current density. For a simple direct current supply voltage  $V_{DC}$ , the main sources of loss are shown either as opposing voltages, or as resistances in Figure 1-1.

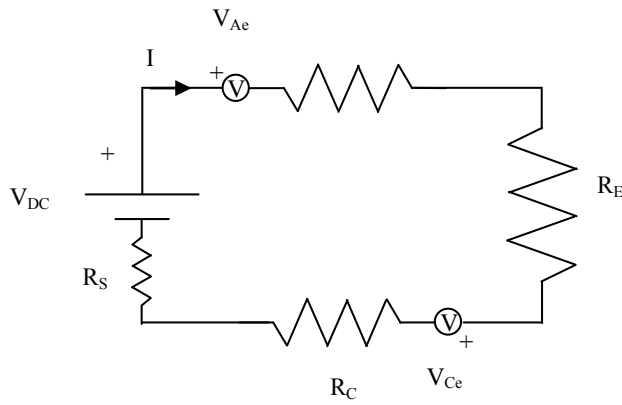


Figure 1-1 The DC electrical equivalent of an electrolytic cell.

The equilibrium potentials for the anode and cathode are  $V_{Ae}$  and  $V_{Ce}$  respectively. The resistance of the supply,  $R_S$ , including metallic leads and the electrolyte are considered to be ohmic (linear) functions of the current. This is well justified for  $R_S$ , but the electrolyte resistance is likely to depart from ohmic behaviour at high current density. The anodic and cathodic over-voltages,  $\eta_A$  and  $\eta_C$ , are equivalent to the voltages across the non-linear resistors  $R_A$  and  $R_C$  respectively. This is reflected in Equation 1-6 which shows components of voltage in the electrolytic cell circuit displayed in Figure 1-1. Equation 1-7 shows the electrochemical efficiency ( $\epsilon$ ) of an electrolytic cell.

Equation 1-6 
$$V_{DC} = V_{R_S} + V_{Ae} + V_{R_A} + V_{R_E} + V_{Ce} + V_{R_C}$$

Equation 1-7 
$$\epsilon = \frac{V_{Ae} + V_{Ce}}{V_{DC}} = 1 - \frac{V_{R_S} + V_{R_A} + V_{R_E} + V_{R_C}}{V_{DC}}$$

Equation 1-4 shows that in order to enable current to pass, over-potential must be applied, yet Equation 1-7 shows that over-potentials contribute directly to energy losses. Hence, all practical designs must apply some form of compromise, so that the area of the electrodes is not too large, while the energy efficiency is not too low. The acceptable limits for either depend on the application.

Standard industrial electrochemical processes use high concentration, high conductivity electrolytes, since this minimises the loss attributed to the term  $V_{R_E}$  in Equation 1-7. However, dilute electrolytes have conductivities several orders of magnitude lower than industrial electrolytes, which are commonly dominated by the contribution of NaCl. A graph of conductivity versus [NaCl] is shown in Figure 1-2. Higher salt concentrations result in a sub-linear response according to the Debye-Huckel and Fuoss-Onsager relations (Wright 1988).

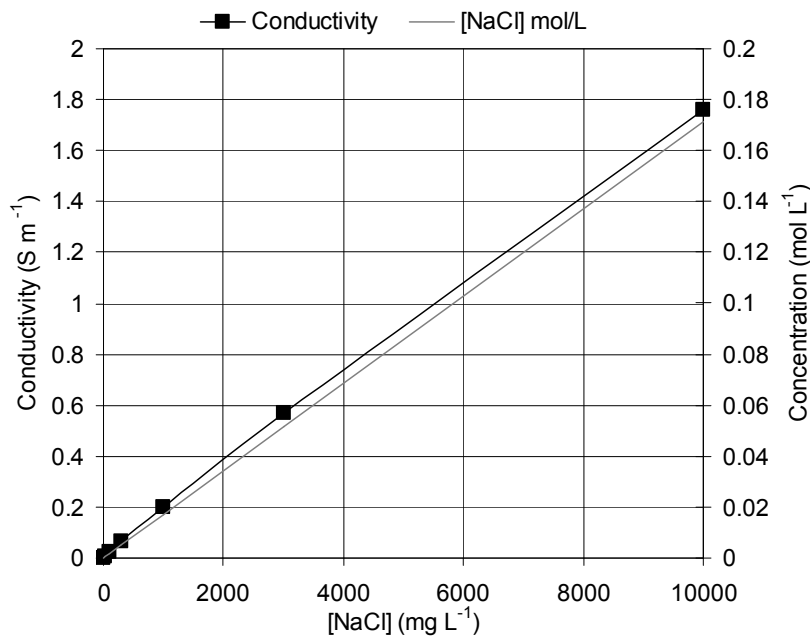


Figure 1-2 Conductivity of dilute aqueous NaCl solutions at 25 °C (Bryan 2003).

For situations where the electrolyte is dilute and cannot be altered for economic or environmental reasons, such as in wastewater, the loss due to electrolyte resistance can dominate. This is because the electrode over-potentials are logarithmic functions of the current density but the voltage across the electrolyte is almost linear with current. The conductance of the electrolyte is estimated from its conductivity ( $\sigma$ ), the area of the electrode interface ( $A$ ) and the average gap between the electrodes ( $l$ ) as in Equation 1-8.

Equation 1-8 
$$S_E = \sigma \frac{A}{l}$$

Overcoming the limitation of poor electrolyte conductivity is central to making cost-effective electrolytic water and wastewater processors. According to Equation 1-8 increasing the surface area offers lower losses. It also leads to an increase in size and capital cost. Indeed, increased surface roughness or porosity of the electrodes is of little use when the electrolyte conductivity is low because the shortest current path is so strongly favoured. However, an area-increasing surface structure that is very fine compared to the gap between the electrodes is advantageous. The next obvious target is to lower the distance between the electrodes. By this simplistic theory there is no limit to the size of the plates, or how closely they may be arranged. However, when it comes to making a real electrolyser, practical difficulties very quickly come to the fore.

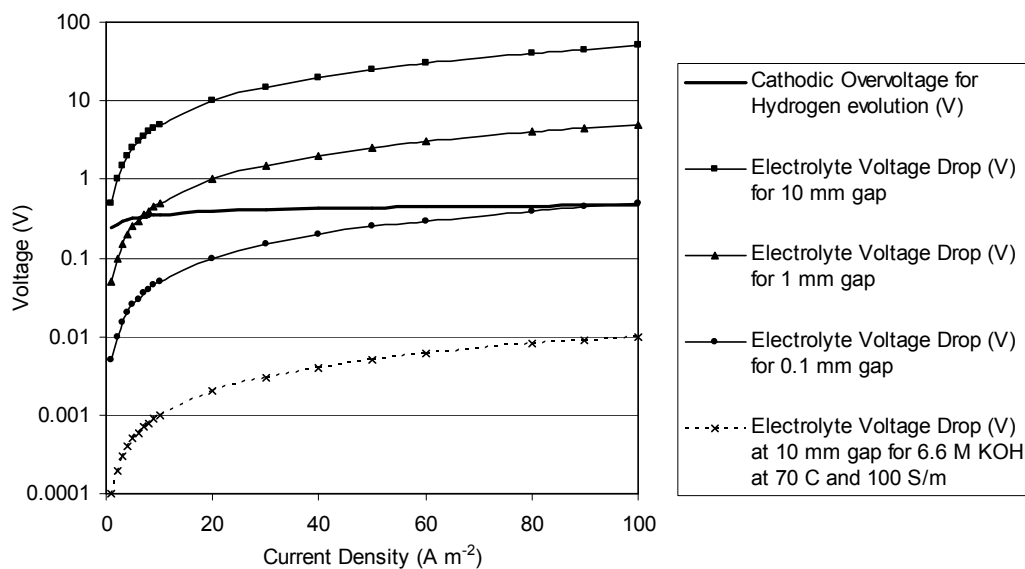


Figure 1-3 How electrolyte voltage drop is lowered to the order of the cathodic overpotential by reducing the gap. Based on an iron cathode and fluid with a conductivity of  $0.02 \text{ S m}^{-1}$ . Result for concentrated electrolyte shown for comparison.

Figure 1-3 shows how the voltage drop across the electrolyte gap becomes dominant if the electrolyte conductivity is reduced, and how reducing the gap size can lower the losses. This figure is based on published data for iron cathode exchange currents (Pletcher et al. 1990).

Partial occlusion of the electrolyte gap by gas bubbles leads to an increase in effective electrolyte resistance. Two extreme forms are explored for illustration: if a contiguous sheet of gas forms between two electrodes, from bubbles that

coalesce, this will grossly increase the effective resistance of the electrolyte even if it does not fill the entire space. Hence, this is to be avoided if at all possible; evenly dispersed fine bubbles will reduce the electrolyte conductivity from  $\kappa_0$  to  $\kappa$  slightly more than predicted by the linear gas void to total volume ratio,  $\varepsilon_g$ , (Wendt et al. 1999).

Theoretical estimates of the conductivity ratio are in a narrow range defined by Equation 1-9 so that if the gas bubbles occupy half the space then the resistance will be a little more than doubled. As the electrolyte gap is reduced, this limitation becomes more prominent, though the primary determinant of gas voidage is the ratio of gas volume production rate to fluid flow rate.

*Equation 1-9*

$$(1 - \varepsilon_g)^{\frac{3}{2}} < \frac{\kappa}{\kappa_0} < 1 - \varepsilon_g$$

For the simple case of parallel electrodes with plug flow of fluid that controls the motion of the bubbles, the terminal part of the flow will have the highest gas loading. The build-up may be modelled as spatially linear so that the average level is the same as the level at the halfway point in the flow, leading to the term triangular gas void ratio,  $\varepsilon_\Delta$  defined in Equation 1-10. This is equal to half the value of the voiding at the exit point, and is used in place of  $\varepsilon_g$  in Equation 1-9. Given that  $V_m$  is molar volume in  $\text{m}^3 \text{mol}^{-1}$ ,  $D_I$  is the faradic dose and the current efficiency of gas production is 100%, a value of  $D_I$  of  $60000 \text{ C m}^{-3}$ , equivalent to  $1 \text{ A (L min}^{-1}\text{)}^{-1}$  results in a  $\varepsilon_\Delta$  of 1%. This does not depend explicitly on the gap size, though for very narrow gaps, coalescence will cause the sheeting problem. The analysis above is an oversimplification because the gas is not distributed evenly across the electrolyte, being largely concentrated close to the electrodes where it causes diffusion limitations and raises the required over-potentials at a given current density. More detailed analysis is available in the literature (Sides 1986). Furthermore the positive return gained by reducing the gap size is limited by increases in fluid pressure drop and greater difficulty in preventing contact of the electrode pairs. For example, the pressure drop in laminar flow between

parallel plates is proportional to the cube of the reciprocal of the gap (Wendt et al. 1999).

Equation 1-10 
$$\varepsilon_{\Delta} = \frac{3}{4} \frac{IV_m}{F} D_l$$

### 1.5.2 Current fraction and current efficiency

In situations where more than one electrochemical reaction can occur at an electrode, the electrical current is distributed into fractions for each reaction. If one reaction is preferred, then the current fraction for that reaction is considered to be the current efficiency. While an electrochemically-driven reaction cannot have more than 100% current efficiency, based on the external current, it is possible for a similar (corrosion) reaction to occur passively and simultaneously using a local short-circuit of current. For measurement based on the outflow composition, this will raise the apparent current fraction for that reaction. Conversely, a back reaction could occur at the opposing electrode to consume the products of the preferred reaction, as an electrochemical short-circuit, lowering the apparent current fraction for that reaction. Therefore the total of the apparent current fractions could be more or less than 100% and a single reaction could have greater than 100% apparent current efficiency.

### 1.5.3 Mass transport limitations

While the electrodic equations in §1.5.1 are accurate at low to moderate current densities, at high current densities the over-potential is raised by inadequate diffusion of dissolved reactants to the electrode, inadequate diffusion of dissolved or precipitated products from the electrode and poor clearance of gas bubbles from the electrodes. However, if bubbles of around 10  $\mu\text{m}$  to 100  $\mu\text{m}$  diameter are released rapidly enough from the surface they stir the diffusion layers effectively, greatly improving mass transport (Wendt et al. 1999).

Stirring and dwell time between the electrodes have a number of conflicting effects. Stirring certainly assists reactants to reach the appropriate electrode and



products to leave the site of production, but it also causes useful products to meet the opposite electrode where they could be destroyed. If the fluid is passed through the electrode space rapidly, turbulent flow is more likely to occur, but the time available for back-reactions to occur is reduced.

Convection and gas pumping cause fluid movement whether or not fluid flow is driven externally. If necessary, this can be restricted by closing off all but the top face of the electrode cavity. Localised heating, concentration and dilution can occur in at least two forms. One is due to diffusion rate limitations, exemplified by the pH extremes close to the active electrode surfaces. Another is due to positive feedback on local current density – if the gap between the electrodes is uneven then the closer parts have higher current density, leading to higher local temperatures and therefore higher current density, until limited by gas void fraction and movement of electrolyte.

#### 1.5.4 The effect of pH

The standard oxygen potential drops at higher pH according to the Nernst equation (Bard et al. 1985), as shown in Equation 1-11.

$$\text{Equation 1-11} \quad E_{O_2} = 1.229 - 0.05916pH$$

At pH 0,  $E_{O_2}$  is 1.229 V, at pH 7 it is 0.815 V and at pH 14 it is 0.401 V. The variation with pH from the standard potential for production of chlorine from chloride (1.358 V) is not as extreme as for oxygen (Prokhorov 1963). For voltages in excess of the chlorine potential, decreasing the anodic pH by raising the current density will increase the chlorine current fraction at the expense of oxygen production until balanced by chloride depletion. Note also that increasing the bulk fluid pH will not directly lower the minimum voltage for electrolysis of water because the change in the hydrogen potential according to Equation 1-12 tracks the change in the oxygen potential (0V at pH 1, -0.414 v at pH 7, -0.828 v at pH 14).

$$\text{Equation 1-12} \quad E_{H_2} = -0.05916pH$$

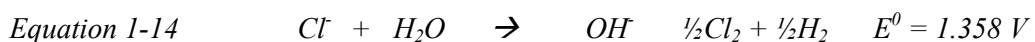
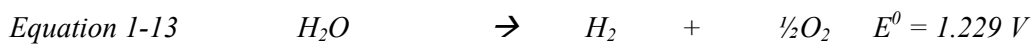
Hence, for all uniform pH values at 298 K, the standard potential for electrolysis of water is 1.229V. The surface of the electrolytic anode will tend to be strongly acidic, and the electrolytic cathode surface will tend to be strongly alkaline.

Therefore the cell voltage of the overall reaction of electrolysis of water could easily exceed  $1.229 - (-0.828) = 2.05$  V. One of the few ways to affect this is to alter the fluid flow through the electrodes. A low-flow-through system will exacerbate the lowering of anodic pH therefore favouring chlorine production ahead of oxygen. Higher inflow fluid pH will offset the acidity at the anode, thereby favouring oxygen production, though the cathode is more likely to be plated with metals and carbonates.

## 1.6 Electrochemical water treatment processes

### 1.6.1 General reactions and conditions

If materials and conditions are set so that the anode is non-corroding, the two main electrolytic reactions of interest in water, if the major solute is NaCl, are Equation 1-13 and Equation 1-14 (following from Equation 1-11 and Equation 1-12):



Analogous reactions are likely for other halide salts. Any gaseous chlorine produced will rapidly form active hydrolysed species in the water and commence

reacting with oxidisable impurities. Hence, the current fraction that goes to each reaction determines whether the system favours disinfection or flotation. The products of both reactions are cleared from the surface of the electrodes by flotation and fluid flow. The reverse reactions at the opposite electrodes are limited by clearance of the prospective reactants.

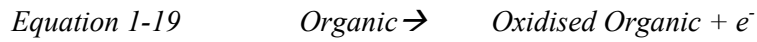
If the anode is corrodible then either the metal (M) is oxidised directly or subsequently consumes the oxidising agents produced at the anode. Maximisation of the corrosion current fraction is achieved by setting the cell voltage so that the reversible potentials for unwanted reactions are not exceeded (Lu, G. et al. 1999). Crucially, the current density for such small electrode voltages tends to be very low so that the effective electrolyser surface has to be large, with low resistance between the electrodes.

Electrons are extracted from the anode by the external driving voltage resulting in the oxidation of the solvent, solutes or anode. Water splits to produce oxygen and  $H^+$ , and  $OH^-$  is oxidised to form water and oxygen according to Equation 1-15 and Equation 1-16, considered as an acid or basic solution respectively.



Hence, the electrolyte close to the anode is acidified compared to the bulk solution. Anions, metals and organics are oxidized according to Equation 1-17, Equation 1-18 and Equation 1-19 respectively.

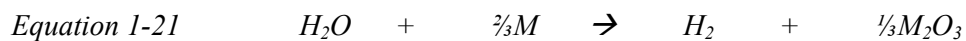




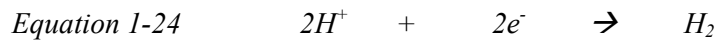
$H_2O_2$  is not a stable intermediate at the anode in the oxidation of water to oxygen (Bard et al. 1985). However, it is possible for hydrogen to decompose at the anode, as shown in Equation 1-20.



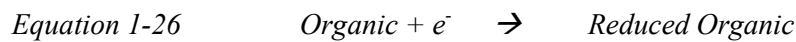
Metals passively corrode to form a stable oxide coating, according to Equation 1-21. In water Equation 1-22 is kinetically favoured, because of the ready availability of reactants, and the product is a flocculent. Both of these passive reactions are assisted electrolytically by the disruption of protective layers (Moriizumi et al. 2000).



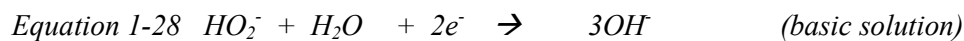
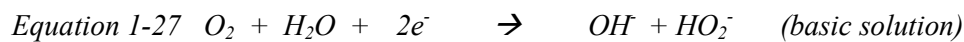
Reduction occurs at the cathode.  $H_2O$  or  $H^{+}$  is reduced according to Equation 1-23 (considered as a basic solution) and Equation 1-24 (considered as an acid solution) respectively. Hence, electrolyte at the cathode is de-acidified.



Metals and organics are reduced according to Equation 1-25 and Equation 1-26 respectively. Electrowinning of metals is an example (Rengakuji et al. 1998; Bestetti et al. 2001). Cathodic reduction of metal ions in a concentrated electrolyte to the metallic form is a well known industrial process (Delplancke et al. 1999).



O<sub>2</sub> is reduced back to water or OH<sup>-</sup> at the cathode. Hydrogen peroxide is an intermediate of this reaction and is present in measurable quantities at high current densities (Bard et al. 1985).



When there are other solutes and suspended solids in the water, there is a myriad of possibilities for minor reactions that have disproportionate consequences. The most damaging prospect is adherence of non-conductive precipitates to either of

the electrodes. This can be limited by maintaining high fluid velocity over the entire electrode surface (Donini et al. 1994) or periodically reversing the polarity (Zhurkov et al. 1977). The latter method in particular has the potential to capture heavy metals and release them during the period of polarity reversal – an electrolytic analogue of back-flushing a loaded filter.

### **1.6.2 Electroflocculation by electrolysis of aluminium or iron**

The most challenging aspect of deliberate electrolytic corrosion of an anode is maximizing the mass conversion of solid metal to metal flocculent in the outflow fluid using the least possible energy. Any of the following problems will limit this conversion: low current efficiency for anodic corrosion; poor clearance of the corrosion products from the anode; re-attachment of concentrated corrosion products to the anode toward the outflow and high cell resistance.

Normally, solid iron in water will corrode slowly, consuming oxygen, whereas aluminium is self-protected by an impervious thin oxide layer. When either of these metals is forced to be an acidic anode by an external voltage, and the corrosion products are removed by flowing water, the rates of both the faradic (dependent on external current) and passive (local short-circuit current) corrosion rates are enhanced. Hence, it is possible for the production rate of metal ions to exceed the maximum available from complete use of the transferred charge. That is, the apparent corrosion current efficiency can exceed 100% (Lu, G. et al. 1999; Jiang et al. 2002). What is not clear from the literature is the rate of chemical corrosion for a given rate of electrochemical corrosion at known current densities, particularly for dilute and poorly conductive solutions of moderate pH that require very high cell voltage. The production of persistent disinfectant is severely limited because even if an oxidising agent is formed, it is likely to be consumed by the metal. Crucially, both the metal oxide and the metal chloride can hydrolyse into a form that flocculates. The possibilities for side reactions are extensive, particularly for iron anodes. For example products with mixed oxidation states such as magnetite ( $\text{Fe}_3\text{O}_4$ ) can form (Tsouris et al. 2001). Aluminium has various thermodynamically favoured states depending on both the voltage and pH. This is shown in the Eh diagram in Figure 1-4 (Bard et al. 1985; Terryn 2002).

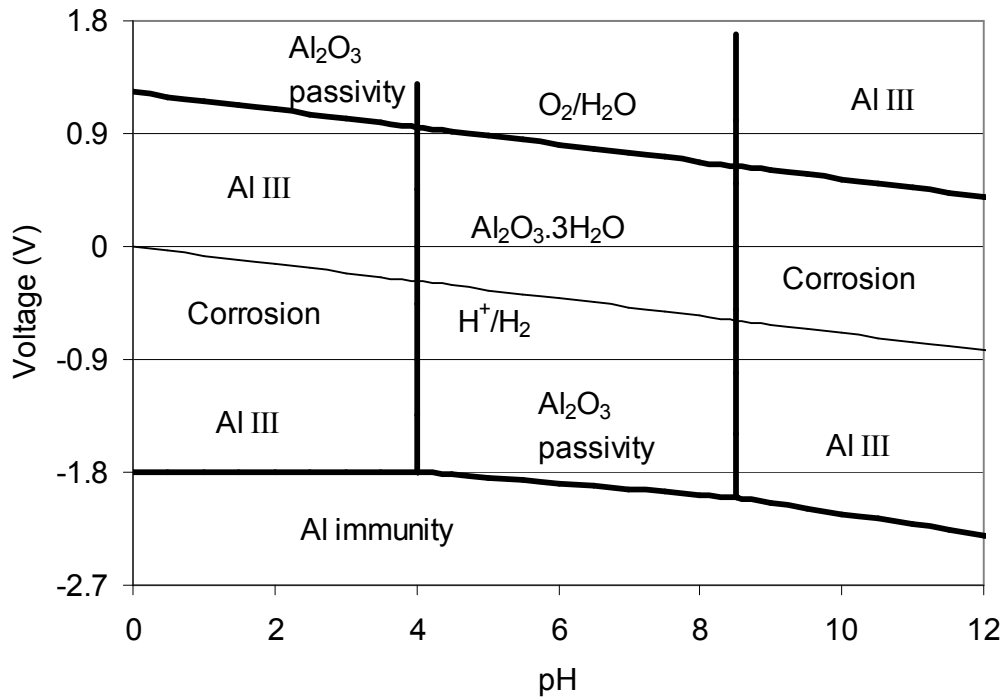


Figure 1-4 Pourbaix diagram for aluminium.

Figure 1-5 shows the levels of both amorphous and crystalline (gibbsite,  $\alpha$ -Al(OH)<sub>3</sub>) forms of aluminium that are dissolved in water at 25 °C as aluminate Al(OH)<sub>4</sub><sup>-</sup> for alkaline pH (Baes et al. 1976; Pontius 1990). Only aluminate levels in excess of those indicated are thermodynamically subject to precipitation. Figure 1-5 shows that it is very difficult to achieve a low residual of aluminium in water when flocculating at high pH using aluminium salts, particularly as the floc could be amorphous. At or below neutral pH the solubility of other aluminium species becomes significant, limiting the minimum solubility of gibbsite to 0.09 mg L<sup>-1</sup> (Baes et al. 1976).

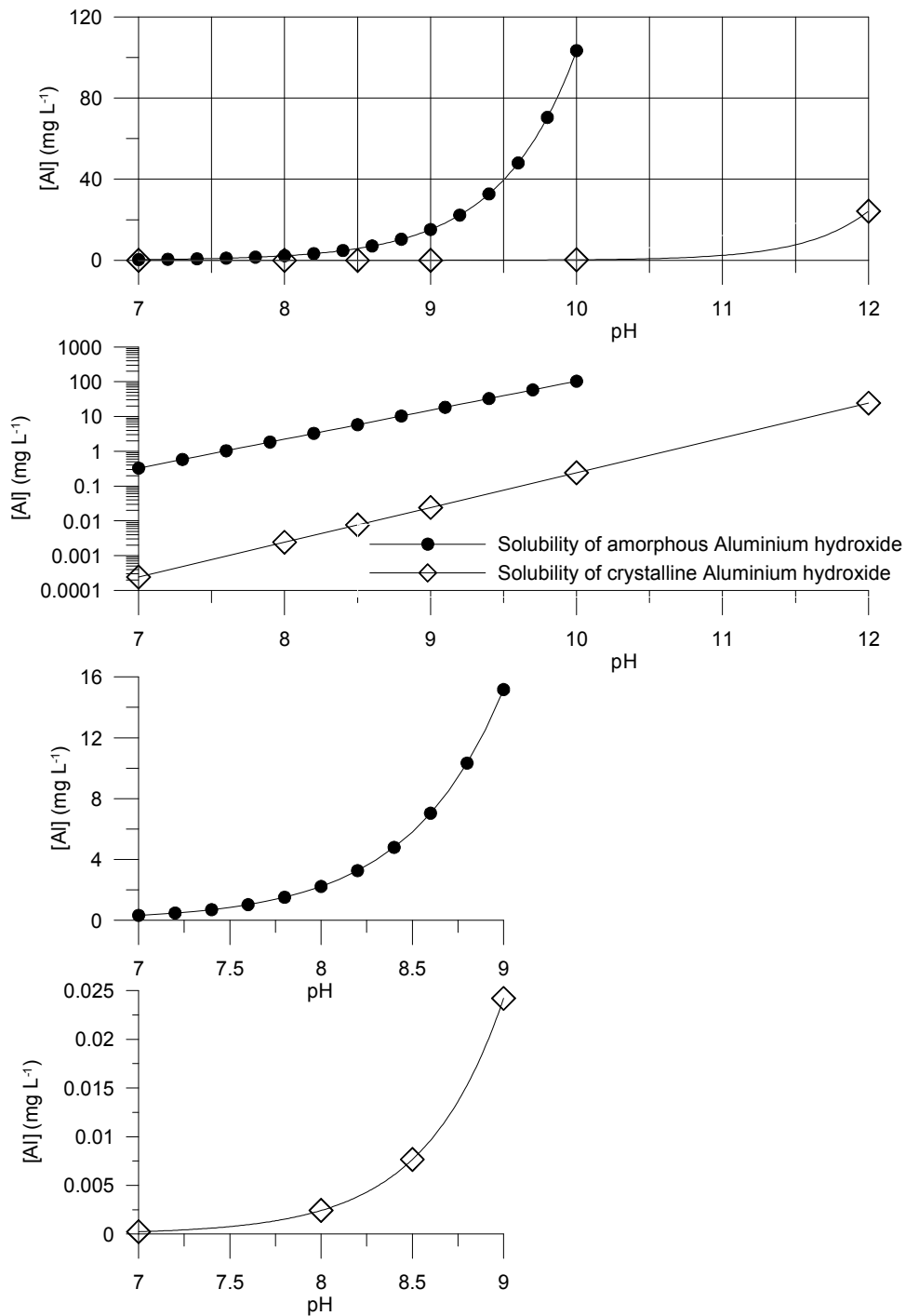


Figure 1-5 Saturation concentration of aluminium (mg L<sup>-1</sup>) for alkaline pH at which  $Al(OH)_4^-$  precipitates as either amorphous or crystalline forms of  $Al(OH)_3$ . Multiply  $[Al]$  by 1.889 to find the  $[Al_2O_3]$  equivalent.

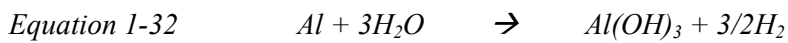
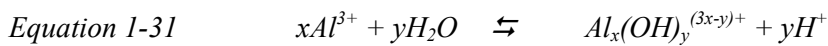
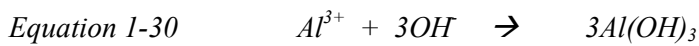
Anodic and cathodic reactions for systems with aluminium anodes and cathodes have been considered by other researchers (Jiang et al. 2002). While species such as chlorine are rapidly hydrolysed in aqueous solution, either the nascent chlorine or its derivatives can corrode additional aluminium in secondary reactions.

Equation 1-29 to Equation 1-34 examine the possible means of anodic aluminium

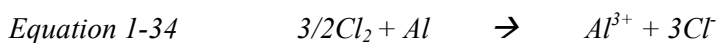


corrosion in the context of electrolysis in dilute saline solutions. Chloride ions, which are oxidised at the anode, are not spectator ions for the electrochemical reactions.

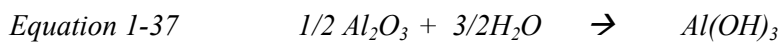
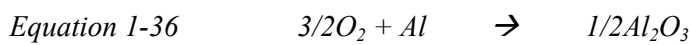
Direct electrolytic corrosion of an aluminium anode occurs according to Equation 1-29.  $Al(OH)_3$  is formed according to Equation 1-30 at the isoelectric point but the equilibria shown in Equation 1-31 (Baes et al. 1976) and Equation 1-42 are more general. Equation 1-32 shows passive hydrolysis at the isoelectric point.



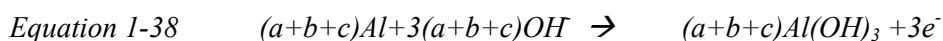
Reaction of aluminium with electrolytically formed chlorine as shown in the sequence Equation 1-33 to Equation 1-34 will result in a further hydrolysis similar to Equation 1-30.



Electrolysis of water will produce oxygen at the anode in basic conditions, according to Equation 1-35, that could attack the aluminium (Equation 1-36) with the resulting oxide then hydrolyzing, albeit slowly (Equation 1-37), to the usual hydroxide at the isoelectric point.



If the proportions of current (the current fractions) going into the primary reactions Equation 1-29, Equation 1-33 and Equation 1-35 are a, b and c respectively and the secondary and tertiary reactions go virtually to completion then the overall anodic reaction is represented by Equation 1-38.



If  $a+b+c=1$ , the above equations predict that 1 net mol of acid is added at the anode per mol of electrons transferred, irrespective of the individual current fractions.

The cathodic reaction (at a non-corroding cathode) is shown in Equation 1-39.



Equation 1-39 indicates that 1 mol of acid is consumed per mol of electrons transferred. If the cathode is also aluminium then other aluminium corrosion reactions can occur there too (Jiang et al. 2002).

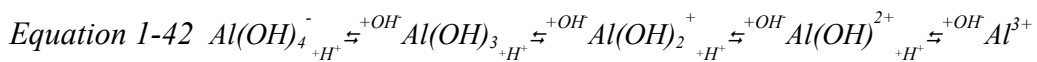
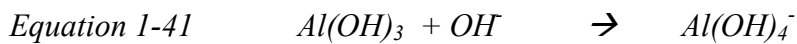
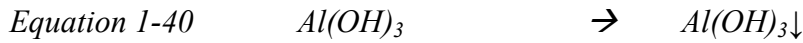
If the anodic reactants and products are kept separate from the cathodic versions by a membrane and the bulk of the flow goes through the anode compartment as anolyte, with a small seepage on the other side of the membrane as catholyte, the separately collected outflows are of different pH. The anolyte is slightly acidified and the catholyte is extremely de-acidified. The dual pH adjustment effect has been observed and identified as useful by other researchers (Yamamoto 2005).

Equation 1-39 suggests that if the anolyte and catholyte are mixed then the outflow will have the same pH as the inflow. If gaseous products partly escape the system or any of the secondary or tertiary reactions do not go to completion, then a net pH increase would be expected. In fact, for neutral to moderately alkaline pH inflows, significant pH drops in the mixed outflow lasting many hours were observed in both field and laboratory conditions during this research.

Simple chemical corrosion of aluminium by water according to Equation 1-32 and further dissolution in alkaline conditions according to Equation 1-41 (Meixner 2005), produces 1 net mol of acid and 1.5 mol of hydrogen per mol of aluminium consumed. Applying a positive voltage to aluminium makes it possible for the corrosion to proceed at a fast rate at extremely alkaline pH (Krasnobryzhii et al. 2004) or in acid conditions (Mazzone et al. 1969). The purity of the metal is probably crucial as studies using highly pure aluminium in pH adjusted saline have found weak dependence of corrosion rate upon voltage compared to the dependence on pH, but much more sensitivity to voltage for alloys (DiBari et al. 1971).

At the isoelectric point of  $\text{Al(OH)}_3$ , by definition, the resulting  $\text{Al(OH)}_3$  remains uncharged and will precipitate, as in Equation 1-40. At a pH more alkaline than the isoelectric point net hydroxide will be absorbed, producing a negatively charged aluminium species and lowering the pH, as shown in Equation 1-41. The series  $\text{Al(OH)}^{2+}$ ,  $\text{Al(OH)}_2^+$ ,  $\text{Al(OH)}_3$ ,  $\text{Al(OH)}_4^-$  is produced by removal or addition of either  $\text{H}^+$  or  $\text{OH}^-$  in appropriate conditions. This hydrolysis series is represented

in Equation 1-42. At a pH more acidic than the isoelectric point, net protons are absorbed producing a more positively charged aluminium species and raising the pH.

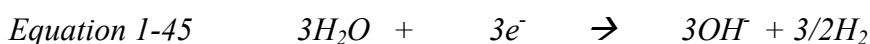
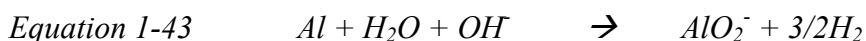


Ingress of oxygen from the atmosphere into the system is also possible, enabling more corrosion of aluminium according to Equation 1-36 followed by pH adjustment via Equation 1-42.

The extent of the pH adjusting reactions is controlled by equilibrium constants and will depend on pH. The solubility of aluminium species according to pH is significant at non-neutral pH (see Figure 1-5) and suggests the more extreme pH the greater the amount of Al(OH)<sub>3</sub> dissolved. Hence, the amount of OH<sup>-</sup> or H<sup>+</sup> consumed will be greater.

Other researchers have found that anomalously large hydrogen production, according to Equation 1-32, occurs in proportion to the anodic current density – the so-called negative difference effect (Drazic et al. 1997; Barteneva et al. 1999; Drazic et al. 1999a, 1999b). Hence, the total corrosion would exceed the faradic corrosion more at higher anodic current density. The negative difference effect also depends on chloride concentration, as a study using AD-1M aluminium alloy has shown (Barteneva et al. 1999), and is inhibited by indium in the alloy (Purenovic et al. 1976; Krasnobryzhii et al. 2004). Another mechanism for the pH modification has been expressed recently for the case of extremely alkaline electrolyte (Krasnobryzhii et al. 2004) and is shown in Equation 1-43 which is

based on the half-reactions Equation 1-44 and Equation 1-45. In this case  $\text{AlO}_2^-$  is used as an alternative representation to  $\text{Al}(\text{OH})_4^-$  (Krasnobryzhii et al. 2004).



While Equation 1-29 to Equation 1-42 explain the hydrolysis to single aluminium (mononuclear) monomers, the literature (Baes et al. 1976) also presents a consensus for the following sequence in which formation of dissolved mononuclear species is the first step: rapid and reversible formation of mononuclear hydrolysis products as in Equation 1-31 and Equation 1-42; small polynuclear species such as  $\text{Al}_2(\text{OH})_2^{4+}$  or  $\text{Al}_3(\text{OH})_4^{5+}$  are formed less rapidly from the mononuclear forms; large stable polymeric species, most notably  $\text{Al}_{13}\text{O}_4(\text{OH})_{24}^{7+}$ , are formed even more slowly.

The first solid phase to precipitate is probably an amorphous form that is meta-stable  $\text{Al}(\text{OH})_3$  or basic  $\text{AlCl}_3$  (Turner et al. 1970; Jiang et al. 2002). This converts slowly to the stable crystalline form by first-order kinetics with a half-life of 20 days (Smith et al. 1972) so long as the chloride ion concentration is not too high (Turner et al. 1970). Similar ageing by crystallisation is noticeable in commercial PFS (Jamieson, G. 2003, pers. comm., March 15<sup>th</sup>).

Alkalinity is clearly defined (Rounds et al. 2001):

*“Alkalinity is the acid neutralizing capacity of solutes in a water sample, reported in equivalents per litre (or milliequivalents or microequivalents per litre).*

*Alkalinity consists of the sum of titratable carbonate and noncarbonate chemical*

*species in a filtered water sample (filter membrane of 0.45- $\mu\text{m}$  pore size or smaller).”*

Aluminium floc formation requires a certain amount of available alkalinity to permit rapid hydrolysis (Jamieson, G. 2005, pers. comm., April). For example, adding an acidic flocculent to fluid of pH 8 with no buffering could cause the pH to drop below 6, not only limiting the flocculation but causing dissolution of the aluminium, whereas a buffered fluid at pH 8 will respond to the same dose more favourably. Recycling of aluminium coagulant is also possible (Kul'skii et al. 1989).

For water with sodium chloride-based conductivity in the range  $0.05 \text{ S m}^{-1}$  to  $0.1 \text{ S m}^{-1}$ , electroflocculation is achieved at a volumetric energy density of 2 to  $6 \text{ kWh m}^{-3}$  (Tiemann 2003) depending on contaminant concentration. Other researchers have reported that the amount of electrolytically produced aluminium flocculent required for good results with rendering plant effluent is less than direct chemical addition (Tetrault 2003).

Either aluminium or iron anodes are used as the source of flocculent. There a number of reports in the literature showing preferences for iron anodes and reporting good results (Tetrault 2003; Marconato 1998; Berg 1977; Fassina 1938). While rotating electrodes are commonly used in electrochemical studies it has been found that a rotating 6061 aluminium alloy anode does not corrode uniformly beyond a threshold oxide thickness (Gao et al. 2000). Electrochemical studies of the corrosion of aluminium have indicated several distinct corrosion mechanisms. Anodised aluminium in saline corrodes by forming pits, (Zhang et al. 2002), aluminium foil in hydrochloric acid solution permits transport of chloride ions through the oxide film via oxygen vacancies (Feng et al. 2001) and 6060 aluminium alloys undergo filiform corrosion if the copper fraction in the alloy is  $> 0.1\%$  (Stuckart et al. 1998).

### **1.6.3 Electroflotation versus dissolved air flotation**

The faradic production rate of hydrogen and oxygen gas from electrolysis of water is up to  $1.7 \times 10^{-7} \text{ m}^3 \text{ s}^{-1}$  per Ampere-cell. That is, for 10 A flowing through 10

cells in series, the gas production rate is  $1 \text{ L min}^{-1}$ . Mine waste or ore refining applications have been reported (Matis et al. 2002).

For combined electrocoagulation-flotation, where the gas production is partly replaced by anodic corrosion, current consumption and energy consumption between  $1 \text{ A (L min}^{-1})^{-1}$  to  $10 \text{ A (L min}^{-1})^{-1}$  and  $0.1 \text{ kWh m}^{-3}$  to  $2.5 \text{ kWh m}^{-3}$  respectively have been reported (Rogov et al. 1978).

#### **1.6.4 Electrosterilisation and electro-oxidation**

The space between close electrodes is a very harsh environment. The electric field is high and the gradient of pH from extremely acidic to extremely caustic occurs over a very short distance. Reactions at the electrodes surfaces have free radical intermediates and produce highly reactive forms of oxidising agents (Chou et al. 1995; Salama 2001). Even if the water does not entirely flow through the electrode space, the persistent disinfectants that are produced are highly effective in eliminating microbes. These persistent disinfectants include hypochlorite (Kasai et al. 2001), ozone (Demmerle 2002) and peroxide (Drogui, Rumeau et al. 2001). Specific systems with high current efficiency for  $\text{OH}^\cdot$  radical production have been reported (Troester et al. 2004). Mixed oxidant disinfection systems using electrolysis have better performance than simple gaseous chlorine addition (Herrington et al. 1997). Some researchers have claimed order of magnitude advantages (Wilk et al. 1987). Algae can provide a suitable habitat for bacteria and bio-films are a resilient multi-species structure (Lewis, G. 2003, pers. comm., June).

There has been a surge of activity in prevention of legionellosis by electrolysis recently. These efforts have included dissolution of toxic metals like silver (Khaydarov et al. 2004) to specific cooling-tower case studies (Forstmeier et al. 2005) to more general work in Japan (Kondo et al. 2003; Feng et al. 2004; Furuta et al. 2004; Nakajima et al. 2004; Tanaka et al. 2005). The recent action (2003 to 2004) of the New Zealand Police to prevent legionellosis at a South Auckland Police Station by dosing the entire water supply with silver is noted. Colloidal silver is generated commercially by electrolysis (Klein 2003).

While the form of an electro-oxidiser is similar to that of an electro-steriliser, the function is different because the types of impurities that are treated are oxidisable reducing agents and electrochemical reactions occur directly at the anode. Where particular species are to be selectively oxidised and others left intact, specific anode coatings should be used. For example a MnO<sub>2</sub> coating could enhance oxygen production by raising the over-potential for chlorine production (Bennett 1980).

### 1.6.5 Electrolytic production of hydrogen

This is an established industrial process (Vezev et al. 1902; Carrara 1918; Norsk Hydro 1928; Filippov et al. 1983; Kruger 2001). The key parameter is efficiency of production. As shown in Figure 1-6, derived from §1.5.4, §1.6.1 and Equation 1-7, at room temperature the efficiency of water electrolysis is simply the ratio of the equilibrium potential for electrolysis of water (1.229 V) divided by the actual cell voltage ( $V_{DC}$ ) as shown in Equation 1-46. Hence, there is a strong incentive to minimize the cell voltage.

$$\text{Equation 1-46} \quad \eta_{H_2/H_2O} = \frac{1.229}{V_{DC}}$$

A plot of this function is shown in Figure 1-6.

If the goal is to disinfect a fluid with both solutes and suspended solid, then all of the three effects, electroflotation, electroflocculation and electrosterilisation must be utilised. Because the flocculation and disinfection effects are most sensitive to contaminant concentration, it seems sensible to arrange the water flow so that the electroflotation is applied, followed by the flocculation, and finally the disinfection. However, the flocculation and flotation can work well in tandem because the very fine bubbles can attach to the floc particles as soon as they appear, and remain attached as the floc coalesces, causing a large proportion of the floc to float along with the suspended solid. This effect is temporary, as the



gas escapes into the atmosphere, leaving the floc to sink, but there is a window of at least a few minutes in which to collect the floated floc. Furthermore, the nucleation of fine bubbles is synergistic with nucleation points for the formation of floc (da Rosa and Rubio 2005).

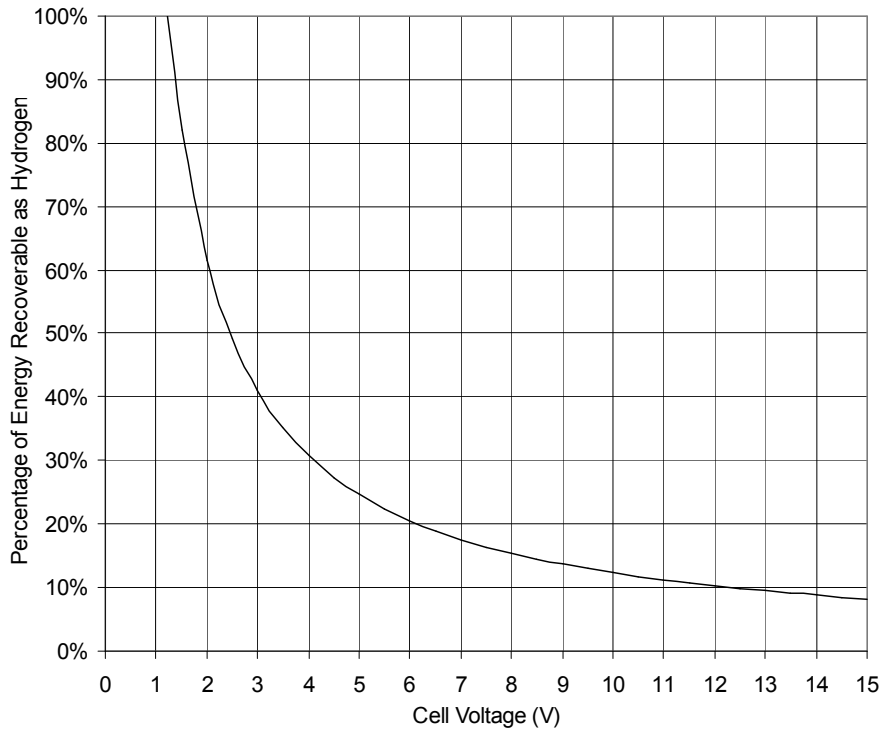


Figure 1-6 The fraction of energy recoverable as hydrogen from electrolysis of water.

### 1.6.6 Combined effects and limitation of combinations

A non-corroding anode specialised for gas production will not produce flocculent unless the source is in the water. Any disinfectant produced and consumed will detract from the oxygen production. A non-corroding anode specialised for disinfectant production will not produce flocculent either, unless the source is in the water. A corroding anode specialised for flocculation will release less oxygen than usual and the flotation gas will be mainly hydrogen.

Where it is possible to achieve complete treatment using only two of the three mechanisms, the only combination that is not possible with a single anode type is flocculation and disinfection. In order to obtain the full benefit of all three

mechanisms, it is necessary to use at least two cells in series or parallel and at least two different types of anode.

## **1.7 Hypothesis and research questions**

### **Hypothesis**

The central hypothesis motivating the proposed research was that electrochemistry provides unexplored opportunities to develop improved methods of water and wastewater treatment. The central research question was - under what circumstances can electrochemical water and wastewater treatment processes enhance or surpass the effectiveness of chemical treatment processes? Subsidiary research questions follow.

#### **1.7.1 Electro-flocculants**

In what cases are flocculants produced by corrosion of a metal anode in dilute electrolytes more effective than traditional chemical flocculants? Are they more effective because they lower the total amount of metal added, have a lower operating cost, have independent pH adjustment or have a lower residual metal content in the outflow?

#### **1.7.2 Overcoming low conductivity**

Is it possible to electrolytically purify water and wastewater economically even though it has much lower conductivity than standard electrolytes, as least as effectually as traditional techniques, through the application of various means to reduce the effective resistance of the electrolyte?

#### **1.7.3 Benign anodes**

Anodes that corrode either very slowly or corrode in a way that improves the quality of the water are defined as benign. How can an electrolytic purifier be configured so either that corrosion products are produced at a low rate thereby causing less harm than the existing contaminants, or configured to produce corrosion products that are flocculants which are removable?

#### **1.7.4 Recovery of by-products**

Are there by-products that can be extracted in sufficient quantity and concentration to offset the cost of electrolytic processing? How can these by-products be extracted at sufficient rate and concentration to be useful?

#### **1.7.5 Ability to configure function**

How can the basic functions of electroflocculation, electroflotation, electro-oxidation, electrowinning, pH-splitting and electrosterilisation be achieved independently or in combination by choosing appropriate electrode materials, arranging flows to take best advantage of the effects and applying control to the cell voltage or current? Does the direct electrical sensing and control of an electrolyser offer greater flexibility than adjustment of chemical dose?

#### **1.7.6 Turning waste into a resource at the point of production**

The standard method of treating effluents is to gather them together and treat them in a central facility. This certainly offers economy of scale but the different impurities require different forms of treatment and some minor components will antagonise removal of the majority. For example heavy metals will contaminate a biological oxidation process. Conversely, there will be valuable impurities (perhaps the very same heavy metals) in a fluid stream that could be recovered more easily if they were extracted before being diluted in an aggregated wastewater flow.

How can specialised small-scale electrolytic waste-water treatment process at the point of production be configured to extract useable resources before they enter an aggregated waste stream?

## **2 Materials and methods**

### **2.1 Experimental philosophy**

#### **2.1.1 Selection of methods for experiments**

The aim of this project was to develop sufficient understanding of electrochemical water purification for designing systems for industrial sites. Field trials were invaluable for garnering information about the usefulness of processors. However, understanding of the basic mechanisms of successful treatment remained elusive in the field, so laboratory experiments were designed to simulate the essential features of the functional field systems.

#### **2.1.2 Selection of case studies**

The case studies were influenced by water and wastewater treatment requirements in Australasia. Interactions with clients and potential clients of Works Filter Systems Limited clarified the problems that had to be solved. By attempting to solve the problems directly in the field, the appropriate context of literature searches and laboratory studies was established.

#### **2.1.3 Selection of methods for controlled laboratory conditions**

A typical cycle of discovery and confirmation was: discover that a processing technique worked in the field; perform laboratory experiments to increase the reliability of the processor and clarify the mechanism of the technique; declare and test possible improvements in function and understanding of the processing technique. The laboratory work was directed toward using the largest possible models of the field equipment to simulate real behaviour as closely as possible.

### **2.2 The essential parts of an electrolytic water processor**

#### **2.2.1 Electrodes**

The choice of electrode materials greatly influences the capital cost and functionality of the electrolyser. The cathode is not prone to corrosion, so stainless

steel is sufficient in most cases. A stainless steel cathode is recommended where there is significant magnesium or calcium in the water (Kul'skii et al. 1978). Stainless steel is also hard enough that it could be re-polished if necessary. Titanium also makes a good cathode - it is even harder than steel, though more expensive.

For a corroding anode, the cheapest relatively pure aluminium or iron is ideal. There is no advantage in using a harder grade alloy unless it is particularly cheap, as the main additives such as magnesium and copper for aluminium, and chromium and nickel for steel, will undoubtedly be added to the water, though in trace amounts. This is described for iron based materials in Table 2-1 and for 6060 aluminium in Table 4-1.

Mild steel is the most convenient source of iron. However, even this has a number of troublesome impurities. Cast or pig irons are purer sources. The anode material is more difficult to choose if corrosion resistance is required. 316 stainless steel has a large proportion of toxic metals that will leach out as part of the corrosion process as shown in Table 2-1 (MatWeb 1996). However, the corrosion rate of iron alloys is reduced by lowering the current density. Alternatively it is possible to offset the anodic acidity by using high pH fluid, which also lowers the equilibrium potential for production of oxygen.

*Table 2-1 Percentages of additives in ferrous metals (MatWeb 1996).*

Material%	C	Mn	P	S	Si	Al	Cr	Ni	Mo	Slag
Pig iron	0.02		0.02	0.108	0.12					0.07
Mild steel	0.06	0.20	0.03	0.02	0.04	0.08				
	max.	to	max.	max.	max.	max.				
		0.30								
316 stainless steel	0.08	2.00			0.75		17	12	2.5	
Material%	C	Mn	P	S	Si	Al	Cr	Ni	Mo	Slag

Table 2-2 Comparison of some anode material components.

	Platinum (1)	Iridium (2)	316 Stainless Steel plate (3)	Titanium plate (4)	Carbon (5)
Price USD kg <sup>-1</sup> (Jan 2006)	32000	6000	4.5	100	4
Corrosion Resistance	Excellent	Excellent	Moderate	Good	Poor

Sources for Table 2-2:

1. Kitco Bullion Dealers 2006.
2. Tax Free Gold 2006.
3. MEPS International 2006.
4. Alpha Knife Supply 2004.
5. Tokai Carbon Co. 2005.

More exotic anode materials are not economic. Ti is highly resistant to bulk corrosion because it forms an oxide layer (Rembar 2005). Unfortunately, the oxide layer has a very high electrical resistivity ( $10^{11}$  to  $10^{16}$   $\Omega$  m) and a breakdown field of 4 to 8 MV m<sup>-1</sup> (MatWeb 1996). So even a 1  $\mu$ m thick coating will require 6 V to initiate conduction. The well-accepted industry standard anode for brine electrolysis is the dimensionally stable anode DSA®, which refers to an anode coated with mixed oxides of ruthenium, iridium and titanium. This anode coating favours chlorine production (Millet et al. 1993). Pt is a standard anode in laboratory situations. However, this is an expensive option. Other coatings are of some interest, though they tend to crack and degrade rapidly. In particular, MnO<sub>2</sub> coatings suppress chlorine production by raising the anodic over-potential for chlorine production (Bennett 1980). Another industrially accepted anode material is carbon, but this also suffers from gradual oxidation.

## 2.2.2 Electrolyte and compartments

The space between the electrodes must be electrically conductive, though to ions rather than electrons, and is therefore defined as an electrolyte. In the context of this research, the electrolyte is simply the fluid to be treated. If a membrane is placed between an electrode pair (see §2.2.3), the electrolyte is separated into two compartments – anolyte and catholyte. This means that fluids of different composition can pass in, through or out of either compartment.

The conductivity of the fluids to be treated is generally low by the standard of industrial electrolysis. The conductivities of typical electrolytes are shown in Table 2-3. Nafion® also doubles as a separating membrane.

Table 2-3 Conductivity ( $S m^{-1}$ ) of electrolytes (*italic*) and typical fluids for purification.

6.6 M KOH (1)	Nafion® solid polymer in acid (2)	Conc. NaCl Brine (3)	Sea water (4)	Municipal wastewater terminal effluent (5)	Tannery effluent (6)	Ground water (7)	Pulp mill effluent (8)
100	10	23	5 to 6	0.01 to 0.05	1 to 2	0.01 to 5	0.1

Sources for Table 2-3:

1. Vennekens et al. 2001.
2. Mazur et al. 2005.
3. Calder 2003.
4. Direct measurement of seawater sampled from Raglan harbour, New Zealand.
5. Direct measurement of Hamilton City Council terminal effluent wastewater.
6. Direct measurement at a tannery in the Waikato, New Zealand.
7. Minerals Council of Australia 2005.
8. Direct measurement of alkaline effluent from a New Zealand kraft process pulp mill, New Zealand.

## 2.2.3 Separating membranes

To prevent contact between close opposing electrodes and allow separation of the anolyte and catholyte, a separating membrane should be used. For dilute

electrolytes reducing the gap between the electrodes to an absolute minimum, while still enabling gas release, is crucial, as shown in Equation 1-10 and Figure 1-3. In this context a separating membrane must be very thin. While Nafion® (DuPont 2005) and other ionic polymers are well known as combined solid electrolytes and thin sheet membranes, they are proprietary and expensive. They also have particular bathing fluid requirements, having much higher conductivity in highly acidic fluids. Hence, cheaper alternatives were considered first – see §2.3.3.

#### **2.2.4 Electrical components**

The power supplies described in §2.6.1 were connected to the electrolyser by the shortest possible insulated cables with appropriate current ratings, terminated with bolt-on crimp-lugs.

Currents were switched using an N-channel TMOS E-FET Device STP60NF06, labelled SEC SSP60N06, catalogue number Z1853 at Dick Smith Ltd. This was known as the MOSFET (Chipcatalog 2005).

#### **2.2.5 Flow control**

The inflow to a processor was controlled by a manual valve with continuously variable constriction. In some cases, the outflow was re-directed by a range of valves. There was a fail-safe overflow to drain in all cases.

### **2.3 Materials for electrolytic processing**

#### **2.3.1 Using the fluid to be treated as an electrolyte**

While it would have been technically feasible to construct an electrolyser that operated efficiently using highly conductive concentrated electrolytes and delivered the products to the fluid to be treated, there were compelling reasons for using the product to be treated as an electrolyte: a separate electrolyte would be consumable; gas bubbles and disinfectants are more effective when small or particularly fresh respectively; in cases where the fluid contaminant is to be



directly electrochemically modified, it must pass close to an electrode to be treated.

Hence, the difficulties of working with low conductivity electrolytes were accepted. Real effluents were left unmodified where possible. Synthetic effluents were made with similar conductivities to real effluents. Properties are shown in Table 2-4.

Table 2-4 Properties for fluids to be treated (see Table 2-3 and Table 4-7).

	Conductivity (S m <sup>-1</sup> )	Chemical/ biochemical oxygen demand (COD/BOD) (mg L <sup>-1</sup> )	Total Suspend ed Solids (TSS) (mg L <sup>-1</sup> )	Coliform count (CC), as colony forming units (cfu/100 mL)	Other
HTE	0.01 to 0.05	<5/<5	10 to 20	100000	
Tannery Effluent	1 to 2	100 to 1000	1000 to 2000	<10 to 1000000	Cr <sup>3+</sup> at about 20 mg L <sup>-1</sup>
Municipal Leachate	0.1 to 1	10 to 100	<10	Variable but often low.	Many toxic solutes
Cooling Tower fluid	0.03 to 0.1	100	<100	Variable, but often < 100	Could have <i>Legionella</i> <i>sp.</i> bloom
Waikato Bore Water	0.02 to 0.1	<1/<1	<1	<1	Fe <sup>2+</sup> up to 30 mg L <sup>-1</sup>

### Hamilton City Council waste water treatment plant terminal effluent (HTE)

HTE is the result of treatment of Hamilton City's municipal wastewater. The conductivity varies from 0.05 S m<sup>-1</sup> to 0.01 S m<sup>-1</sup> depending on the amount of storm-water ingress to the process inflow. It is a relatively pure wastewater, which

is discharged to the river after tertiary UV disinfection. Other characteristics are given in Table 2-3 and Table 2-4.

Since the average flow of around  $50000 \text{ m}^3 \text{ day}^{-1}$  requires an energy input to the UV treatment in the order of 100 kW, there is some scope for a process that requires less than  $0.05 \text{ kWh m}^{-3}$  to replace or assist the UV disinfection, particularly if there are additional treatment benefits. The final treatment before disinfection is up-flow clarification, whereby suspended solids are settled passively by gravity, so the terminal effluent tends to contain suspended solids that are either extremely fine or of similar or lower density to water. Hence, a subsequent flotation step, prior to disinfection, would target the remaining contaminants. This includes algal colonies and animals which are opaque and hence hinder UV treatment. Flocculation would assist in converting the significant fine colloidal fraction of the suspended solids into filterable material. Combining flocculation with flotation, as is possible in electrolytic processing, is advantageous. Otherwise additional filtration or settling steps are required. Electrochemical sterilisation of low conductivity water with significant organic content is liable to be energy intensive, especially as the current density has to be high to achieve significant current efficiency for production of disinfectants or the cell voltage must be high to achieve electric field-dependent effects – in either case the energy recovery by hydrogen is limited. HTE was sampled from a point before UV treatment and was therefore clarified effluent, not the disinfected (tertiary treated) effluent.

### **2.3.2 Electrode materials**

Many of the case studies in this project that required a non-corroding anode used stainless steel electrodes (both anode and cathode) that were operated at low current density to minimise corrosion. These electrodes were easy to fabricate and form into test modules.

Attempts were made to form non-corroding anodes by partial reduction at high temperature of monolithic  $\text{TiO}_2$  to the Magnéli series  $\text{Ti}_n\text{O}_{2n-1}$ , particularly  $\text{Ti}_4\text{O}_7$  in 5% hydrogen in  $\text{N}_2$  mixture. The challenge in this case is to reduce the  $\text{TiO}_2$  without forming nitrides. The greatest reductions achieved were to  $\text{Ti}_8\text{O}_{15}$  (a dark blue material) at  $1190 \text{ }^\circ\text{C}$  and the best bulk material created was similar in

composition to  $\text{Ti}_{20}\text{O}_{39}$ . Even these materials offered good conductivity, within 2 orders of magnitude of graphite. While none of the created materials were used in electrolyzers, further work in material development is strongly recommended. Non-porous forms offer the most promise because they would resist ingress of water to the electrical connections (Clarke, R. 2004, pers. comm., 3<sup>rd</sup> December).

### **2.3.3 Separating membranes**

In many cases, separating membranes were not used because they added no advantage. However, where pH modification was required, a membrane was very useful.

Uncoated parka nylon is used to make clothing that is windproof but not waterproof. While not previously known as useful material for industrial electrochemistry, at \$4 m<sup>-2</sup> it is one of the cheapest commercially available membranes. The parka nylon used in this project had a density of 52 g m<sup>-2</sup> and 8 threads per millimeter with an open area fraction of 0.4. The very fine pores allow passage of ionic current while resisting, though not preventing, bulk flow. At 0.1 mm thick it allows construction of large area electrodes with sub-mm gaps, although with reduced effective area for conduction. If the membrane is sandwiched between the electrodes, filling the gap, the electrodes must have gas venting features.

### **2.3.4 Synthetic fluids**

Synthetic fluids and flocculating agents were made using the following chemicals:

Polyaluminium chloride (10.05%  $\text{Al}_2\text{O}_3$ ) sourced from HamChem, New Zealand.

NaCl pharmaceutical grade.

CAS 7647-14-5 sourced from Dominion Salt, New Zealand.

NaCl Grade 23 Solar Salt. Sourced from Dominion Salt, New Zealand.

HCl, Univar AR 36%.

NaOH, Applichem 99%, Maximum 1% carbonate.

Albumin Sigma Grade 11 Ovalbumin crude powder No. A-5253.

$\text{Cr}_2(\text{SO}_4)_3 \cdot 15\text{H}_2\text{O}$  LR >96%.

$\text{AlCl}_3 \cdot 6\text{H}_2\text{O}$  BDH LR 96%.

One-tonne prices for flocculants were used in cost comparisons.

### **2.3.5 Catholyte modification**

Pharmaceutical Grade NaCl and tap water were used to make up concentrated brine stock solution. The pH of the stock was modified by addition of concentrated HCl or concentrated NaOH.

### **2.3.6 Chemical flocculants and coagulants for comparison**

Several chemical flocculants were used to compare their function with that of the electro-flocculator. PAC23 (polyaluminium chlorohydrate) is a form of polyaluminium chloride that is normally used in final stage purification of water where only small amount of suspended solid has to be removed (Leitzau 2004a). PACl is a polyaluminium chloride that is used as a general purpose flocculent (Leitzau 2004b). PFS is polyferric sulphate, a flocculent that is highly effective over the wide range of pH encountered in wastewater applications (Leitzau 2004c). All of the flocculants listed above are sold to end users in a concentrated form, partly hydrolysed, but still low in pH so that they do not complete hydrolysis and flocculate in storage. They have to be mixed rapidly into the water they are to treat so that the floc particles that form are still small when mixing is complete. Further slower stirring allows sweep flocculation of suspended solid to occur (Jamieson, G. 2003, pers. comm., March). This mixing regime was as achieved consistently by a jar stirrer (see §2.6.3).

While PFS treatment leaves lower residual metal levels in the water than aluminium based flocculants, it causes a distinct rusty discolouration of the water, especially if incorrectly dosed, which discourages its use in drinking water

applications. However, it is generally considered to be better at removal of very fine suspended solid or dissolved materials than aluminium flocculants (Jamieson, G. 2003, pers. comm., March).

## **2.4 Post-processing**

### **2.4.1 Acidification**

In order to dissolve floc but not metal fragments prior to total hydrated metal analysis, acidification was limited to drop-wise addition of sufficient concentrated hydrochloric acid to visibly dissolve any floc and colloid without altering the dilution significantly.

### **2.4.2 Settling and stirring**

Settling was achieved by leaving sealed samples motionless for between 24 hours and 96 hours. Stirring was achieved by tumbling and shaking sealed samples. Ultra-sonication was by placing sealed samples in the University of Waikato Chemistry Department ultra-sonicator for 90 minutes.

## **2.5 General measurement methods and instruments**

### **2.5.1 Conductivity**

For the crucial parameter of electrical conductivity, a conductivity meter built by Auckland University Chemistry Department #AG24997, with cell of  $K = 1.38 \text{ cm}^{-1}$ , was used. This instrument gave results that were reproducible within 1%. For indicative measurements, even moving fluids could be probed, though the measurements tended to be elevated by up to 20%. The fluid to be probed had to be galvanically isolated from other electrical circuitry – otherwise leakage currents could distort the readings grossly. For best accuracy, samples of at least 50 mL were removed from flowing or electrified bodies of water and allowed to settle in plastic or glass containers for 10 s with the rinsed probe in place. Where possible the least attenuation factor of the signal was used, where the choices were 1, 10 and 100 and the maximum display reading was 2000. The display reading was multiplied by the attenuation factor and  $K$  to give a measurement in  $\mu\text{S}\cdot\text{cm}^{-1}$ .

### **2.5.2 Turbidity**

A portable turbidimeter (Hach 2100P turbidimeter, model 46-500) set to auto-scale, reading in nephelometric turbidity units (NTU) was used. Calibration to standards in the range of < 0.1 NTU up to 800 NTU was provided by the Hamilton City Council wastewater treatment laboratory.

### **2.5.3 Trace element analysis**

GBC Integra XL ICP-OES for elemental trace analysis in fluids by Inductively Coupled Plasma – Optical Emission Spectroscopy. This device is able to analyse for multiple elements in an aqueous solution sequentially, using less than 10 mL of sample per element. The methods were software configured and could be tailored to achieve optimal sensitivity for a combination of elements. The larger the number of elements present in the sample, the more difficult it was to find combinations of resonant peaks that did not interfere with each other. For example, the most sensitive peak for aluminium could only be used if the sample was known to be free of iron. Some of the method configurations for low levels (below 1 mg.L<sup>-1</sup>) of aluminium and chromium are shown in Appendix A.

### **2.5.4 pH measurement**

For pH measurements in the laboratory the Radiometer Copenhagen MeterLab PHM290 and PHM240 instruments were used. These instruments use twin probes: a pH sensitive glass electrode and a saturated-KCl reference electrode. The instruments were calibrated regularly.

### **2.5.5 Particle sizing**

The Malvern Instruments laser particle sizer, model MasterSizer 2000S was used for particle sizing.

### **2.5.6 Electrical measurements**

The following instruments were used for electrical measurements:

- Hewlett Packard 3468B Voltmeter (laboratory use).

- Fluke 337 Voltmeter with 2 kHz bandwidth (both field and laboratory).
- Fluke 337 Ammeter clamp-meter with 2 kHz bandwidth (both field and laboratory).
- Tektronix TDS720 digital sampling oscilloscope with greater than 1 MHz bandwidth (laboratory use).

### **The four-wire method of measuring cell voltage when passing heavy current**

Cell voltages were measured at dry contacts by the four-wire method, shown in Figure 2-1. The principle is to remove as much of the lead and contact voltages as possible from the measurement by connecting the voltage probes within the entry and exit points of current to the test circuit. This meant attaching high-impedance voltmeter probes on dry electrode metal, within any welded, fastened or draped power contacts.

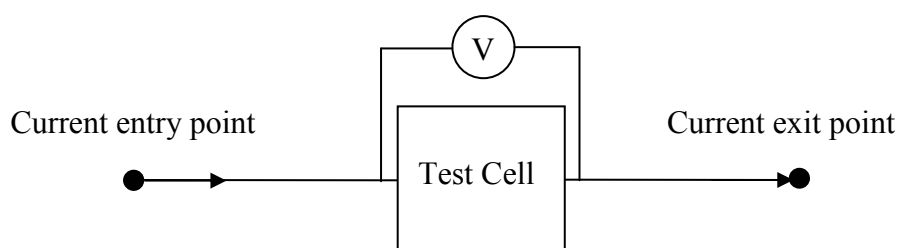


*Figure 2-1 The four-wire method of voltage measurement as applied to an entire electrochemical cell.*

Because the voltage drop across the dilute electrolytes that were used dominated the overall cell voltage, measurement of half-cell voltages or over-voltages was not attempted. Hence, no three-terminal measurements were made, nor were any potentiostatic experiments carried out. While this prevented resolution of the different effects on either the anode or cathode voltages due to changing experimental conditions, the focus for this project was minimisation of total cell voltage to achieve the best efficiency. Furthermore, the coarse nature of the fluids under test, especially in the field, made use of fine and delicate instrumentation impossible. Other researchers have carried out extensive potentiostatic studies (DiBari 1970; Buso et al. 2000; Rios et al. 2005).

### **2.5.7 Automated measurements**

The ISCO Autosampler model 6700 with a YSI Sonde probe automatically measured pH, dissolved oxygen, conductivity and temperature and delivered them to a PC using ISCO Flowlink software. The pH and conductivity measurements were calibrated to values reported by finer instruments. The temperature measurement was accurate to within 1 °C. While the best feature of the instrument was the short sample period, which could track sudden changes caused by step changes in conditions, the pH meter had a response time in the order of 10 minutes which meant that realistic measurements in the course of step changes could only be made by taking frequent manual samples at accurately known times.

### **2.5.8 Software for modeling, data recording and presentation**

Microsoft Excel®, the CVT100 terminal emulator and MathCAD were used.

### **2.5.9 Microbiological counts**

Coliform count is the most common method of measuring the level of microbial contamination of water. Most probable numbers (MPN) of coliforms were calculated by sampling, making multiple dilutions, culturing the different dilutions and counting colonies according to standard procedures. Both Total Coliforms (MPN/100 mL) and the subset *Escherichia coli* (MPN/100 mL) were usually estimated for samples. These procedures were carried out by laboratories with ISO 9001 certification, namely Hill Laboratories, Alpha Scientific (now known as e-Lab), and the Hamilton City Wastewater Treatment Plant Laboratory, all in Hamilton.

*Legionella pneumoniae* is a human pathogenic form of the Legionella family, infamous for its association with outbreaks for Legionnaires disease. Trials of electrolytic disinfection of live cultures of this pathogen were carried out in secure facilities at WaterCare Services Laboratory in Auckland. WaterCare Services Laboratory staff subsequently carried out enumeration tests according to their standard procedures.

Bacteriophage-viruses and enteric bacteria were cultured and enumerated by Auckland University's School of Biological Sciences.



### **2.5.10 Dissolved oxygen**

The University of Waikato Chemistry Department dissolved oxygen meter, Mettler Toledo MO128 and the Materials and Process Engineering Department dissolved oxygen meter Cyberscan 100 (University of Waikato inventory number 5256) were used.

### **2.5.11 Residual chlorine**

Measurements were based on immediate titration with ferrous ammonium sulphate reagent in conjunction with sharp transition DPD1, both supplied by HamChem of Hamilton, New Zealand. Measurement of  $0.1 \text{ mg L}^{-1}$  to  $5 \text{ mg L}^{-1}$  was possible with  $\pm 0.05 \text{ mg L}^{-1}$  accuracy.

## **2.6 General equipment and techniques**

### **2.6.1 Power supplies**

- 3.3 V 20 A switch-mode power supply (SMPS) model JWS100-3A (Innovative Energies 2004) with  $< 1\%$  voltage ripple.
- Continuously adjustable full-wave rectifier comprised of an earth-leakage protected 230 V single phase supply, a 4 A variac supplied by the Physics Department of Waikato University, a step-down transformer, and four 50 A bridge-rectifier modules in parallel on a car stereo heatsink. The output was fed to the electrolyser through 80 A cable, and protected from short-circuit by a 100 A high rupture current (HRC) fuse. This power supply could operate continuously at 0 V to 25 V full wave rectified RMS at 0 A to 50 A RMS, and supply up to 60 A for a few minutes at up to 10 V, limited by rectifier heatsinking. This supply was known as the “50 A rectified supply”. The peak voltage of this supply was approximately 1.5 times the RMS value, and the 100 Hz harmonic component was significant. The continuous variability enabled fine control of the current delivery during experimental work. Two 180000  $\mu\text{F}$  capacitors, also supplied by the University of Waikato Physics Department, were available to test the

effect of smoothing of the rectified waveform. When applied in parallel the total capacitance of 0.36 F reduced the voltage ripple to less than 1.5 V for the rated current.

- Dick Smith 3.5 V to 15 V, 0 A to 20 A, voltage source power supply, model D3800. Minimum load resistance of 0.5  $\Omega$ .
- Trio Power Supply 0 V to 35 V, 0 A to 20 A, model PD35-20, configurable as either a voltage source or a current source and able to drive constant current into a short circuit.

### **2.6.2 Filters**

The effectiveness of Works Filter Systems' proprietary filtration system, Porous Ceramic Dual Media (PCDM), in removing suspended solids, including well-formed floc from a liquid flow, is well established (Hill et al. 1991; Langdon, A. G. et al. 1995). PCDM uses both modified pumice and sand filter media over a nozzle composed of a titanomagnetite-glass composite (Langdon, A. et al. 1995).

In this context, PCDM filters and their derivatives were used as reliable indicators of the relative effectiveness of flocculation induced by electrolytic processing and comparative methods. Flow speeds of between 0.5 m s<sup>-1</sup> and 20 m s<sup>-1</sup> and different grades of media were used to check the quality of the flocculation. In some practical applications, entire capture of the suspended solid is not required because partial removal may meet discharge requirements. Furthermore, disposal of the large quantities of extracted solids is problematic.

In order to determine the level of dissolved substances, an arbitrary definition of soluble was assumed to be the part that could pass through a Sartorius Minisart 0.45  $\mu\text{m}$  single use filter unit, part number 16555. This was a repeatable method, particularly helpful when measuring differences between unsettled metal floc, colloidal suspensions of metals and dissolved metals. In combination with acidification it was used for preparation of ICP-OES samples.

### **2.6.3 Jar stirrer**

The dosing method for chemical flocculent (see §2.3.6) was standardised by using a Boltac Industries JarStar jar tester with a square cross-section 1 L vessel, usually set for 10 s pre-stirring at 100 rpm, then dose injection followed by 30 s at 250 rpm, then 3 minutes at 100 rpm, followed by a known settling time without further disturbance.

### **2.6.4 Presentation of multiple graphs and traces in a single figure**

Multiple graphs in a figure are presented with a common independent variable axis and several dependent axes. Common dependent variable groupings were flow rate and pH, cell current and cell voltage, and metal concentrations. The different graphs are referred to by graph number from the top of the figure. Individual traces are referred to by trace name from the legend for that graph. For example, the Inflow pH in the top graph would be referred to as the inflow pH trace in graph 1.

## **3 Development of bipolar stack processors**

### **3.1 Introduction**

The advantages of series stacks of bipolar cells include lower power supply current, less electrical interconnection and more compact hardware. Hence they were considered a good form to use as a base for development of working systems.

The terminal effluent at Hamilton City Council's wastewater treatment plant was used to test different models. The inflow sampling point was after the secondary clarifier, but before the tertiary UV treatment. The water had conductivity of  $0.05 \text{ S m}^{-1}$  with diurnal and seasonal variability of 50%, turbidity between 5 NTU and 10 NTU, and coliform counts of  $10^5$  per 100 ml. Hence, it was a good fluid for testing both physical and biological effects, available at about  $50000 \text{ m}^3 \text{ day}^{-1}$ .

### **3.2 Stages of development**

#### **3.2.1 Starting point - Model 0: jubilee clips on porous ceramic**

At the time the doctoral project commenced, Works Filter Systems had trialed water processors incorporating an electrolytic function into titano-magnetite/glass composite ceramic (TMGCC) filter. By attaching two or more stainless steel jubilee clips to the outside of a tube and making power supply connections to the clips, a device that could simultaneously filter and sterilise waste water had been made. Typical operation was with a full wave rectified mains voltage of  $215 \text{ V}_{\text{RMS}}$ . A schematic is shown in Figure 3-1. This system was the starting point for development of other processors.

The role of the TMGCC component in the electrolyser was intended to be that of a conductor or electrolyte. However, the material was found to be a weakly conducting dielectric, with a breakdown field of  $10^6 \text{ V m}^{-1}$ . This was because the insulating silicate fraction coated the metal oxide particles during the heat treatment phase of production.

The dielectric properties of TMGCC could be exploited by using high voltage alternating current connections, perhaps of higher frequency than the usual mains, in order to apply rapidly changing electromagnetic fields to the water as it passes through the TMGCC. However, this would be a high-voltage low-current method that is not predominantly electrolytic in effect, nor likely to result in efficient recovery of the energy input as hydrogen.

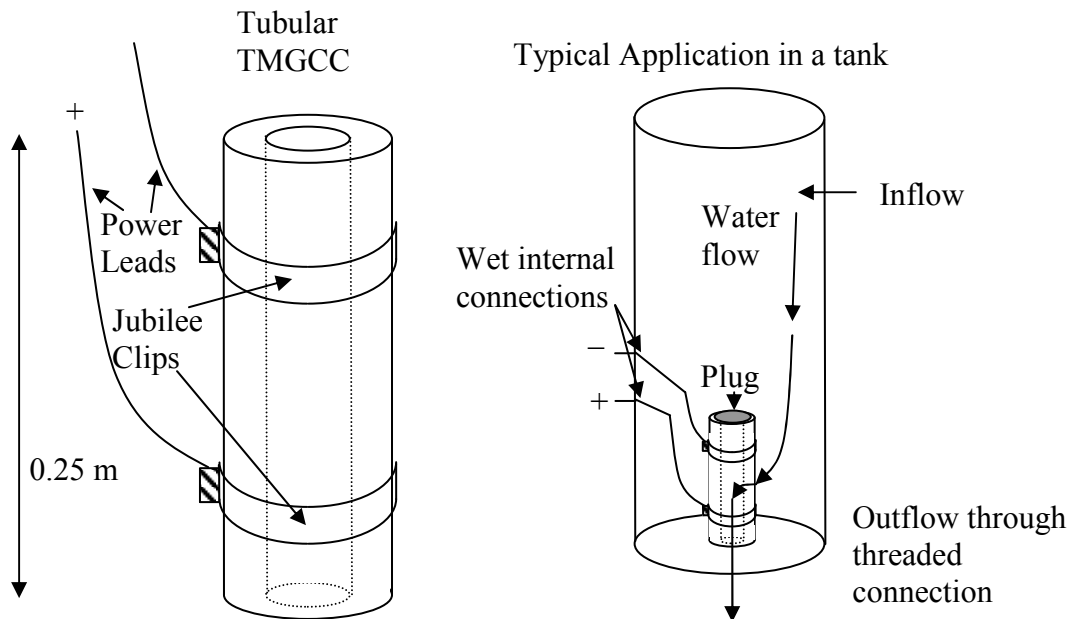


Figure 3-1 Tubular TMGCC as an electrolytic filter (left) and a typical application (right).

### 3.2.2 Narrowed gap, increased area, lower voltage

The conductivity of fluids likely to be treated electrolytically is low and so taking note of Equation 1-8 is important. For this reason, the first attempted improvement was to bring the jubilee clips closer together so that the current path through dilute electrolyte was shortened. The most obvious change was that the current increased for a given supply voltage. This could be taken to the point where the edges of the clips were almost touching and the voltage had to be lowered to prevent the supply from going above its current capability. By this means, the cell voltage for adequate treatment was reduced from the initial 215 V to 42 V. 42 V is the new standard for automotive batteries (Society of Automotive Engineering 2005) so this may become a standard for portable power supplies much as 12 V is at present.

As the current density was increased, the problem of anodic corrosion became visible. This also applied to all wet connections especially where dissimilar metals were in contact.

The intention of electrolysing water at the inflow side of the TMGCC was to capture electro-generated floc in the filter. However, the sharp treatment-level threshold for flocculation meant that either very little floc was produced, or a strong floc that could be filtered using a coarser filter was produced. The TMGCC was such a fine filter that it could capture very small particles. In order to remove as much suspended solid from the fluid prior to attempting sterilisation the flow direction was reversed so that the filtered water was electrolysed. Each TMGCC filter could pass 3 m<sup>3</sup> of terminal effluent before requiring back-flushing.

### **3.2.3 Optimisation for hydrogen production or sterilisation**

The lower the cell voltage, the more efficient the production of hydrogen. However, lowering the cell voltage will de-emphasise other reactions that are more important to the disinfection capability of the electrolyser. That is, the current fraction for production of chlorine derived compounds or other microbial poisons will be reduced at lower cell voltages. So a decisive point in the optimisation process was reached - either minimum energy for hydrogen production or minimum energy for sterilisation. By retaining just two external connections but placing additional jubilee clips along the barrel of the filter, it was possible to construct bipolar stacks of cells, where the number of cells was one less than the number of conductors attached (shown for two cells in series in Figure 3-2a). Hence, the voltage per cell was lower than for a single cell with the same supply voltage and the faradic effects were to be multiplied by the number of cells. Normally bipolar cell stacks are sealed to prevent leakage currents (Pletcher et al. 1990) but because the fluid bathing the cells was so poorly conductive, so long as the clips were wider than the gaps between them, the electrical leakage current was expected to be small. That is, the majority of the current was expected to pass through all the cells in series. A lower voltage per cell or higher gap width to conductor width ratio will reduce the effective Ampere-cells of a bipolar series by increasing the fraction of the current that bypasses at least one of the cells in the series stack.

Figure 3-2b shows the greater complexity of possible leakages about four cells in series. A notation that numbers the electrodes cells in ascending order from the most positive voltage to the lowest voltage is used. Leakage currents are named by the electrodes at which they start and end. For example, in a four cell, five conductor stack,  $E_1$  is the most positive electrode and  $I_{L14}$  starts at the most positive anode and ends at the lowest voltage cathode. Series cell currents are denoted by just the anode number at which they originate, for example  $I_{S1}$  is the current leaving the most positive anode and entering the most positive cathode. If the number of cells in a stack is even, there is a central electrode that will be at approximately half the potential of the external positive connection. If odd, there will be two electrodes physically and electrically straddling the mid-point. Because the leakage currents leaving an electrode are greater than those entering for all electrodes on the positive side of the mid-point, and vice-versa on the negative side of the mid-point, the amount of series cell current decreases monotonically toward the centre of the stack.

The level of electrical leakage was modelled, for the simple case of two cells in series, with 0.01 m wide conductive bands like jubilee clips. Figure 3-3 shows the Ampere-cell factor, where 2 would be the ideal for two cells passing all the current in series and 1 is the worst case if all the current bypasses the central electrode, as a function of the gap width. Electrode over-potentials per cell were assumed constant, limiting the range of prediction. Assumed conditions:  $0.1 \text{ S m}^{-1}$  conductivity; 0.01 m conductor thicknesses; reversible cell potential of 2 V and constant over-potential of 1 V per cell. For example, an Ampere-cell factor of 1.5 out of a possible 2 in a two cell stack indicates that half the current is leaking around the central electrode; the Ampere-cell factor has two additive components (in this case, two cells in series by half the total current, plus one outer cell in parallel by half the current:  $2 \times \frac{1}{2} + 1 \times \frac{1}{2} = 1.5$ ). The modeling was corroborated by the observation of greater rates of both bubble production and corrosion on the most positive anode of a bipolar series compared to the inner electrode surfaces.

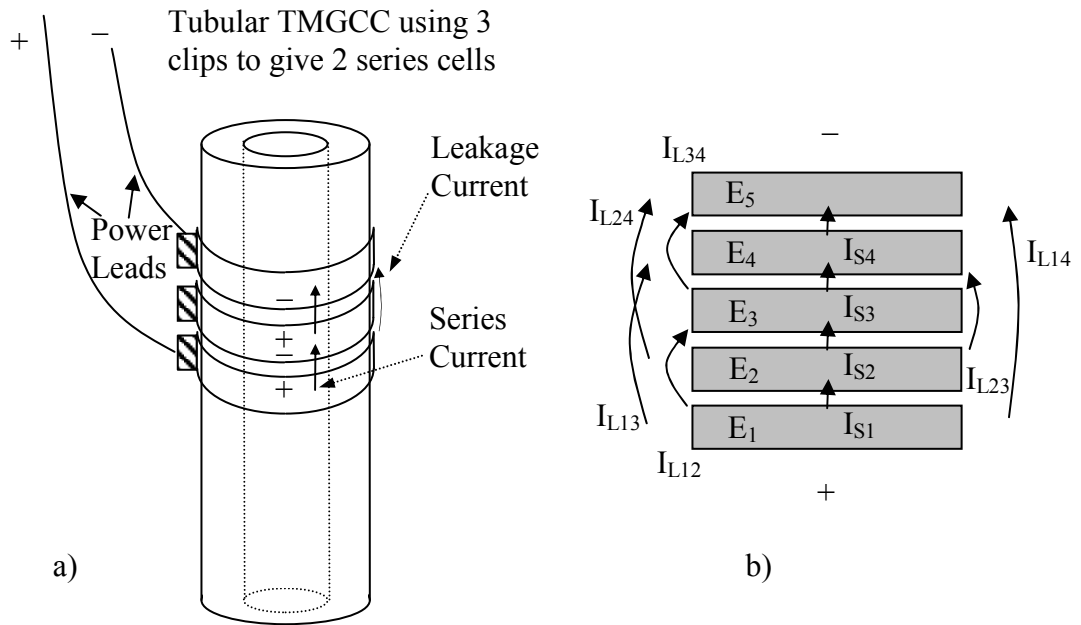


Figure 3-2 Left: Two cells in series on a TMGCC with a central bipolar electrode and two terminal unipolar electrodes (endplates). Right: notation for leakages, series current and total current in a four-cell stack.

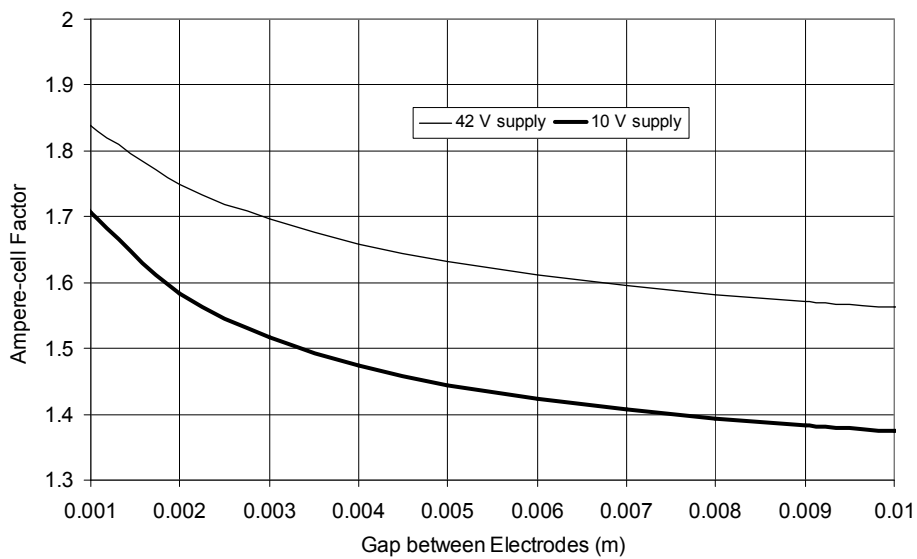


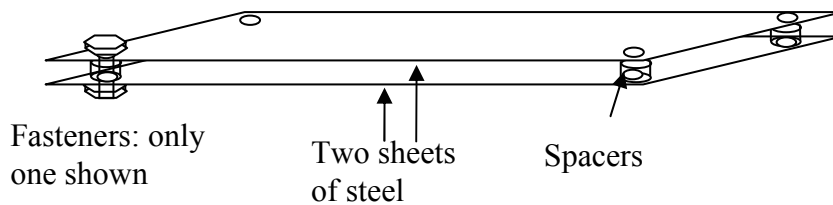
Figure 3-3 Modeled 2-series-cell response to changes in gap between the electrodes: how decreasing the gap between stainless steel electrodes in a bipolar stack bathed in dilute electrolyte can reduce leakage current.

Figure 3-3 shows that in order to achieve an Ampere-cell factor of greater than 1.7 at less than 5 V per cell in a 2-cell series stack, for the practical lower limit of 0.001 m gaps, the effective electrode thickness should be greater than 0.01 m.



### 3.2.4 Model 1: stainless steel plates single cell

In order to increase the active surface area to total volume ratio, the edges of jubilee clips were swapped for flat plates of 316 stainless steel. These could be spaced and fastened accurately and securely. A typical cell was composed of two plates of 0.001 m thick steel, 0.2 m by 0.06 m with four holes, one in each corner, separated by small thin plastic washers and fastened with 6 mm nylon bolts or threaded rod and nuts shown in Figure 3-4.



*Figure 3-4 Single cell composed of stainless steel plates. External connections were made by either welding a rod to each plate or clamping a wire to each plate using the fasteners.*

The conductance of fluid between closely spaced plates was greater than that between the edges of widely spaced jubilee clips. This meant that the energy consumption for a given gas production was much lower. Again the amount of power input per flow rate required to sterilise wastewater was not lowered significantly compared to higher resistance systems.

When driven to very high current density, the rate of anodic corrosion was sufficient to cause iron based flocculation of terminal effluent. This was both encouraging, because the treated water had low turbidity after settling, and problematic, because the heavy metals in the steel were also released into the water. It was observed both when using complete stainless steel construction and when using mild steel fasteners.

### 3.2.5 Model 2: stainless steel plates in a bipolar stack

By analogy to the bipolar stack of clips, stacks of plates were constructed. Thus, the effect of a single relatively low current power supply could be magnified by the number of cells in a compact processor.

A 12-cell (13-electrode) processor composed of 0.2 m by 0.127 m plates was made using the same type of steel plates as Model 1, 0.001 m thick plastic washer spacers (setting the *intra-electrode* gap) and nylon threaded rod as for the single cell version. Rather than use thick plates to reduce the current leakage, stainless steel nuts were used to increase the effective thickness of each bipolar electrode (forming the *inter-electrode* conductor space, bounded by two plates) to 0.01 m. These wet contacts, though tightly fastened, were prone to corrosion. Two single plates formed the outer electrodes, making a total of 24 plates. Figure 3-5 shows the effective electrical shape on the left, with conductors in grey, and the practical realisation on the right.

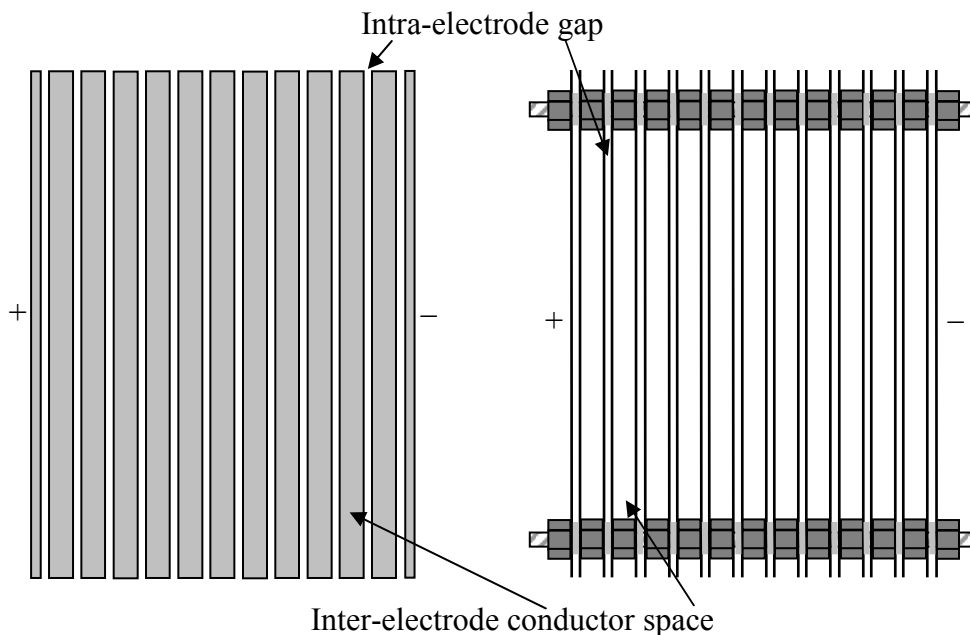


Figure 3-5 12 cell plate electrolyser: cross-sections of concept (left) and realisation (right).

The problem of leakage current could be seen as an outer-edge effect, because the shortest path for leakage current was from the outside edge of the outer anodes to the outer edge of the cathodes on the far side of the stack. So the large area was an

advantage because the leakage current mainly emanated from a small proportion of the total area.

The performance data for both an 8-series-cell and 15-series-cell stack immersed in Hamilton City Council waste water plant clarified effluent (conductivity around  $500 \mu\text{S cm}^{-1}$ ) is shown in Table 3-1. Fluid was pumped through the immersion chamber but was not constrained to flow through the electrode gaps. The stainless steel electrode thickness the same as the electrode gap – 1 mm – so there was significant current leakage around the central cells. Given better spacing ratios the current leakage would be insignificant. Current density in excess of  $25 \text{ A m}^{-2}$  is achievable at 5 V per cell and is possible at 3 V per cell. This is particularly useful data for formulation of larger scale designs.

*Table 3-1 Performance of bipolar cell stacks in clarified terminal effluent.*

Parameter and units	Data from 24 February 2003	Data from 3 March 2003
Cells in series	8	15
Voltage (V) full wave rectified	42.8	44
Current (A)	1	0.4
Length (m)	0.2	0.2
Width (m)	0.06	0.06
Area ( $\text{m}^2$ )	0.012	0.012
Current density ( $\text{A m}^{-2}$ )	83	33
Voltage per cell (V)	5.35	2.93

### **3.2.6 Model 3 (minimum gap) and Model 4 (maximum area)**

The reduction of gap and increase in area were taken to their respective extremes. Gaps of 0.0001 m could be arranged easily for small plate single cells using plastic film washers, but the problem of bubbles filling the gap and limiting the current became apparent. For larger areas, up to 0.5 m by 0.2 m, even 0.001 m gaps were problematic, due to the number of spacers required to prevent contact between electrodes. It was considered too difficult to construct series stacks of either the 0.0001 m gap or  $0.1 \text{ m}^2$  area cells. Depictions of the minimum gap

(Model 3) and maximum area (Model 4) cells are shown in Figure 3-6 and Figure 3-7 respectively.

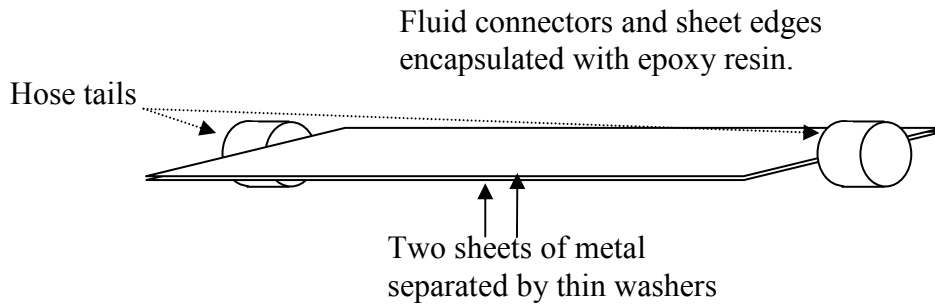


Figure 3-6 Minimum gap-width cell – Model 3.

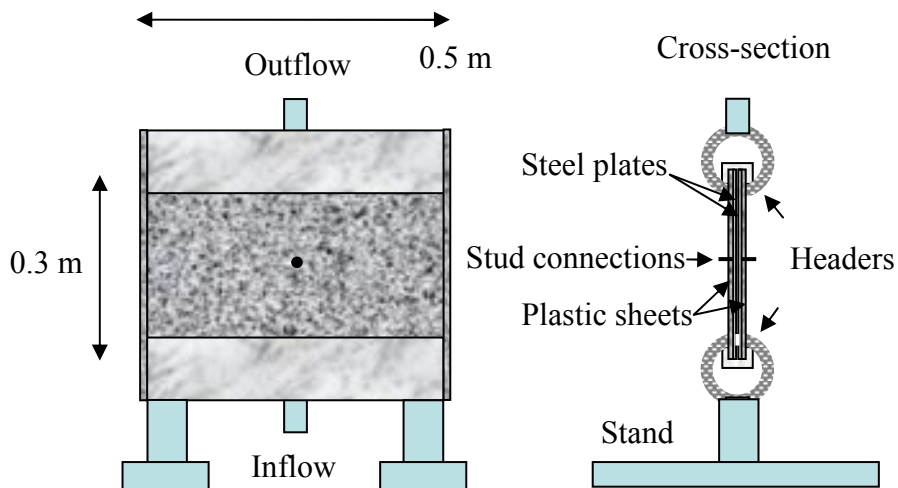


Figure 3-7 Maximum area cell – Model 4.

### 3.2.7 Model 5: stainless steel plates bipolar stack with forced flow

The main weakness of the first multi-cell bipolar plate stack was that of fluid leakage through the inter-electrode space. It was assumed that there would be advantages in forcing all the water to be treated to pass close to an electrochemically active zone. By sealing the inter-electrode paths, fluid flow was restricted to the electrode gap.

### 3.3 Applications of bipolar stacks

#### 3.3.1 Treatment of iron laden bore water (iron-water)

##### Rationale of treatment

The peat-soils that cause reducing conditions in deep aquifers in the Waikato basin in the North Island of New Zealand also leach small but significant amounts of iron (in the order of tens of  $\text{mg L}^{-1}$ ) and manganese (usually less than five  $\text{mg L}^{-1}$ ) into the water. While  $\text{Mn}^{2+}$  and  $\text{Fe}^{2+}$  ions are very soluble and almost colourless, upon exposure to atmospheric oxygen they are converted to less far less soluble black  $\text{Mn}^{4+}$  and brown  $\text{Fe}^{3+}$  respectively. As a result, freshly raised bore water can change from clear to a laundry and sanitary-ware staining fluid in a few hours. The fine precipitate may take many weeks to settle. The conductivity is between 100 and 1000  $\mu\text{S cm}^{-1}$ , mainly due to sodium chloride and other salts. According to Figure 1-2, this is in the range of 1 to 10  $\text{mmol L}^{-1}$  sodium chloride. The pH is usually near neutral so sodium and chloride ions dominate the ionic conductivity of the prospective electrolyte.

The deleterious effect of excessive dietary iron on dairy cows (Coup et al. 1964) and bulls (Stoyanov et al. 1987) is well established. Where iron-water is used for irrigation, the iron is concentrated on the pasture, affecting not only the bovines that ingest it, but also the pasture plants. Reduction of the iron level in bovine drinking water to below 2  $\text{mg L}^{-1}$  is recommended (Stoyanov et al. 1987). The New Zealand drinking water standard 2005 recommends that iron be limited to 0.2  $\text{mg L}^{-1}$  (aesthetic guideline value) and manganese must be below 0.4  $\text{mg L}^{-1}$  (maximum acceptable value) (Ministry of Health 2005). In 2003, a Waikato Dairy company specified a prospective limit of 5 NTU for water used on farms that supply it – at this turbidity the water is noticeably orange (Allen, M. 2003, pers. comm., 21<sup>st</sup> November).

Rapid oxidation of the freshly raised water, prior to commencement of the slow formation of colloid, is required to make a precipitate that is coarse enough to filter with sand or pumice media. The rapid oxidation is typically achieved by spray aeration, but can also be arranged by chlorination of freshly raised water (Yiasoumi 2003), which has the additional benefit of persistently disinfecting the

water. Spray aeration produces a fine floc which is filtered to reduce the iron content consistently to less than 5 mg L<sup>-1</sup>.

Bacteria that oxidise the iron could be used to supplement the other means of treatment (Sharma et al. 2005). Iron reducing bacteria are active in the anaerobic conditions of the bore (Kanso et al. 2002). Hence, disinfection in-ground by chlorination could have unexpected consequences depending upon both the microbes present and the spread of disinfectant dose in an aquifer. Any process that forms fine colloidal iron (III) species in the water, either in-ground or after it is raised to the surface, is not desirable (Hill, T. 2003, pers. comm., August).

### **Strategy**

Electrolytic treatment was used to both rapidly oxidise the iron to a form that flocculates and produce both immediate and persistent disinfection agents. Thus treatment is achieved by converting the contaminants and does not require addition of chemicals. Other functions like flotation were not anticipated but were used if possible in combination with the flocculation.

### **Equipment**

After successful initial batch trials at several different sites using the Model 2 bipolar stack, described in §3.2.5, an improved processor for in-line use was designed and built. Series bipolar 316-stainless steel electrodes of approximately 0.04 m<sup>2</sup> active area (0.2 m side length) were assembled inside a plastic welded PVC box, named the Breadbox, depicted in Figure 3-8. The electrodes were hollow rectangular prisms that prevented leakage through the inter-cell space by occupying it. Each electrode had a small hole in the top face to allow gas to escape. The electrodes were spaced by 1 mm thick PTFE washers glued in place and the entire 12-cell assembly was close-fitted into a PVC box. The endplates at both ends had connector stud bolts welded to the outside surface which were sealed in the PVC wall. The inflow at the middle of the base through ½ inch connectors was spread by a tapered baffle and the flow exited at the top. The thickness of the hollow electrode was 15 mm and the gap between the electrodes was 1 mm so the level of parasitic current (not passing through all 12 cells) was low, particularly as the main trial location had water with conductivity of greater

than  $500 \mu\text{S cm}^{-1}$  and the voltage per cell usually exceed 5 V (see Figure 3-3). The power supply was an RCD protected 4 A variac and a 50 A rectifier which could supply 80 V RMS (full wave rectified) at 3 A indefinitely. The trials were carried out at a Waikato farm.

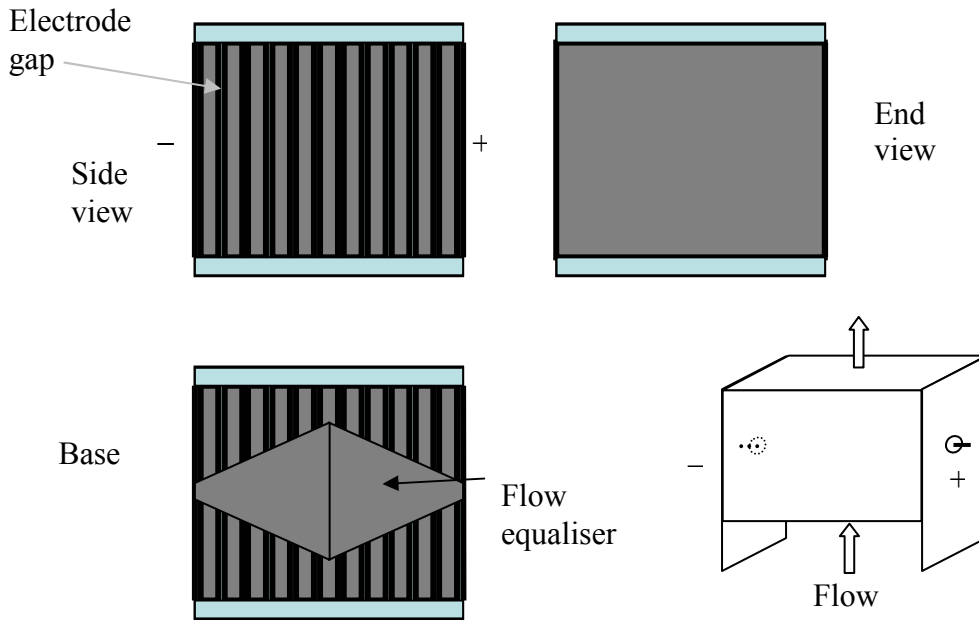


Figure 3-8 The Breadbox – used for processing Fe-laden bore water.

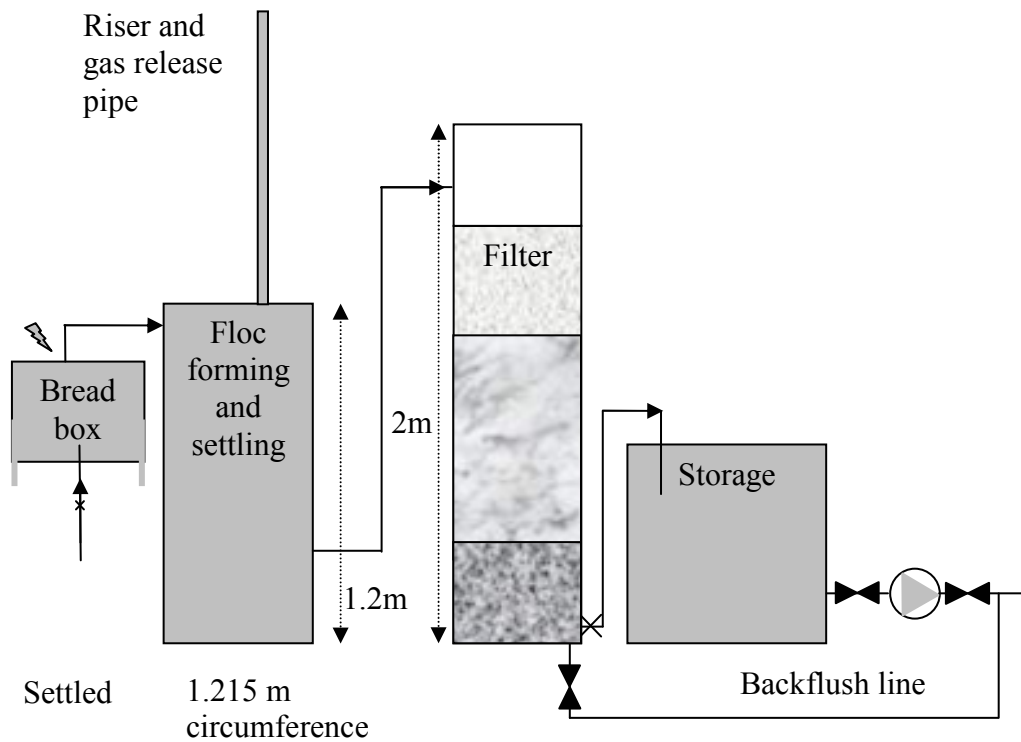


Figure 3-9 Complete iron water processing system.

The system shown in Figure 3-9 was used as a complete processor, incorporating a settling tank and dual media (sand and pumice) both supplied by Works Filter Systems.

### **Flocculation combined with flotation and chlorination**

Electrolysis caused production of coarse floc. Unexpectedly, bubbles entrapped in the floc lead to floc-flotation within a few minutes. Within an hour most of the floated floc had lost the buoyant bubbles and begun to sink at  $0.1 \text{ mm s}^{-1}$ . By that time non-floated floc had already settled.

The complete processing system shown in Figure 3-9 was demonstrated at the trial site, to a group of local farmers who supply the local dairy factory with milk, on November 21<sup>st</sup> 2003. Bore water with a total iron content of  $26.5 \text{ mg L}^{-1}$  was processed continuously at  $4 \text{ L min}^{-1}$ , using 3 A through 12 cells at 5.5 V per cell (65 V supply). This equated to an electrical energy treatment density of  $0.81 \text{ kWh m}^{-3}$  for with a current-cell dose of  $9 \text{ A (L min}^{-1})^{-1}$  at a current density of  $75 \text{ A m}^{-2}$ . After 24 hours settling the supernatant contained  $12.3 \text{ mg L}^{-1}$  iron. When filtered, the water had only  $0.24 \text{ mg L}^{-1}$  iron (all analyses are total iron, made by Hill Laboratories, Hamilton). Acceptable taste and clarity of the processed and filtered water were confirmed on the day by at least two people, including the author, and the turbidity was consistently well under 5 NTU.

Numerous tests before and after the demonstration date were carried out.

Electrolytic processing failed to significantly improve water that had already been spray aerated and filtered. Under-treatment by raising the flow rate or lowering the supply voltage tended to result in immediate formation of colloidal iron. Over-treatment resulted in measurable residual chlorine of up to several  $\text{mg L}^{-1}$ .

Treatment at another site, of bore-water that had in-ground chlorination and lower conductivity than the main site, resulted in formation of colloidal or weakly flocculated iron irrespective of the treatment level (up to  $18 \text{ A (L min}^{-1})^{-1}$ ).



## **Electrode degradation**

Because the Breadbox was sealed and opaque for commercial reasons, it was not possible to see the electrodes. The first indication of corrosion was a slight elevation of the manganese levels after processing. Significant amounts of chromium and nickel were also added to the water by electrolytic processing. The manganese was not easily filterable but the chromium and nickel were readily filtered out to acceptable levels. Evidently the stainless steel electrodes were corroding, although slowly, adding more iron to the water.

## **Discussion**

The Breadbox was able to convert the ferrous iron in bore water to a ferric form that flocculated strongly. This function was enhanced by combination with flotation because the floc formed so quickly that gas bubbles still in the fluid were able to combine with the floc. After the iron was fully oxidised, further treatment resulted in residual chlorine levels of up to 5 mg L<sup>-1</sup>.

As pointed out in §1.4.1, the subtle difference between direct anodic oxidation of iron II to iron III, and reaction of iron II with anodically produced oxidising agents to produce iron III, can only be resolved by voltammetric methods. These were not used, but it was assumed that in either case it would be best if all the water passed close to the active anode surface to facilitate either direct oxidation or reaction with nascent oxidising agents. There were no separating membranes between the anodes and cathodes. It is possible that reduction of Fe<sup>3+</sup> back to Fe<sup>2+</sup> occurred at the cathode. It was not easy to check if chlorine or OH<sup>-</sup> was the primary oxidiser for the iron. The presence of measured free available chlorine only at treatment levels above that required to completely oxidise the iron suggests that chlorine compounds have a role.

In order to ease the load on the subsequent filtration, or perhaps even make filtration unnecessary, the observed rapid flotation of iron floc and subsequent settling could be utilised more effectively. By skimming the floated floc before it settles (Jamieson, G. 2003, pers. comm., November 21) and allowing the remainder to settle in a counter-cross-flow or lamella settler (Gomella 1974; Pontius 1990) it is possible that the majority of the iron could be concentrated in a

small fraction of the water leaving the outflow adequately purified without filtration. If further filtration were required, the time between back-flushes could be greatly increased compared to a system without settling.

There is no point in trying to lower the corrosion rate by increasing the expense of the anode material. Hence, all the components of the anode should be relatively cheap and the corrosion products should be benign (to lower toxicity). According to Table 2-1 and Table 2-2, a likely candidate is graphitic carbon. Replaceable slabs of graphite with the favourable conduction axis parallel to the current flow could be used as substitutes for the hollow stainless steel bipolar electrodes.

The compact nature of the Breadbox meant that the both the current density and energy consumption were high. If the current density was lowered both the anodic corrosion rate and energy consumption could be reduced greatly. At some point the effectiveness would be compromised because the current fraction for chlorine production would drop. Further study is required to find an optimum for a commercial product.

## **Conclusion**

Electrolytic processing of iron laden bore water makes a dense floc that is floated or settled out of the water. Polishing of the processed water by filtration would produce high quality water. The capital cost of processors and post-processing equipment must be minimised to maintain interest from potential users. A benign anode is crucial to the success of this application (see §6.5.3).

### **3.3.2 Treatment of cooling tower water to prevent legionellosis**

#### **Rationale for treatment**

Rare but dangerous outbreaks of Legionnaires Disease have occurred when susceptible people are exposed to liquid and aerosols containing certain serotypes of the microbe *Legionella pneumophila*. Sporadic cases greatly outnumber mass outbreaks, and a mild form known as Pontiac Fever is far more common. However, the fatality rate for legionellosis is 15% on average, but higher in immuno-compromised patients (Public Health Commission 1995).

*Legionella* genus microbes are common in natural waterways, can survive temperatures of up to 60 °C, multiply in temperatures between 20 °C and 45 °C, and thrive in waters between 35 °C to 43 °C. Favourable conditions for multiplication are commonly experienced in building cooling towers with the added risk of aerosol dispersion from these towers (Public Health Commission 1995). Even though the risk of infection is not directly proportional to the number of *Legionella pneumophila* in a cooling tower (Public Health Commission 1995), disinfection of cooling tower water is a way to lower the risk of legionellosis.

Enumeration of *Legionella pneumophila* is a specialised and expensive laboratory task. Just as coliform counts are used as indicators for sewage contamination, heterotrophic plate counts (HPC) are used to gauge the likely level of *Legionella pneumophila* in a fluid. However, a low HPC could favour *Legionella pneumophila* multiplication due to lack of competition, so readings must be taken with caution (Public Health Commission 1995).

The standard method of preventing build-up of *Legionella* genus microbes in cooling towers is to maintain 5 mg L<sup>-1</sup> of free chlorine residual in the cooling tower water. Chlorine based decontamination, as well as routine disinfection, is also detailed in the prescribed guidelines (Public Health Commission 1995). Electrolytic treatment cooling tower water has been shown to be feasible in another study (Forstmeier et al. 2005).

Tap water is normally used to replenish the water lost from evaporative cooling towers. The evaporation tends to produce a more concentrated electrolyte, and conductivity is further enhanced by addition of contaminants leached in from the pipes and heat exchangers during recirculation, as well as ingress of material such as dust into the outdoor cooling tower. The pH is likely to be near-neutral so salt conductivity dominates.

### **The laboratory trial**

Two small single-cell processors made of encapsulated stainless steel plates (200 mm by 62 mm) were made; one with a 1 mm gap and one with a 2 mm gap. These were used on live cultures of *Legionella pneumophila* in saline at WaterCare Services' laboratory in South Auckland. The saline was either 500 µS cm<sup>-1</sup>,

achieved by using a solution of 0.25 g L<sup>-1</sup> of NaCl in distilled water, or 200 µS cm<sup>-1</sup>, achieved by using a solution of 0.1 g L<sup>-1</sup> of NaCl in distilled water. The saline was spiked with microbes at 10000 cfu mL<sup>-1</sup>. Fluid was pumped at a fixed rate through the processor in a single pass. The inflow and outflow microbial counts were made by WaterCare Services. Table 3-2 shows the conditions used for treating water with conductivity of approximately 500 µS cm<sup>-1</sup>. The treatment resulted in complete disinfection in all cases.

*Table 3-2 Electrolytic treatment of saline spiked with Legionella pneumophila at 10000 cfu mL<sup>-1</sup> showing Legionella pneumophila levels below the minimum resolvable amount of 10 cfu L<sup>-1</sup> (December 3<sup>rd</sup> 2003).*

Flow (mL min <sup>-1</sup> )	Current (A)	W (L min <sup>-1</sup> ) <sup>-1</sup>	Energy density (kWh m <sup>-3</sup> )
Cell Voltage 5 V			
10.5	1	476	7.9
85	1.25	74	1.2
500	1.5	15	0.25
2100	1.25	3	0.05
3000	1	1.7	0.028
1 mm rig at 3.5 V			
100	1	35	0.6
Cell Voltage 10 V			
85	4	470.6	7.8
250	4.5	180.0	3.0
300	4.5	150.0	2.5
450	4.75	105.6	1.8
2400	5	20.8	0.3
Cell Voltage 15 V			
130	7	807.7	13.5
300	8	400.0	6.67
750	8	160.0	2.67
2400	9	56.3	0.94

Table 3-3 shows the conditions used for treating water with conductivity of approximately 200  $\mu\text{S cm}^{-1}$ .

*Table 3-3 Log<sub>10</sub> reduction of Legionella pneumophila by electrolytic treatment of low conductivity microbe-spiked saline (March 17<sup>th</sup> 2004).*

Flow (mL min <sup>-1</sup> )	Current (A)	W (L min <sup>-1</sup> ) <sup>-1</sup>	Energy density (kWh m <sup>-3</sup> )	Outflow <i>Leg. p.</i> count (cfu L <sup>-1</sup> )	Log <sub>10</sub> reduction
Cell Voltage 5 V					
1300	0.5	1.9	0.032	<10	≥ - 6
2000	0.5	1.3	0.021	300	- 4.5
Cell Voltage 10 V					
1300	2	15.4	0.3	<10	≥ - 6

Table 3-3 shows that the outflows had *Legionella pneumophila* levels below 300 cfu L<sup>-1</sup>. The minimum energy density for treatment was 0.03 kWh m<sup>-3</sup>.

### **The field trial**

The maximum area cell (Model 4, see Figure 3-7 in §3.2.6) was installed at a plastics factory (in Hamilton, New Zealand) to process a side-stream of the plastic production factory's cooling tower water according to the scheme shown in Figure 3-10. The water was taken from the cooling tower and siphoned into the storage tank via the processor. The conductivity was around 500  $\mu\text{S cm}^{-1}$ . Clear plastic hoses were used to make connections and these were in direct sunlight. Water flowed upward through the processor. The processor was powered by a D3800 voltage source from Dick Smith Pty. The processor was left in place for 12 days and samples were taken every few days. These were cultured and enumerated by e-Lab Alpha in Hamilton, New Zealand.

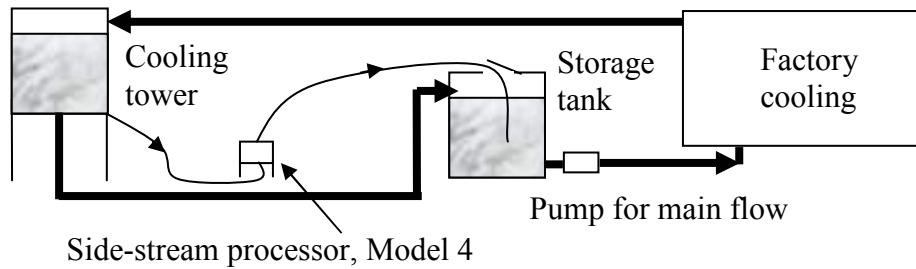


Figure 3-10 Side-stream processing scheme for cooling tower water treatment.

The results of the twelve day trial are shown in Figure 3-11.

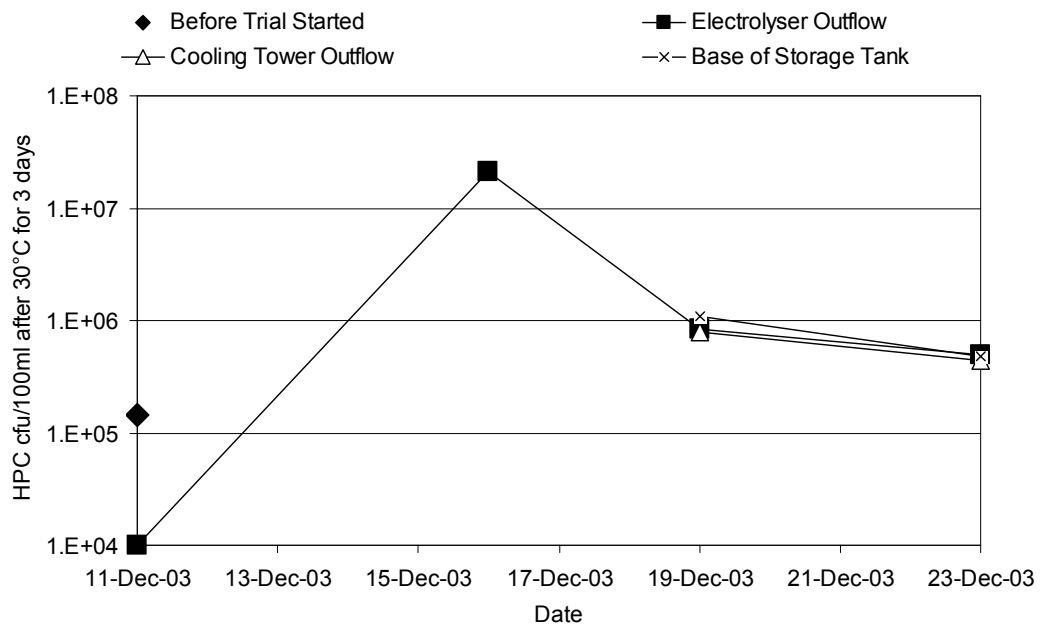


Figure 3-11 Result of electrolytic processing of cooling tower fluid.

Figure 3-11 shows that while the outflow had a much lower heterotrophic plate count three hours after beginning processing than the initial inflow, all the counts went up drastically over the ensuing 10 days. The pH of the entire stream climbed from 7 to above 8 and algae colonized the inflow line to the processor. This was in contrast to the ease of disinfection in saline in the laboratory. The influence of algal growth could have been significant. The raised pH, which would weaken the effectiveness of chlorination, is not easily explained.

### Discussion and conclusion

There were several reasons why the electrolytic processor failed to achieve disinfection of the cooling tower fluid. The residual chlorine level could not be

raised above 2 mg L<sup>-1</sup> without increasing the pH to greater than 8 (rendering the chlorination ineffectual), the amount of organic matter in the fluid was significant and the clear hoses enabled growth of algae.

The effectiveness of disinfection systems that do not rely entirely on chlorination must be proven to regulatory authorities, so that such systems are ratified in standards. In this context, over-treatment should normally be arranged to give a safety margin.

Electrolytic processing of chloride ions to chlorine in a single pass system is an excellent way to kill *Legionella pneumophila* in saline but work is required to perfect a system that can continuously sterilise a real cooling tower side-stream.

### **3.3.3 Electrosterilisation of virus-contaminated water**

#### **The vitality of enteric viruses compared to *E. coli***

Bacteriophage MS2 virus (*Leviviridae. levivirus*), grown in *Escherichia coli* C3000 was used as a test virus. MS2 is a viral and faecal contaminant indicator for wastewater that can persist in water longer than most other viruses (Douglas 1975; Hurst 2000). The bacteria tested for comparison were *E. coli* C3000 and *Enterococcus faecalis* 1240 (Em 2003).

#### **Electrolytic processor**

Figure 3-12 shows the processor that was used for trials of electrolytic disinfection of viral and bacterial microbes at the School of Biological Sciences, University of Auckland. The work was carried out in partnership with a student of the University of Auckland (Em 2003).

The core of the processor was a six cell electrolyser made of bipolar stainless steel plates similar to the (twelve cell) Model 2 as shown in Figure 3-5, fixed within a cubical stainless steel container. The electrodes were 0.1 m by 0.05 m in size. Although the processor could be configured for many different flow directions, the flow for this trial was not through the electrode space, as the main disinfection effect was expected to be due to the action of persistent oxidizing agents produced at the anode.

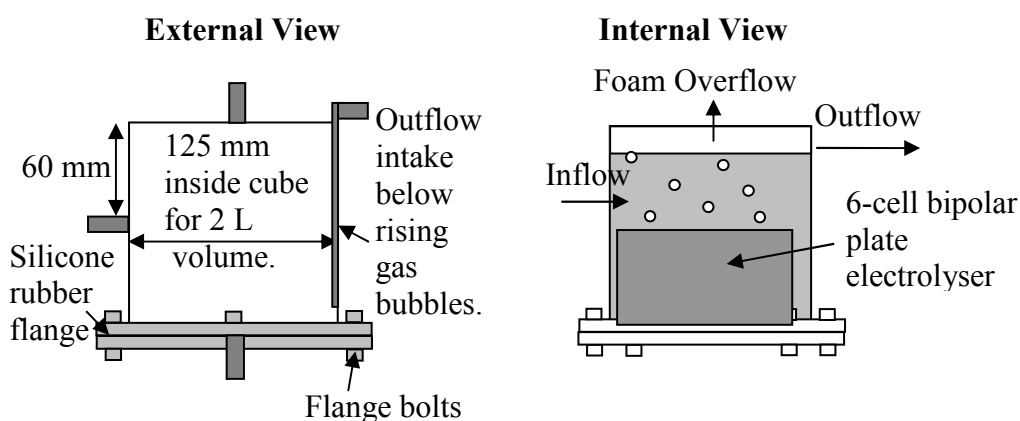


Figure 3-12 The electrolytic processor designed for the trial at the University of Auckland.

The power supply was a 4 A variac feeding a single 50 A rectifier. The voltage was varied according to the conductivity of different water samples. Safety protection was by an earth-leakage breaker. The processor was used in a fume-hood and stood on a 0.3 m high platform to enable fluid connection and lower possible earth leakage. The fluid paths (hoses) to and from the processor were 1 m long to minimise earth leakage. Plastic valves were used for safety. Before each use the metallic parts of the rig were autoclaved along with the silicone tubing used in the peristaltic pump. The plastic attachments, hoses and containers were sterilised before use, by soaking in 3%  $\text{Cl}_2$  overnight, followed by rinsing with tap water twice then deionised water once, then de-chlorinated in  $\text{Na}_2\text{S}_2\text{O}_3$  solution for approximately 30 minutes before a final rinse in deionised water (Em 2003).

### Test fluid and media formulations

Model wastewater was made in 20 L batches from deionised water with 300 mg  $\text{L}^{-1}$  of yeast extract. To test the effect of various salts on the electrolytic treatment, either  $\text{NaCl}$  or  $\text{MgSO}_4$ , at 0.1%, 0.05% or 0.01%, was added to the water. The measured conductivity of 0.1% solutions of  $\text{NaCl}$  was  $2114 \mu\text{S cm}^{-1}$  while 0.1%  $\text{MgSO}_4$  solutions were  $150 \mu\text{S cm}^{-1}$ . All materials were used and kept at room temperature. The model wastewater was seeded with microbes which were in either an exponential growth phase or a stationary phase, and pumped through the electrolytic apparatus at  $1.1 \text{ L min}^{-1} \pm 0.2 \text{ L min}^{-1}$  using a peristaltic pump operating at fixed speed. The suspension was exposed to treatment by a current of 4 A of passing through six cells (approximately  $24 \text{ A (L min}^{-1})^{-1}$  at  $800 \text{ A m}^{-2}$ ).



Inflow samples, three outflow samples taken at two-minute intervals and foam overflow samples were tested for culturable counts in duplicate (Em 2003). The media for microbial culture, both broth and agar, were made at Auckland University (Em 2003). Table 3-4 summarises the type of inflows used (Em 2003).

*Table 3-4 Summaries of organisms and electrolyte composition, as well as control voltage and flow rate.*

Micro-organism	Voltage (V) (setting on variac)	Flow Rate (L min <sup>-1</sup> )	pH	NaCl %	MgSO4 %
MS2	264	1.25	6.43	0	0
MS2	266	1.10	6.50	0	0
MS2	230	1.25	6.83	0	0
MS2	218	1.10	6.23	0	0
MS2	242	1.20	5.71	0	0
MS2	230	1.25	6.37	0	0
MS2	35	1.00	6.37	0.1	0
MS2	38	1.00	6.51	0.1	0
MS2	42	1.00	6.45	0.05	0
MS2	42-45	1.10	6.50	0.05	0
MS2	80	1.00	7.09	0.01	0
MS2	110-115	1.10	6.65	0.01	0
<i>E.coli</i>	82	1.00	6.24	0.01	0
<i>E.coli</i>	85-95	1.00	6.67	0.01	0
<i>E.coli</i> + <i>Ent.facalis</i>	85	1.10	- <sup>a</sup>	0.01	0
<i>Ent.facalis</i>	90	1.00	-	0.01	0
<i>E.coli</i>	115-17	1.00	-	0	0.01
<i>E.coli</i> + <i>Ent.facalis</i>	125-140	1.00	6.57	0	0.01
<i>Ent.facalis</i>	130-135	1.10	-	0	0.01
<i>E.coli</i> early stationary	200-220	1.00	-	0	0
<i>E.coli</i> exponential	220-230	1.10	6.52	0	0
<i>E.coli</i> exponential	220-230	1.00	-	0	0
<i>E.coli</i> stationary	220-240	1.00	6.47	0	0
<i>E.coli</i> stationary	230-235	1.00	-	0	0

## Comparison of efficacy for viruses and bacteria

As shown in Table 3-5, the effectiveness as measured by log reduction was good for bacteria but less for viruses.

Table 3-5 The  $\text{Log}_{10}$  microbial reduction rates achieved by electrolytic processing of model wastewater (Em 2003).

	0% salt	0.01% NaCl	0.05% NaCl	0.1% NaCl	0.01% MgSO <sub>4</sub>
MS2	2.0 ± 0.5*	1.3 ± 0.1	3.3 ± 0.3	3.7 ± 0.3	-
<i>E.coli</i>	0.5 ± 0.2	6.3 ± 0.2	-	-	0.1 ± 0.1
<i>Ent.facalis</i>	-	2.2 ± 0.8	-	-	0.3 ± 0.2

\* showing reduction of  $\text{log}_{10}$  units and the standard deviations of these.

- these conditions were not tested.

Table 3-5 shows that reduction of viruses was generally improved by increasing NaCl addition to the electrolyte, which would be expected if the current efficiency of conversion to chlorine was increased. The difference between the nil NaCl addition and 0.01% NaCl addition was not significant. MgSO<sub>4</sub> addition resulted in lower reduction than for nil NaCl addition. The high voltage used for the nil NaCl addition trials contributed to a disinfection effect based on the voltage or electric field. After the trial the electrodes were found to have corroded significantly.

## Discussion and Conclusion

Electrode corrosion would have released metallic toxins that assisted disinfection when the cell voltage was higher. This is evident in the nil NaCl addition samples. In order to test the effect of electric field-dependent effects it would be advisable to conduct another trial with the inflow connected to the base-port so that the water flows at least partly through the electrode gaps.

### 3.3.4 Electroflotation of laundry water

#### Synthetic laundry water

A synthetic laundry water was made from tap water and commercially available materials - Ocean Fresh Surf Concentrate containing anionic & non-ionic

surfactants, sodium polyphosphate, zeolite and suspending agent, sodium silicate and sodium carbonate, sodium sulphate, fluorescer, enzymes and colour; sodium hydroxide (> 99% purity) was added later in the trial, when the majority of the detergent was flushed out, as a reference for the effect of high pH alone.

### **Laundry water in Geelong, Australia**

A processor was sent to a commercial laundry in the suburb of Geelong near Melbourne, Australia. This facility normally processed laundry from hotels and provided a suitable test fluid.

The goal of treatment was to produce recyclable water and a fraction with concentrated contaminants that was within discharge limits according to the following specifications set by Geelong municipal authorities:

*Inflow at 1.2 m<sup>3</sup> h<sup>-1</sup> for 8 hours per day with 20 mg L<sup>-1</sup> suspended solids. The recycled outflow must be free of faecal coliforms. The rejected water must be no more than 100 mg L<sup>-1</sup> suspended solid and also be free of faecal coliforms.*

Given low suspended solid in the recycled fraction, no more than 80% of the inflow could be recycled. Concentrating the suspended solid by a factor of around five into a flow of around 0.24 m<sup>3</sup> hour<sup>-1</sup> was considered possible. However, both of the outflow fractions had to be disinfected.

### **The electrolytic processor**

Stainless steel electrodes were used for both the synthetic water and the field trials. A single cell plate unit similar to Model 1 shown in §3.2.4 (Figure 3-4) was used for the synthetic water trials. A specialised three-cell unit in the style of Model 2 shown in §3.2.5 (Figure 3-5) was made with larger inter-cell gaps of 15 mm to minimise parasitic current.

A 60 L open-top rectangular plastic container was modified by placing a weir across the width to force the flow to go over the top, as shown in Figure 3-13. This enhanced flotation by bringing all the fluid close to the surface after processing. Only very dense contaminants would sink after this stage.

Contaminants and foam were to exit the upper outflow while purified water was to exit the lower outflow port. A D3800 dc voltage source was used (supplied by Dick Smith Pty.)

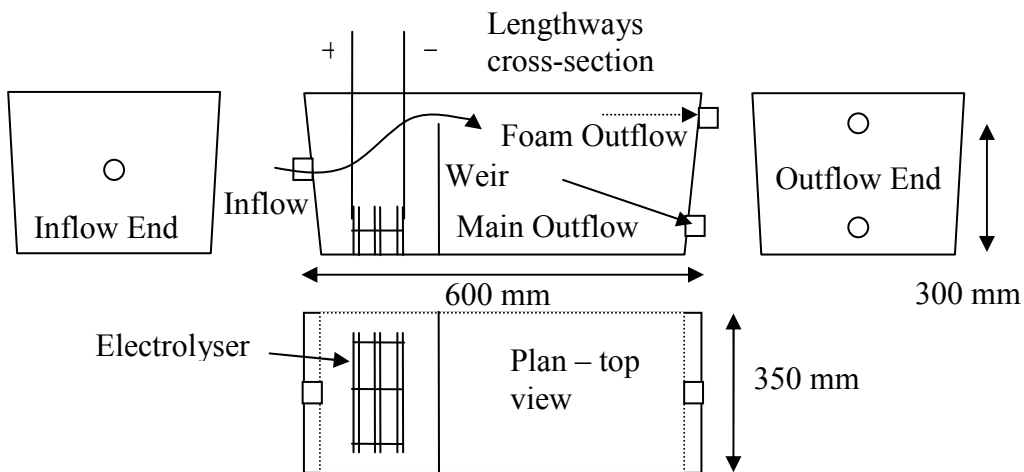


Figure 3-13 The device for laundry water recycling including a 3 cell electrolyser.

### Synthetic laundry water

The results for processing of synthetic laundry water are shown in Table 3-6. Table 3-6 indicates that most of the current went into making bubbles of hydrogen and oxygen, with a small fraction directed to chlorine formation. The effect of the processing was that fine bubbles from the electrolyser, in conjunction with the detergent surfactant, made stable floating foam. By adjusting restrictions on the outflow ports, the foam could be removed by a periodic siphon into the upper port.

### Field trial report

The conductivity of the laundry water was lower than expected, based on the reported current. The operator also reported a darkening of the outflow that may have been due to corrosion of the electrodes. The effect of high pH on disinfection is unknown. The trials are on-going and we await the return of the unit for examination and improvement.

Table 3-6 Chlorine production for synthetic laundry water using a single cell electrolyser operated at 17 V.

Electrolyte (mg L <sup>-1</sup> )	Conductivity ( $\mu\text{S cm}^{-1}$ )	I (A)	Current density (A m <sup>-2</sup> )	Flow (L min <sup>-1</sup> )	pH	Cl <sub>2</sub> (mg L <sup>-1</sup> )	Cl <sub>2</sub> current efficiency (%)
Add Detergent							
0	483	0	0	15	7.7	0.05	0.0%
0	483	2.5	403	15	7.7	0.1	2.7%
211	828	5	806	15	9.9	0.275	3.7%
1000	2484	10	1613	15	10.6	0.2	1.4%
1293	2760	15	2419	15	10.6	0.175	0.8%
1293	2760	15	2419	15	10.6	0.35	1.6%
add NaOH							
0	1050	0	0	15	7.7	0.05	0.0%
0	1750	2.5	403	15	7.7	0.1	2.7%
80	1104	5	806	15	11.1	0.35	4.8%
147	2500	10	1613	15	12.1	0.6	4.1%
233	4140	15	2419	15	12.2	0.5	2.3%

## Discussion and conclusion

This case study showed that getting an appropriate mix of flotation and sterilisation in a compact package is possible with a single electrode type.

However, it is advisable to use stainless steel electrodes at low current density for flotation and a separate corrosion-resistant anode specialised for disinfection of both the recycle fraction and the water to be discharged.

This application seems feasible due to the relatively low recycle fraction that is enforced by discharge standards. Based on a 5 V cell and a requirement of 380 mL m<sup>-3</sup> (flotation gas volume per volume of laundry water, see §1.4.1) the energy consumption could be as low as 0.1 kWh m<sup>-3</sup>.

### **3.3.5 Treatment of municipal wastewater**

#### **Terminal effluent**

The Hamilton City Council changed from a final chlorination step to UV tertiary treatment because release of organochlorine compounds into a river was seen as inappropriate. Given the existing investment in UV disinfection, the most promising potential improvement appeared to be pre-treating the water using low voltage cells so that the UV treatment became less energy intensive and the outflow becomes lower in suspended solids. The processors shown in §3.2 were developed by trials with terminal effluent. A side-stream of effluent was extracted from the main stream at a point just before the UV-disinfection and returned, after electrolytic processing, to the same point.

#### **Development models**

Processors were enclosed within either cylindrical or square cross section containers with a selection of inflow and outflow ports. While the initial commercial imperative was to find an entire replacement for the UV treatment, which directed the study toward electrosterilisation, it quickly became apparent that flotation and flocculation were more cost-effective and would greatly assist the UV treatment.

#### **Electrosterilisation**

Attempts at electrosterilisation of terminal effluent were made using stainless steel plate processors Model 1 to Model 3 shown in §3.2 as part of side-stream processors. The summary of results over many days and many different cell voltages is shown in Figure 3-14, and indicate that thorough disinfection is likely to require around 10 kWh m<sup>-3</sup>.

#### **Electroflotation**

Figure 3-15 shows a square cross-section processor into which a 12-cell stainless steel plate processor similar to Model 2 shown was placed in a transparent flow vessel. Terminal effluent is shown flowing downward through the stack of plates, but most of the prolific bubble production traveled upward making the water appear opaque.

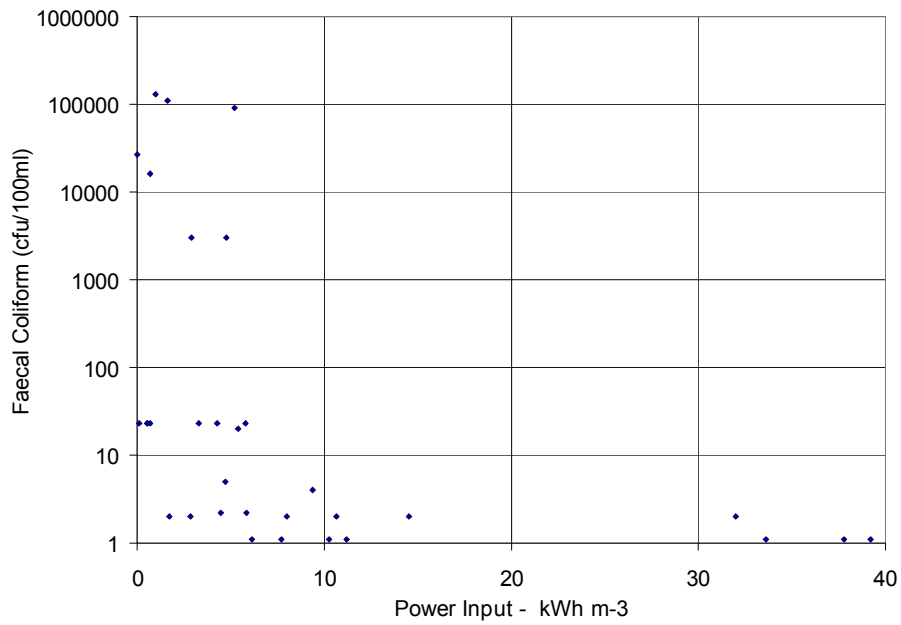


Figure 3-14 Aggregated results of attempted electrosterilisation of terminal effluent.



Figure 3-15 Down-flow electroflotation clarifier. Algae and other particulates were raised above the inflow point in sturdy foam. Some small bubbles passed down beyond the processor to the outflow stream at the bottom. Some of these small bubbles coalesced to form larger bubbles that rose back up through the processor.

Figure 3-15 shows that a compact layer composed of suspended solid from the effluent, including algae, was raised to the top of the liquid level (just above the danger sign). The key hydraulic parameter was flow speed. It was estimated that more than 90% by volume of the electrolytically produced gas was able to travel upwards against a downward fluid flow speed of  $3 \text{ mm s}^{-1}$ . Constraining the flow to pass through the narrow electrode gaps meant that coarse contaminants could not pass the closely spaced gas bubbles passing upward, but the downward flow speed would be increased leading to downward escape or coalescence of the smallest and most effective flotation bubbles along with the finest suspended solids. The bubbles that rose above the processor quickly dispersed to evenly occupy the entire cross-section of the flow vessel. The energy density of electroflotation of terminal effluent could be as low as  $0.1 \text{ kWh m}^{-3}$ .

### **Electroflocculation**

When terminal effluent was treated at greater than  $10 \text{ kWh m}^{-3}$  using steel plates with cell voltages in excess of 20 V, enough anodic corrosion occurred to induce iron based flocculation. While the effect on supernatant clarity was dramatic the effect was not pursued because of the excessive energy consumption and the likelihood of additional toxic metals leaching from the steel into the water.

### **Discussion and conclusion**

Electroflotation of clarified effluent appears to be the most feasible means of electrolytic treatment as it will enable the existing UV to sterilise with lower energy density. If electrolytic sterilisation is to be performed then it should be after a step that removes suspended solid. Flotation is the most useful function of electrolytic processing in treatment of previously up-flow clarified effluent. One of the three existing clarifier ponds at the Hamilton City Council Wastewater Treatment plant could be converted to an electroflotation tank, and the by-product hydrogen could be ducted to the existing bio-gas driven electrical generators on-site.



### **3.4 Proposed effluent processor**

#### **3.4.1 Emphasis on electroflotation of suspended solids**

The Hamilton City Council requested the development of a  $500 \text{ m}^3 \text{ day}^{-1}$  recycled water plant with their wastewater plant terminal effluent as inflow. The outflow was specified as wash-water quality. A suitable  $500 \text{ m}^3 \text{ day}^{-1}$  module could be replicated to supply the approximately  $1500 \text{ m}^3 \text{ day}^{-1}$  demand for wash water at the municipal waste water plant. Electroflotation was considered to be the most important function for this application. It is also clear that pure electroflotation does not add any persistent impurity to the fluid. The gas released is energy-rich and the energy is recoverable in an existing on-site gas burning electrical generator. The low concentration of suspended solid in the terminal effluent (less than  $20 \text{ mg L}^{-1}$ ) means that that up to  $7.6 \text{ L}$  of gas would be needed per cubic metre of fluid treated. A novel flow configuration is proposed that should lower the amount of gas required for treatment to  $1 \text{ L m}^{-3}$  by using an inversion of the principles used in floc blanket (Pontius 1990) and teacup (Wilson 1980) devices. Lower gas production directly lowers the operating cost. Collection of hydrogen gas is also easier and purification efficiency will be improved. The proposed scheme is shown in Figure 3-16. Conservative specifications are shown in Table 3-7, assuming use of stainless steel electrodes. An unfiltered full-wave rectifier power source will make smaller bubbles than a DC power supply due to release of the bubbles between pulses.

The outflow from the processor will have very low suspended solid compared to the inflow, and the algal colonies that microbes could shelter in are very likely to be removed. If the inflow is UV-treated terminal effluent then the outflow will need a relatively light dose of chlorine to be acceptable as wash water. The electrical cost and the fraction recoverable as hydrogen are not significant at this scale, though the operating cost could be reduced by lowering the cell resistance. Since the outflow is wash water, not potable water, some electrode corrosion is tolerable, and stainless steel or graphitic carbon electrodes should be used instead of more exotic materials.

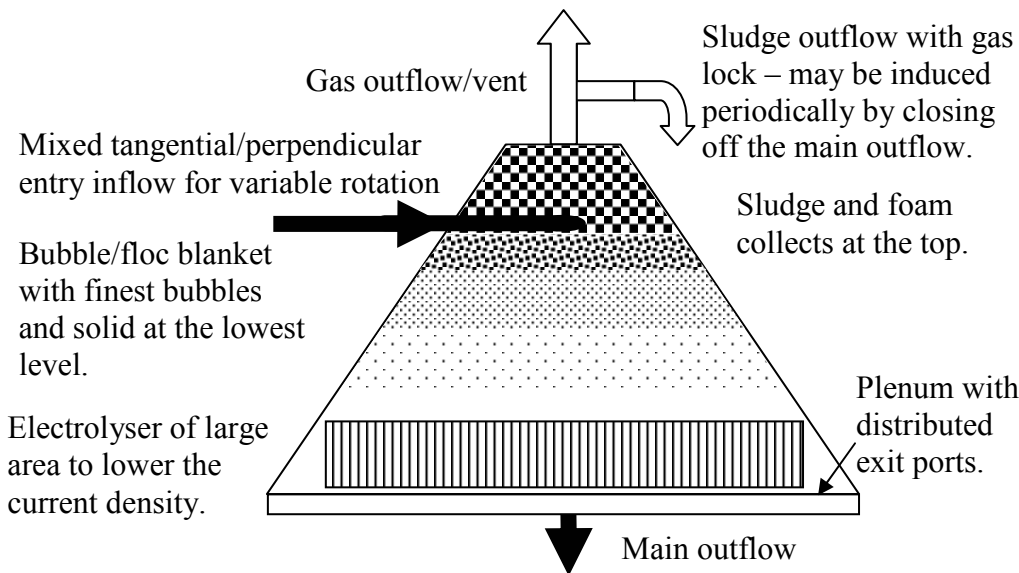


*Figure 3-16 Proposed scheme for electroflotation of municipal waste water plant terminal effluent. A truncated cone with down flow ensures lower flow speed toward the bottom so that small bubbles will rise to some level in the tank where a floc-bubble blanket will form, preventing suspended solids from progressing downward. Rotational flow like an inverted teacup will concentrate the bubbles and solids in the centre at the top.*

The scheme shown in Figure 3-16 could be up-scaled to treat the entire waste water flow of up to  $150000 \text{ m}^3 \text{ day}^{-1}$  in a clarifier of approximately 15 m radius. Since there are three appropriately sized clarifier basins in place already and the system can operate on two, one could be converted to an electroflotation tank. However, the cost of similar electrodes used at the same current density would increase by a factor of 300 to be in the order of hundreds of thousands of dollars. This alone could be considered prohibitive and it would be difficult to engineer thousands of square metres of electrode with an even 1 mm gap and regular gas release ports. Hence, it would be expected that the cost of electrode manufacture and installation would be an order of magnitude higher than the electrode material cost.

However, experience with the proposed  $500 \text{ m}^3 \text{ day}^{-1}$  unit will provide some lessons that enable production of a low resistance cell and a system that does not need so much gas to achieve adequate treatment. This could then be up-scaled. If the cell voltage is reduced to 3 V for the same current density and the gas requirement per volume of fluid could be reduced to  $1 \text{ L m}^{-3}$  by a scheme similar

to that in Figure 3-16 then the power consumption for treatment of the entire flow would be lower than that of the UV system.

*Table 3-7 Operating parameters of a terminal effluent recycling plant assuming a current density of 25 A m<sup>-2</sup> that would require an electrode gap of 1 mm (see §3.2.5).*

Parameter	Value	Unit
Container base radius	1	m
Area X-section	3.14	m <sup>2</sup>
Max flow	500	m <sup>3</sup> day <sup>-1</sup>
Max flow speed at base	1.84	mm s <sup>-1</sup>
Minimum conductivity	250	μS cm <sup>-1</sup>
Cell voltage	5	V
Current density	25	A m <sup>-2</sup>
Total suspended solid	20	mg L <sup>-1</sup>
Gas dosage	7.6	L m <sup>-3</sup> fluid
Gas production rate	44	mL s <sup>-1</sup>
Faradic gas production rate	0.17	mL gas s <sup>-1</sup> per Ampere-cell
Current required	253	Ampere-cells
Current dose	0.73	A (L min <sup>-1</sup> ) <sup>-1</sup>
Anode or cathode area	10.1	m <sup>2</sup> of anode or cathode
Total Electrode area	20.2	m <sup>2</sup> of electrode total
1 mm stainless steel plate	\$49	m <sup>-2</sup>
Electrode cost	\$1000	
Electrical energy input	1300	W
Electrical energy input density	0.06	kWh m <sup>-3</sup>
Power recoverable as H <sub>2</sub>	7	kWh day <sup>-1</sup>

The specifications of such a system are shown in Table 3-8. 30 kW of electrical input would be required and 10 kW (240 kWh day<sup>-1</sup>) of this could be recovered as hydrogen production. If the UV power requirement is reduced by 30 kW, the overall scheme will save 10 kW of net power input. Assuming capital cost of \$200000 the payback period is 15 years. In addition, the quality of the outflow would be improved to a point where the entire flow is recyclable.

*Table 3-8 Specifications for a possible electroflotation treatment system for the entire flow of previously up-flow clarified effluent at the Hamilton City Council Waste Water Treatment Plant. The cell voltage and gas dose have been reduced to the point where the energy requirement per volume is less than that of the UV system. Subsequent UV disinfection would require less energy input. Overall operating cost savings are possible.*

Parameter	Value	Unit
Container base radius	15	m
Area X-section	700	m <sup>2</sup>
Max flow	150000	m <sup>3</sup> day <sup>-1</sup>
	1.7	m <sup>3</sup> s <sup>-1</sup>
Max flow speed at base	2.5	mm s <sup>-1</sup>
Minimum conductivity	250	μS cm <sup>-1</sup>
Cell voltage	3	V
Current density	25	A m <sup>-2</sup>
Total Suspended Solid	20	mg L <sup>-1</sup>
Gas dosage	1	L m <sup>-3</sup> fluid
Gas production rate	1700	mL s <sup>-1</sup>
Faradic gas production rate	0.17	mL gas s <sup>-1</sup> per Ampere-cell
Current required	10000	Ampere-cells
Current dose	0.096	A (L min <sup>-1</sup> ) <sup>-1</sup>
Anode or cathode area	400	m <sup>2</sup> of anode or cathode
Total electrode area	800	m <sup>2</sup> of electrode total
1 mm stainless steel plate	\$49	m <sup>-2</sup>
Electrode cost	\$30000	
Electrical energy input	30	kW
	720	kWh day <sup>-1</sup>
	0.005	kWh m <sup>-3</sup>
Power recoverable as H <sub>2</sub>	290	kWh day <sup>-1</sup>

The lifetime of an electrode is inversely proportional to the square of the current density (see §1.4.1). Hence, a compromise must be made between initial capital cost and life-cycle cost. Where minimal contamination of the fluid by either electrode corrosion products or chlorination is paramount, the balance tips toward using extremely large area electrodes. The form of the electrodes should be an up-scaling of the bipolar stack shown in §3.2.5, though regularly spaced gas vents would be essential to prevent excessive gas voidage of the electrode gap. An

extreme form of this would be a membrane cell with mesh electrodes, as shown in Figure 3-17.

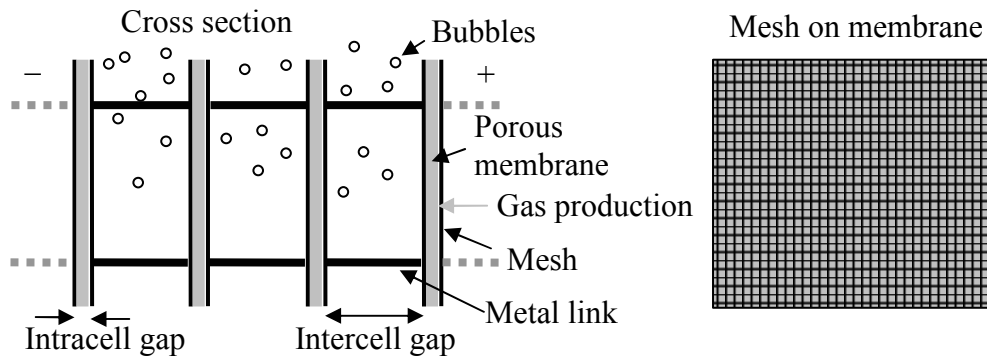


Figure 3-17 Mesh and membrane bipolar cell stack for large scale electroflotation. While gas is produced mainly at the mesh membrane contact surfaces it is able to depart via the inter-cellular gap which is relatively large. Thus current leakage and gas voidage are eliminated. This form is mass-producible as the only close-tolerance dimension is the intracell gap and this is assured by the membrane.

## 4 Development of corroding anode processors

### 4.1 Development sequence

#### 4.1.1 Model 6: corroding anode plates.

In order to examine electroflocculation, systems with anodes that corroded deliberately were developed, first by making encapsulated single cell units with aluminium plates, just like the stainless steel versions described in Chapter 3. These were disposable, because the anode disintegrated, disrupting the encapsulation. The problems of uneven corrosion and poor clearance of the corrosion products from Model 6 anodes were observed in the form of fouling and increasing electrical resistance.

#### 4.1.2 Model 7: corroding anode disc.

Radially symmetric submersible designs of various forms using either iron or aluminium disc anodes were built to try to overcome the problems of Model 6. Either the water flow was directed perpendicularly at the anode surface through a porous cathode, or it drained out through a porous cathode as illustrated in Figure 4-1. The cathode porosity ranged from a single central hole to perforated stainless steel with 0.005 m diameter holes and 30% open area.

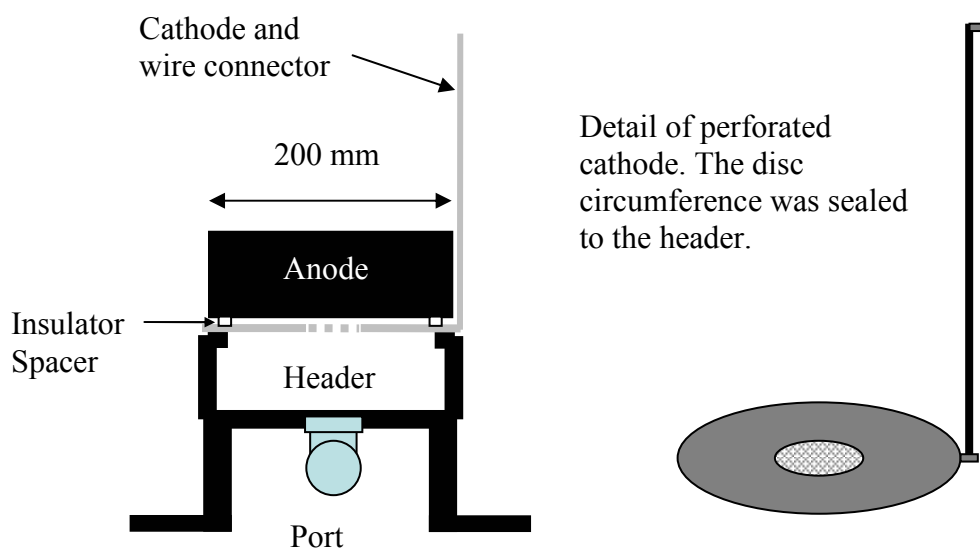


Figure 4-1 Perforated cathode and radial flow over a corroding anode.

It rapidly became apparent that it was difficult to achieve uniform corrosion of a bulk material. Water jetting caused uneven erosion of the anode, tracking of radial flows occurred almost inevitably and large sections of the anode were under-utilized. A crucial observation was that the hydrolysed corrosion products were self-limiting the electroflocculation process by forming a sludge layer on the anode, particularly where water flow was too low to dislodge the sludge. Rotating disc corroding electrodes were not considered because they would require the complication of moving parts and would not necessarily be self-cleaning.

#### **4.1.3 Model 8: corroding anode made of shavings – the Tower.**

A breakthrough was made by realising that the ideal corroding anode material should be, in at least one dimension, smaller than that which could result in a thickness of corrosion-product sludge that prevented further corrosion. That way the fabric of the anode would disintegrate entirely before the corrosion products could foul it. This is the basis of NZ Provisional Patent 537700. The first form considered, but not trialed, was metal foil, either in a single sheet or multiple layers. This was thought to be either too short-lived (single sheet) or prone to the same problems under compression as a single plate (multiple layers).

The next readily available materials considered were aluminium or iron shavings. These had a thickness of less than 0.001 m and a ribbon-like aspect ratio, up to 0.1 m long and 0.05 mm wide, with great variation. Curls and spiral forms were common. Aggregates of shavings could be packed in loose bundles. The shavings were the basis of a porous anode. The porosity did not increase the electrochemically active surface area, due to the low conductivity of the fluid, but did allow a fast fluid flow in the region close to where the shavings were corroded. An inert but porous membrane, in the form of a sock of parka nylon, was used to prevent direct electrical contact between the shavings and the cathode (see Figure 4-2).

After brief initial trials, a moderate scale prototype was developed. The design principles incorporated all that had been gleaned from the previous models; dry electrode connections to prevent contact corrosion, high flow speeds in large reaction areas and a low flow speed zone after the reactions to promote floc formation. It was composed of two tubes of steel forming an annular space which

was packed with aluminium shavings. The tubes were also the cathodes. The resulting device shown in Figure 4-2 held promise but required significant modification to achieve good performance.

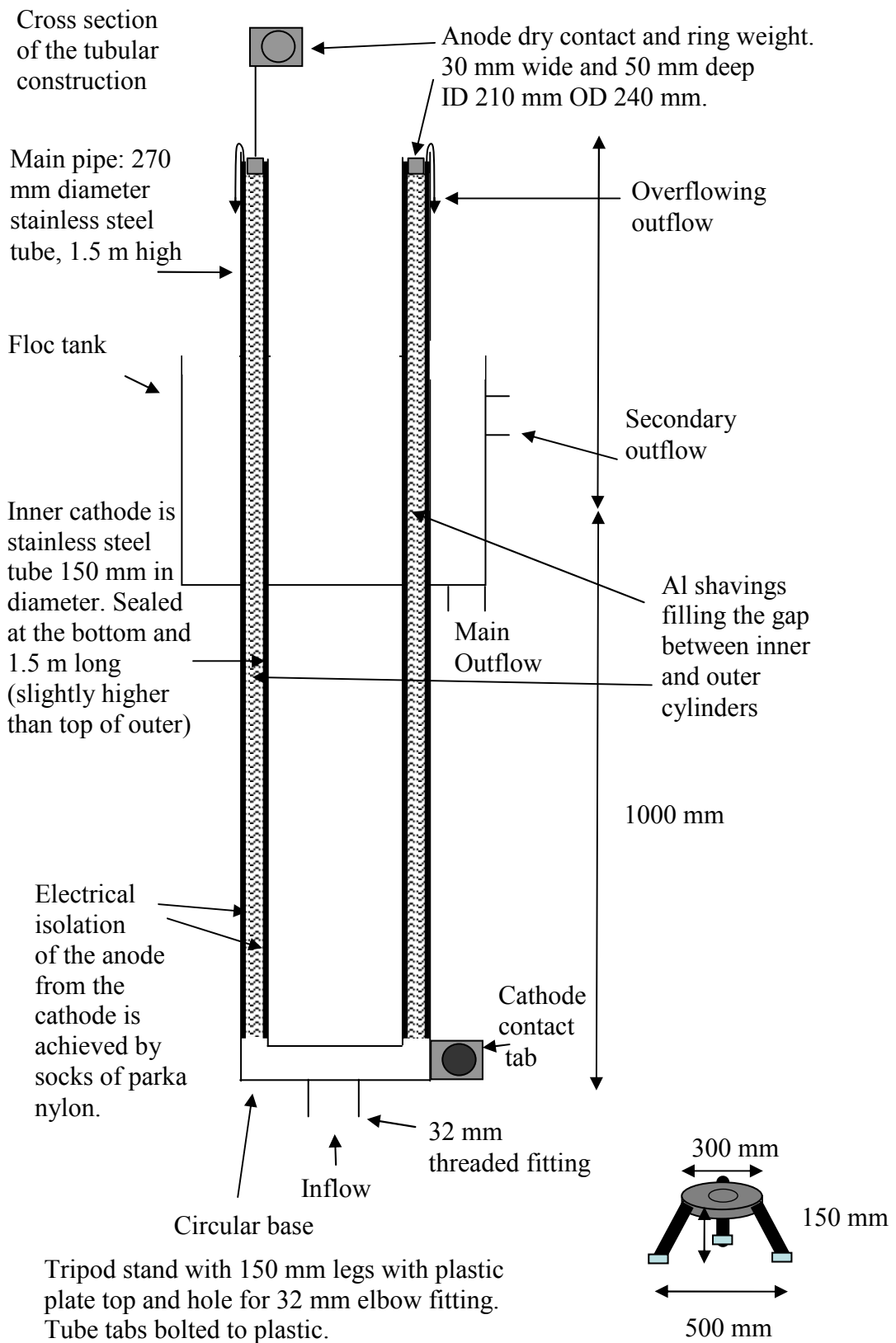


Figure 4-2 Aluminium shavings corroder – the Tower.



Aluminium shavings of 6060 alloy with a scrap value of \$1 kg<sup>-1</sup>, supplied by Ullrich Aluminium of Hamilton from their cutting waste, filled the interior of the Tower and were used as an anode. The composition of 6060 alloy is shown in Table 4-1.

*Table 4-1 Impurities in aluminium Alloy EN AW-6060. All in weight % (Matter Project 2001).*

Element	% in AW-6060
Mg	0.35 - 0.6
Si	0.30 - 0.6
Fe	0.10 - 0.30
Cr	≤ 0.05
Zn	≤ 0.15
Ti	≤ 0.10
Mn	≤ 0.10
Cu	≤ 0.10
Other elements not listed	≤ 0.05
Total other than Mg, Si and Fe	≤ 0.15

Table 4-1 indicates that for levels of up to 100 mg L<sup>-1</sup> of aluminium added by corrosion, the total level of additional metals will be less than 1 mg L<sup>-1</sup>.

Most of the basic operational features of the Tower were discovered during a month of trials at the Hamilton City Council waste water treatment plant. The electrical resistance was 0.5 to 1 Ω with fresh aluminium for a wide range of voltages, indicating that the fluid resistivity dominated. But as the aluminium corroded the total resistance increased. Because the flow through the Tower was not restricted to the zone of corrosion (indeed most of the flow was free to pass through the middle of the annular gap) the highest level of highly active flocculent that could be delivered to the flow in *steady state* was limited to a few mg L<sup>-1</sup> of aluminium, which was barely adequate to floc the terminal effluent. When the flow rate was increased markedly the flow speed in the corrosion zones was sufficient to clear stored corrosion products and produced a transient of outflow with a high dose of floc. However, if a flow rate sufficient to clear the corrosion

products was maintained the steady state outflow was under-dosed. If the flow rate was lowered to 5 L min<sup>-1</sup> at a constant voltage, the immediate effect depended upon the prior history, because of the capacity of the Tower to hold corroded material. This is shown in Table 4-2.

Table 4-2 shows that when the Tower was already loaded with corrosion products and significant partial corrosion of shavings had already occurred then it could effectively be saturated, as indicated by the steadily increasing clearance rate with time. The greater than 100% apparent clearance rate at 5 L min<sup>-1</sup> seemed to be a coincidence whereby many partially corroded shavings finally broke free of the body of shavings. This high apparent clearance rate was subsequently found to be a long-lasting steady effect, based on passive extra-faradic corrosion. The effect appeared to be based on anodic current density, which could be controlled by cell voltage.

*Table 4-2 Corrosion product saturation and greater than faradic clearance from the Tower while processing clarified effluent at the Hamilton City Council Wastewater Treatment Plant. Total aluminium analysed by Hill Laboratories (January 18<sup>th</sup> 2005).*

Elapsed Time (min)	Flow Rate (L min <sup>-1</sup> )	Current (A)	Dissolved Al (mg L <sup>-1</sup> )	Total Al (mg L <sup>-1</sup> )	Apparent aluminium current efficiency.
18	25	5	0.046	3.65	13%
25	20	5	0.048	3.87	17%
35	15	5	0.072	4.35	26%
48	10	5	0.101	5.37	48%
75	5	5	0.179	9.94	178%
85	30	5	0.045	75.2	224%
90	25	5	0.042	1.8	6%
100	40	20	0.063	7.63	68%

Flushing at 30 L min<sup>-1</sup> caused a massive release of corroded aluminium, eventually clearing the Tower of corroded aluminium so that when the flow rate was reduced to 25 L min<sup>-1</sup> a few minutes later, the apparent clearance rate was

very low as the Tower was well below saturation with floc and was largely storing it. If the flow rate was held steady at  $5 \text{ L min}^{-1}$ , products of corrosion were cleared at a rate well below their production rate and the current soon dropped as the metal forming the current path to the outside surfaces of the aluminium shavings became oxidised or coated with products of oxidation. If the flow rate was then increased to  $20 \text{ L min}^{-1}$ , the products of corrosion were largely cleared and the current was more stable, declining to half after several hours of operation. At higher flow rates the products of corrosion were cleared almost fully, but in insufficient concentration to cause flocculation. This is shown in Table 4-3.

Table 4-3 shows that effect of poor clearance of corrosion products. This tended to happen at the top, which was the exit point of the fluid, and led to a sudden drop in current that could be relieved only by disturbing the top layer, and cured only by replacing the entire body of aluminium. This problem was slowed, but not prevented, by the use of an aluminium skewer (0.008 m diameter rod) pushed down into the annular space. Because the skewer was wet, it suffered from the same slow corrosion problem as the mid-space shavings and had to be polished frequently. While it was hoped that the bed of shavings would sink and spread sideways to replace the corroded shavings, this did not occur, and the bed had to be re-distributed manually or replaced.

At flow rates between  $5 \text{ L min}^{-1}$  and  $10 \text{ L min}^{-1}$  the Tower was able to cause HTE to flocculate for a limited time, until corrosion products caused the current to collapse due to increased electrical resistance and increased hydrodynamic resistance in the reaction zone. The effective clearance of the Tower with fresh aluminium could be consistently above 100% for over 1 hour at a high flow rate, reflecting an apparent current efficiency of greater than 100%. This cannot be explained solely by consumption of the dissolved oxygen in the water, because even if the dissolved oxygen content had been  $10 \text{ mg L}^{-1}$ , the additional aluminium added would have been just over  $1 \text{ mg L}^{-1}$ . The dissolved oxygen could not be replenished easily in the Tower because it is sealed from the atmosphere. The most likely explanation in this case came from visual observation of the fresh outflow, in which flecks (less than 2 mm size) of partly corroded aluminium were present. At very high voltages the aluminium shavings are broken up as well as having their surfaces corroded, resulting in release of un-

corroded aluminium that contributes to the total aluminium measured in the outflow, as measured by acid digest method. However, the possibility of extra-faradic aluminium corrosion was now evident and considered thoroughly in the tests and trials that followed.

*Table 4-3 The effect of high cell voltage on aluminium corrosion. Total aluminium analysed by Hill Laboratories (January 24<sup>th</sup> 2005).*

	Elapsed Time (min)	Flow Rate (L min <sup>-1</sup> )	Voltage (V)	Current (A)	Total Al (mg L <sup>-1</sup> )	Apparent aluminium current efficiency.
Filtered Outflow	-	30	35	25	0.1	35
Terminal Effluent	-	-	-	-	0.2	-
Inflow	-	15	20	20	6.57	157%
Initial result at normal polarity	-	-	-	-	-	-
Polarity Reversal	0	15	-20	17	7.03	-
Reset to normal Polarity	5	30	35	35	11.7	244%
	30	30	35	35	11.3	236%
	45	30	35	35	11.1	232%
	60	30	35	30	10.9	195%
	90	30	35	25	8.59	128%

To test the effectiveness of flocculation, a trial of porting the outflow from the flocc tank directly to a filter was carried out. The flow rate was 5.5 L min<sup>-1</sup> and the current was 17.5 A. The filter was cylindrical with a radius of 0.1 m so the filter flow speed was 14 m hour<sup>-1</sup>, which is relatively rapid. The filter was loaded with a

300 mm bed of Works Filter Systems' Silicon Sponge 14/25 mesh grade (fine) media. The turbidity of the inflow to the electrolyser was 7 NTU. The turbidity of the filtered outflow versus time is shown in Figure 4-3.

Figure 4-3 shows that a fast flow speed of  $14.3 \text{ m hour}^{-1}$  could be filtered effectively. However, loading to the capacity of the filter and filter breakthrough could begin within half an hour of operation.

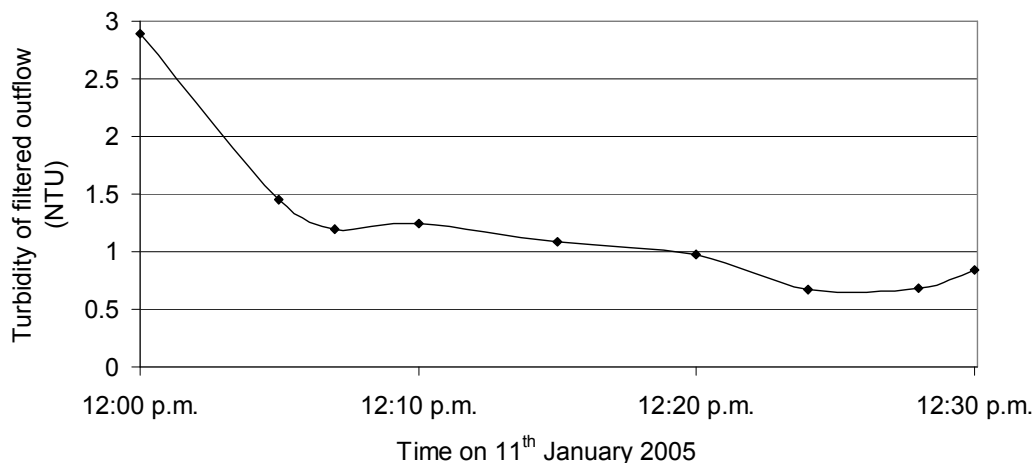


Figure 4-3 Immediate turbidity after filtration of outflow from the Tower.

Another trial with lower filter flow speed was carried out. While the Tower was operated at a fixed cell voltage of 35 V and flow of  $25 \text{ L min}^{-1}$ , only part of the outflow was directed to the filter and the filter flow speed was  $3 \text{ m hour}^{-1}$ . The turbidity of terminal effluent after processing and filtration are shown in Figure 4-4.

The freshly processed effluent and after filtration traces in Figure 4-4 show that electrolysed effluent was loaded with floc and that the floc was coarse enough to be filtered at a moderate speed. The amount of dissolved material, shown in the filtered at  $0.45 \mu\text{m}$  trace, was not changed significantly by electrolytic processing.

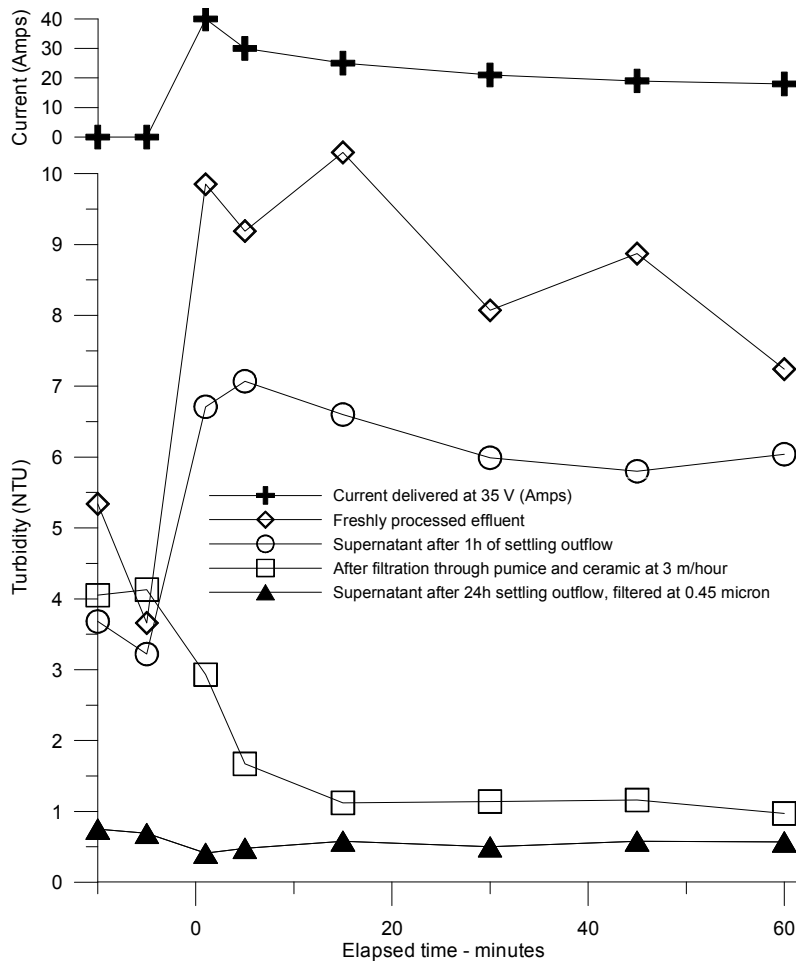


Figure 4-4 The turbidity of terminal effluent at different stages after processing in the Tower at 35 V (January 26<sup>th</sup> 2005).

#### 4.1.4 Model 9: the Flume processor.

The Flume was developed in response to the need for better clearance of corrosion products from a corroding anode. The crucial feature parameter was the flow speed in the vicinity of the site of production of flocculent. Prior studies on rivers (Hjulstrom 1935) indicate that for particles up to 0.001 m in size, flow speeds greater than 0.1 m.s<sup>-1</sup> will favour transport to deposition, and as the flow speed approaches 1 m s<sup>-1</sup> erosion and transport will become dominant. Hence, high flow speed was expected to encourage good clearance of floc from the shavings. The simplest measure of the flow speed was made by turning the inflow off briefly then on again before the shavings drained significantly and measuring the delay before the on-flow reached the outflow. This could be applied at any time to see how the flow speed was changing during trials. The steady state flow speed could be calculated from the flow rate divided by the cross-section of the flow, which was proportional to the thickness of the flow.

The Flume design is shown in Figure 4-5. A 2.5 m length of galvanized mild steel U-section was cleaned with dilute  $\text{HNO}_3$ , and used as a cathode. Parka-nylon cloth sheet (uncoated, sourced from Duncan's Canvas, Hamilton) with a thickness of 0.1 mm was used as the insulating lining membrane on the inside of the U-section.

A number of optimisations came together in this design. The current distribution was in a dry zone yet the subsequent path to the anode reactions zone was short. The fluid layer was thin and forced close to the cathode by gravity. Hence, the flow speed was high in the vicinity of the anodic reaction and the rest of the anode was dry. The gap between the anode and cathode was very low. The consumed shavings were replaced by gravity, and the entire bed could be lifted or shaken easily. Replenishment of the shavings with fresh stock could be achieved with minimal downtime. The elongated aspect ratio of the Flume in parallel with the flow direction meant that the flow speed was high. The maximum steady state dose, clearance of corrosion products and longevity of operation were expected to be greatly improved in comparison to the Tower. The flow head was also reduced.

The flow was mainly down the anode side as anolyte. The rate of seepage across the membrane was in the range of 0.1% to 1% of the total flow, resulting in a small catholyte flow. The absolute rate of plating-out would be expected to be low due to the low catholyte flow but the fraction of aluminium or chromium plated out of the catholyte was unknown.

The first trials of the Flume were made using tap water of pH 8 that was modified to have conductivity similar to tannery effluent by addition of NaCl. A 3.3 V SMPS with very little low frequency voltage ripple was used as a power supply. There were immediate improvements. Instead of decaying, the current steadily increased over several hours, and flocculation was reliable, even without other contaminants to build on. The basic physical parameters of the Flume during this operation are shown in Table 4-4.

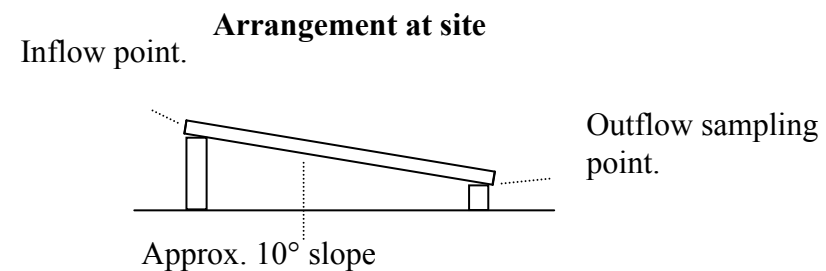
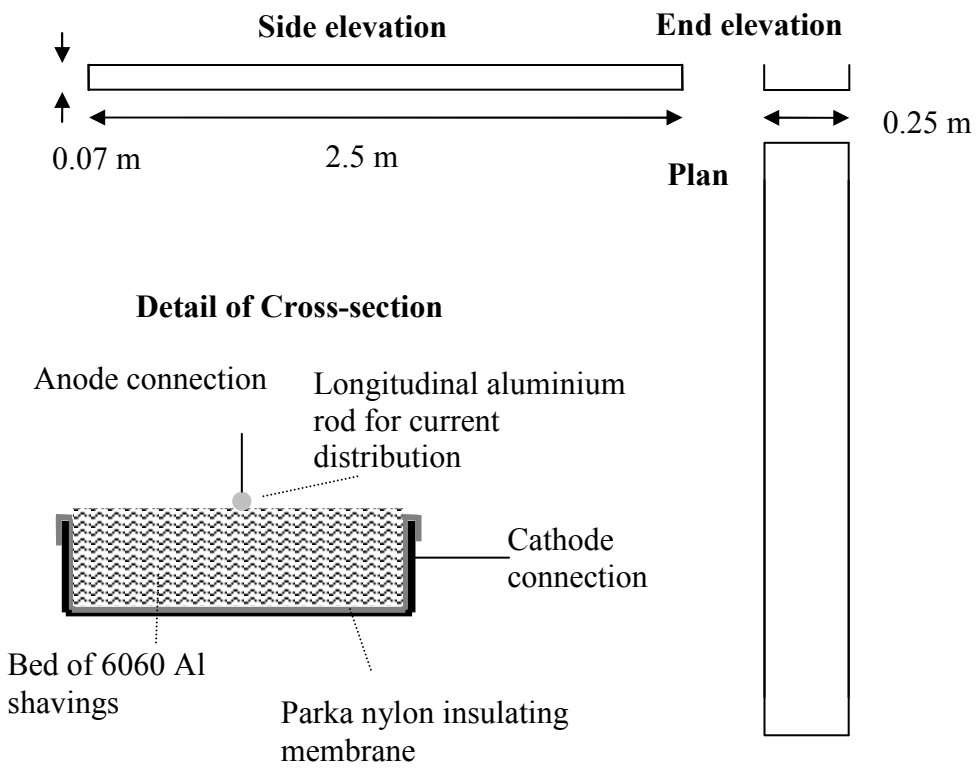


Figure 4-5 Model 9 system - the Flume processor.

Table 4-4 Test flume basic parameters.

Parameter	Value	Unit
Slope	10	degrees
Width	0.15	m
Length	2.5	m
Minimum head	0.20	m
Bottom area	0.375	m <sup>2</sup>
Current	7.5	A
Current density based on bottom area	20	A m <sup>-2</sup>
Thickness of shavings	0.07	m



Table 4-4 shows that for a moderate current of 7.5 A the current density over the bottom area would be 20 A m<sup>-2</sup>.

The Flume was operated with flow of saline but without power, in order to focus on flow thicknesses and speeds. The results are shown in Table 4-5.

*Table 4-5 Flow characteristics of the Flume with aluminium shavings in place, using salted tap water without electrical power.*

Flow (L min <sup>-1</sup> )	Thickness of flow the top of the Flume (m)	Thickness of flow at flume bottom (m)	Flow speed the top of the Flume (m s <sup>-1</sup> )	Flow speed the bottom of the Flume (m s <sup>-1</sup> )
13	0.03	0.005	0.048	0.289
6	0.015	0.003	0.044	0.222
24	0.07	0.010	0.038	0.267
20	0.02	0.008	0.111	0.278

Table 4-5 shows that for a wide range of flow rates the flow speed at the bottom of the Flume was well in excess of 0.1 m s<sup>-1</sup>. It also shows that the flow was in a thin sheet for flows up to 20 L min<sup>-1</sup>. Hence, it was expected that any corrosion products would be removed from the shavings and mix with the effluent. Subsequently, the Flume was taken to a tannery and tested on real effluent.

## **4.2 Treatment of landfill leachate**

### **4.2.1 Rational for treatment**

Leachate from the Hamilton municipal landfill, in the Waikato, is produced at a variable rate depending on seasonal rainfall, though usually 2 m<sup>3</sup> day<sup>-1</sup>, and is pumped back to the Hamilton City Council waste water treatment plant for incorporation in municipal sewage treatment. The conductivity also varies with rainfall patterns but, unlike municipal sewage, it can have a higher conductivity (8000 μS cm<sup>-1</sup>) when rainfall has been high due to leaching of salts from the soil.

Since the dried solid matter resulting from the municipal waste water treatment process is delivered to the landfill, a closed circuit is apparent with steadily increasing amounts of recalcitrant material in the circuit. While the landfill is due to be closed within a few years the leachate circuit will remain active for many decades – gradually running down as contaminants escape the leachate collection system. It is necessary to remove contaminants from the leachate and convert them into a material that does not break down. The purified water would ideally be of sufficient quality to be delivered to storm-water drains.

#### **4.2.2 Materials and methods**

The Flume and power supply were transferred to the landfill site and a brief trial was conducted.

#### **4.2.3 Results**

The conductivity of leachate was found to be  $8000 \mu\text{S cm}^{-1}$  in June, which is high enough to enable cost-effective processing. However, the pH was 7 which prevented flocculation by corrosion of aluminium.

#### **4.2.4 Proposed leachate processor**

##### **Strategy: breaking the loop**

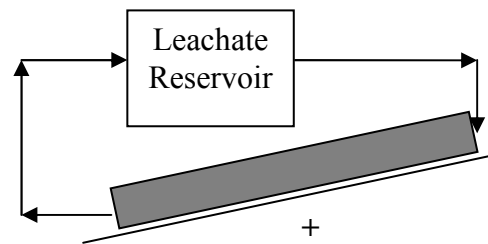
If the goal of artificial wastewater treatment is to remove noxious impurities and return the purified water to the natural water cycle, the part that is often overlooked is disposal of the removed impurities. If these impurities are not dealt with effectively then they can re-enter the natural water cycle. This is particularly crucial for landfill leachate. The traditional strategy seems to have been slowing the rate of re-entry to that which the natural water cycle can tolerate. This leads to a large storage of noxious contaminants in a contained loop that must be continually re-processed.

##### **Schematics**

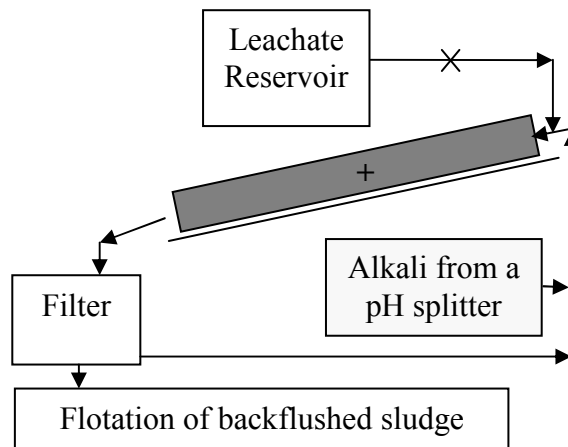
The schemes shown in Figure 4-6 are a possible means of further concentrating the contaminants found in landfill leachate and producing a purified fluid that may be discharged to storm-water drains (see §5.4 for a description of a pH splitter). These means are likely to succeed if the pH and effective conductivity are

manipulated correctly. The more interesting challenge is what to do with the material that is produced by back-flushing the filters shown in Figure 4-6. If the back-flush water is further treated by electroflotation and a concentrated sludge is produced then the sludge can be dried to a combustible form. The final form would be a metal-rich ceramic with no organic toxins.

A. Plating mode with porous electrode as collection cathode for trace metals. High re-circulated flow, low voltage and only very current fraction for plating. The anode material must be benign, with large area to avoid making chlorine compounds.



B. Flocculation mode with porous electrode as corroding anode. Reservoir fluid is added until there is enough liquid to run the filter then closed off. After power-on the floc is captured in a standard filter. The filter outflow is re-circulated and the pH is raised sufficiently to make the flocculation effective, while the electrolyser voltage is set to lower the pH to reduce metal solubility.



C. Continuous flocculation mode with porous electrode as corroding anode. Floc is captured in a standard filter. The reservoir fluid is pH-adjusted by a pH-splitter to make the corrosion-flocculation effective, while the electrolyser voltage is set to lower the pH to reduce metal solubility. Acidic disinfectant from the pH splitter conditions the outflow to a standard that can be discharged to a storm-water drain. Catholyte brine enhances conductivity without salinating the main flow significantly.

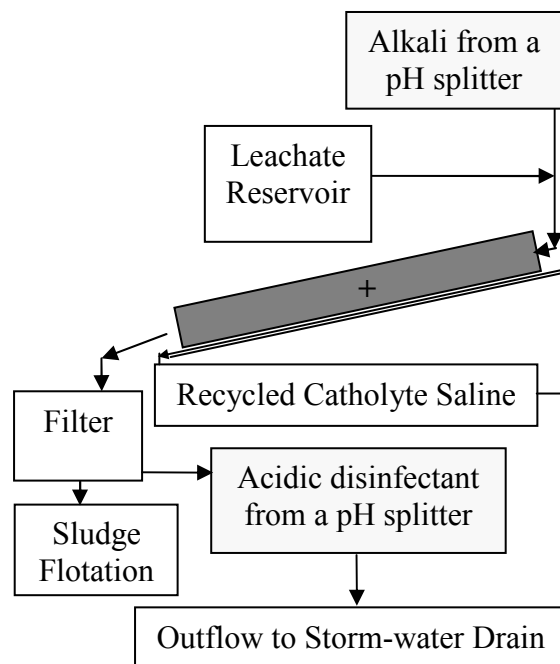


Figure 4-6 Bi-modal (A and B) and uni-modal (C) treatment schemes.

#### **4.2.5 Discussion and conclusion**

Processing of leachate is hampered by the neutral pH of the fluid. However, the low flow rate and difficulty of treating it by any other method provides an opportunity for design of a specialised small-scale electrolytic processor. Catholyte salinisation and pH adjustment, as described in §5.6 was considered as a means of overcoming the low pH of the leachate. Alternatively, an anode made of iron ribbons will produce a less pH-sensitive floc.

### **4.3 Pulp mill effluent**

#### **4.3.1 Rationale for treatment**

Pulp mill effluent has many forms depending on the type of pulp process and the stage of processing at which the effluent is drawn. Two effluent streams are produced from the kraft process, one extremely acidic and the other extremely alkaline. These are not mixed until both streams have cooled from the temperatures of the early flows that can exceed 60 °C. The most problematic contaminant is usually described as “colour” often meaning dissolved phenolic substances (tannins) that resists biological degradation or filtration and stains the water brown even when present in very low concentrations. Such effluent is produced at large rates – typically 1 m<sup>3</sup> s<sup>-1</sup>.

#### **4.3.2 Materials and methods**

The conductivity of a sample of alkaline effluent (pH 9) from the clarifier ponds of a kraft process pulp mill in New Zealand was only 1600 μS cm<sup>-1</sup>, an order of magnitude lower than tannery effluent. It was determined that a trial using a Flume in the laboratory (a smaller version of the Flume - see §5.2.2) would be required. A flow rate of 3.4 L min<sup>-1</sup>, current of 10.5 A and cell voltages of between 10 V and 15 V were used. The fluid had a temperature of 13 °C.

#### **4.3.3 Results**

As Table 4-6 shows electrolytic processing at 3 A (L min<sup>-1</sup>)<sup>-1</sup> was ineffectual, despite the high cell voltages used. The cell resistance increased steadily.

*Table 4-6 Colloidal precipitate produced by electroflocculation of low-conductivity alkaline pulp mill effluent.*

Cell Voltage (V)	Current (A)	Time on September 22 <sup>nd</sup> 2005	24 hour supernatant turbidity (NTU)
10	10.5	16:00	28
15	10	16:27	30

#### **4.3.4 Discussion**

The low conductivity of the pulp mill effluent meant that the electrical cost of effective treatment, based on using unmodified electrolyte, would be more than 1 kWh m<sup>-3</sup>. This is unacceptable when the plant flow rate is 1 m<sup>3</sup> s<sup>-1</sup>, not only from the point of view of operating cost, but also from the size of the power supply (greater than 3.6 MW). This inspired the work described in §5.6, to increase the effective conductivity of fluids during electrolysis without significantly increasing the salinity of the outflow compared to the inflow.

A field trial using high temperature water (up to 70° C at the exit from the mill) is likely to produce some interesting results depending on the effect of temperature on corrosion and flocculation rates. It is possible to exploit the two streams of opposing pH (acidic and alkaline) by making them catholyte and anolyte respectively.

#### **4.3.5 Conclusion**

The pH of the alkaline stream of effluent is ideal for electroflocculation but the attempted treatment was ineffectual because the conductivity was too low. A means of increasing the effective conductivity of the effluent (such as described in §5.6) is crucial to the cost effectiveness of a full scale operation.

## **4.4 Treatment of tannery effluent**

### **4.4.1 Introduction**

#### **History and Geography**

Raw tannery effluent is particularly noxious, because the chemicals used in the tanning process include chromium compounds, tissue preservatives, fungicides, and organic dyes. The pH tends to be high due to addition of lime. Electrolytic processing is feasible because the high sodium chloride content of the effluent gives a high electrical conductivity. While research on the subject dates back to early in the 20<sup>th</sup> Century (Landreth 1914; Fassina 1938), commercialisation has not occurred, perhaps due to excessive power consumption. Other researchers have produced promising results with rendering plant effluent (Tetrault 2003), but with cell voltages of 50 V (Tetrault, A. 2003, pers. comm., September 2003). Toward the end of 2004, an opportunity arose to trial an electrolytic effluent processor at a tannery in the Waikato region of New Zealand.

#### **Emphasis on flocculation and flotation**

The high suspended solids and chromium content of the DAF outflow set the emphasis on electroflotation and electroflocculation. Although the final goal for the tannery company was to reduce the coliform count in the terminal effluent, direct electrosterilisation of the tannery effluent was considered to be prohibitively energy intensive and counter-productive to subsequent oxidation pond function.

Because the main treatment function was flocculation, the processing systems were designed to corrode an anode with high current efficiency. In addition it was hoped that the previously observed floc-flotation function could be achieved. Hence, electrolytic processors specialised for electroflocculation with simultaneous bubble production were used. The first model trialled was the Tower and the second was the Flume processor. These used aluminium shavings as a corroding anode.

## **Rationale and goal**

If the standard approach to water purification research had been followed, the first task would have been formulation of a model effluent. This would be used to develop a process that performs reliably and repeatedly in controlled laboratory conditions. Because there was no readily available realistic model of tannery effluent, an active research case study had to be carried first out in order to determine the parameters of a model effluent. Field experience also gives a more realistic view of the challenges that would have to be met by any commercial processing system so that they could be incorporated at an early stage of the development sequence.

The primary goal of the trials was to determine whether anodic dissolution of aluminium could produce a flocculent that could economically remove both dissolved chromium and suspended solids while leaving low residual aluminium, despite uncontrollable variations in inflow salinity, turbidity and pH. This is effectively a test of the hypothesis in §1.7. The effectiveness was measured in terms of both achievable outflow quality and the time it took for flocculation and settling to occur. The trials were carried out in parallel with jar-testing using standard chemical flocculants (PFS, PAC1 and PAC23) for comparison.

### **4.4.2 Trials**

A total of six trials with the Flume were carried out over a 3 month period. Data obtained from these trials were used to investigate the following aspects of function: removal of suspended solids; floc removal by flotation; treatment of moderate-to-high pH effluent; treatment of near-neutral pH effluent; cost effectiveness of chromium removal; the effect of processing on microbes.

### **4.4.3 Site and trial conditions**

The tannery is situated adjacent to a river. There is also a rendering plant on-site that processes carcasses of farm animals. The rendering plant effluent is heavily laden with organic matter that is treated by a standard sequence of processes, including a DAF plant, aerated oxidation-settling ponds, and a wetland drainage scheme. A site process diagram is shown in Appendix B. The tannery effluent is treated in a separate DAF and oxidation pond (the Hides and Skins (H&S) pond

before being added to the rendering plant waste stream at the oxidation-settling stage (pond 3), resulting in an average daily total effluent flow of 1350 m<sup>3</sup>, of which 500 m<sup>3</sup> is from the tannery. The final effluent is discharged from the last settling pond (Pond 6) to the river in times of high river flow and is otherwise discharged as irrigation to farmland.

The tannery DAF uses polymer coagulant (Crystal Floc type B 340L) dosed at a constant rate of 7 mg L<sup>-1</sup> from a stock of 2500 mg L<sup>-1</sup> and generally treats a constant flow from a balance tank which supplies the DAF inflow. The composition of the inflow was subject to sudden variation muted slightly by the balance tank. For example, the DAF outflow pH varied from 9.6 to 8.6 in 6 hours, and was low as 7.1 on days when low quantities of lime were added, or the lime was neutralised by acid as a part of the usual tannery process sequence. The measured electrical conductivity of the tannery effluent always exceeded 1 S m<sup>-1</sup> and never exceeded 2 S m<sup>-1</sup>. It changed by up to 10% in an hour. The conductivity was due largely to the sodium chloride content (0.1 mol L<sup>-1</sup>) and hydrated lime (up to 0.001 mol L<sup>-1</sup> at the highest pH). The average suspended solids content of the DAF outflow for 2004 was 1000 mg L<sup>-1</sup>, with a conservatively estimated 15 mg L<sup>-1</sup> of chromium. The residual polymer floc content in the DAF outflow was unlikely to have exceeded a few mg L<sup>-1</sup> but even this level was likely to be significant as a coagulant.

Data for the DAF outflow is approximated by historical sampling from the oxidation pond which receives the DAF outflow – the H&S pond, and this is shown in Table 4-7. For comparison, corresponding data for pond 6, the source of terminal effluent, is shown in Table 4-8.

Because the tannery DAF effluent varied in composition so quickly, the trials were usually conducted within a 30 minute period. It took 10 minutes to stabilise the Flume to new conditions, only three samples for different process conditions could be taken in this time. In some cases the pH dropped so quickly that a trial effectively became a test of performance during a pH ramp.



Table 4-7 “H&S pond” (supplied by DAF outflow) analytical data supplied by the tannery company.

Date	Suspended solid (mg L <sup>-1</sup> )	E.coli (cfu/100mL)
15-Apr-04	1340	
13-May-04	1310	
23-Jun-04	1510	139000
13-Jul-04	1460	299000
25-Aug-04	1140	816000
19-Sep-04	790	>2420000
13-Oct-04	1440	
17-Nov-04	877	86000
15-Dec-04	973	41000
12-Jan-05	717	173000

Table 4-8 Pond 6 (source of final effluent) composition data - supplied by the tannery company.

Date	Electrical conductivity (S m <sup>-1</sup> )	Suspended solid (mg L <sup>-1</sup> )	E.coli (cfu/100mL)
14-Apr-04	0.995	101	57900
5-May-04	0.798	100	2880
9-Jun-04	0.782	193	6690
7-Jul-04	0.75	156	43500
4-Aug-04	0.771	240	141000
1-Sep-04	0.77	158	92100
29-Sep-04	0.806	180	9060
1-Nov-04	0.871	219	7800
24-Nov-04	0.796	145	10000
22-Dec-04	0.802	100	9700

#### 4.4.4 Materials and methods

##### Electrolytic processors

The Flume processor was chosen for use at the tannery, because it was specialised for electroflocculation (see §4.1.3 and §4.1.4 respectively). The flow schematic is shown in Figure 4-7.

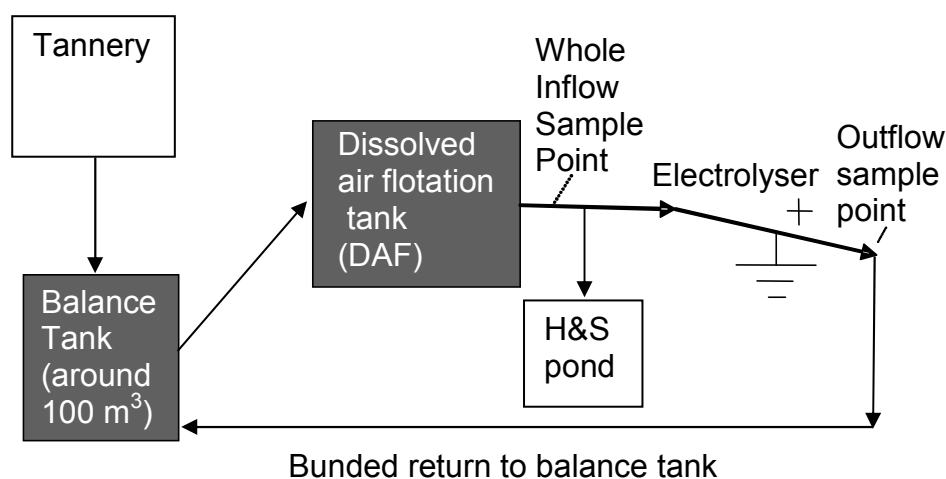


Figure 4-7 Flow schematic for tannery effluent trials.

##### Power supplies

A 3.3 V voltage regulated 0 to 20 A switch-mode power supply (SMPS) and a continuously voltage-adjustable full-wave rectifier able to deliver 0 A to 50 A, known as the “50 A full-wave rectified supply,” were used (see §2.6.1).

##### Costs of treatment

The cost of PACl bought by the tonne in New Zealand is \$20 per kilogram of aluminium (Orica Chemnet sales staff 2005, pers. comm., 3 May). The cost of scrap machine shavings from Ullrich Aluminium in Hamilton was \$1 per kilogram of near-pure aluminium (Wright, S. 2005, pers. comm., April 2005 and 28 November). This highlights the major cost advantage of using a solid source of flocculent, and freight costs would be lower due to not transporting a heavy liquid solution that is 5% active metal by weight. The cost of electricity was assumed to be \$0.15 per kWh.

## **Analytical tools**

In the field a portable pH meter, supplied by HamChem Ltd, Hamilton, New Zealand and the Hach 2100P Turbidimeter were used (see §2.5.2).

## **Allowance for extra-faradic corrosion**

More aluminium was corroding in the anodic alkaline conditions (see Figure 1-4) than would be predicted by faradic estimation (DiBari 1970; DiBari et al. 1971; Barteneva et al. 1999). Storage of corroded aluminium (floc) within the body of the shavings had already been observed during trials with the Tower at high flow rates using near-neutral terminal effluent and 35 V cell voltage. Those trials also confirmed the possibility of total corrosion at up to three times the faradic rate (see §4.1.3). In order to allow for the possibility of extra-faradic corrosion, and for the purpose of calculating the operating cost of electrolytic processing, the amount of consumed aluminium estimated by faradic means was tripled. Even though the current efficiency of oxygen production was significant and analysis of the total aluminium in the outflow indicated faradic or sub-faradic clearance into the water, the triple faradic dose was used as a conservative reference.

## **Effects of pH and alkalinity**

The pH of the water to be treated is crucial to the effectiveness of Al-based flocculation because it determines the long-term solubility of  $\text{Al}(\text{OH})_3$ . A pH of 6.2 is usually considered to be the point of minimum solubility for aluminium (Pontius 1990) and this is well below the pH of the tannery effluent. The current density at the surface of the metal shavings determines the localised acidification, which is depletion of  $\text{OH}^-$  or repletion of  $\text{H}^+$ , which can occur as a result of either hydrolysis of  $\text{Al}^{3+}$  ions or direct oxidation of  $\text{H}_2\text{O}$ . This means that the hydrated aluminium species formed close to electrodes are more likely to be the cationic or polycationic forms such as  $\text{Al}_{13}\text{O}_4(\text{OH})_{24}^{7+}$  (Lu, G. et al. 1999; Qu et al. 2004). These species develop to form stable floc particles when they are exposed to the higher pH of the bulk solution. The high protein content of tannery effluent raised the alkalinity of the fluid so it could be treated by an acidic flocculent.

#### 4.4.5 Removal of suspended solids

An experiment was performed to test the effectiveness of the Flume processor at removing suspended solids and the results were compared with jar trial flocculation using PFS. The effluent used was DAF outflow and after processing it was allowed to settle for an hour. Suspended solids in the supernatant were measured by drying. Results are shown in Figure 4-8.  $\text{Al}_2\text{O}_3$  equivalents were used for molar comparisons of aluminium and iron dosage.

The first positive indication that an electro-flocculator using an aluminium shavings anode was capable of treating tannery effluent is shown in Figure 4-8. A heavy electrolytic dosage of around  $8 \text{ A (L min}^{-1}\text{)}^{-1}$  resulted in excellent flocculation, comparable with heavy treatment by PFS (at three times the threshold dose for flocculation). PFS addition also caused formation of black material which remained suspended in the supernatant for many days. This material was most likely to have been a sulphur compound, formed by reaction of the PFS with sulphur compounds in the effluent. Hence iron anodes were not considered suitable for treatment of this particular tannery effluent.

At moderately alkaline inflow pH, between 8 and 10, the Flume processor was able to reliably and repeatedly cause flocculation of the DAF outflow using the anodic corrosion products of 6060 aluminium alloy shavings as the flocculent. When the inflow pH was lower than 8, the alkalinity was insufficient to enable good flocculation. At the highest inflow pH experienced, above 10, flocculation was poor and the residual aluminium level was high. A range of pH drops from inflow to outflow were observed but it was difficult to distinguish the effect of the rapidly varying inflow pH from the effect of the process.

The electrical resistance when passing tannery effluent was low, less than  $0.5 \Omega$ . This was probably because gravity was compressing the shavings against the membrane. The resistance often dropped slightly from its initial value during the first hour of operation to a level that remained steady for up to several hours. This indicated that the clearance of corrosion products was much better in the Flume than in the Tower.

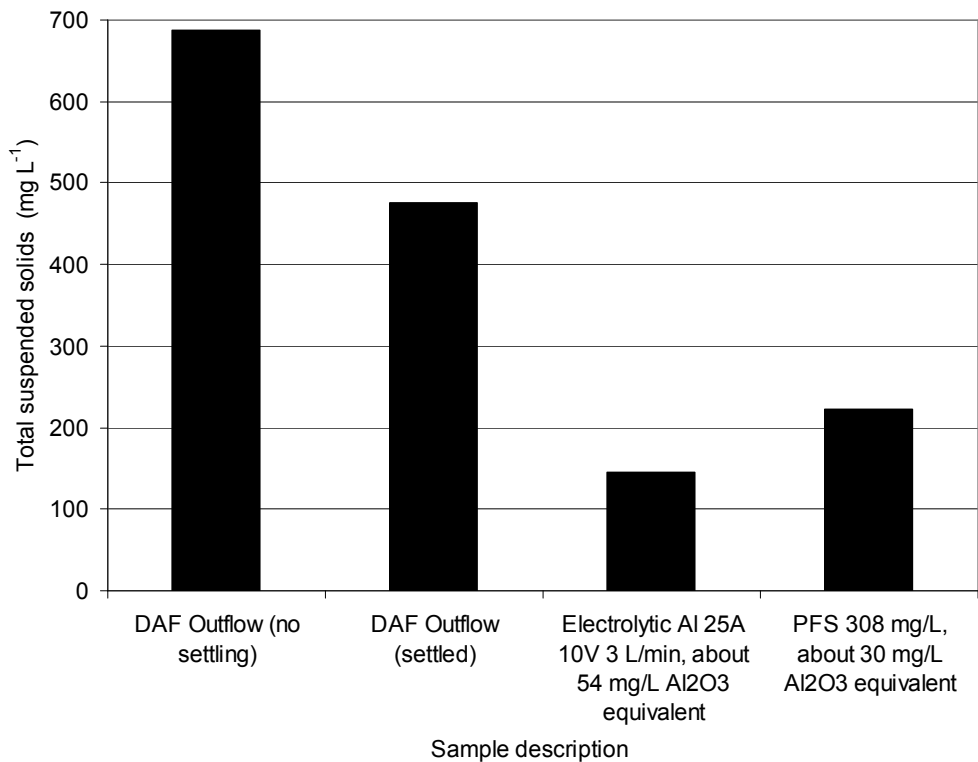


*Figure 4-8 Comparison of electrolytic treatment with PFS dosing for reducing supernatant suspended solids in DAF outflow (inflow to Hides and Skins Pond). One hour settling times were used (March 4<sup>th</sup> 2005).*

#### **4.4.6 Floc removal by flotation**

Floc that formed within a few minutes could be floated to the surface by the fine bubbles that travelled out of the Flume. This floc could be decanted, thereby removing a considerable fraction of the suspended solid including flocculated chromium, without requiring settling or filtration. If the portion of the liquid left after decanting was allowed to settle, it tended to produce a less turbid supernatant than if the early decanting had not been applied. A schematic is shown in

Figure 4-9. Results for the trial of this method, on 8th April 2005, are shown in Figure 4-10. The inflow pH was  $8.5 \pm 0.5$  and the effluent pH was lowered slightly by the process. Cell voltage was 3.6 V dc (full-wave rectified but not smoothed) and the current was 30 A dc into 6 L min<sup>-1</sup> of DAF outflow.

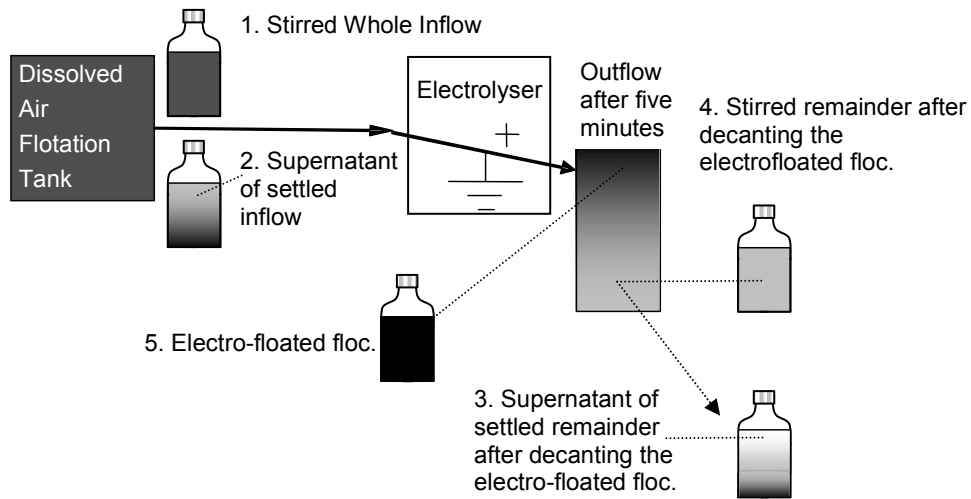


Figure 4-9 Schematic of electrolytic processing, followed by electroflotation then mixing or settling. Sample numbers 1 to 5 are used in Figure 4-10.

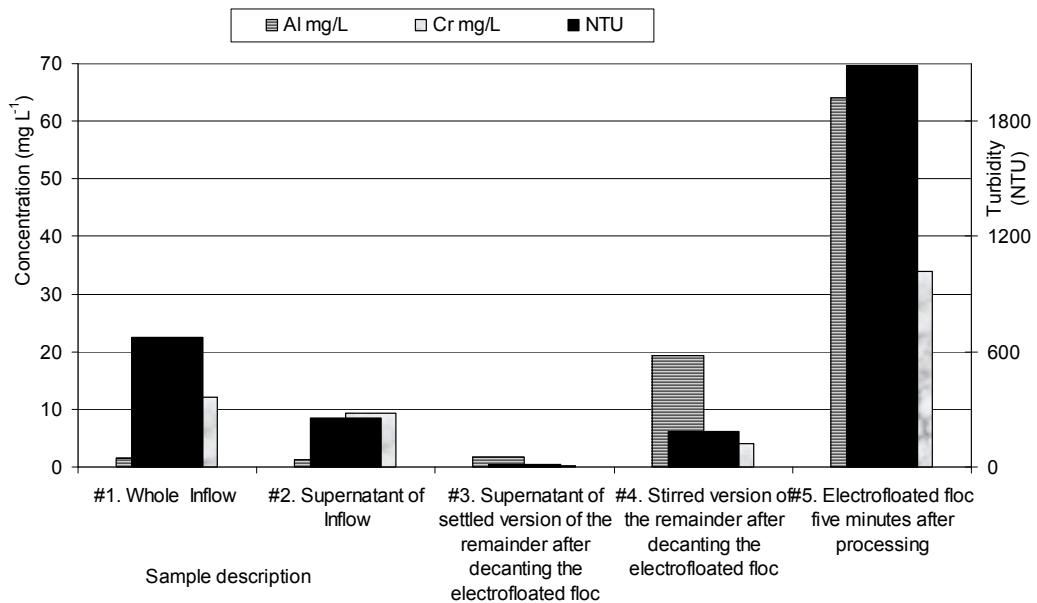


Figure 4-10 The turbidity and metal concentration at the sample points shown in Figure 4-9. This shows the improvement due to removing the electro-floated floc that formed less than five minutes after processing (April 8<sup>th</sup> 2005).

Figure 4-10 shows that for whole DAF outflow turbidity of 600 NTU, passive settling for 72 hours lowered the supernatant turbidity to 250 NTU. For processed

fluid, after decanting the floated floc within five minutes, the remainder settled to give a supernatant turbidity of 10.6 NTU in the same time period. The vast majority of the settling of the processed fluid occurred within 4 hours. When the settled processed fluid was re-stirred, it had a turbidity of 187 NTU. Similar trends were found for chromium content. If the floc was not decanted, it eventually de-gassed and largely settled. However, over many trials the supernatant turbidity achieved by this method was always above 15 NTU. This reinforced the effectiveness of the flotation-decanting-settling sequence, which removes positively and negatively buoyant portions of the flocculated suspended solid in sequence.

The average aluminium concentration of all the outflow components, for the trial on 8<sup>th</sup> April 2005, was 32 mg L<sup>-1</sup>, equivalent to 60 mg L<sup>-1</sup> of Al<sub>2</sub>O<sub>3</sub>. This is high, but appropriate for the amount of suspended solids to be captured in floc. The aluminium concentration in the supernatant after flotation and settling was 1.7 mg L<sup>-1</sup>, just slightly higher than in the DAF outflow, and is the level that would be expected in water of pH 8.4 (see Figure 1-5). Hence, the amount of aluminium in the final outflow from Pond 6 after settling is unlikely to be increased significantly by electrolytic processing of the entire tannery effluent flow, because the pH of Pond 6 is near-neutral with little variance, maintaining the low solubility of aluminium. However, the total amount of aluminium in all the collected sludge would be increased by one or two orders of magnitude.

#### **4.4.7 Treatment of moderate to high pH effluent**

A trial was conducted to test the effectiveness of electrolytic treatment for high pH DAF outflow and compare it with chemical flocculation using PACl. The DAF outflow had a pH of 9.9 and conductivity of 1.2 S m<sup>-1</sup> during the trial. The conditions for the trial are shown in Table 4-9.

As shown in Table 4-9, the faradic dose was 25 mg L<sup>-1</sup> Al<sub>2</sub>O<sub>3</sub>-equivalent of aluminium, but the measured total aluminium at the highest flow rate was equivalent to 75 mg L<sup>-1</sup> Al<sub>2</sub>O<sub>3</sub>, indicating that the level of corrosion was indeed three times faradic. According to Table 4-5 and §4.1.4, a flow rate of 10 L min<sup>-1</sup> should be sufficient to transport the corrosion products out of the Flume. At 3 L min<sup>-1</sup>, with similar current and voltage, the level of total aluminium in the outflow

was similar to that at 10 L min<sup>-1</sup> despite the tripled dose, indicating poor clearance at the lower flow. The costs for electrolytic treatment are shown in Figure 4-11, using the electrolytic process conditions shown in Table 4-9, and reflect an assumption of triple-faradic consumption of aluminium. Costs are based on industrial sized lots of PACl (1000 L IBC), commercial electricity rates and the scrap aluminium shavings price.

*Table 4-9 The conditions of electrolysis for results shown in Figure 4-11 (April 15<sup>th</sup> 2005).*

Current (A)	Flow at 20 °C (L min <sup>-1</sup> )	Voltage (V)	Total aluminium by ICP-OES (mg L <sup>-1</sup> )	3-times faradic aluminium (mg L <sup>-1</sup> )	Al <sub>2</sub> O <sub>3</sub> equivalent of 3-times faradic (mg L <sup>-1</sup> )
16	10	5	10	27	51
18	9	5	9	34	63
17	3	5	13	95	180

The results shown in Figure 4-11 indicate that electrolytic treatment levels above 2 A (L min<sup>-1</sup>)<sup>-1</sup> were effective in lowering turbidity and supernatant chromium (graphs 1 and 2 respectively) and could be achieved at much lower operating cost (graph 4) than treatment than with PACl. A similar level of chromium removal using PACl addition required 100 mg L<sup>-1</sup> as Al<sub>2</sub>O<sub>3</sub>. The levels of aluminium in the supernatants of the PACl treated waters were higher than the average of the inflow, except for the highest level of treatment which required 200 mg L<sup>-1</sup> Al<sub>2</sub>O<sub>3</sub> equivalent and would cost over \$2 per cubic metre of water treated. The supernatants of the electrolytically treated fluid had an aluminium level comparable to or slightly higher than the average of the inflow.

Another trial with tannery DAF outflow (pH of 8.5 and conductivity of 1.7 S m<sup>-1</sup>) was carried out to confirm the previous results and determine if treatment was effective at moderate pH. Further comparisons with PACl and PFS were carried out. Conditions of treatment are shown in Table 4-10 .



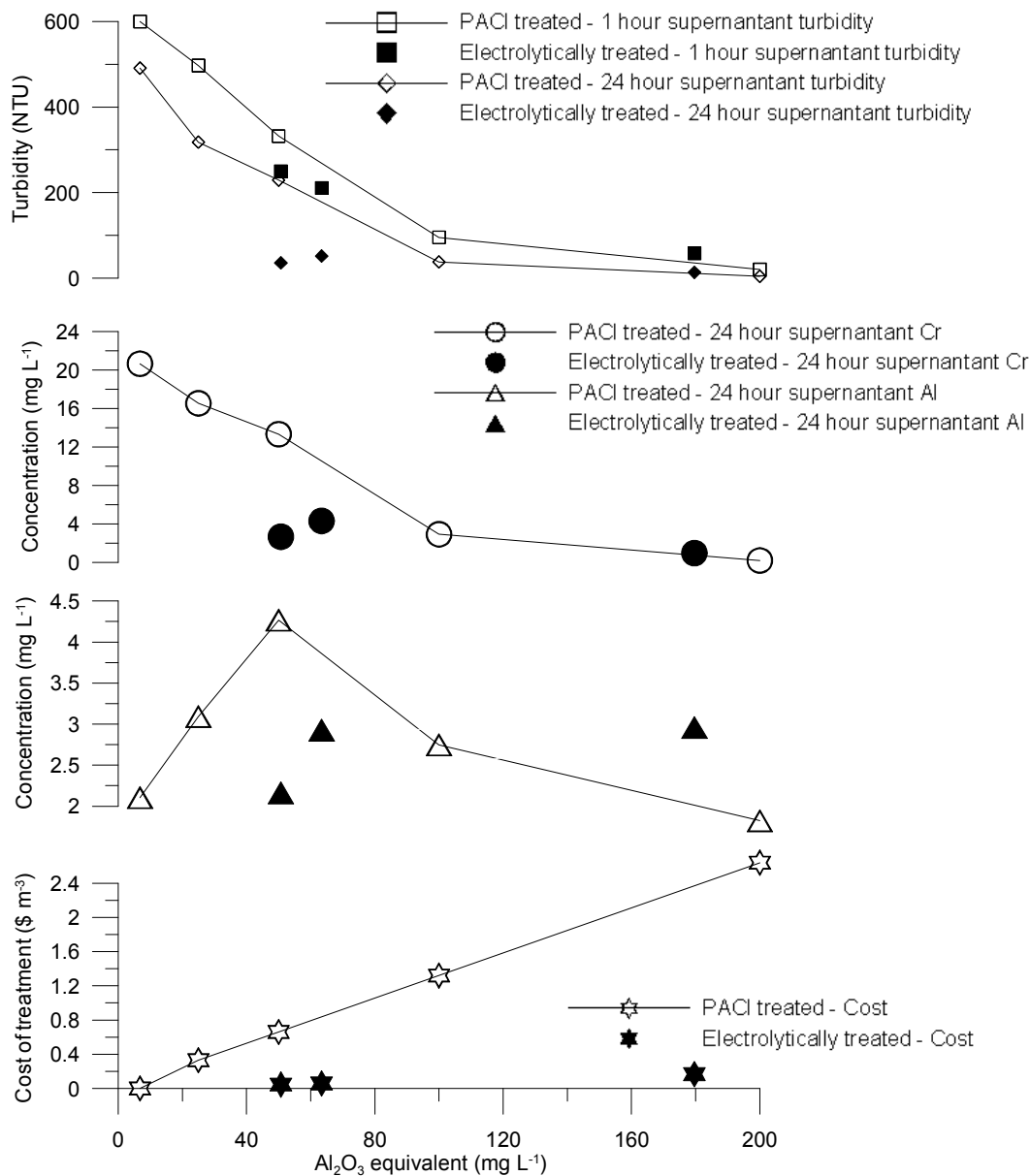


Figure 4-11 Effectiveness and cost of electrolytic addition of aluminium versus PACI dosing. (April 15<sup>th</sup> 2005).

A compact form of the results shown in Figure 4-13, Figure 4-14 and Figure 4-15 is shown in Figure 4-12, based on the conditions shown in Table 4-10, using Al<sub>2</sub>O<sub>3</sub> equivalent as the dependent axis. Both measured total aluminium (ICP-OES) and triple-faradic data points are used. All data points shown with Al<sub>2</sub>O<sub>3</sub> > 60 mg L<sup>-1</sup> assume three times faradic rate of corrosion of aluminium, to make a conservative comparison with chemical flocculent, even though the measured total outflow aluminium from the electrolytic processing was close to or lower than faradic – see Table 4-10. Conservative cost comparisons were made using triple-faradic corrosion rates of aluminium.

Table 4-10 Conditions and sample details for Figure 4-12 (May 12<sup>th</sup> 2005).

Sample type	Measured Total aluminium (mg L <sup>-1</sup> )	3-times Faradic aluminium (mg L <sup>-1</sup> )	Al <sub>2</sub> O <sub>3</sub> Equivalent (mg L <sup>-1</sup> )
Inflow 2:30 pm	2		4
Inflow 3:00 pm	2		4
PACl at 2:50 pm	5		9
PACl at 2:50 pm	7		13
PACl at 2:50 pm	9		18
PACl at 2:50 pm	13		25
PACl at 2:50 pm	23		44
PFS at 3:10 pm	34		63
23 A 6 V 10 L min <sup>-1</sup> 2:30 pm	11	39	73
25 A 6 V 10 L min <sup>-1</sup> 2:35 pm	11	42	79
28 A 6 V 10 L min <sup>-1</sup> 2:40 pm	12	47	89
36 A 6 V 10 L min <sup>-1</sup> 2:45 pm	13	60	114
21 A 3 V 10 L min <sup>-1</sup> 3:00 pm	9	35	67

PACl treated – 24 hour supernatant chromium and PACl treated 24 hour supernatant aluminium in graph 2 of Figure 4-11 show the greater reduction of supernatant chromium and aluminium that occur with greater dose of PACl. Based on measured total outflow aluminium, electrolytic treatment (Electrolytically treated – 24 hour supernatant chromium for Total measured Al) gives similar chromium reduction to PACl treatment (PACl treated – 24 hour supernatant chromium in graph 2 of Figure 4-12). Despite the rapid drop in pH from 8.8 to 8.4 (Inflow pH of graph 4 of Figure 4-12) during the trial, good flocculation was achieved consistently. The data shown in Figure 4-12 were split up by treatment type to show turbidity and cost, supernatant metals and pH in Figure 4-13, Figure 4-14 and Figure 4-15 respectively.

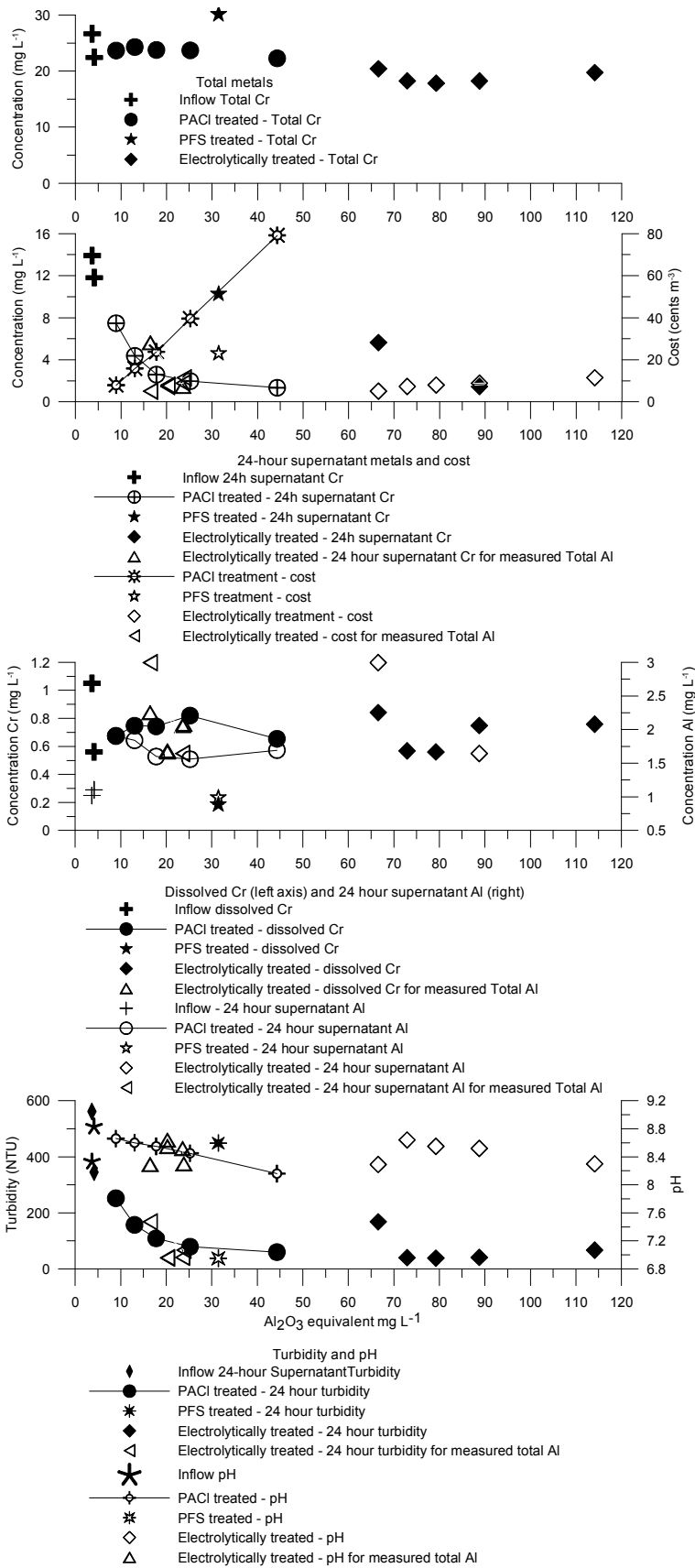


Figure 4-12 Comparison of electrolytic treatment with PACl dosing (May 12 2005).

Figure 4-13 shows that effective PACl dosing was more expensive than electrolytic treatment. Turbidity increase and pH drop in the inflow during the trial made it difficult to compare the early samples with the later ones. For example the 36 A, 6 V, 10 L min<sup>-1</sup> outflow sample at 2:45 pm had high turbidity but the inflow turbidity was increasing at that time.

At a dose of 2.1 A (L min<sup>-1</sup>)<sup>-1</sup> using 3 V, as seen on the right of Figure 4-14, the treatment was less effective. PFS again produced a poor result due to the formation of black colloids, though it had to contend with the most turbid and lowest pH inflow at the end of the trial.

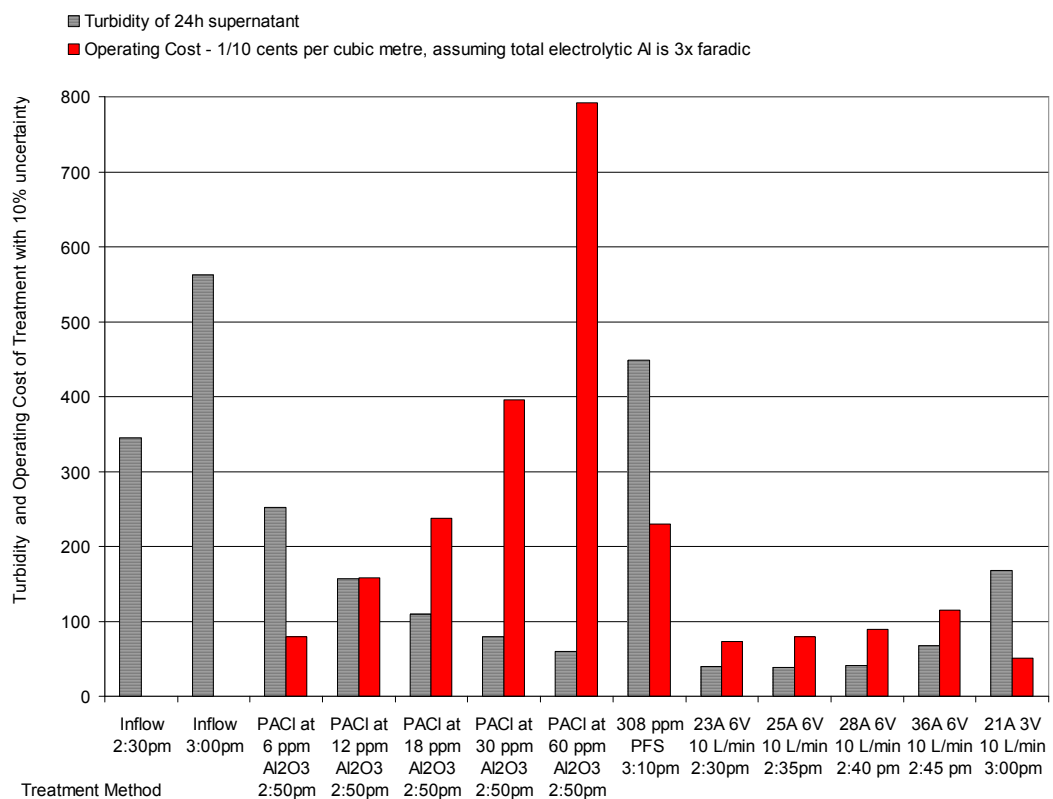


Figure 4-13 The superior turbidity removal of electrolytic treatment compared to dosing with PACl in terms of outflow supernatant turbidity for operating cost (May 12<sup>th</sup> 2005).

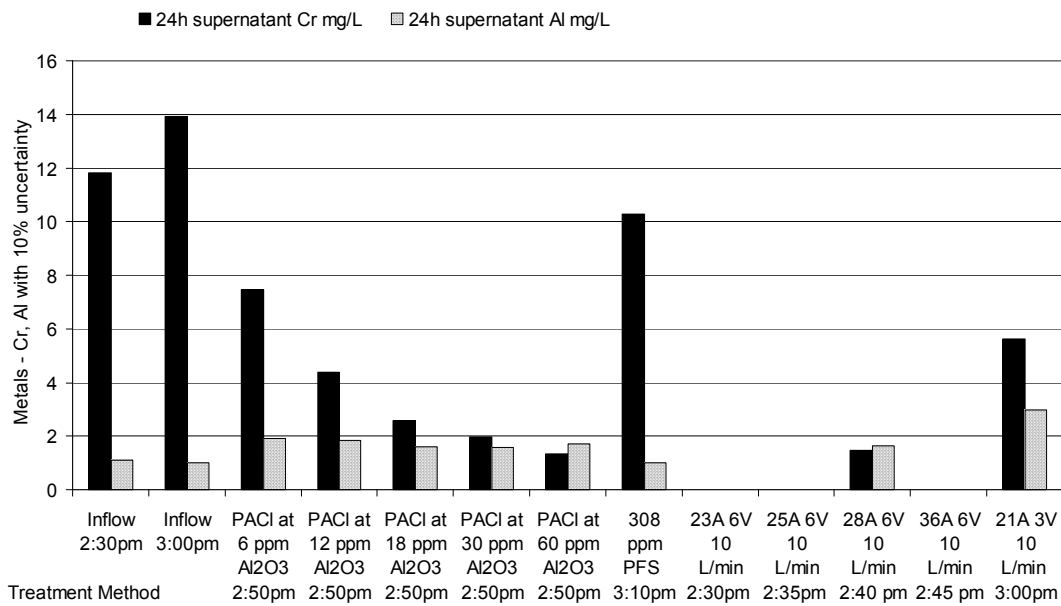


Figure 4-14 Supernatant aluminium and chromium and total aluminium levels measured by ICP-OES (May 12<sup>th</sup> 2005).

Figure 4-14 shows that high PACI dosing was required to achieve a good result. Electrolytic treatment was effective when the cell voltage was 6 V but not when the cell voltage was 3 V.

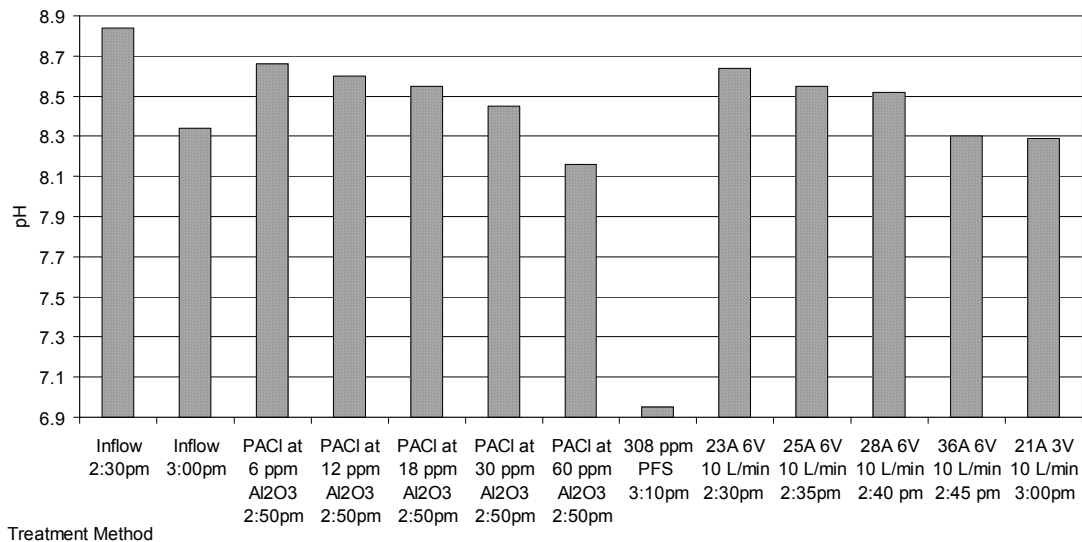


Figure 4-15 pH of inflow and processed effluent (May 12<sup>th</sup> 2005).

Figure 4-15 shows the drop in inflow pH between 2:30 pm and 3:00 pm. Hence, the apparently low pH for the sample on the right, 21 A, 3 V and 10 L min<sup>-1</sup> is

actually the same pH as the corresponding inflow. At low cell voltage the pH drop was small.

#### **4.4.8 Treatment of near neutral pH effluent**

Given the awareness of extra-faradic corrosion, alkalinity requirement and possible pH changes raised by trials at high pH, further trials were carried out at the tannery using lower pH effluent. However, treatment conditions of earlier trials were replicated as much as possible.

The first trial was conducted at Pond 6, the source of terminal effluent from the combined tannery and rendering effluent. The composition of the fluid in Pond 6 was much more stable than the tannery DAF outflow and also had much lower pH and contaminant levels. Inflow turbidity was 132 NTU, conductivity was 13000  $\mu\text{S cm}^{-1}$ , pH was 7.36 and the temperature was 20 °C. The electrolytic aluminium corrosion rate was assumed to be that measured by the outflow total aluminium, due to the near-neutral pH.

The results are summarised in Figure 4-16. The dissolved iron resulting from PFS treatment uses a larger scale on the right y-axis of graph 1.

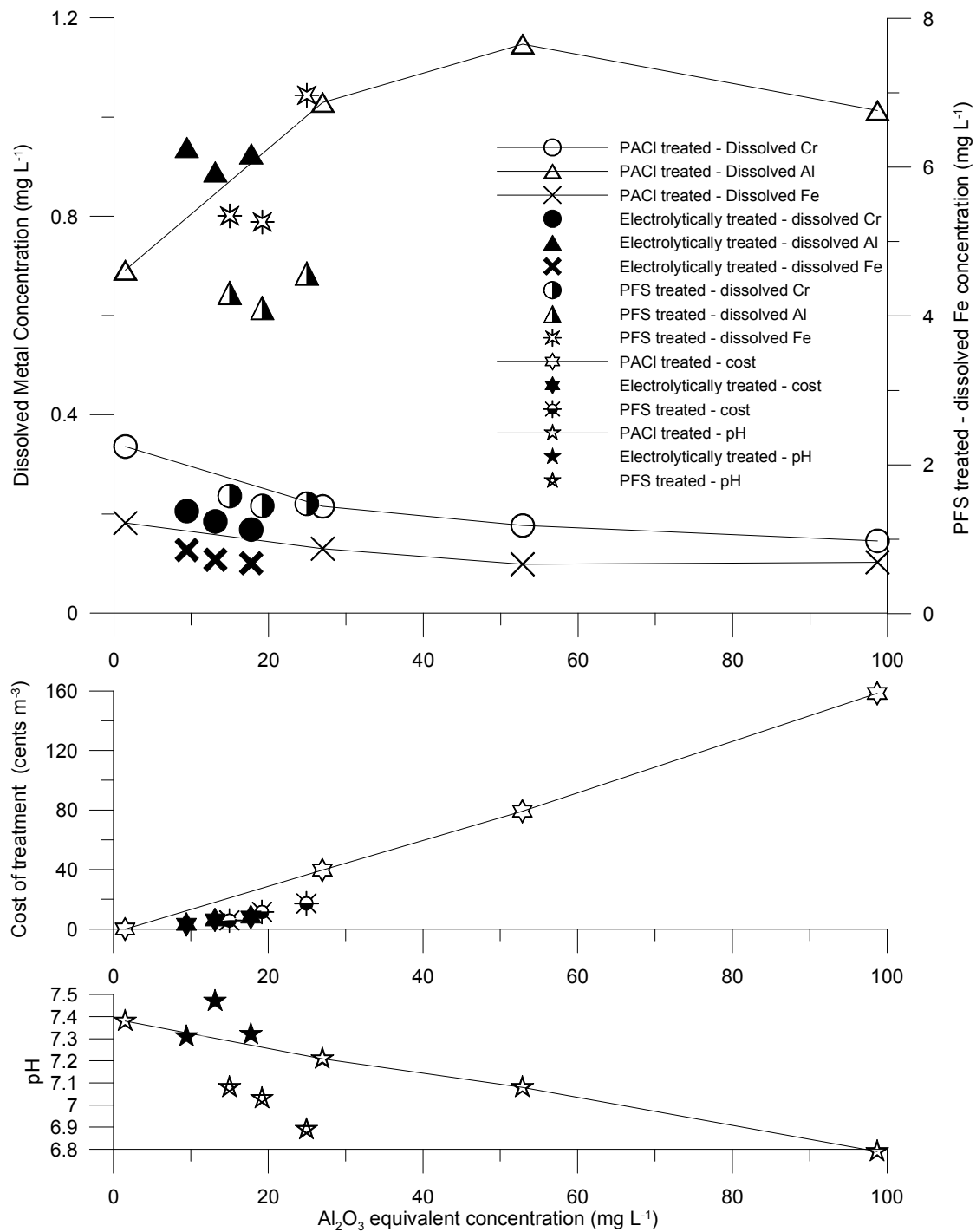


Figure 4-16 Comparison of PACl/PFS dosing and electrolytic processing, based on  $Al_2O_3$  equivalents, on Pond 6 terminal effluent at the tannery (May 4<sup>th</sup> 2005).

As shown by the pH plots in graph 3 of Figure 4-16, the pH of the influent was below 7.5 and treatment by PACl reduced the pH while electrolytic treatment did not. The dissolved metal plots in graph 1 indicate that chromium reduction by any of the methods tried was poorly effectual, even at high levels of treatment. The floc formed by both the electrolytic and chemical addition of aluminium varied from weak to near-colloidal, despite the high conductivity of the water and

relatively low loading of suspended solids. The cost plots in graph 2 shows that addition of iron based flocculent was cheapest, but caused formation of black colloids. The high dissolved iron levels suggest that iron was part of the colloid. The most obvious cause of treatment failure was low pH. The poor treatment of Pond 6 water could also be due to the quality of the inflow water compared with the tannery DAF outflow. It was more difficult to remove the last traces of diluted metals than remove the majority of metals from extremely contaminated water, indicating that the concentrated tannery effluent stream is a better treatment target. The total aluminium in the outflow of the electrolytic treatment was sub-faradic, as shown in Figure 4-17.

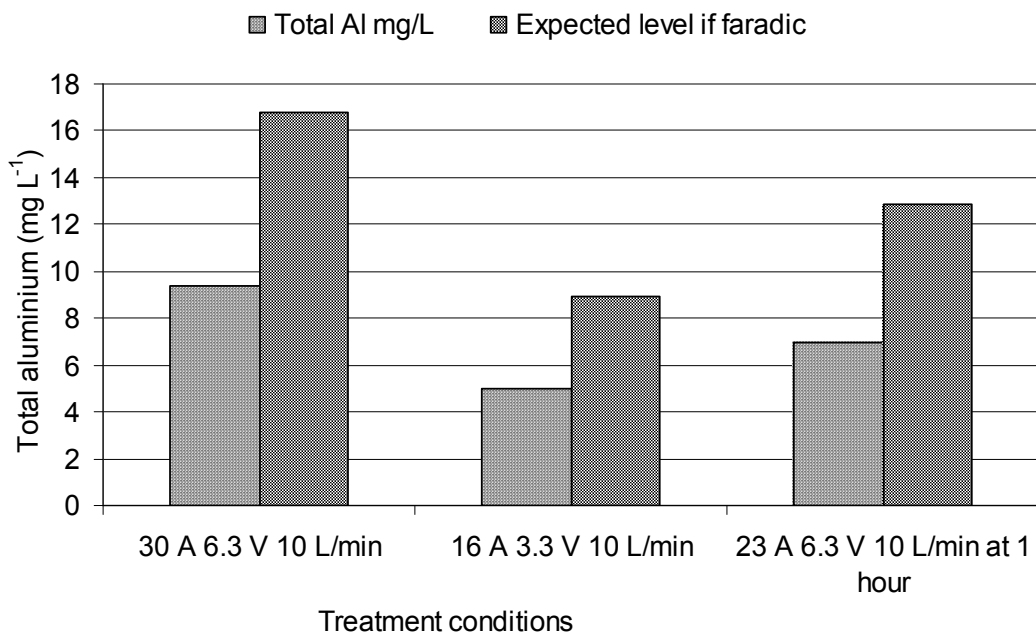


Figure 4-17 Lower current efficiency at near-neutral pH of Pond 6 water shown by measured total aluminium compared with the faradic prediction for treatment (May 4<sup>th</sup> 2005).

While a faradic dose of  $3 \text{ A (L min}^{-1}\text{)}^{-1}$  would give an equivalent of  $30 \text{ mg L}^{-1} \text{ Al}_2\text{O}_3$ , the 30 A,  $10 \text{ L min}^{-1}$  conditions shown at the left side of Figure 4-17 indicate an aluminium corrosion current efficiency of just over 50%. Floc storage in the shavings was not as pronounced as for treatment of DAF outflow as the floc was weak and largely passed out with the effluent. The other two results are consistent with sub-faradic aluminium corrosion despite the different treatment conditions. Furthermore, dissolved oxygen measurements using the Mettler



Toledo dissolved oxygen meter (see §2.5.10) indicated that the outflow of electrolytic treatment was saturated with oxygen whilst the inflow was low in oxygen, also suggesting that the aluminium corrosion efficiency was low. Extra-faradic corrosion did not occur when processing near-neutral pH effluent at low voltage. The advantages of extra-faradic corrosion were lost. The possible association of extra-faradic current with pH drop was observed. Since noticing that the pH of the DAF outflow dropped sharply at 3 pm on Thursdays, another trial was conducted with DAF outflow when the pH was low and dropping. At 2:40 pm the inflow had pH 7.11, turbidity of 474 NTU, and conductivity of 8300  $\mu\text{S cm}^{-1}$  at 20 °C; at 3:15 pm the inflow pH was 6.62, turbidity was 697 NTU, and the conductivity was 8846  $\mu\text{S cm}^{-1}$  at 19 °C. PAC23 was used for chemical flocculent comparison. A fresh set of shavings was used for the electrolytic trial and very little storage of floc in the shavings was observed at the end of the trial. Hence, total aluminium measured in the outflow was used rather than triple-faradic. A summary of results is shown in Figure 4-18.

The PAC23 treated – 24 hour supernatant chromium and electrolytically treated – 24 hour supernatant chromium for measured total aluminium plots in graph 2 of Figure 4-18 show weak flocculation similar to that seen at the Pond 6 trial. The data shown in Figure 4-18 were split up by treatment type to show turbidity, cost and supernatant metals as well as pH in Figure 4-19 and Figure 4-20 respectively. Aluminium corrosion was assumed to be faradic because the pH was low. This agreed closely with the measured outflow levels.

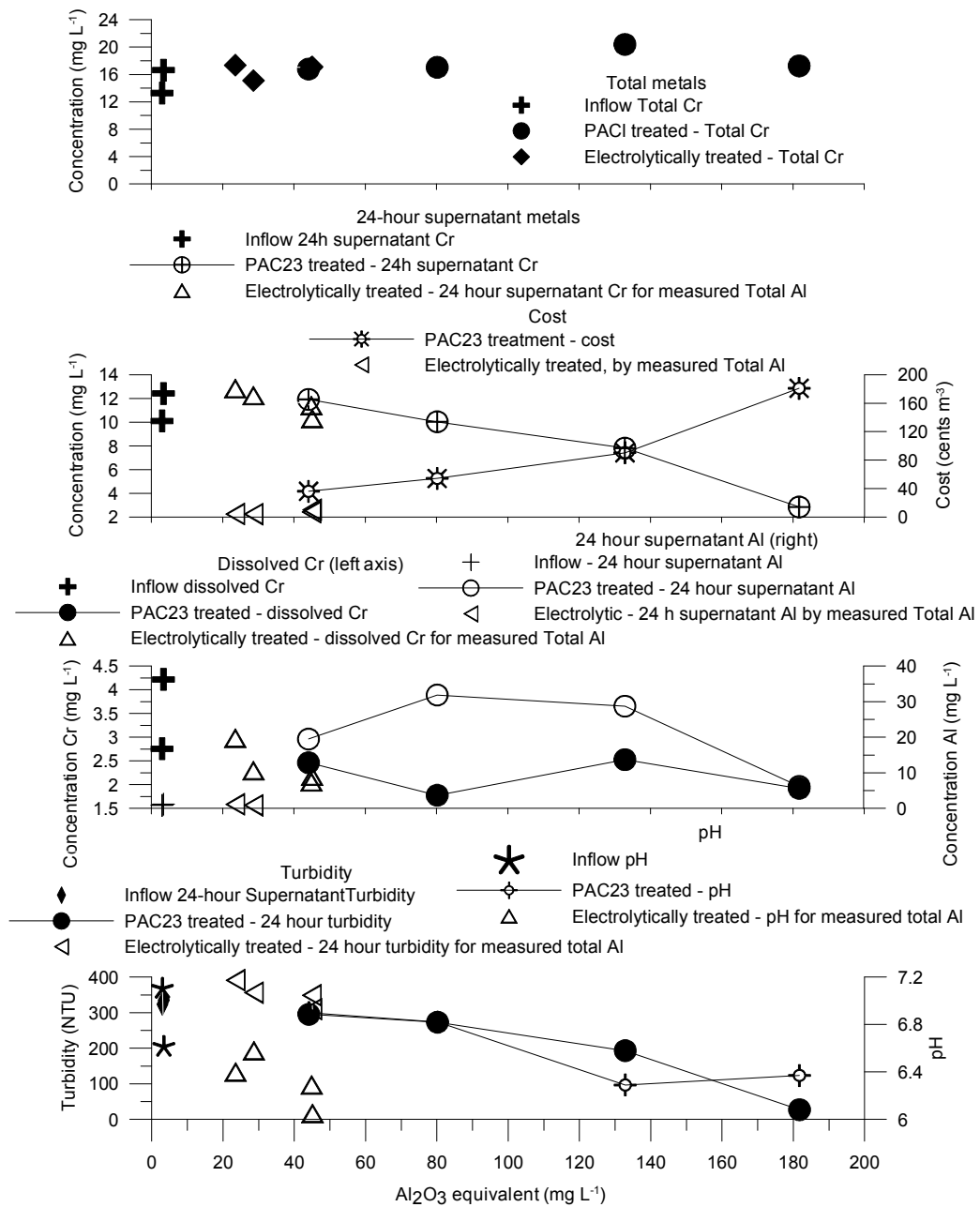


Figure 4-18 The poor performance of both electrolytic treatment and PAC23 dosing when treating tannery DAF outflow (inflow to H&S pond) that was relatively low in pH (19 May 2005).

As Figure 4-18, Figure 4-19 and Figure 4-20 show, even high levels of treatment by either PAC23 or electrolysis were not effective.

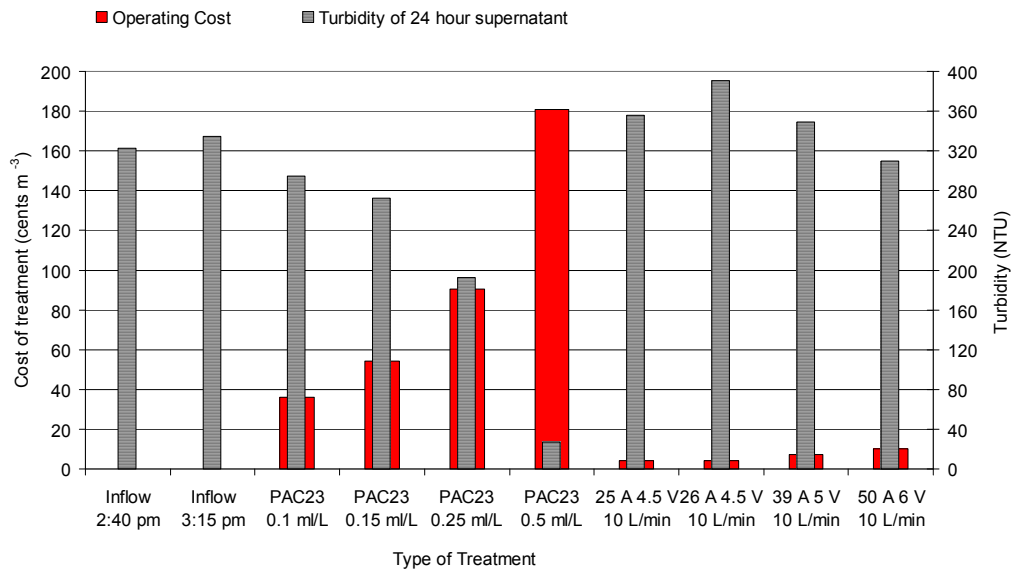


Figure 4-19 24 hour turbidity and cost for PAC23 and electrolytic treatment (19 May 2005).

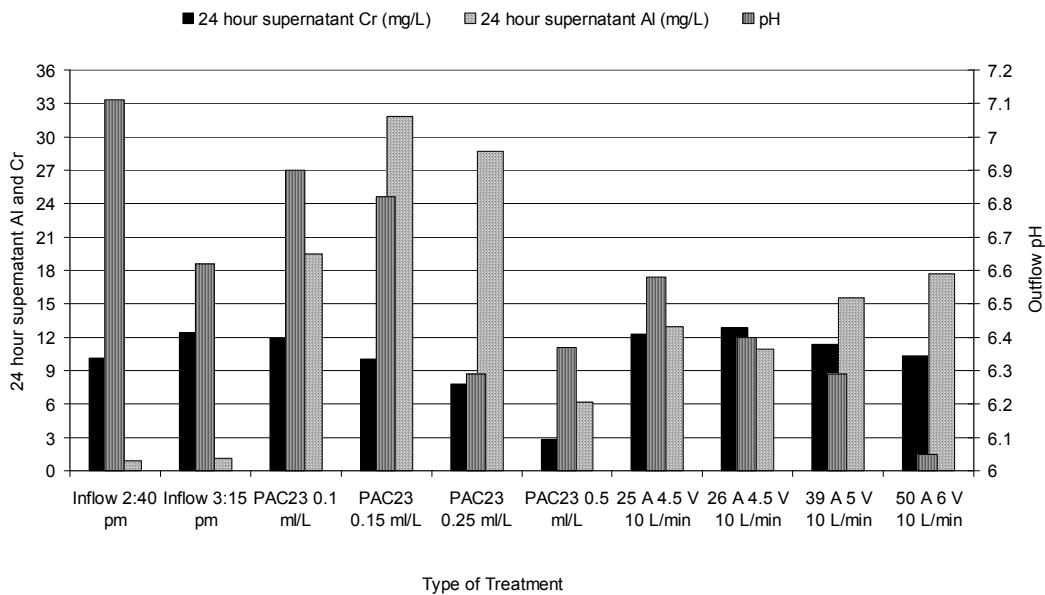


Figure 4-20 High levels of supernatant metals at low pH for both electrolytic treatment and flocculent dosing of DAF outflow (19 May 2005).

#### 4.4.9 Cost effectiveness of chromium removal

The cost effectiveness of chromium removal from DAF effluent by flocculation and settling was tested. The Flume processor was used to treat DAF outflow (conductivity  $1.4 \pm 0.1 \text{ S m}^{-1}$ , temperature  $24 \text{ }^\circ\text{C} \pm 4 \text{ }^\circ\text{C}$ ). Total inflow chromium was  $15 \text{ mg L}^{-1}$ . Inflow pH dropped from 9.2 to 8.6 during the trial. The treatment conditions used are shown in Table 4-11. Figure 4-21 shows chromium remaining

in the supernatant after settling for 24 hours where the operating cost of treatment was based on electrical power at \$0.15 per kWh and the scrap aluminium at \$1 per kg. The inflow supernatant value was taken from samples settled for 24 hours.

Table 4-11 Conditions to achieve dose shown as dependent variable in Figure 4-21.

Flow (L min <sup>-1</sup> )	Current (A)	Voltage (V)	Dose (A (L min <sup>-1</sup> ) <sup>-1</sup> )	Energy Density (kWh m <sup>-3</sup> )
Inflow	0	0	0	0
15	15	4	1	1.67
15	30	6	2	0.83
20	50	10	2.5	0.42
10	50	10	5	0.20
5	50	10	10	0.07

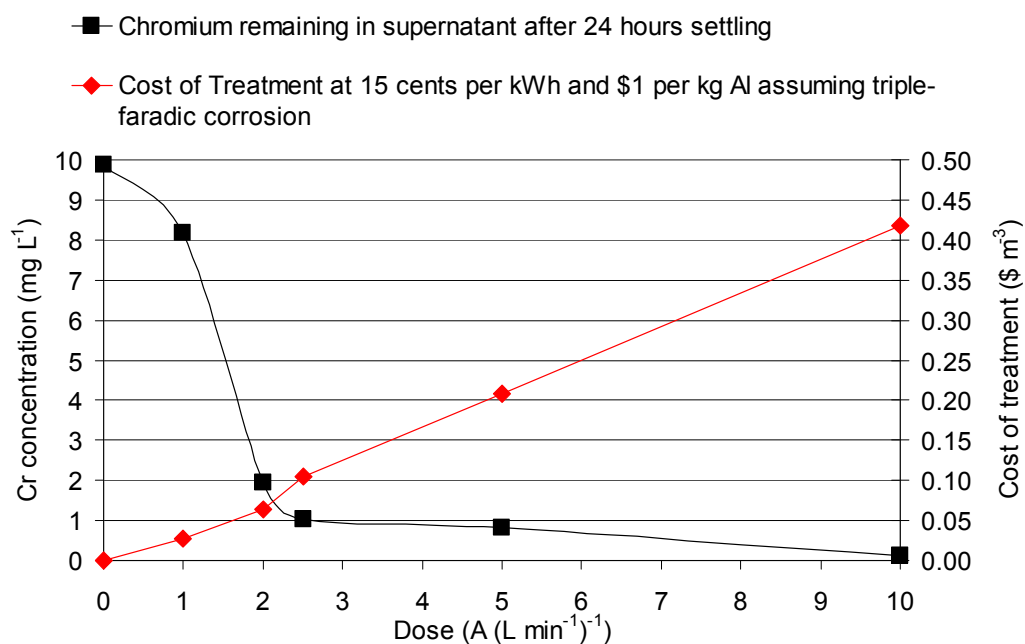


Figure 4-21 Chromium remaining in the supernatant and operating cost for electrolysis of DAF outflow, based on measured aluminium in the outflow. The changes in slope of the cost graph occurred at changes in supply voltage (March 10<sup>th</sup> 2005).

Figure 4-21 shows that treatment was effective at doses above 2 A (L min<sup>-1</sup>)<sup>-1</sup> of liquid flow, equating to \$0.10 m<sup>-3</sup> at a cell voltage of 6 V. Below this dose

flocculation failed abruptly, as shown by higher chromium levels in the supernatant.

#### 4.4.10 The effect of processing on microbes

All the samples taken indicated that the flocculated outflow, from either electrolytic processing or PFS treatment of tannery effluent, is a better growth medium for coliforms than the inflow. An example is shown in Table 4-12. This could be expected, given the removal of toxic chromium as well as lowering of the pH toward neutral, and should improve downstream oxidation pond function.

*Table 4-12 The positive effect on bacterial growth of chromium removal by flocculation.*

Sample Name	Lab No.	Escherichia coli	Total Coliforms
4/03/05	(Hill Laboratories)	(MPN/100 mL)	(MPN/100 mL)
#10 Inflow = DAF Outflow	370771/10	< 100	41000
#11 AI 25 A 10 V 3 L min <sup>-1</sup>	370771/11	1070	>24000000
#12 PFS 200 mg L <sup>-1</sup>	370771/12	< 100	5470000

#### 4.4.11 Blockage at the top and bottom of the Flume processor

##### Top-end blockage

A problem first experienced in the solids removal trial was blockage at the top of the Flume by coarse suspended solid. When this section of shavings was replaced and the system was operated for a further period, blockage at the bottom end by nascent floc was observed. When the pH was close to neutral the flocculation was poor and bottom-end blockage was much slower to arise. For higher inflow pH resulting in strong flocculation, the buildup of floc at the bottom end was rapid, despite flow speeds in excess of 0.1 m s<sup>-1</sup>. Hence, it was difficult to determine the actual rate of corrosion at high pH by means of outflow analysis because some of the corrosion products were stored in the processor. However, the processor could pass well over 10 m<sup>3</sup> of unfiltered DAF outflow before blocking at the bottom.

Direct electroflotation of the coarse solids entering the processor was not possible,

so a conventional filter should be incorporated into any commercial product to give longer Flume run-times.

### Bottom-end blockage

The entire vertical wall of the Flume was wet due to the capillarity of the nylon membrane. Hence, shavings close to the vertical walls, where the flow speed was very low, corroded without clearance of the products. The current in this region was eventually limited by the increased resistance. The flow speeds at the outer margins of the bottom face of the Flume were also low due to flow resistance. This was exacerbated by the build-up of corrosion products by the vertical wall. Hence, a bottom-end blockage proceeded by first filling in the lower corners of the Flume where the corrosion product concentration was greatest, and then moving toward the centre and upwards along the Flume. This is illustrated in Figure 4-22.

The end results were an overflow over the top of the Flume walls near the bottom, and reduced current as the active electrode area was reduced by electrical increasing resistance in the blocked zones.

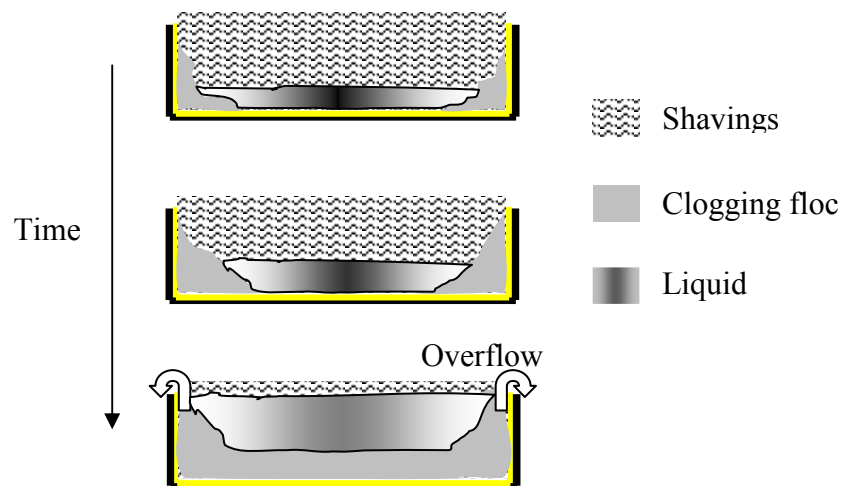


*Figure 4-22 The progress over time of bottom end blockage by accumulated corrosion products, shown in cross-section of the Flume. The flow (shown darker where faster) lifts through the body of shavings over time and becomes thicker, lowering the flow speed and accelerating the blockage, eventually overflowing. Because corrosion products are still delivered from higher up the Flume, the blockage continues to develop higher up the Flume even after the onset of overflow.*

The vertical wall problem is minimised by insulating the vertical walls so that blockage is not initiated there. If the corners were slightly lower than the centre part of the bottom face as illustrated Figure 4-23 it would also help to maintain an adequate flow speed over the entire active surface. A wider flume would have proportionally more bottom face area than side wall area.

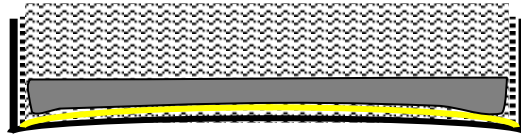


*Figure 4-23 Possible means of leveling the flow speed by lowering areas of higher flow resistance to slow or prevent blockage. The walls are electrically insulated to prevent initiation of blockage there and greater bottom area to side wall area ratio is illustrated.*

#### **4.4.12 Release of aluminium fragments.**

At flow speeds well in excess of  $0.1 \text{ m s}^{-1}$  the smallest fragments of the shavings, were released from the body of the shavings and entered the outflow. As the body of shavings was corroded from the bottom and dropped, more dry fragments entered the flow stream.

Evidently, while shavings with at least one dimension smaller than the self-limiting corrosion thickness were essential, fragments with three small dimensions were not helpful. The smaller pieces would best be removed from the main body before deployment in the Flume.

#### **4.4.13 Discussion and conclusions**

##### **Dependence of flocculation on high pH**

Normal treatment sequences would usually delay flocculation until later in the chain when the majority of the coarse solid was already removed by microbiological action and settling or flotation, lowering the required dose of flocculent. In the case of tannery effluent, removal of chromium and other poisons has to precede the biological settling pond stage. In this case, the required dose of

flocculent is so high that the pH drop is significant. It is advantageous to lower the pH toward neutral, to favour both low solubility of aluminium species and high biological activity in downstream processing. However if the alkalinity is too low flocculation will fail. Because tannery effluent is usually strongly alkaline and buffered, use of acidic flocculants is feasible. However, using a single chemical flocculent does not give independent control of flocculation and pH drop. For example, when the pH is low and the solids loading is high, the pH will be reduced below the minimum solubility point of aluminium species and the alkalinity is insufficient to enable flocculation. PFS would normally be considered the better choice for broad pH application, but again the high solids loading of the effluent, in particular the S content, caused problems. For electrolytic treatment it was noticed that increasing the voltage while attempting to maintain the same faradic dose seemed to lower the pH more than at low voltage.

Using the H&S pond as the inflow source for electrolytic processing would be very helpful as the composition of the fluid would be less variable and the rate of change would be slower. The average pH of the H&S pond is 9, which is ideal for electrolytic processing.

### **Clearance of corrosion products**

The prototype development sequence described in §4.1.1 to §4.1.4 was driven by the need to clear products of corrosion so that the electrolyser could continue operating indefinitely while converting a very high fraction of the corroded anode material to flocculent in the outflow.

The conditions for producing a good floc described in §4.4.13 also caused the same floc to block the lower end of the Flume over time. Aluminium floc, which is by definition cohesive, needs a higher flow speed to ensure clearance than most other fine particulates. Hence, further developments were required.

### **Cost effectiveness of the treatment**

Electrolytic treatment is more cost-effective than chemical treatment with standard flocculants. The energy requirement of electrolytic processing of tannery effluent using the Flume is in the range of 0.2 kWh m<sup>-3</sup> to 1 kWh m<sup>-3</sup> depending on the pH and conductivity of the water. The cost of scrap aluminium is of the



same order as the energy cost. The total cost of treatment is therefore less than \$0.30 m<sup>-3</sup> of effluent. This compares favourably with chemical flocculation and has the added function of flotation. The cost reduction compared to chemical treatment was due to the much lower cost of transporting pure aluminium compared to an aqueous solution. Electrolytic treatment enabled independent pH adjustment and flocculent addition. pH adjustment was used to lower residual metal content in the outflow.

Based on total measured aluminium in the outflow, electrolytic processing adds comparable amounts of metal as either PACl or PFS dosing. The rapid and wide variation of the inflow conditions, as well as the uncertainty over how much corroded aluminium was stored in the body of the shavings made fair comparisons difficult. Within the range pH of 8 to 10, the Flume processor was able to treat a rapidly and widely varying inflow successfully.

#### **4.4.14 Unresolved issues suggesting further work**

The mechanism of pH drop induced by electrolytic corrosion was still not clear, nor was not possible to consistently electro-float electro-floc.

It was envisaged that the DAF outflow (or the less variable H&S pond fluid) could be treated and released (back) to the outlet of the H&S pond, with collected solids returned to the DAF. Hence, no other settling ponds or filters would be required. However, the loading on the tannery DAF would increase significantly. The key is separation of the metals from the organic material in the sludge, enabling the metallic portion to be returned to the tannery.

The Flume processor worked well for trials lasting a few hours, but was limited by eventual blockage. There are two distinct types of blockage, each with unique cures: if the inflow is loaded with coarse suspended solid this will be lodged in the upper section of the Flume where the shavings act as a filter, leading to blockage. Because the shavings form a coherent bed, they cannot be fluidised easily like ideal filter media; if the corrosion-induced flocculation is at the right level to treat the water successfully, the water at the lower end of the Flume will be loaded with nascent floc that can lodge on the shavings there, leading to blockage that raise the fluid level and slows the flow speed, exacerbating the problem.

The effectiveness of a water treatment system is measured by the ratio of treated water produced to amount of water required to regenerate the system (Langdon, A. 2003, pers. comm., September). In a filter, this is simply the amount of water treated between back-flushes divided by the amount of water required per back-flush. For this system, reversal of the flow is not feasible because the Flume would overflow close to the bottom.

Means to avoid both top and bottom end blockage to enable long term operation must be considered. The simplest solution to top end blockage is to pre-filter the fluid. The solid captured and back-flushed from the filter is remixed with the outflow of the Flume or separated as an organic water stream (as shown in Figure 5-40). For this particular tannery, making best use of the existing DAF will minimise further capital expenditure. Bottom end blockage can be slowed and relieved by combinations of: pulse flow; periodically turning off the electrical power but retaining the flow; periodic polarity reversal; narrowing the flow or increasing the slope toward the bottom to raise the flow speed there; finding the slope that optimises the components of gravitational force to direct the flow along the bottom of the conduit in minimum cross-section.



## **5 Further investigation of the Flume in a laboratory**

### **5.1 Studies in controlled conditions**

#### **5.1.1 Introduction**

While the Flume electrolytic treatment system performed well in the challenging and variable conditions of a real tannery, the details of operation were difficult to discern in the field. This was because of the complex matrix of compounds in the effluent and the rapidly varying absolute and relative levels of the component impurities.

In order to discover means of treating fluids at the extremes of conductivity and pH, laboratory experiments using synthetic effluent with salinity in the range between tap water and tannery effluent and pH between 3 and 10 were carried out. Contaminants based on the chemicals used in the real process were then added to test the effectiveness of contaminant removal without the complication of coarse suspended solid. By analysis and interpretation of these investigations, the basic mechanisms of treatment of tannery effluent were found. It was expected that new means of processing fluids with extremes of pH and conductivity would be discovered.

#### **5.1.2 Targets of investigation**

The excellent reduction of dissolved metal and suspended solids when treating tannery effluent with pH of 9 was unexpected and required explanation as did the poor performance when treating near-neutral fluid. The most difficult conditions to deal with at the tannery were either near-neutral pH with heavy solids and chromium loading, or water with pH greater than 10. The most puzzling aspect of the good performance at the tannery had been the unexplained pH reduction. Means of maintaining the effectiveness of treatment over a wide range of inflow conditions were investigated, to make the system even more robust than it had already been shown to be at the tannery. The first priority for this approach was a self-regulating system, followed by establishing the crucial parameters for an external control system, either open-loop or closed-loop. Operation of the Flume at the tannery was limited by bottom end-blockage.

The primary target was an effective low-cost system that produced an outflow with low suspended solids, chromium and residual metal. Hence, processing conditions that gave consistent combined electroflotation and electrocoagulation were sought. pH manipulation was investigated by means including changing or modulating the cell voltage or current, altering the catholyte pH and separating the fluid flow into anolyte and catholyte. The trials with alkaline but low conductivity pulp mill effluent (see §4.3) highlighted a need to increase the effective conductivity of the fluid to be treated without significantly altering the composition of the treated fluid. Investigation of catholyte salination addressed this need.

Comparisons with chemical flocculants were not considered essential, as they had already been made in more realistic conditions. Exploration of means to improve the cost effectiveness and practicality of electrolytic processing were considered more important. The trials carried out were: aluminium electroflocculation of pH modified saline; pH modification by splitting the outflow; chromium removal from saline and protein contaminated saline; modification of both effective conductivity and pH by modifying the catholyte and pulse modulation of the current or voltage.

## **5.2 Materials and methods**

### **5.2.1 Inflow stabilisation tank**

The experimental system is illustrated in the lower part of Figure 5-1. A 300 L circular open-top tank was placed on the bench-top. A stirrer, tap water inflow, two 50 litre pH adjusted saline stock tanks and pumps for dosing the saline to the large tank were used to produce a flow of stable composition, supplied to the processor through a submersible pump. Additional contaminants were added either as step doses to the main tank or through the stock tanks. Throughout the trials the inflow, was  $18\text{ }^{\circ}\text{C} \pm 4\text{ }^{\circ}\text{C}$ . The ambient air temperature was within  $3\text{ }^{\circ}\text{C}$  of the tap water. It usually took several hours to stabilise the composition of the inflow before switching on the power.

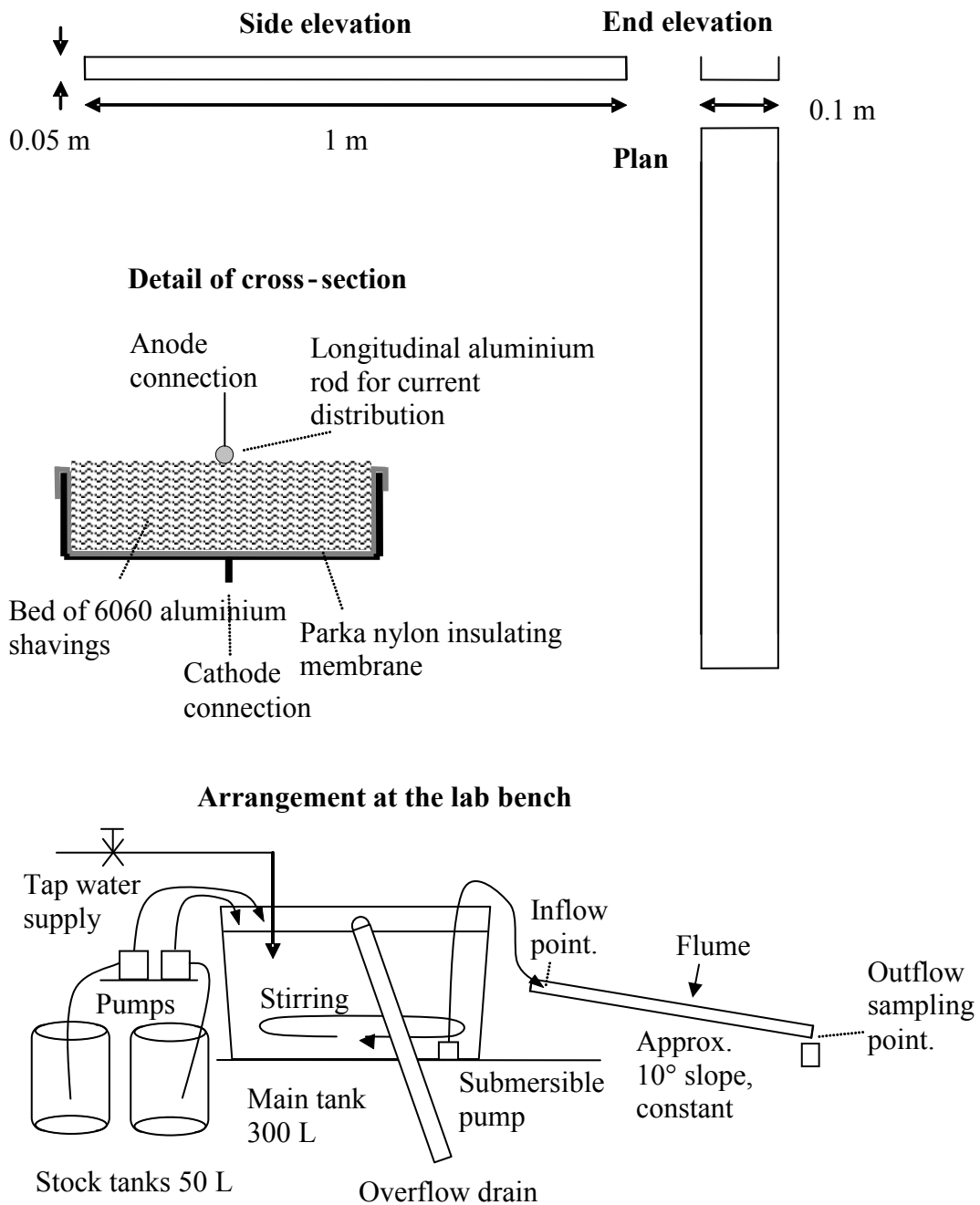


Figure 5-1 The Flume, as used in the laboratory (above) and the experimental system it was part of (below).

The level of the tank was maintained with a higher flow into the tank than that drawn off to the processor. The small excess was passed to waste by a secure wide-bore drainpipe.

### **5.2.2 The laboratory Flume**

The upper part of Figure 5-1 shows a 1 m length of stainless steel plate was folded into a U-section 0.1 m wide and 0.05 m high and used as a cathode. An 8 mm bolt was welded to the underside of the cathode for electrical connection. Parka-nylon and aluminium shavings, identical to the material used at the tannery, were used. Distributed anode connection was achieved by an 8 mm aluminium rod placed on top of the shavings. The electrochemically active surface area was approximately 20% of that for the field equipment. This meant that smaller flows could be treated in a scale model of the field equipment. It also meant that the required current was less than 20 A, which could be delivered by standard power supplies.

The outflow configuration of the Flume was altered for some of the experiments so that the anolyte and catholyte could be separated. Polyethylene sheets were used for this purpose, occupying and preventing electrolysis in the lowest 0.1 m of the Flume.

### **5.2.3 Electrical equipment**

The Trio PD35-20 (see §2.6.1) was used mainly in a voltage-limited constant-current mode, but occasionally in current-limited constant voltage mode. The variation of this supply was found to be lower than 1%.

### **5.2.4 Sampling systems**

The samples taken at the tannery had generally been in 1 L Schott bottles, which were ideal for visual observations. This continued in the laboratory, with manual samples taken in clear glassware of between 500 mL and 3 L. Up to four samples could be taken in a short time to represent the inflow (code: i), whole outflow (w), outflow anolyte (a) and outflow catholyte (c). For example, sample number 258 had four real samples: 258i, 258w, 258a, and 258c. Usually the catholyte flow was too low to allow rapid sampling so a smaller volume, up to 100 mL, was taken instead.

These samples were allowed to settle or post-processed (for example by acidification) in the sample bottles so no further contamination could occur. The bottles were recycled after washing and rinsing with the next sample. Acidified

bottles were used for samples that were to be acidified in turn, to prevent modification of the pH of near-neutral samples.

The pH meter in the Autosampler (see §2.5.7) was found to have a slow (10 minute) response time so was not able to follow step changes. However, it was particularly helpful for monitoring the state of the inflow tank when trying to maintain a constant state. Where fresh outflow pH measurements were made, a PHM meter was used directly. This effectively restricted the time between samples to greater than fifteen minutes.

### **5.2.5 Steady state, ramp and step change experiments**

The stability of the inflow enabled investigation of long-term effects, up to nine hours continuously. The inflow pH and salinity could also be ramped at controlled rates over a set range. By focussing on the range of pH and salinity experienced at the tannery, and extending the boundaries, more general conclusions could be made about the suitability of the process for particular inflow conditions, both for the tannery effluent and other fluids. Step changes to the inflow or operating conditions were made to test the response time and robustness of the system.

### **5.2.6 Contaminants**

To test the effectiveness of electrolytic processing in removing chromium, pH-adjusted  $\text{Cr}_2(\text{SO}_4)_3$  solution was mixed with the inflow. An alkaline stock tank was loaded with concentrated  $\text{Cr}_2(\text{SO}_4)_3$ , which precipitated as a green floc at pH above 11, necessitating re-circulation to prevent settling.

The first experiments used pH-adjusted saline as inflow, with no other contaminants. This enabled simple characterisation of the performance of the electrolyser as an electro-flocculator. Having done this, the next step was to check the chromium removal over a range of pH and salinity. The final type of inflow was a synthetic effluent to mimic tannery wastewater, using addition of chromium with  $500 \text{ mg L}^{-1}$  of egg albumin to test the effect of protein on electroflocculation.



## 5.2.7 Modulation of the power supply

Modulation of the power supply was achieved by the switching circuitry shown in Figure 5-2, based on a signal generator and a 60 V 60 A rated MOSFET (see §2.2.4). The MOSFET on-resistance was less than 16 m $\Omega$ , which is much less than the electrolyser resistance. However, for the purpose of voltage measurement, the cathode of the electrolyser was still significantly different to the negative side of the power supply. The cell voltage was measured with an isolated instrument.

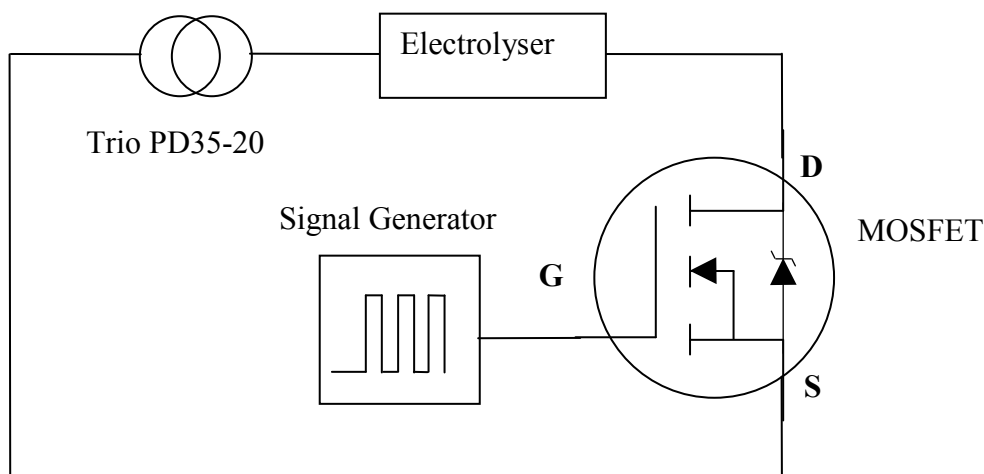


Figure 5-2 The switching circuitry used to modulate the current or voltage of a constant-current (shown) or voltage-source supply. Square wave modulation was used.

## 5.2.8 Analytical tools

For pH measurements, Radiometer Copenhagen MeterLab PHM290 and later a PHM240 were used (see §2.5.4). Conductivity, elemental composition and pH were measured according to §2.5.1, §2.5.3 and §2.5.4 respectively. Levels of aluminium and chromium below mg L<sup>-1</sup> were measurable by ICP-OES in the absence of iron (see Appendix A). Particle size measurements using the Malvern MasterSizer 2000S were used to corroborate the chemical analyses.

### **5.3 Aluminium electroflocculation of pH modified saline**

#### **5.3.1 Elimination of complications due to other contaminants**

By passing a pH-modified NaCl solution down the Flume, complications such as top end blockage, which could arise from the presence of solids, were eliminated. The effect of both pH variation and alteration of process control parameters could be examined closely.

#### **5.3.2 Long-run trials**

The duration of successful long term operation of the Flume at the Tannery had been limited by blockage of the anode with corrosion products. Clearance by flushing with acid flow or similar was considered as a solution. While the system had to be shut down overnight after all-day trials, and required several hours to stabilise after restarting, some multi-day trials including acid flushing were carried out to establish the long term performance of a Flume processor.

The first trial started with fresh aluminium shavings and the following conditions: flume slope of  $15 \pm 2^\circ$ ; inflow conductivity  $3500 \pm 300 \mu\text{S cm}^{-1}$ ; inflow pH of  $7.60 \pm 0.05$  and cell voltage of  $4.00 \pm 0.05 \text{ V}$ . The results for the first day, according to the elapsed time after turning on the power to the electrolyser, are shown in Figure 5-3.

The cell current plot in graph 2 in Figure 5-3 shows a reduction of resistance over time and that the rate of corrosion, as shown by the total outflow aluminium in graph 3, was at least twice-faradic even at a low flow rate. 24-hour supernatant aluminium shown in graph 3 was low for many hours after an initial spike. The pH of the whole outflow shown in graph 1 was significantly lower than the inflow and the difference was proportional to the current.

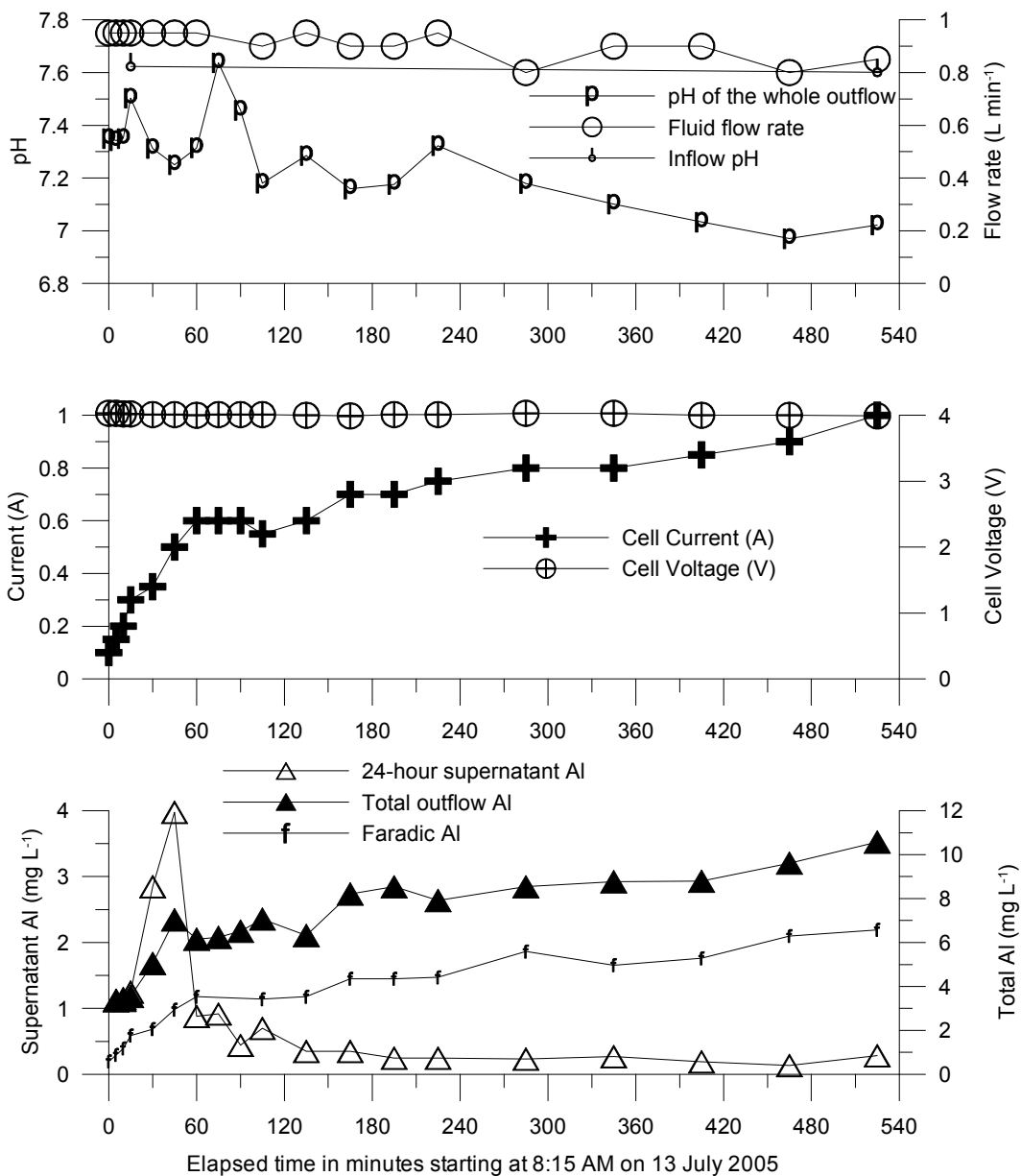


Figure 5-3 The effect of a prolonged run time on process variables and aluminium levels in the outflow for a continuous 9-hour trial of the lab Flume, using saline as electrolyte.

For the next two days, the same shavings were used to continue the experiment. The shavings and dry anode contact were compressed slightly using weights on the anode current distribution rod. Results are shown in Figure 5-4.

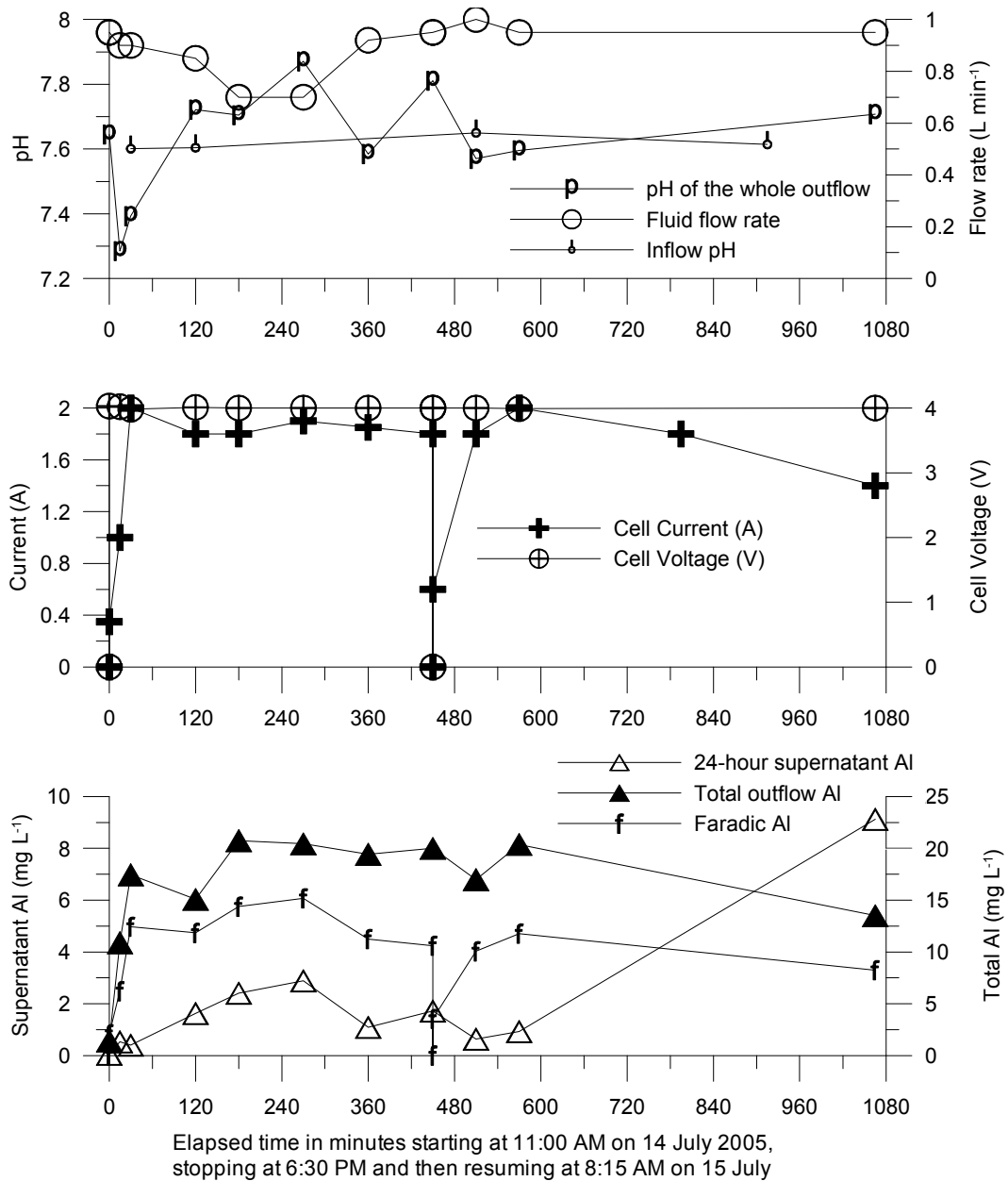


Figure 5-4 The effect of continued use and anode compression during two more days of the trial shown in Figure 5-3.

The cell current plot in graph 2 in Figure 5-4 shows that compression led to a doubling in the initial current but eventual current decay. The higher current due to compression caused greater flow thickness and lower flow speed. The compacted bed of shavings corroded without being cleared, eventually leading to a drop in current during the second day. The plot pH of the whole outflow in graph 1 shows that the pH of the outflow was not lowered significantly compared to the inflow and 24-hour supernatant aluminium of graph 3 shows that the residual aluminium was high toward the end of the trial, especially when the current dropped.

Since trials were not conducted for more than nine consecutive hours, the real lifetime of the system could not be determined precisely, but ten hour run times between deliberate flushing of the shavings seemed feasible. How much overnight breaks (with no power or flow but with the shavings left damp) contributed to the eventual degradation is unknown. As the plot of cell current in graph 2 of Figure 5-4 shows, the system took an hour to recover after a restart in a repeat of the original startup pattern.

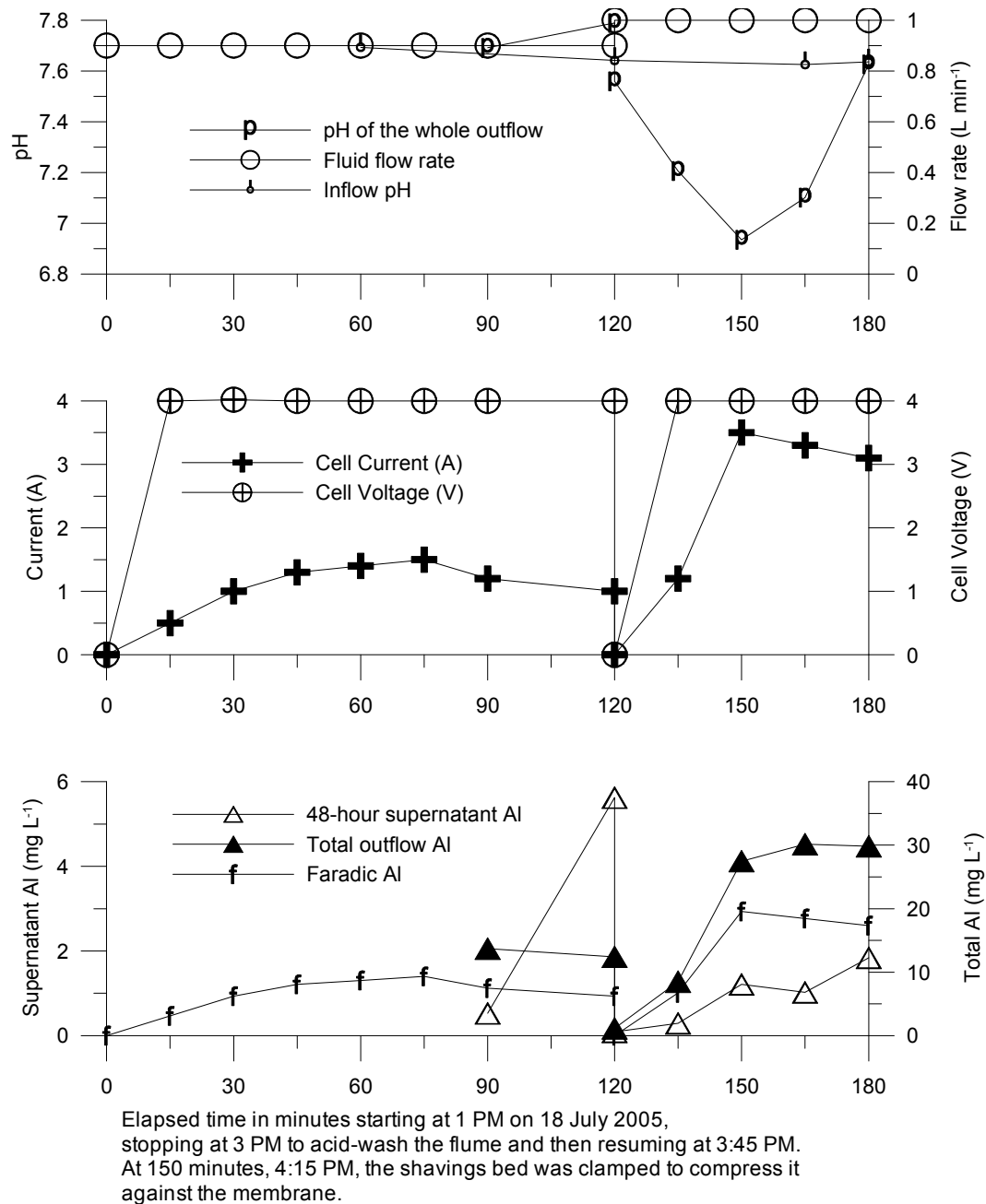


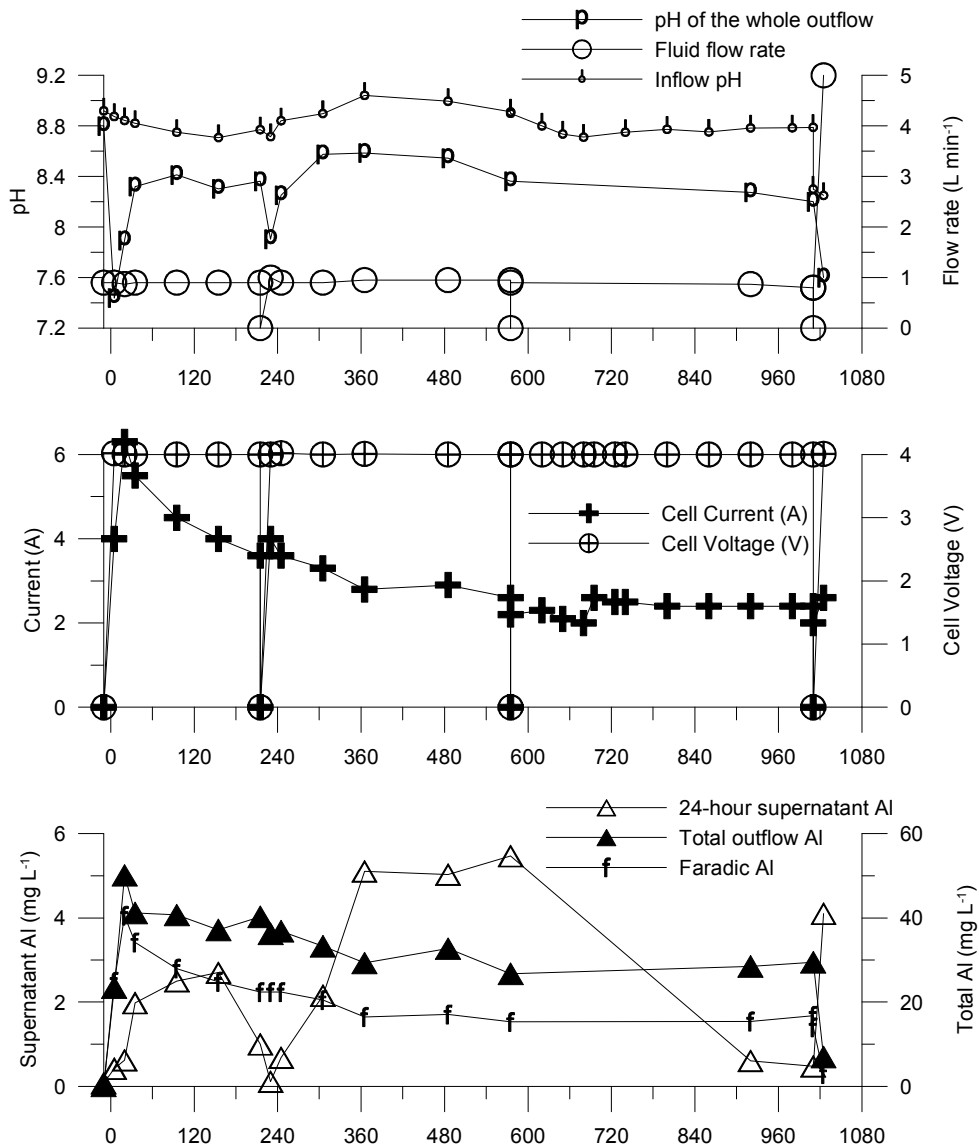
Figure 5-5 The effect of acid rinsing the anode shavings followed by severe compression during continuation of the trial shown in Figure 5-3 and Figure 5-4 for a further day.

Three days later the same body of shavings was rinsed by passing tap water down the Flume and the trial continued. An acid rinse was applied at 120 minutes (elapsed time with power on for the day) and the shavings were compressed into the membrane by mechanically clamping the anode current distribution rod to the cathode just before 150 minutes. Results are shown in Figure 5-5.

48-hour supernatant aluminium plot of graph 3 in Figure 5-5 shows that while it was possible to partly restore the aluminium flocculation function by acid rinsing, this measure was not able to completely restore function. The cell current plot shown in graph 2 was raised by severe compression of the shavings but this led to accelerated blockage. The pH of the whole outflow, shown in graph 1, was lowered directly by the remnants of the acid rinse but remained low for some time until the severe clamping. The measurable symptoms of blockage were now familiar - decay of current, no pH drop and high residual aluminium. The blockage was first observed at the bottom end of the Flume.

To test the long term effectiveness of treatment at higher pH, the inflow pH was raised to 8.8 for a trial starting the next day, and lasting 4 days, with the same shavings as the previous trials. The results are shown in Figure 5-6.

Figure 5-6 shows that the pH of the whole outflow plot in graph 1 is consistently lower than the inflow pH plot of graph 1 and that the 24-hour supernatant aluminium plot in graph 3 tracks the pH of the whole outflow plot in graph 1. The resistance reached a near steady state with 2 A current at 4 V. At the end of the trial the high fluid flow rate plot shown in graph 1 caused a release of stored aged corrosion products from the matrix of the shavings. This caused high residual aluminium (24-hour supernatant aluminium plot in graph 3). A steady flow rate of  $1 \text{ L min}^{-1}$  gave inadequate clearance of corrosion products.



Elapsed time in minutes starting at 1:55 PM on 19 July 2005, stopping at 215 minutes - 5:30 PM to and restarted on 20 July after tap-water rinsing. At 575 minutes the processing was stopped overnight again and restarted on 21 July without rinsing. The processing was stopped at 1010 minutes, then restarted on 27 July for a 15 minute test at high flow.

Figure 5-6 The effect using pH 8.8 inflow on process control variables and outflow aluminium levels for a four day trial.

For continuity of the trials investigating long-term running effects the next trial also used a low flow rate, but with inflow at pH 3.5 and a new bed of shavings. The results are shown in Figure 5-7.

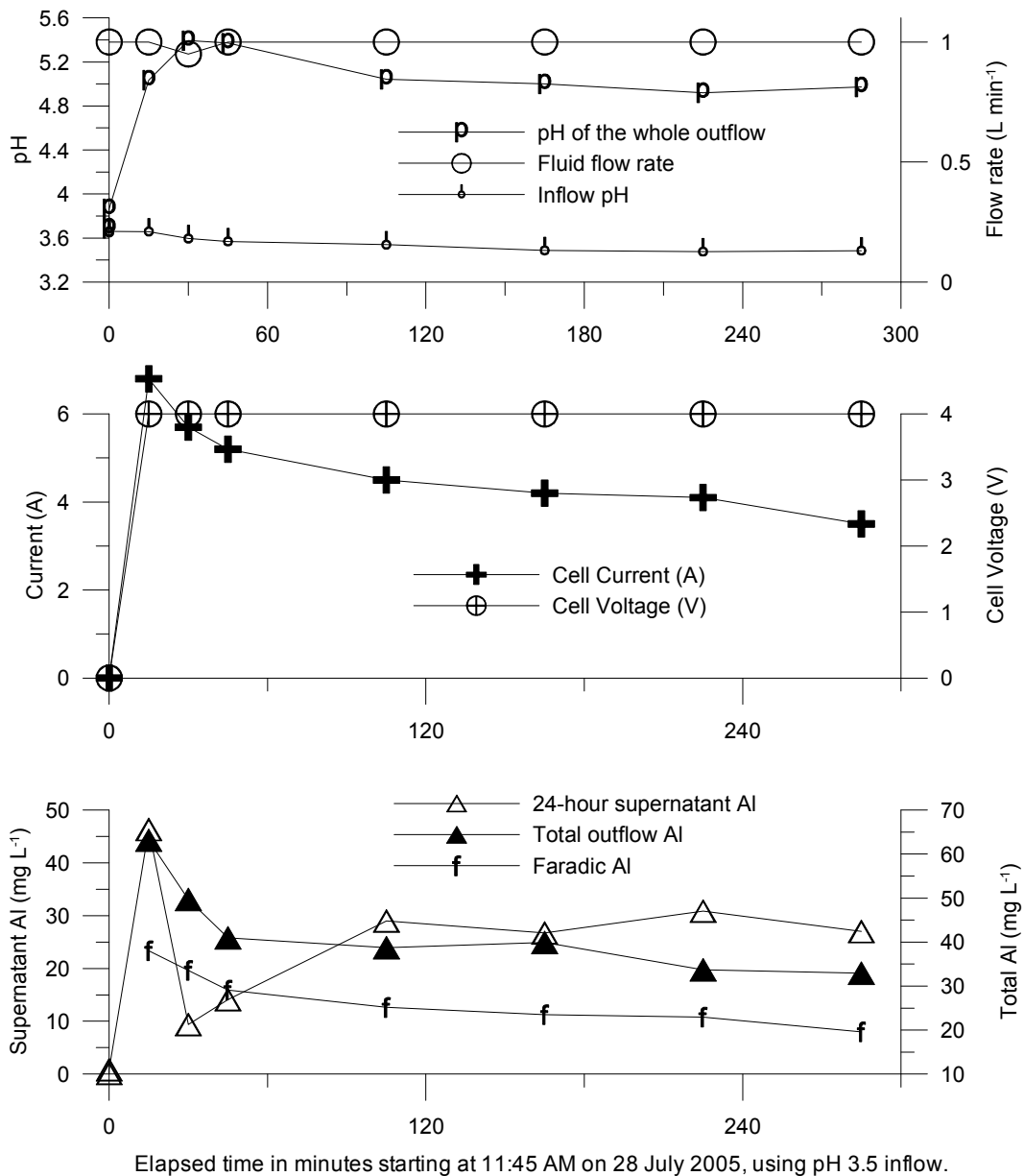


Figure 5-7 The effect of an acid inflow on the process control variables and outflow aluminium levels for a long run trial.

The 24-hour supernatant aluminium plot of graph 3 in Figure 5-7 shows that the residual aluminium level was grossly high. The floc in the outflow was observed to be very fine. The measured total aluminium in the outflow (Total outflow aluminium plot of graph 3) was twice faradic (Faradic aluminium plot of graph 3). The Flume did not block, indicating that the clearance was high. The high clearance left the electrodes un-fouled. This was corroborated by the steady state of moderately high current. The outflow pH was consistently higher than the inflow, but not high enough to achieve good flocculation.



Another acid inflow trial was carried out with the same bed of shavings, but with a slightly lower inflow pH. Controlled current was used and during the trial the current was raised in an attempt to achieve better flocculation. The results are shown in Figure 5-8.

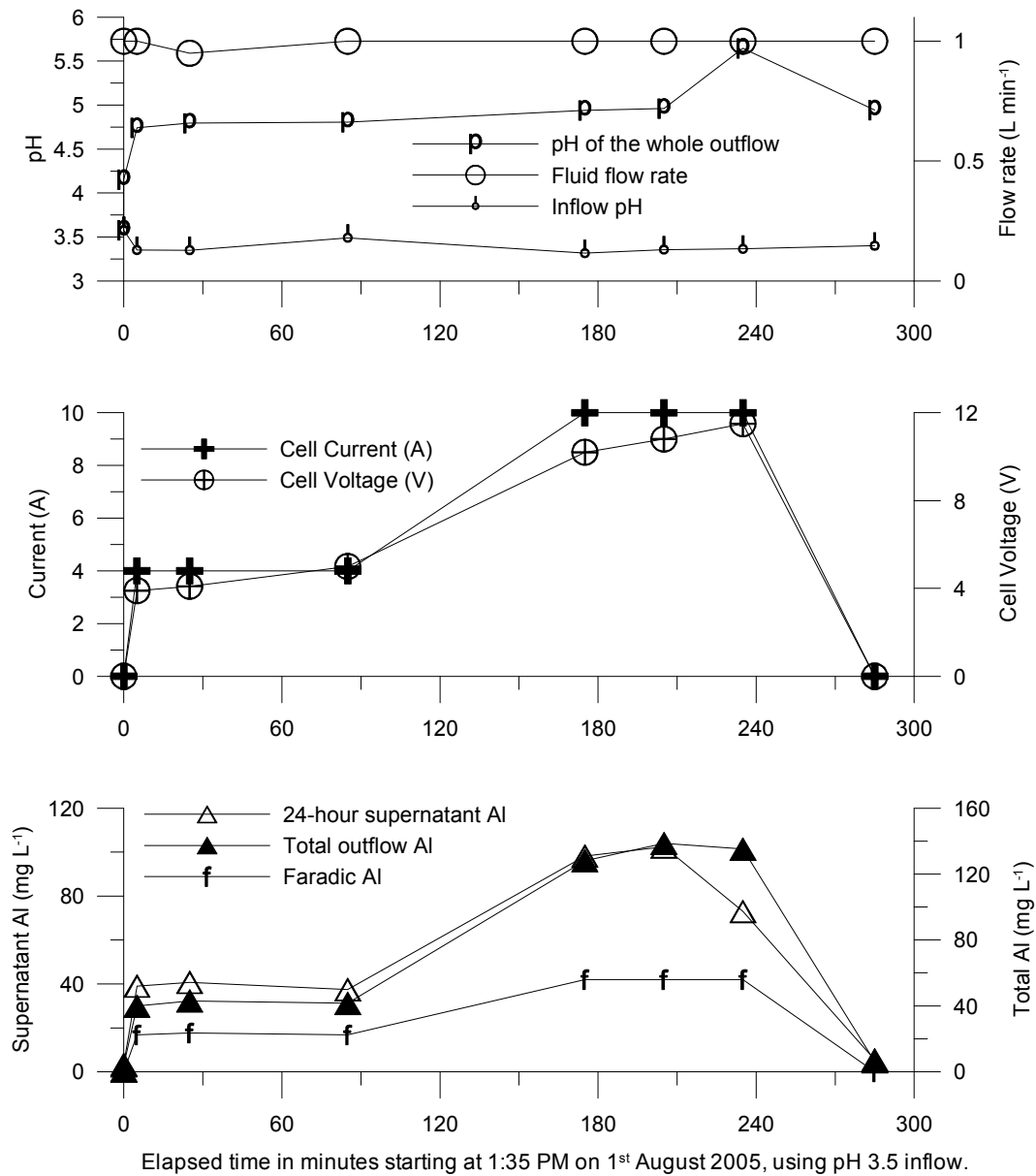


Figure 5-8 The effect of increasing the current on processing of acidic inflow.

The total outflow aluminium and Faradic aluminium plots of graph 3 in Figure 5-8 show that the total corrosion rate was twice faradic initially then increased to three-times faradic when the current was raised by a factor of 2.5. The corrosion rate was low when the power was off and clearance was high throughout the trial. The pH was moderated more by high current. The cell voltage plot shown in

graph 2 was also raised by a similar ratio as the cell current plot in graph 2. These results showed that it was possible to manipulate the pH of the outflow by changing the cell current. While this was for an acidic inflow, it was believed that higher cell current could be used to give greater neutralisation for alkaline inflows too, as anionic aluminium species form at high pH by bonding with  $\text{OH}^-$ .

A trial using an upward ramp of pH from acidic (pH 3) to alkaline (pH 10) was carried out. This trial used a constant current supply (4 A), with no clamping of the shavings. Hence, the cell voltage was higher than the 4 V used for most of the previous trials. The results are shown in Figure 5-9.

The pH of the whole outflow plot of graph 1 in Figure 5-9 shows that the pH was moderated toward 6.4. This closely matches the expected lowest aluminium solubility point. For the initial sub-pH 3 inflow the no-power corrosion rate (shown by the total outflow aluminium plot in graph 3) was significant, but not enough to explain the entire extra-faradic corrosion when the power was on. The 24-hour supernatant aluminium plot shown in graph 3 was low for inflow pH greater than 4 and less than 9. While alkaline inflow caused lower electrical resistance indicated by lowering of the cell voltage plot in graph 2 in the short term, the lower measured outflow aluminium at high pH could indicate poor clearance that would have eventually lead to both a current reduction and flume blockage.

The pH change calculated from the results shown in Figure 5-9 is shown in Figure 5-10. Figure 5-10 shows that for inflow between pH 4 and pH 8.4 the outflow pH was moderated to between pH 5.8 and pH 7 respectively. In this range the outflow supernatant aluminium after 72 hours was below  $1 \text{ mg L}^{-1}$  and as the curve-fit for this range in Equation 5-1 shows that the sensitivity of the outflow pH to inflow pH was low. The energy input per volume of water was between  $0.6 \text{ kWh m}^{-3}$  and  $0.8 \text{ kWh m}^{-3}$  during the trial.

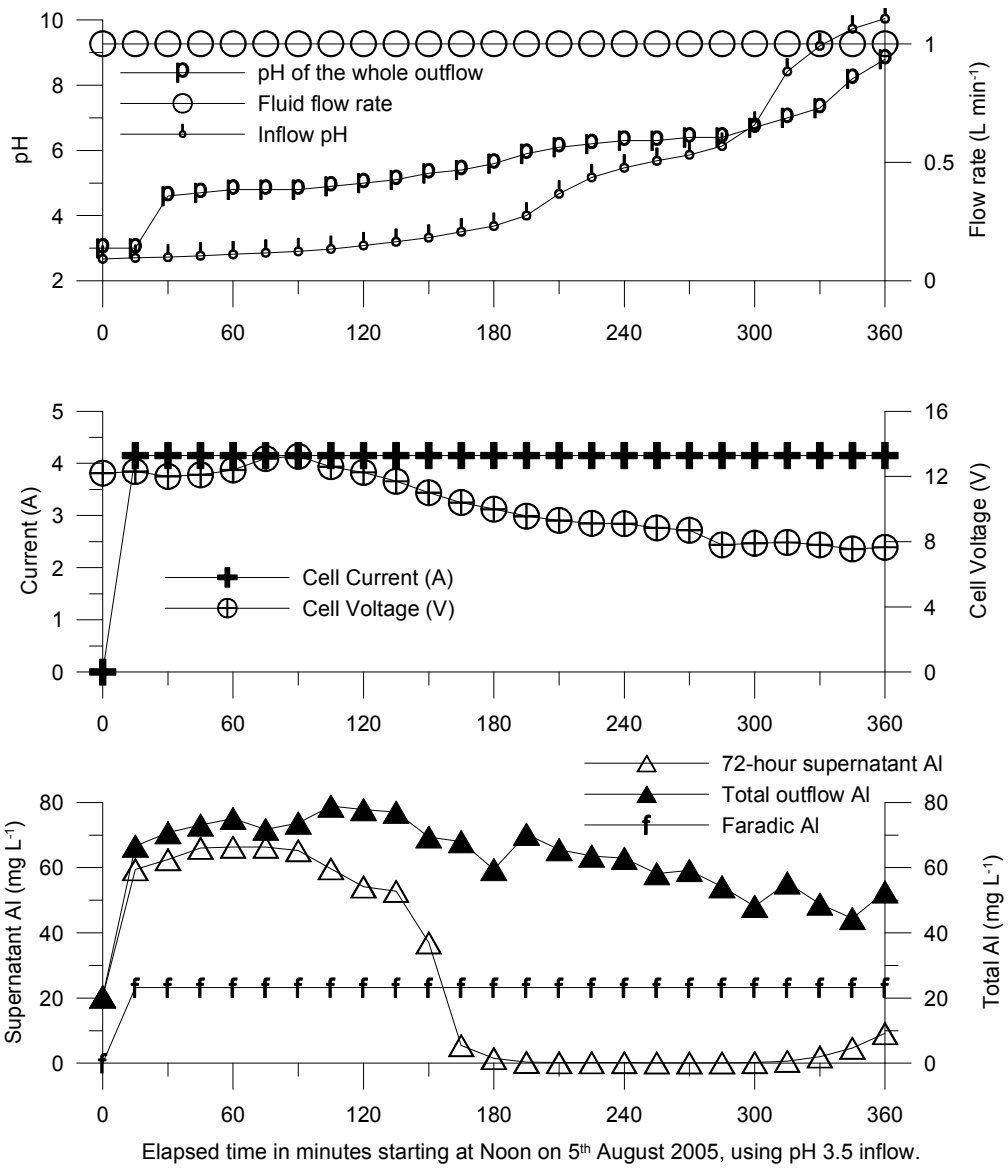


Figure 5-9 The effect of an upward inflow pH ramp from under pH 3 to over pH 10 on process control variables and outflow aluminium levels.

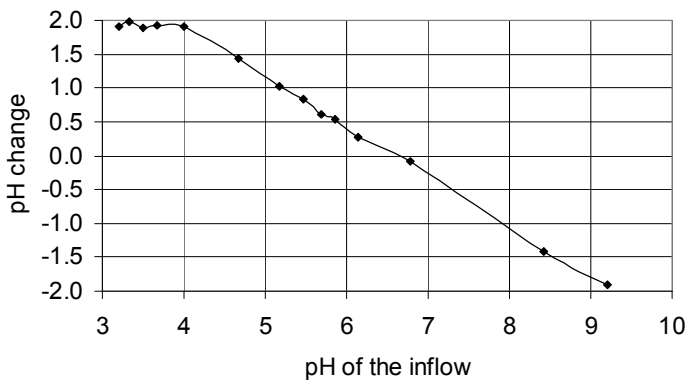


Figure 5-10 The change in pH from inflow to outflow for the conditions shown in Figure 5-9.

Equation 5-1

$$\text{pH}_{\text{out}} = 4.903 + 0.252 \text{pH}_{\text{in}}$$

$R^2 = 0.984$

In order to check the performance for alkaline inflow more thoroughly, a trial using a slow downward ramp of pH from pH 11 was carried out. The results are shown in Figure 5-11.

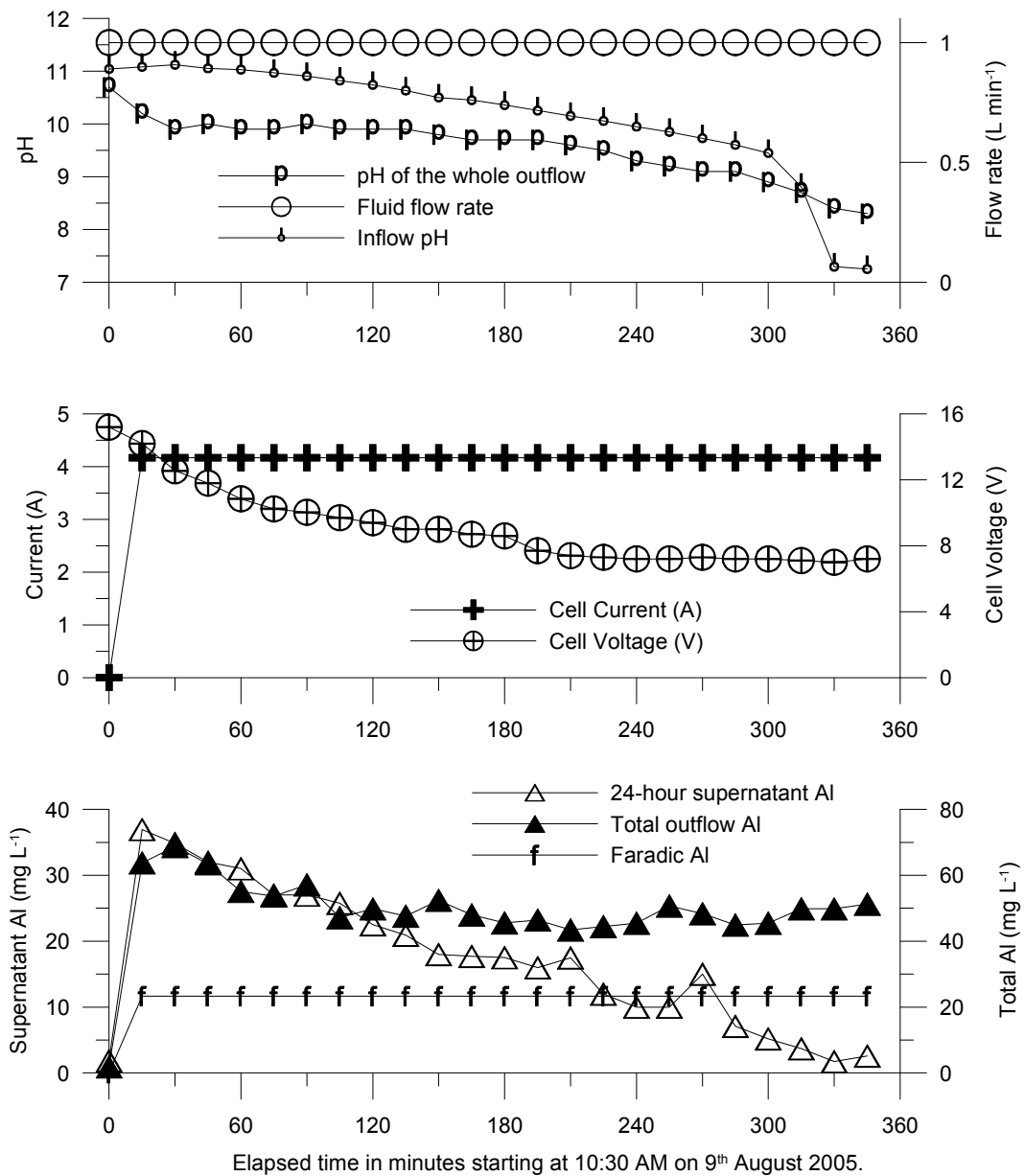


Figure 5-11 The effect of a down-ramp of inflow pH from around pH 11 to near neutral on process control variables and outflow aluminium levels.

Figure 5-11 shows that the pH of the whole outflow pH in graph 1 was slow to respond to the sudden swing of the inflow from pH 9 to pH 7.5 and the 24-hour supernatant aluminium in graph 3 plot reflected this by remaining high. It is likely that significant alkalinity was stored in un-cleared corrosion products at the higher pH. This was released slowly when the inflow pH dropped to near-neutral.

To complete the experimental series investigating pH effects and gain some replicate data, a more rapid ramp of inflow from alkaline to acidic and back again was conducted. This was intended to be an extended simulation of the rapid pH changes that occurred at the tannery. The results are shown in Figure 5-12.

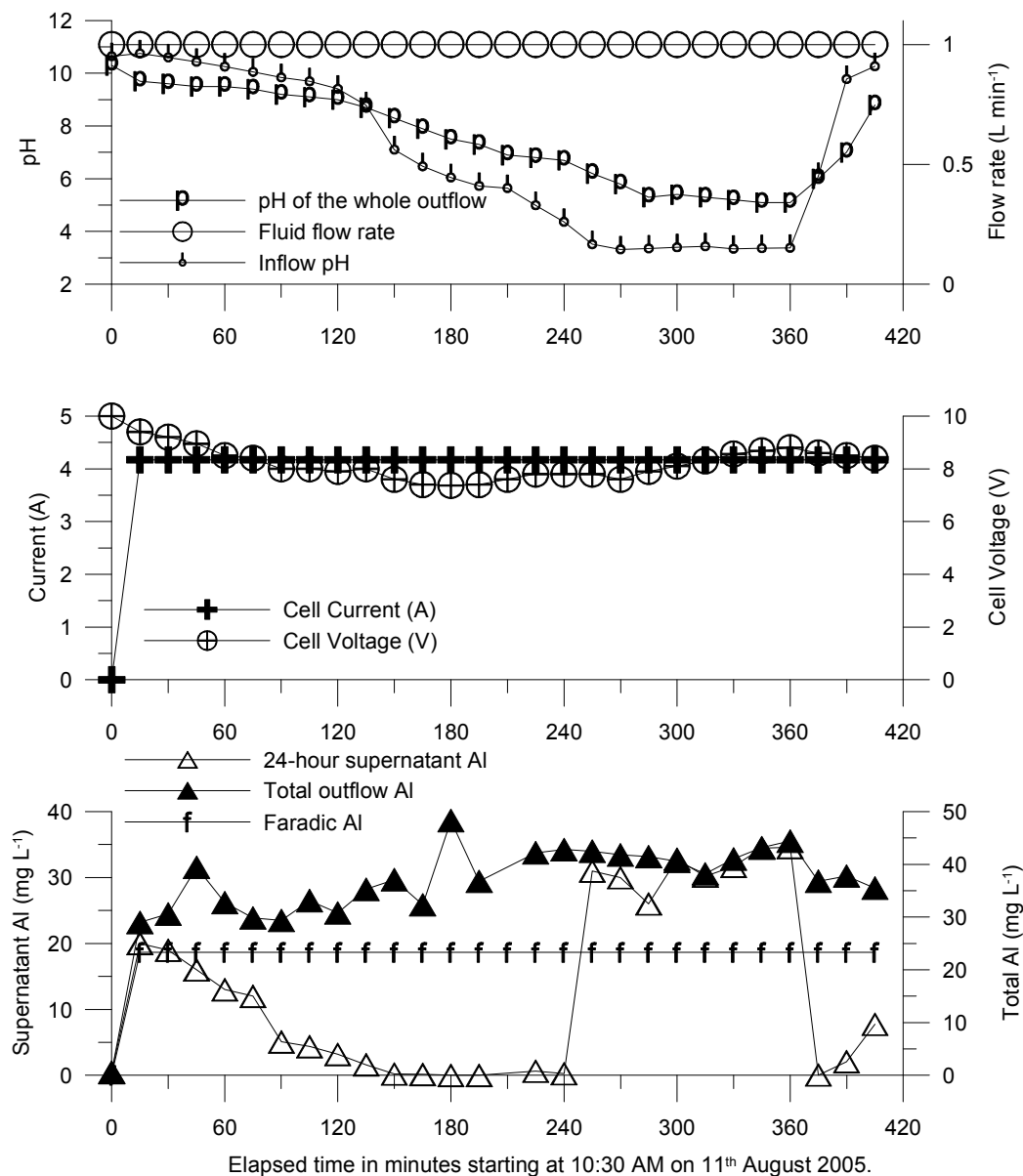


Figure 5-12 The effect of ramping pH down then back up on process control variables and outflow aluminium levels.

The pH of the whole outflow in graph 1 in Figure 5-12 confirmed that when the pH of the inflow was reduced, the crossover inflow pH was 8. This contrasts with the crossover for increasing inflow pH of 6, as seen in Figure 5-9 and Figure 5-11. The 24-hour supernatant aluminium plot in graph 3 reinforced the need for an inflow between pH 8 and pH 10 to be moderated to around pH 8 to achieve good flocculation.

### **5.3.3 Discussion**

The pH of the whole outflow was neutralised by electrolytic treatment. This effect was long-lasting and could have been caused by cathodic plating or dissolution of anodic corrosion products. The dependence of the pH modification on the cell voltage or current density requires further investigation.

The cell resistance usually dropped from the initial value to a plateau, for both constant voltage and constant current power supplies, after a few hours of operation. The reduction in resistance with time was larger for non-neutral pH inflow. The longer term behaviour depended on the pH. Treatment of acid inflow, which could not be flocculated easily, did not cause blockage or clogging with floc. Treatment of alkaline inflow, which could be flocculated easily, did lead to eventual blocking and clogging of the anode. The symptoms of blockage were increased resistance, reduced pH modification and thickening of the flow depth especially near the bottom of the Flume. The Flume stored  $\text{Al}(\text{OH})_3$  in the anode when treating moderately alkaline inflow pH, so that when the inflow pH was reduced the outflow was buffered to relatively high pH. By rinsing the Flume with acidic fluid, in an analogy to back-flushing a filter, the corrosion products could be removed and function partly restored. However the deeper flow during blockage had led to partial corrosion of a thick layer of shavings, so the resistance was still relatively high even after acid-flushing.

Compressing the shavings against the membrane made the resistance lower by both lowering the distance between the anode and the cathode and by increasing the effective cathode area. However, operation under high compression could not be sustained as the clearance of corrosion products was hindered.

## 5.4 pH modification by splitting the outflow

### 5.4.1 Passage of fluid through the membrane

When water was introduced to the Flume in the anode compartment, only a very small fraction, less than 0.1%, passed through the membrane into the cathode compartment due to gravity and capillarity. This seepage was essential because it supplied the part of the electrolyte that carried the ionic current between the anode and cathode.

Because the pore size of the nylon membrane was less than 10  $\mu\text{m}$ , the passage of metal fragments from the main flow stream to the cathode was very limited.

However, both dissolved and colloidal aluminium were able to pass through the membrane by diffusion. Where the anolyte was close to neutral pH, the catholyte had a higher total aluminium concentration than the anolyte, due to the greater solubility of aluminium at the higher pH, though both were sub- $\text{mg L}^{-1}$ . At higher anolyte pH, the catholyte had a similar aluminium concentration to the anolyte, in the range of 10  $\text{mg L}^{-1}$  to 20  $\text{mg L}^{-1}$ . Because the bottom-section of the Flume was not electrochemically active, leakage of anolyte to the catholyte in that section could easily lower the catholyte pH resulting in precipitation of aluminium in the catholyte. The loss of aluminium by electrowinning was expected to be low, even if the fraction of aluminium in the catholyte that is plated was 100%, because of the low catholyte flow.

The separation of the catholyte from the anolyte by the membrane offered a very direct method of modifying the pH of treated water – splitting the whole outflow into anolyte and catholyte. A means of achieving this in the laboratory flume was application of a short section of polyethylene sheet on top of the main membrane at the outlet end, extending beyond the end of the Flume, creating an anolyte funnel. The catholyte continued to drip slowly off the bottom end of the Flume from under the main membrane. The pH of the catholyte was found to be very stable, taking hours to build up to a pH greater than 12 and took hours to decay after the power was switched off. So despite the low catholyte flow, considerable alkalinity was stored in the cathode compartment.

Trials in which the pH of fluids from different compartments were monitored followed. It was also determined that the problem of low corrosion product clearance for alkaline pH inflow should be ameliorated at this stage by raising the flow rate to  $3.5 \text{ L min}^{-1}$  which gave equivalent flow speed as flows of  $10 \text{ L min}^{-1}$  in the larger flume used at the tannery.

#### 5.4.2 Using split flow to achieve lower residual aluminium

New shavings were installed for a trial to test the effect of different currents on anolyte outflow pH. Inflow of pH 9.6 was treated using current that was changed in steps. The results are shown in Figure 5-13.

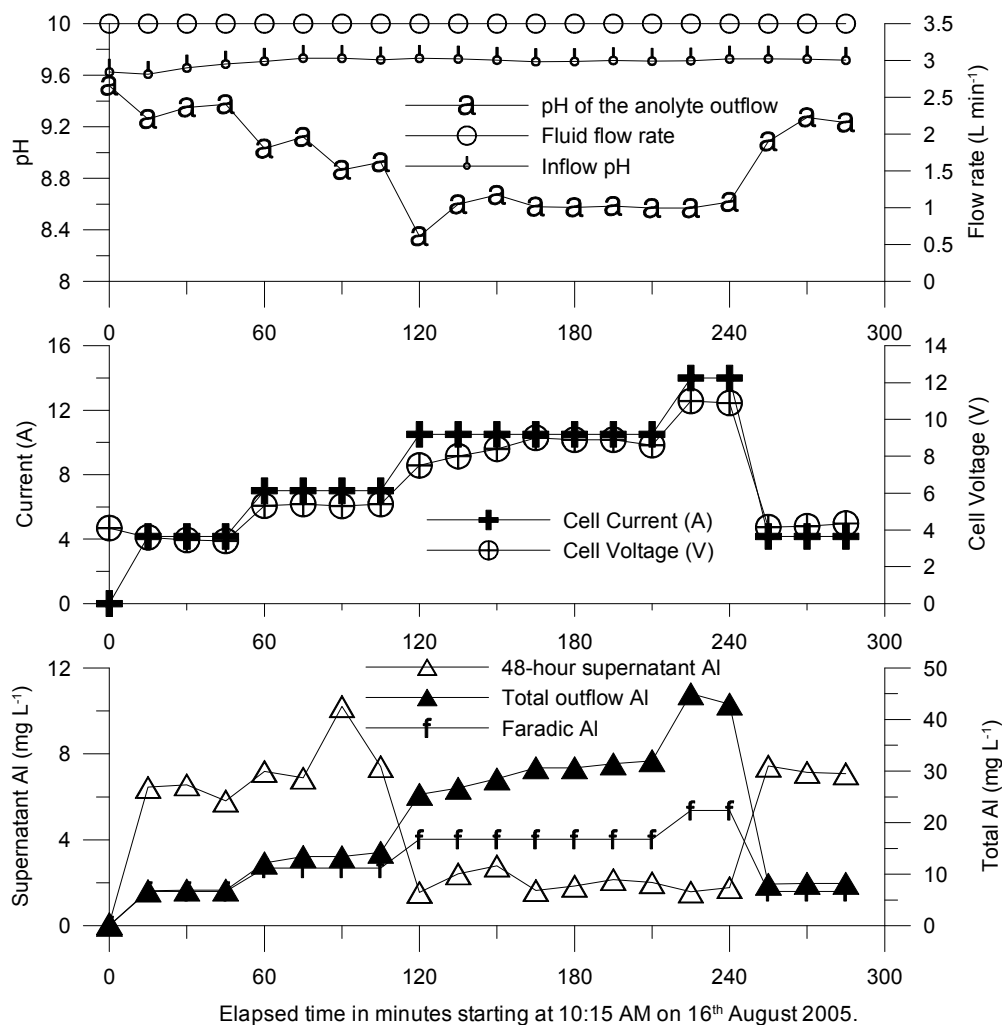


Figure 5-13 The effect of splitting the anolyte and the catholyte while changing the current in steps on process control variables and outflow aluminium levels.



The pH of the anolyte outflow plot of graph 1 in Figure 5-13 shows that pH moderation of alkaline inflow is easily exerted by changing the cell current (of graph 2) using a current-regulated power supply. When the current was higher the extra-faradic corrosion (the difference between Total outflow aluminium and Faradic aluminium in graph 3) was a greater proportion of the total corrosion (Total outflow aluminium of graph 3), in parallel to the moderation of pH. At low current, the extra-faradic corrosion was very low, but there was still some pH moderation of the anolyte due the separation from the catholyte.

To investigate the differences between whole outflow and anolyte further, another trial in which samples of both anolyte and whole outflow were collected was carried out. Similar steps of controlled current to the previous trial were used for a moderate inflow pH of 8 to 8.5. The results are shown in Figure 5-14. Note the log scale for the aluminium level plots in graphs 3 and 4 and low initial levels of aluminium when the power was off.

Figure 5-14 shows that the pH is moderated more in the anolyte (pH of the anolyte outflow in graph 1) than the whole outflow (Whole outflow pH plot of graph 1) and that the residual aluminium in the supernatant is lower in the anolyte (48-hour anolyte supernatant aluminium plot in graph 3) than in the whole outflow (Whole outflow 48-hour supernatant aluminium in graph 3) at all but the lowest dose where flocculation was marginal and limited by alkalinity. The level of dissolved aluminium was consistently lower in the anolyte than in the whole outflow. At high doses or when the dose was reduced there were spikes in both the pH and residual aluminium, particularly in the whole outflow. So the choice between whole or anolyte outflow would depend on criteria of outflow quality, the level of treatment required, and the feasibility of post-processing filtration.

The aluminium concentration data from Figure 5-14 is compared to expected saturation concentration of aluminium, as  $\text{Al(OH)}_4^-$  formed from amorphous  $\text{Al(OH)}_3$ , in Figure 5-15. In order to resolve the low levels of aluminium achieved by this trial, below  $0.1 \text{ mg L}^{-1}$ , sensitive ICP-OES methods were used (see Appendix A).

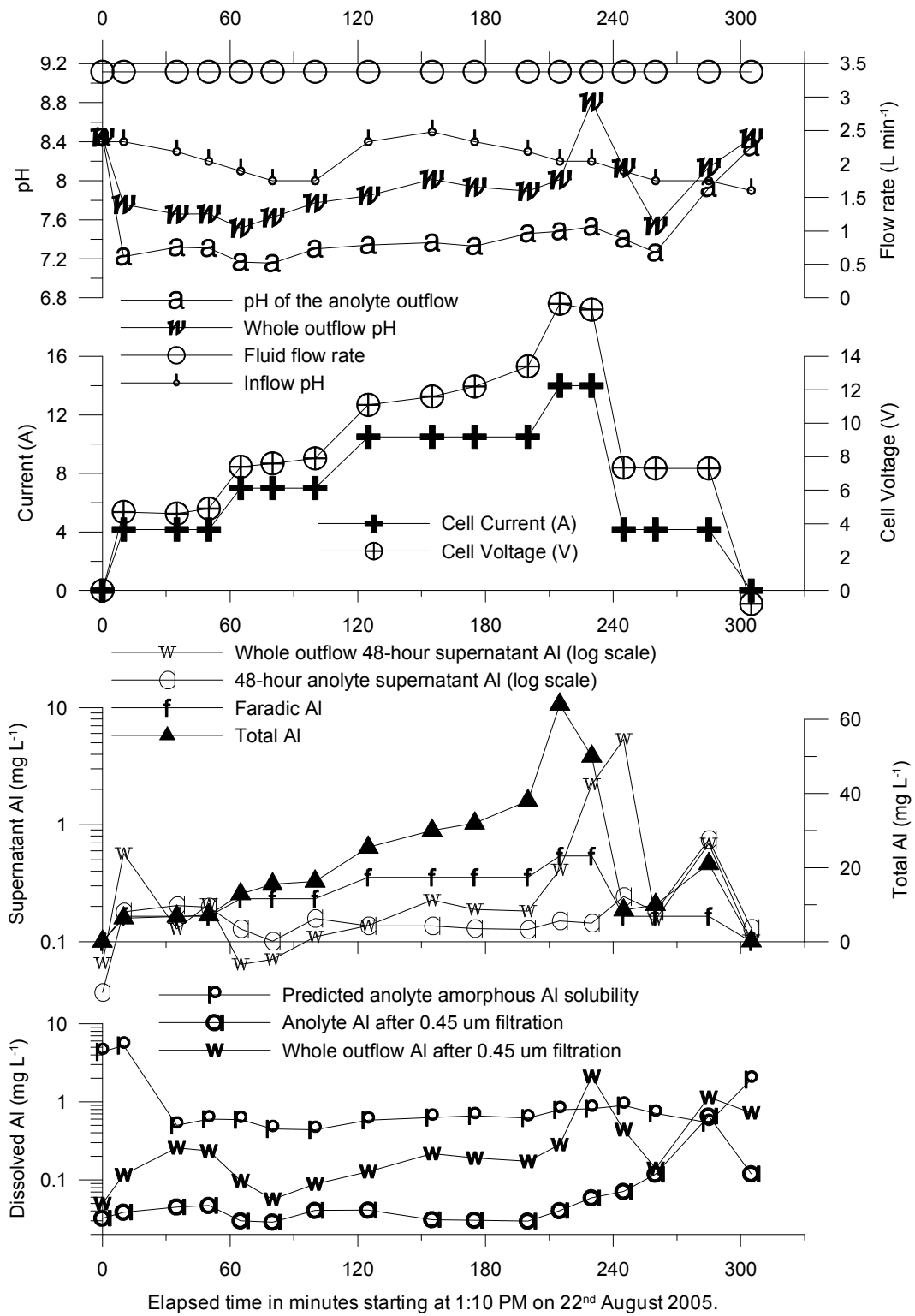


Figure 5-14 Process control variables and outflow aluminium levels showing the greater pH moderation in anolyte compared to whole outflow, corroborated by lower dissolved aluminium in the anolyte.

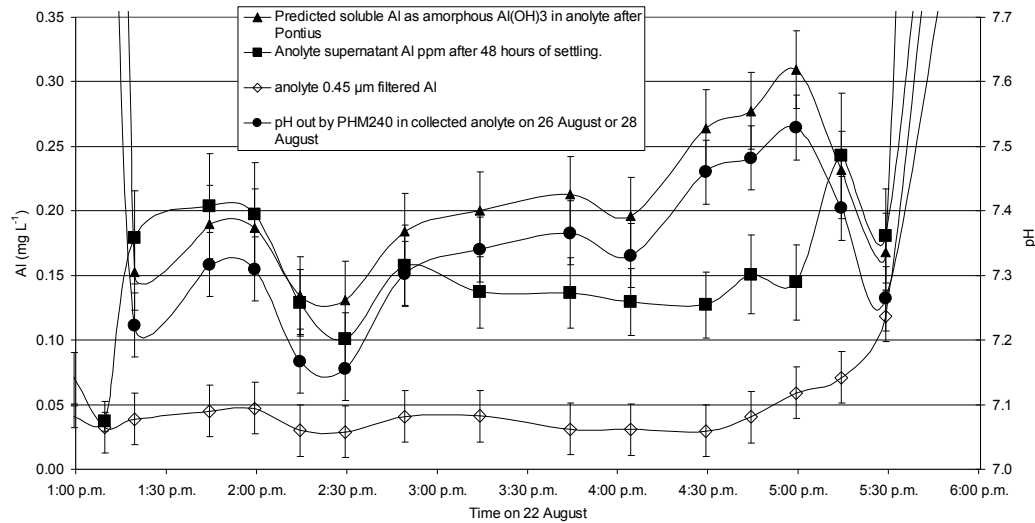


Figure 5-15 Comparison of predicted and measured aluminium in the both the anolyte and whole outflow. The solubility prediction is a function of pH, but both the 48-hour supernatants and the 0.45 µm filtered samples had lower aluminium levels than predicted.

Figure 5-15 shows both the supernatants and the 0.45 µm filtered samples had less aluminium than would be predicted thermodynamically (see Figure 1-5). This seemed rather improbable, so both the theoretical estimates and the experimental results were checked thoroughly.

In case the floc was crystalline, the same data is shown plotted in comparison to predicted levels of aluminium as aluminate formed from both amorphous and crystalline Al(OH)<sub>3</sub> in Figure 5-16.

Graph 3 of Figure 5-16 shows that the anolyte outflow had a lower measured level of dissolved aluminium (0.45 µm filtered plot) than the whole outflow (graph 2) and both had a lower level than would be predicted if the aluminium were part of an amorphous floc (predicted amorphous aluminium solubility traces) but more than if the aluminium were part of a crystalline (gibbsite) precipitate (predicted solubility of crystalline Al(OH)<sub>3</sub> plots). This was also true for the initial no-power samples, indicating that thermodynamic equilibrium had not been established.

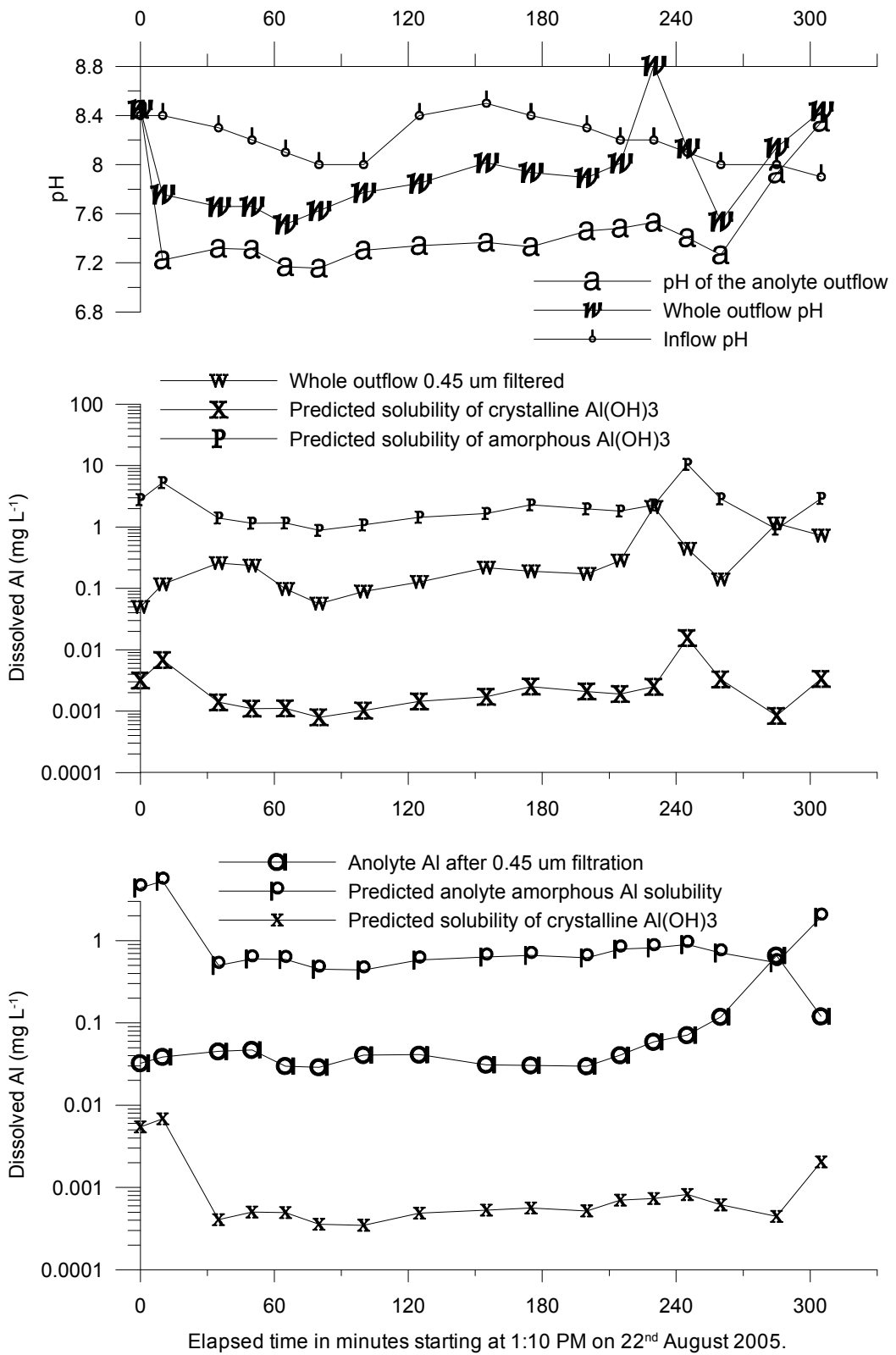


Figure 5-16 Comparison of predicted dissolved aluminium levels, for both amorphous and crystalline forms of Al(OH)<sub>3</sub>, with measured levels of aluminium after 0.45 μm filtration.

To test the limits of pH reduction, a trial with relatively high inflow pH of 10 and high electrical conductivity of  $13600 \mu\text{S cm}^{-1}$ , as would be expected in extreme cases at the tannery, was carried out. The results are shown in Figure 5-17.

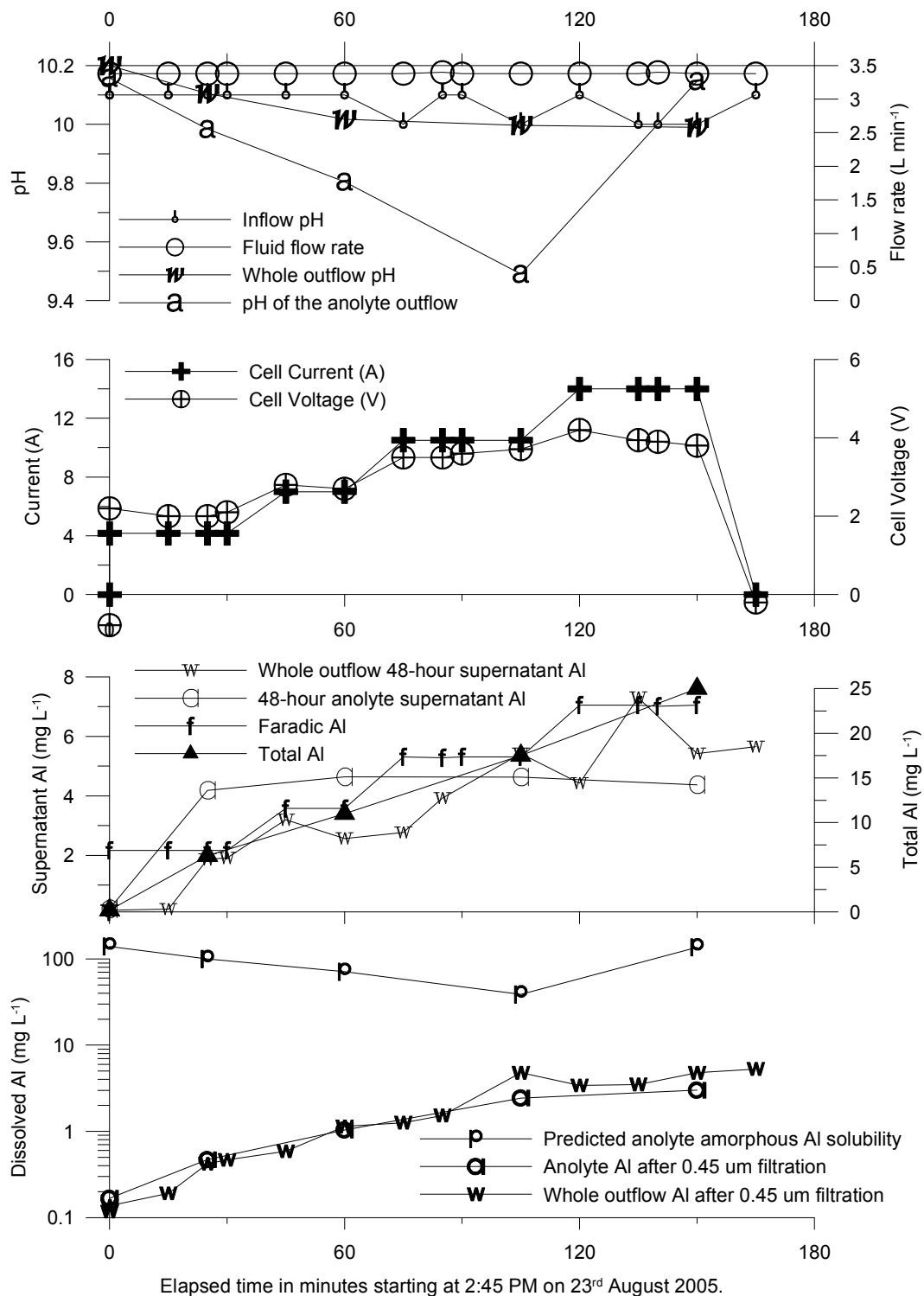


Figure 5-17 The effect of split outflow when treating high pH inflow on process control variables and outflow aluminium levels.

Figure 5-17 shows greater pH drop from that of the inflow (inflow pH plot of graph 1) in the anolyte (pH of the anolyte outflow plot in graph 1) compared the whole outflow pH plot of graph 1 and high residual aluminium (anolyte and catholyte 48-hour supernatant aluminium plot in graph 3 and 0.45  $\mu\text{m}$  filtration traces of graph 3) despite the strong floc observed in the outflow, especially at higher current doses (cell current plot of graph 2).

A comparison of the aluminium levels with theoretical predictions is shown in Figure 5-18.

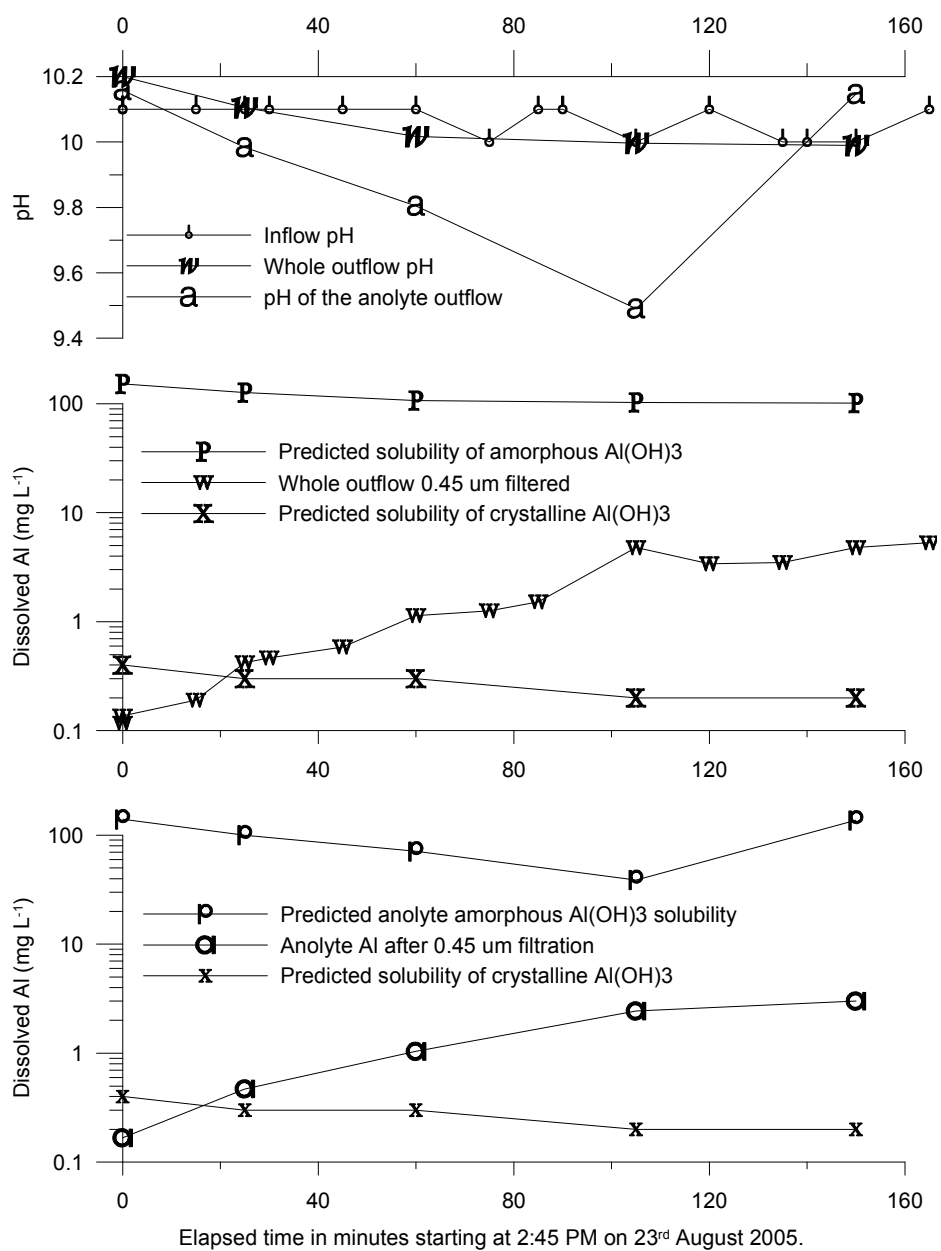


Figure 5-18 Comparison of both whole outflow and anolyte dissolved aluminium with theoretical predictions for solubility of amorphous and crystalline  $\text{Al}(\text{OH})_3$ .

The performance in terms of residual aluminium seemed to be worse than for comparable treatment of water at the tannery with both high pH and high conductivity. This was partly due to traces of polymer coagulant in the DAF outflow at the tannery. The high conductivity meant that the cell voltage was low. The total measured outflow aluminium was almost faradic and the pH drop was small. However, the predicted levels of dissolved aluminium were still an order of magnitude or two higher than the measured levels.

Comparison of the results shown in Figure 5-14 to Figure 5-18 gave some insight into the linkage between extra-faradic corrosion and pH drop, as well as causal factors for these effects. The different results obtained for water of moderate pH and low conductivity, compared with water of high pH and high conductivity were examined by plotting the total measured outflow aluminium against cell current. This is shown in Figure 5-19.

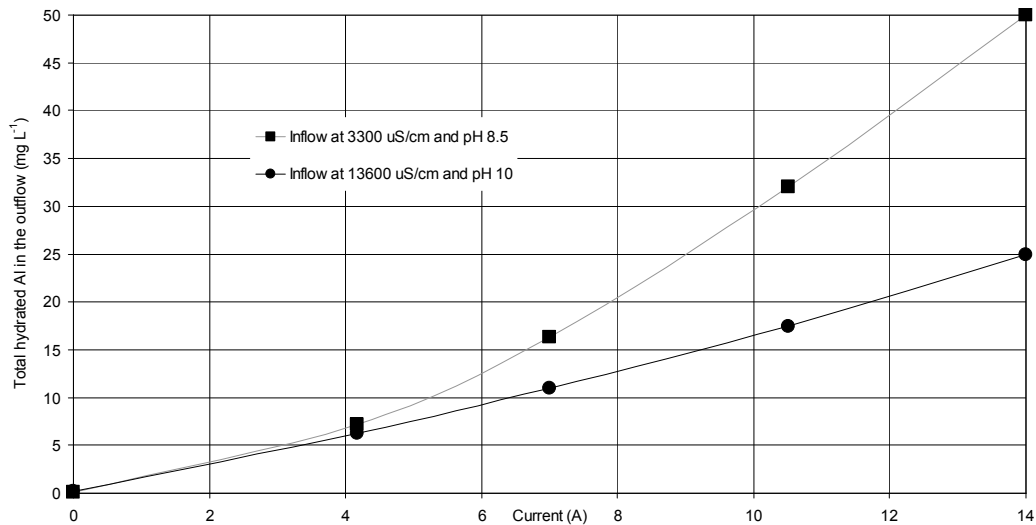


Figure 5-19 Greater extra-faradic corrosion at moderate pH with low conductivity water at a given current than for high pH with high conductivity.

Figure 5-19 shows that the amount of aluminium delivered to the outflow was greater than faradic if the conductivity and pH were low, whereas it was faradic if the conductivity and pH were high. The different results obtained for water of moderate pH and low conductivity compared to water of high pH and high conductivity were reviewed by plotting the total measured outflow aluminium against cell voltage. This is shown in Figure 5-20.

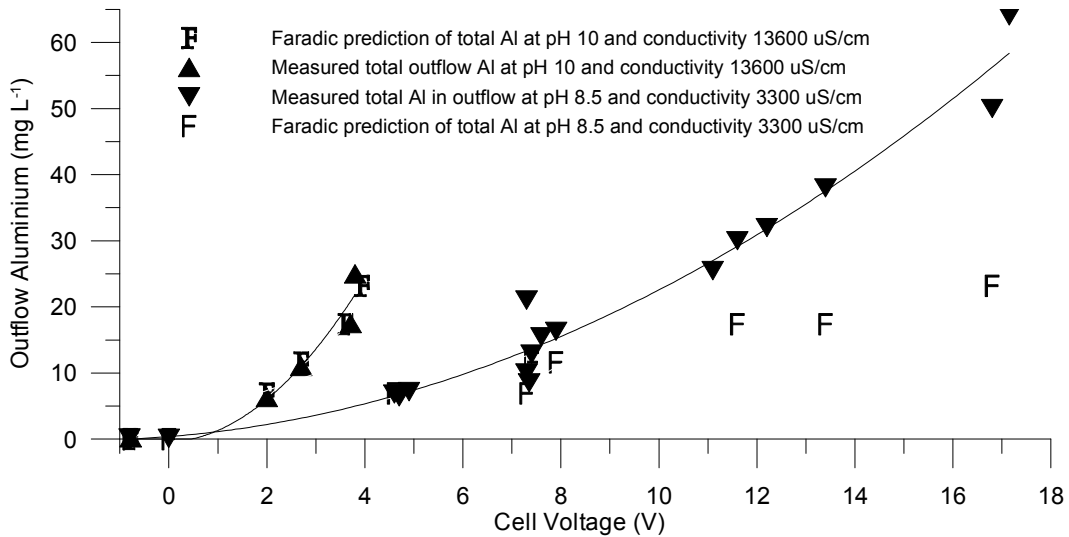


Figure 5-20 Total outflow aluminium versus cell voltage for two different electrolytes.

Figure 5-19 and Figure 5-20 show that there is less extra-faradic corrosion in very conductive high pH inflow for the same current, current density or corresponding voltage as there is for lower conductivity, moderate pH inflow. The cell voltage was less than zero for zero current, as the cell performed as a weak battery or fuel cell. For the relatively weak electrolyte at lower pH, the current is approximately linear with voltage, whereas for more conductive electrolyte at high pH, the current is proportional to the square of the cell voltage. In both cases, the measured outflow aluminium is approximated by a quadratic function of the cell voltage, as shown in Equation 5-2 and Equation 5-3.

$$\text{Equation 5-2} \quad \text{Al (mg L}^{-1}\text{) for pH 10 and } 13600 \mu\text{S cm}^{-1} = 0.374 + 0.593V + 0.163V^2$$

$$R^2 = 0.96$$

$$\text{Equation 5-3} \quad \text{Al (mg L}^{-1}\text{) for pH 8.5 and } 3300 \mu\text{S cm}^{-1} = -0.439 + 0.274V + 1.473V^2$$

$$R^2 = 0.94$$

Because the apparent solubility of aluminium in many of the trials was lower than predicted by the solubility of amorphous  $\text{Al(OH)}_3$ , but higher than would be



expected for crystalline (gibbsite)  $\text{Al}(\text{OH})_3$ , a sample of freshly made floc was freeze-dried immediately. The resulting white powder was examined by X-ray diffraction. As Figure 5-21 shows the sample was found to be amorphous, or least composed of very small crystals.

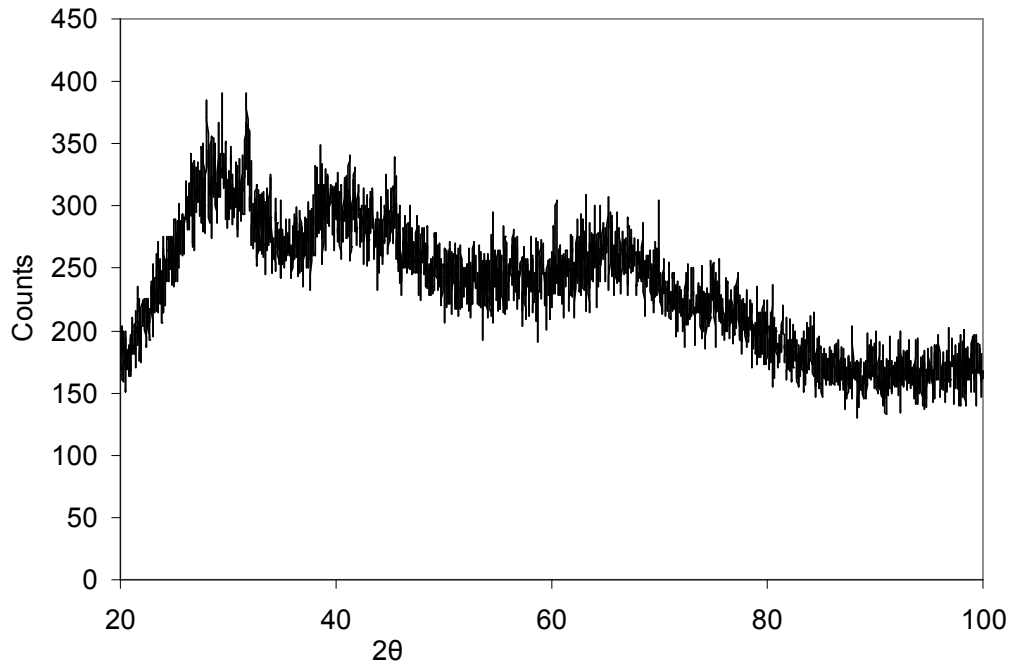


*Figure 5-21 Typical XRD spectrum ( $\text{Cu K}\alpha$ ) of aluminium floc after freeze drying showing no well-defined crystalline structure.*

### 5.4.3 Discussion

Moderation of alkaline effluent pH both lowered the residual aluminium in the anolyte outflow and produced a recyclable caustic catholyte outflow. The pH of whole outflow was moderated by electrolytic processing. Both the pH difference between anolyte and catholyte and difference between the whole outflow pH and the inflow pH are adjustable. Splitting the outflow into anolyte and catholyte flows allows greater pH adjustment. The moderation of pH was controlled by either the cell current or cell voltage.

## **5.5 Chromium removal from saline and saline with protein**

### **5.5.1 Chromium and protein**

Chromium was the most toxic, yet valuable, component in the tannery effluent. Hence, it was crucial to establish the conditions in which it could be removed from the effluent. Chromium was bound to both dissolved and solid protein in the tannery effluent. Dissolved protein in the tannery effluent stabilised chromium in a soluble or colloidal form (Langdon, A. 2005, pers. comm., 1<sup>st</sup> September), making it more difficult to flocculate. By conducting laboratory trials in the laboratory with chromium alone and a combination of chromium and protein it was hoped to gain insight into the mechanism of chromium removal from the effluent.

### **5.5.2 Chromium removal from pH-modified saline**

The result of electrolytic treatment of chromium contaminated inflow, with both pH and conductivity at the upper end of that found in tannery effluent, is shown in Figure 5-22.

The cell voltage plot shown in graph 2 in Figure 5-22 was low. The aluminium corrosion (total aluminium plot of graph 3) was approximately faradic. The pH was not lowered enough to produce a low aluminium residual even in the anolyte (24-hour anolyte supernatant aluminium plot of graph 3). The supernatant and dissolved chromium levels (anolyte 24-hour supernatant chromium and chromium after 0.45  $\mu\text{m}$  filtration of anolyte plots respectively in graph 4) were low even without power but were reduced significantly by electrolytic treatment in step with the cell current in graph 2. At greater than 11 A, a dose of  $3 \text{ A (L min}^{-1}\text{)}^{-1}$ , the flocculation was good and a clear supernatant formed within an hour. The absolute uncertainty of the low-level chromium measurements was  $0.02 \text{ mg L}^{-1}$ , but the resolution, as gauged by the repeatability, was  $0.01 \text{ mg L}^{-1}$ . Both the supernatant chromium and dissolved chromium were reduced to the resolution limit of measurement by treatment with  $40 \text{ mg L}^{-1} \text{ Al}_2\text{O}_3$  equivalent.

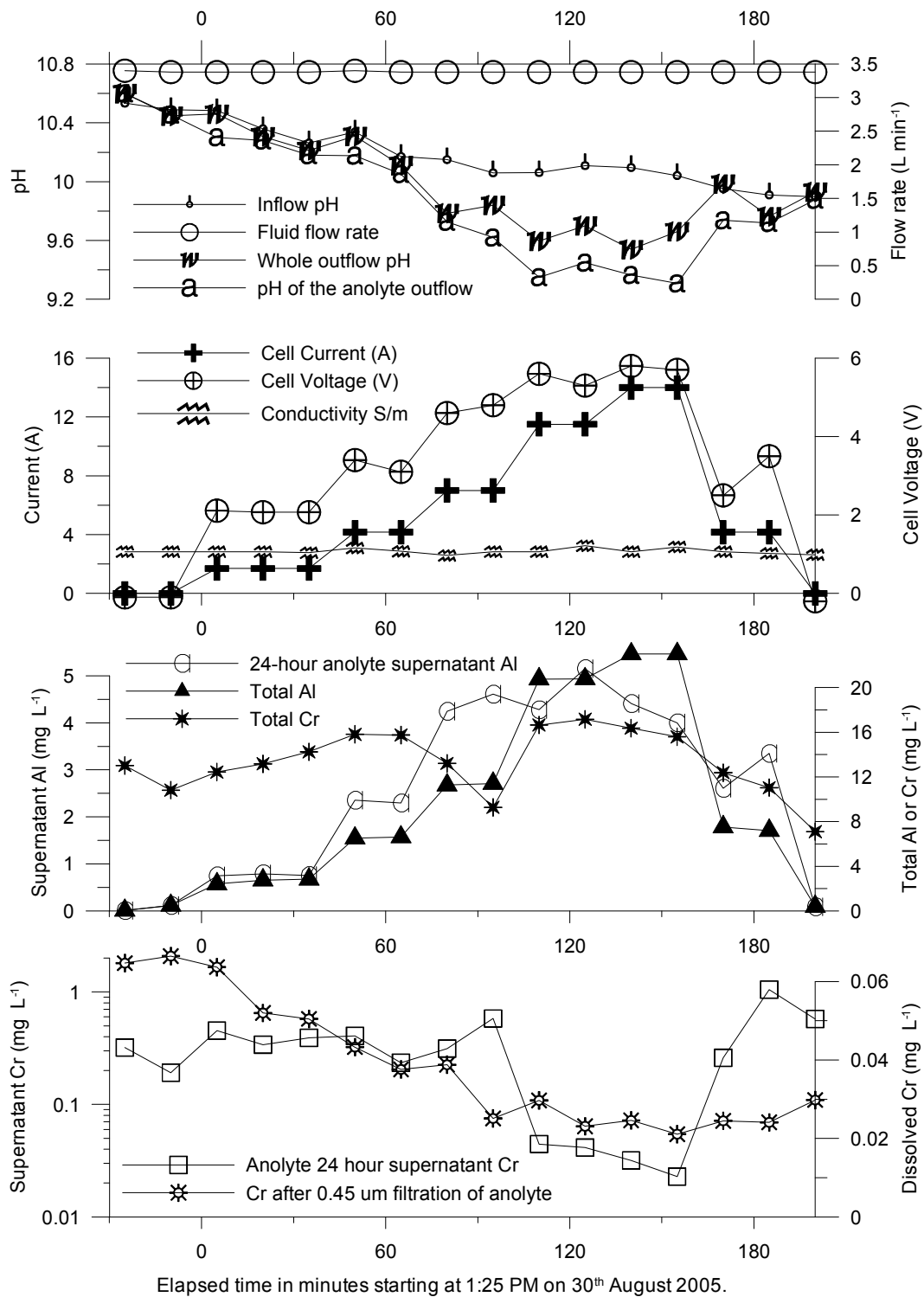


Figure 5-22 chromium removal from high pH and conductivity chromium-laden water by electrolytic treatment.

The measured supernatant levels of aluminium in comparison to the predicted solubility of aluminium as both an amorphous hydroxide and as a crystalline hydroxide are shown in Figure 5-23.

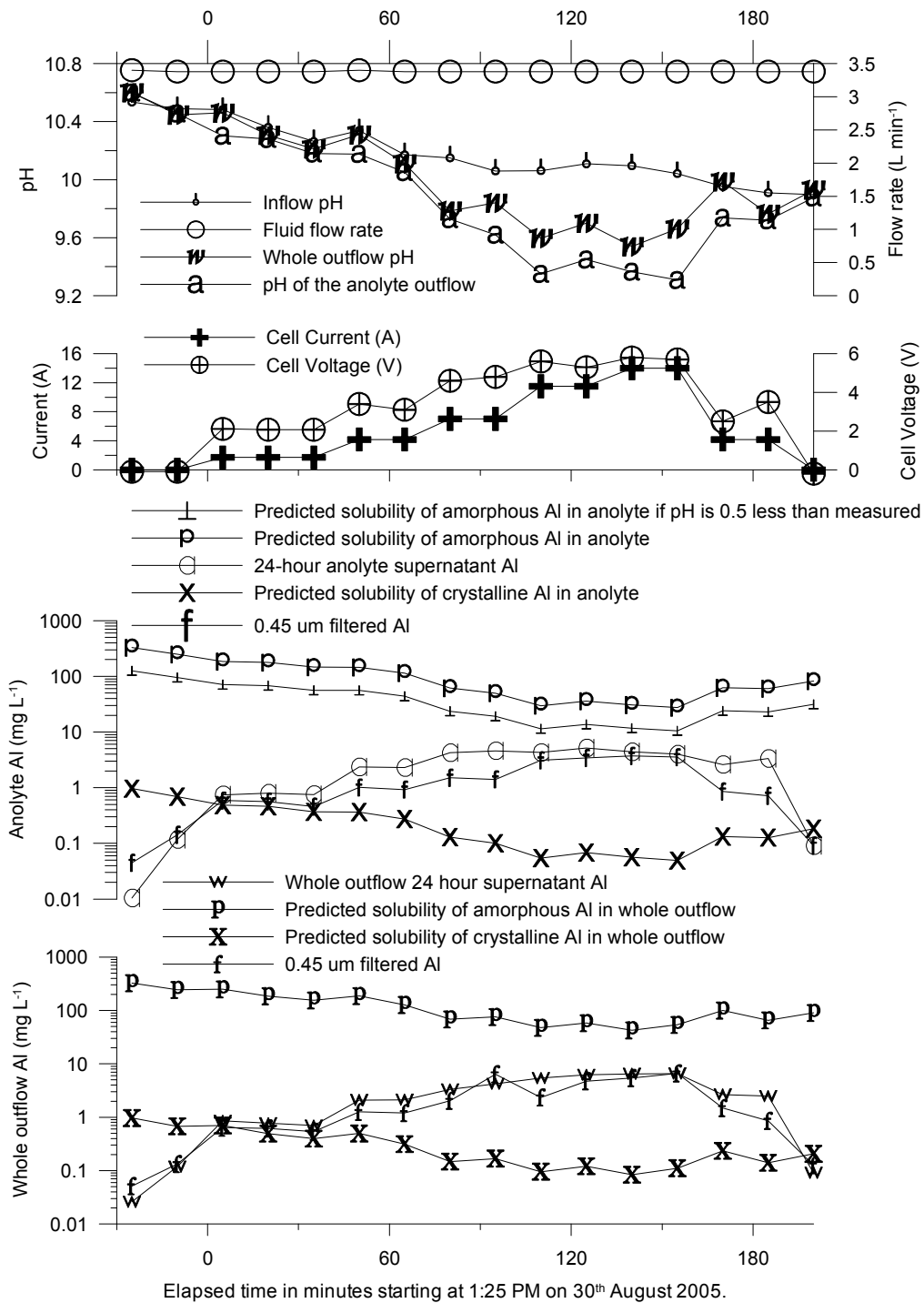


Figure 5-23 Comparison of predicted and actual solubility of aluminium when treating chromium contaminated water.

Graphs 3 and 4 of Figure 5-23 show that the measured supernatant levels of aluminium were between that predicted by solubility of aluminium as an amorphous hydroxide and that predicted by solubility of a crystalline hydroxide. Even if the real pH of the anolyte was 0.5 pH units lower than the measured pH, the predicted solubility of aluminium as amorphous floc (plot of predicted solubility of amorphous aluminium if pH is 0.5 less than measured, in graph 3)

was still higher than the values measured by ICP-OES (24-hour analyte supernatant aluminium in graph 3).

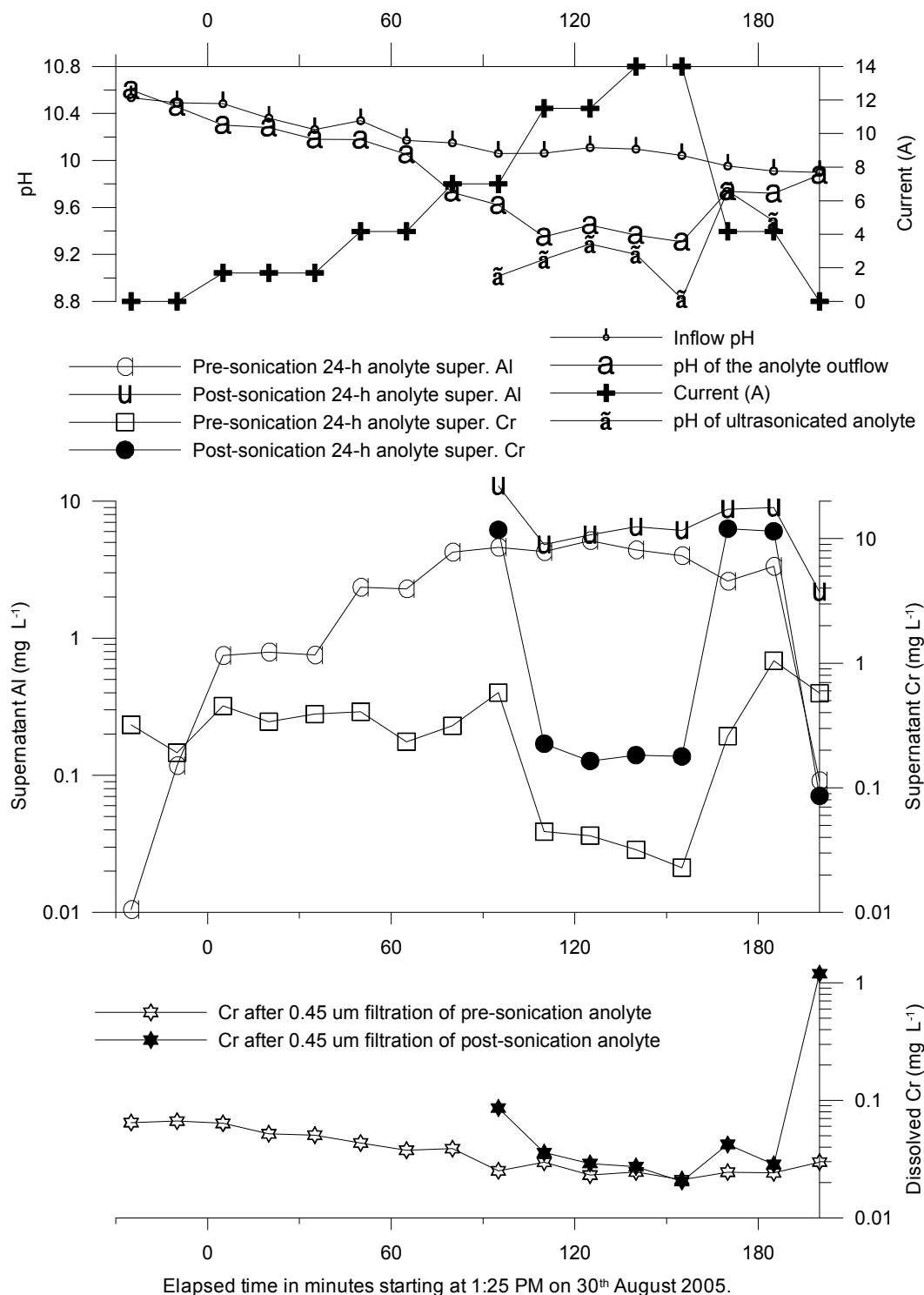


Figure 5-24 Comparison of presonicated and postsonicated metal levels. Note the log scales. The measured analyte pH was lower after standing and ultra-sonication, but both the aluminium and chromium residuals were higher.

The resilience of the floc was tested by ultra-sonication of the samples for 90 minutes, to simulate pumping at the tannery, then re-settled. Trace element analysis results are shown in Figure 5-24.

Comparison of the presonicated and postsonicated anolyte 24-h supernatant aluminium and chromium plots in graph 2 of Figure 5-24 show that the ultra-sonicated samples became colloidal and failed to settle as they did when fresh. The particle sizes of sonicated anolytes were investigated using a Malvern Mastersizer 2000S. The results are shown in Figure 5-25. The 1 A ( $\text{L min}^{-1}$ )<sup>-1</sup> treatment was last and shows a secondary peak possibly due to a faint remnant of the prior treatment at 4 A ( $\text{L min}^{-1}$ )<sup>-1</sup>.

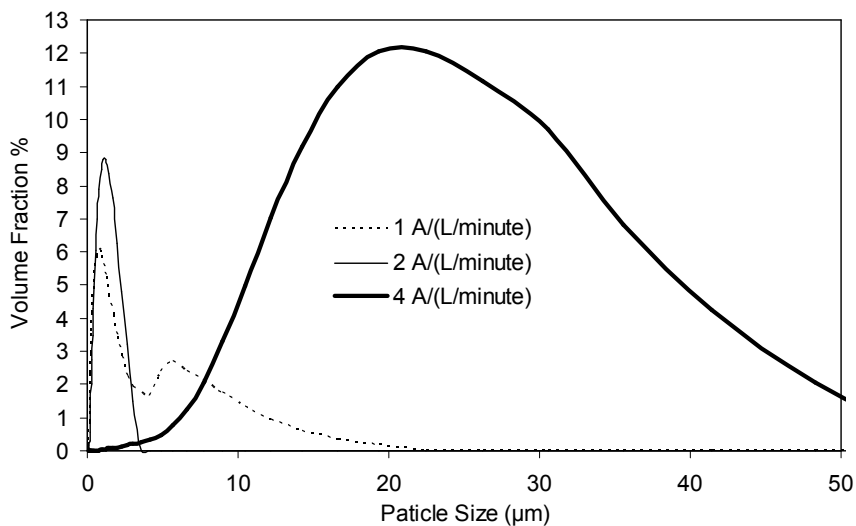


Figure 5-25 Particle sizes in processed and sonicated anolyte at three different treatment levels. The order of treatment was 2, 4, and 1 (August 30<sup>th</sup> 2005).

Figure 5-25 shows that treatment at 4 A ( $\text{L min}^{-1}$ )<sup>-1</sup> produced a robust floc that could be filtered or settled even after vigorous agitation, whereas lower treatment levels were not sufficient if the sample was sonicated after treatment.

### 5.5.3 Chromium removal from protein contaminated saline

Because protein in real tannery effluent can stabilise colloidal chromium, protein was added to the synthetic effluent. Egg albumin was added to the inflow during a trial when the electrolytic dose was 3 A ( $\text{L min}^{-1}$ )<sup>-1</sup> at 148 minutes elapsed time after power-on, by shock dose to the 300 L tank of a slurry of albumin in water, to

make the inflow to the processor contain  $500 \text{ mg L}^{-1}$  of protein for an hour. The chromium in the inflow was  $2 \text{ mg L}^{-1}$  and the inflow pH was lowered to 9.2 which made the chromium more soluble. A moderate conductivity inflow of around  $8000 \text{ } \mu\text{S cm}^{-1}$  was used to make the corrosion at least partly extra-faradic to assist in lowering the pH. Results are shown in Figure 5-26.

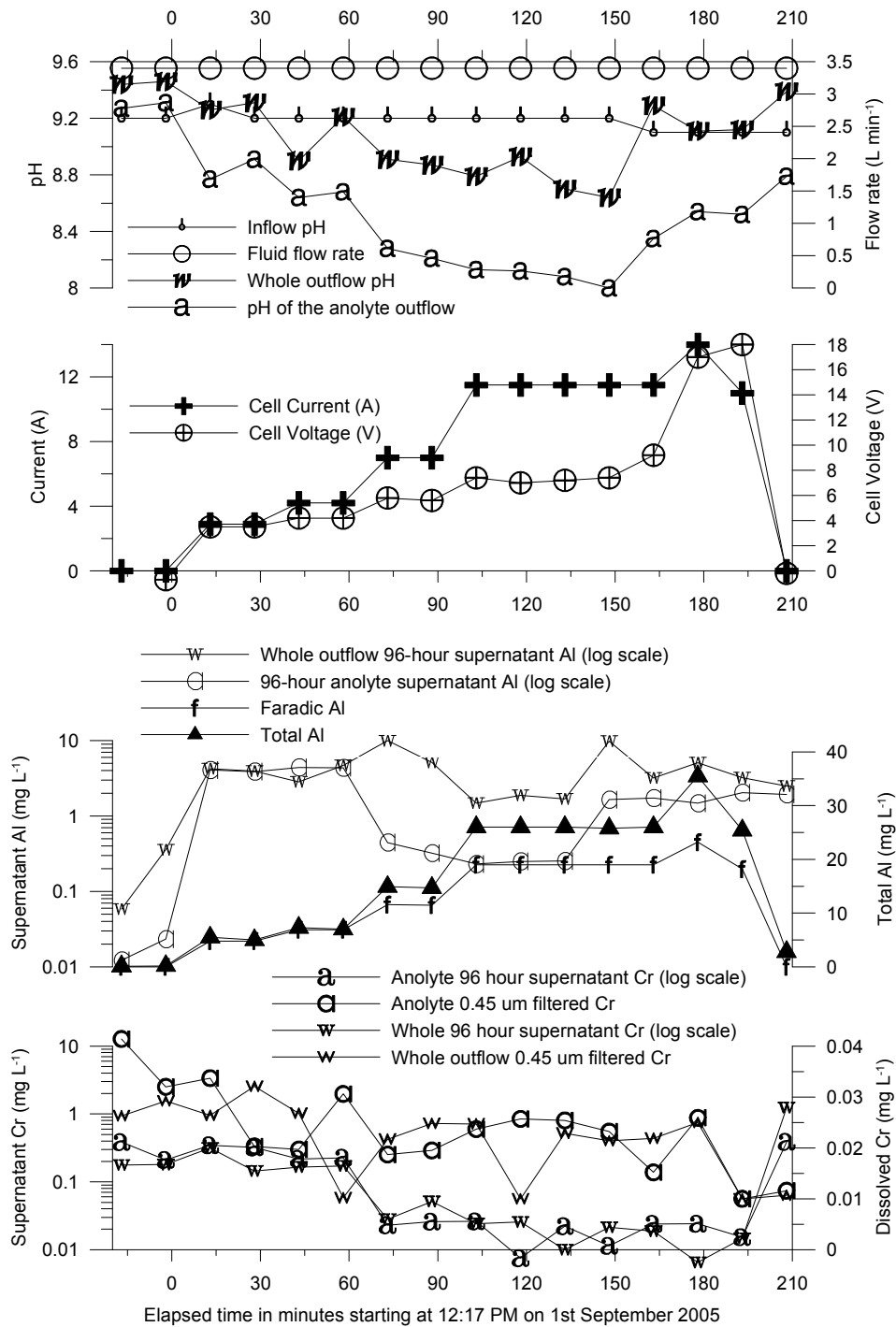


Figure 5-26 The effect of loading the inflow with protein at  $500 \text{ mg L}^{-1}$  on chromium removal and residual aluminium.

The 96-hour anolyte supernatant aluminium plot in graph 3 of Figure 5-26 shows that while treatment at 3 A (L min<sup>-1</sup>)<sup>-1</sup> was adequate before protein addition, it produced a colloidal outflow after protein was added. Treatment at 4 A (L min<sup>-1</sup>)<sup>-1</sup> was sufficient to produce a rapidly settling floc (and clear supernatant) even with protein. Graph 4 shows that most of the chromium was removed whatever the treatment or protein content, but higher levels of treatment gave greater removal. It also shows that even though the whole and anolyte pH (pH of the anolyte outflow and whole outflow pH plots of graph 1) are considerably different, especially at high treatment levels, the residual chromium levels in the anolyte and whole outflow are indistinguishable. A comparison of predicted and actual solubility of aluminium is shown in Figure 5-27.

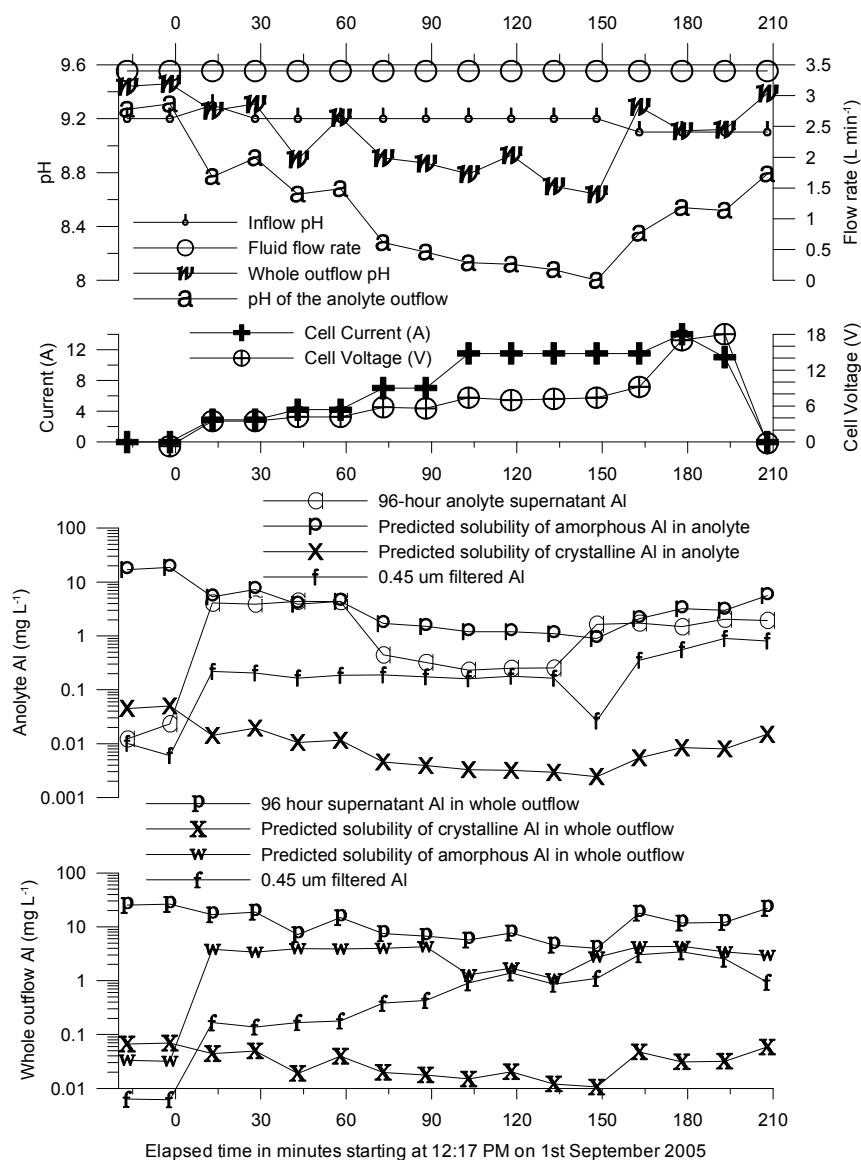
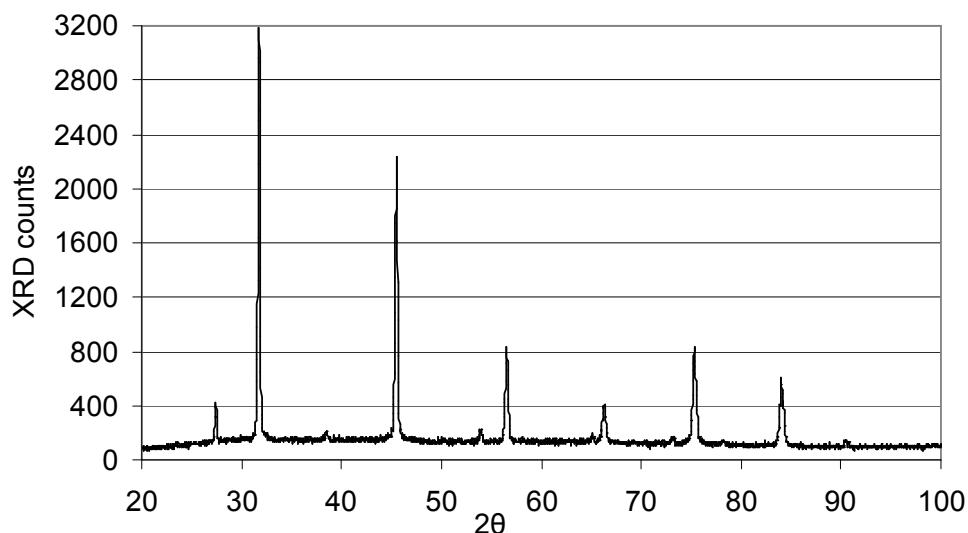


Figure 5-27 Comparison of predicted and actual solubility of aluminium before and after protein addition.



The 0.45  $\mu\text{m}$  filtered aluminium plot of graph 3 and pH of the anolyte outflow plot of graph 1 in Figure 5-27 show that levels of dissolved aluminium were raised when the protein was added and that pH modification was reduced.

Fresh aluminium-chromium floc without protein was tested by XRD after freeze-drying – the spectrum of the light green powder is shown in Figure 5-28. This spectrum was not matched by any substance in known databases (ICDD 2005).



*Figure 5-28 The XRD spectrum (Cu  $K_{\alpha}$ ) of freeze-dried fresh floc containing both chromium and aluminium, analysed on September 16<sup>th</sup> 2005, showing a crystalline structure that contained some peaks of known crystalline aluminium and chromium species but did not match any substance in the Philips X'Pert Database. Provisionally named Alexandrite.*

The key advantage of the electrolytic processing was production of a coarse floc that could be easily filtered or settled. Because a long 96-hour settling period was used for the protein trial, resolution of this advantage was not obvious. Particle size analysis (by percentage volume fraction) was carried out to investigate why the protein-laden sample was best treated using a dose of 4 A (L min<sup>-1</sup>)<sup>-1</sup> rather than 3 A (L min<sup>-1</sup>)<sup>-1</sup>. This analysis is shown in order of particle size range from smallest to largest in Figure 5-29, Figure 5-30 and Figure 5-31. A log scale version of Figure 5-31 is shown in Figure 5-32.

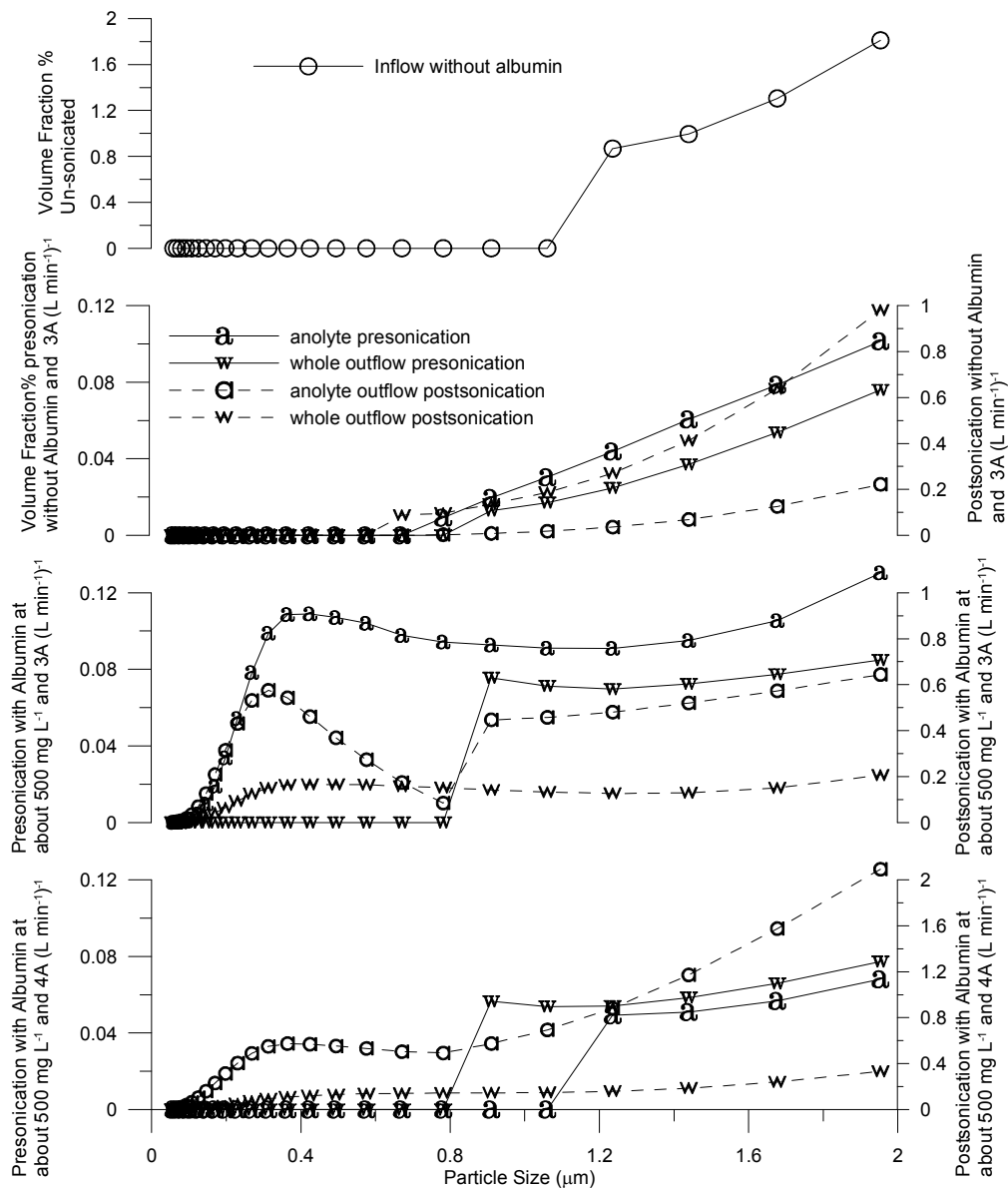


Figure 5-29 Particle size analysis below 2  $\mu\text{m}$ . Particles in this size range are very difficult to filter in practice (trial date September 1<sup>st</sup> 2005).

Figure 5-29 shows that the volume fraction of particles below 1  $\mu\text{m}$  in size increased at 3 A ( $\text{L min}^{-1}$ )<sup>-1</sup> when protein was added to the inflow (compare anolyte presonication of graph 2 with anolyte presonication of graph 3) but dropped again when the treatment level was raised to 4 A ( $\text{L min}^{-1}$ )<sup>-1</sup> (anolyte presonication of graph 4). After ultra-sonication the volume fraction of small particles increased (in all the anolyte outflow postsonication and whole outflow postsonication plots - note the larger scale for the postsonicated samples).

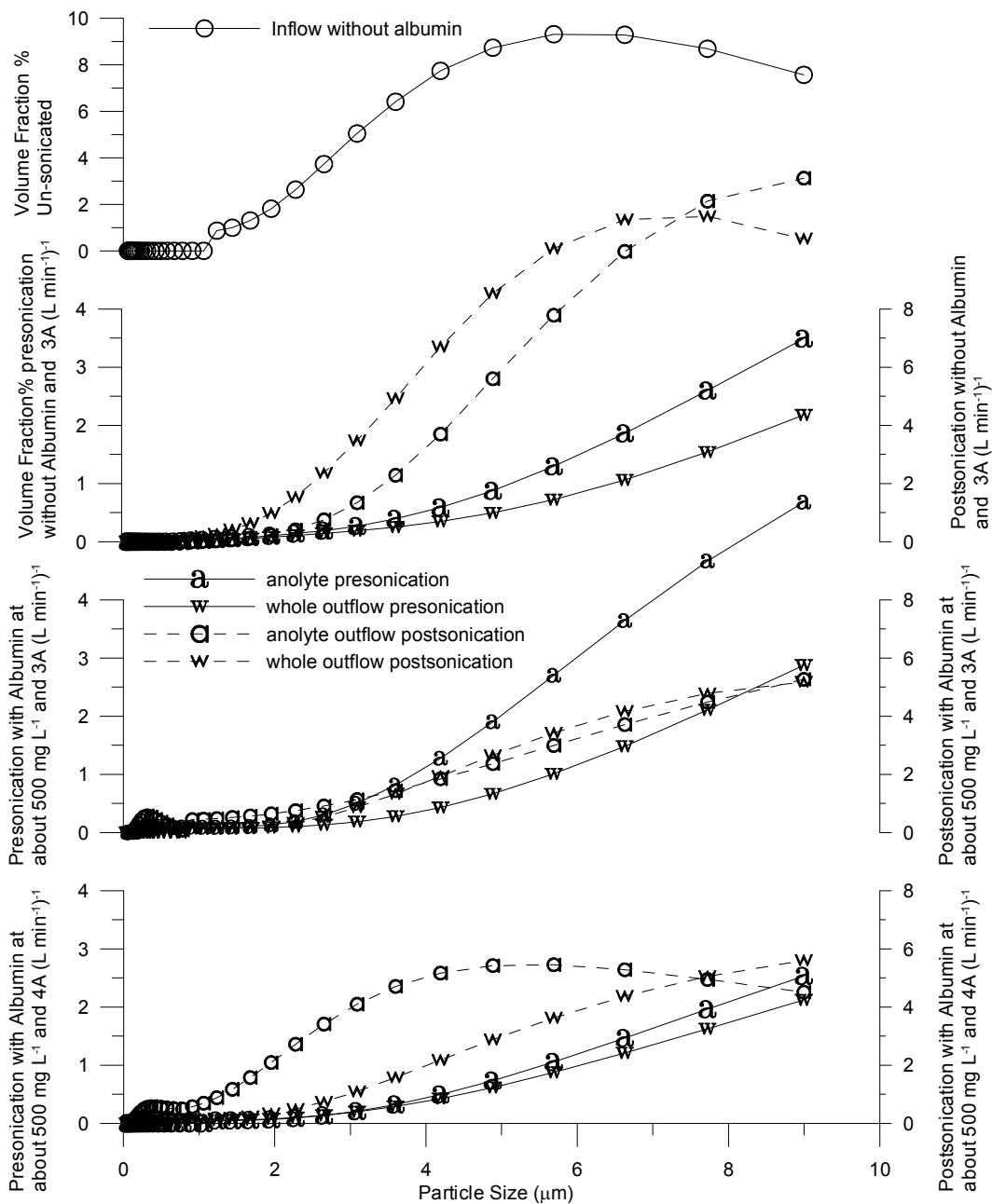


Figure 5-30 Particle size analysis below 10  $\mu\text{m}$ . Significant volume fractions are present in this range, which is marginal for capture in a fast coarse filter (trial date September 1<sup>st</sup> 2005).

The results displayed in Figure 5-30 shows a similar pattern to those of Figure 5-29. The volume fraction below 10  $\mu\text{m}$  increased at 3 A ( $\text{L min}^{-1}$ )<sup>-1</sup> when protein was added to the inflow but dropped again when the treatment level was raised to 4 A ( $\text{L min}^{-1}$ )<sup>-1</sup>. After ultra-sonication the volume fraction of small particles increased greatly (note the larger scale for the postsonicated samples). The higher pH whole outflow produced a floc that was more resistant to break-up by sonication.

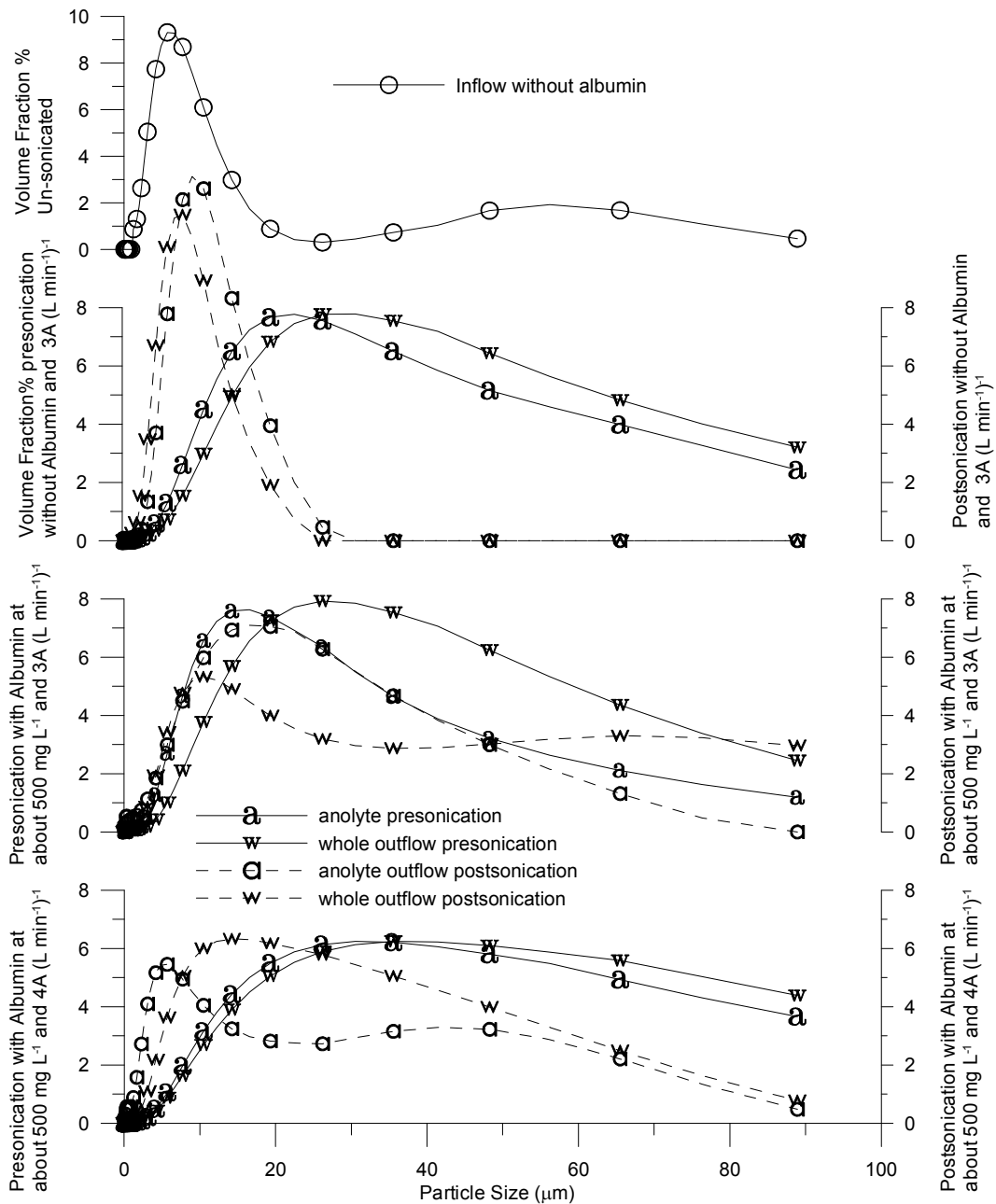


Figure 5-31 Particle size analysis below 100  $\mu\text{m}$ . The upper part of this range could be captured in a fast coarse filter. The inflow would not be easily filterable (trial date September 1<sup>st</sup> 2005).

The patterns shown in Figure 5-29 and Figure 5-30 are again present in the plots of Figure 5-31. The volume fraction at lower sizes increased at 3 A (L min<sup>-1</sup>)<sup>-1</sup> when protein was added to the inflow but drops again when the treatment level was raised to 4 A (L min<sup>-1</sup>)<sup>-1</sup>. After ultra-sonication the volume fraction of small particles increased greatly (note the larger scale for the postsonicated samples). The higher pH whole outflow seemed to produce a floc that was more resistant to break-up by sonication.

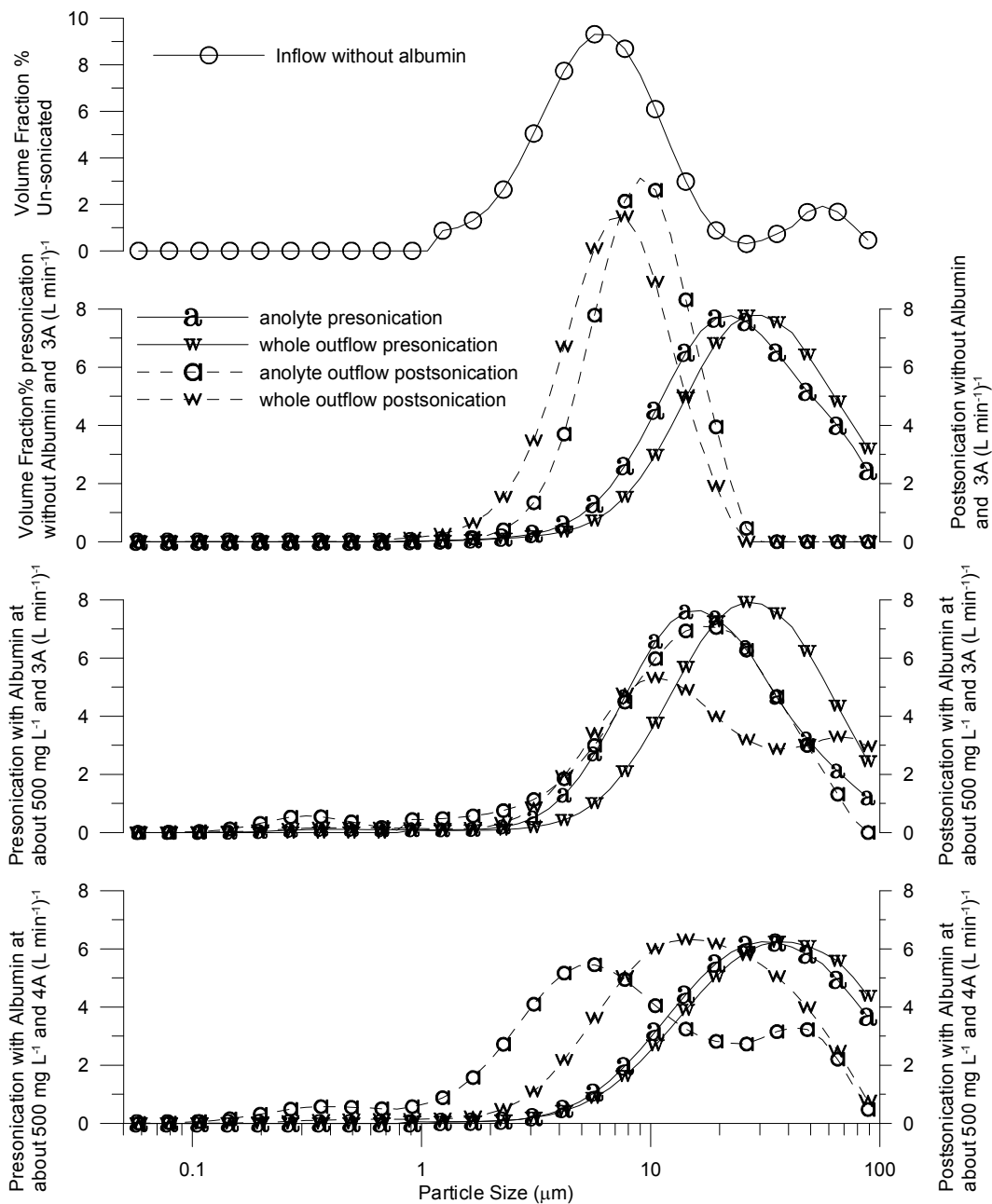


Figure 5-32 A log-scale version of Figure 5-31 – particle size analysis below 100 μm. The peak-shifting is emphasised in this view and reinforces the pattern of 3 A (L min<sup>-1</sup>)<sup>-1</sup> dosage being adequate when there is no protein in the inflow but that 4 A (L min<sup>-1</sup>)<sup>-1</sup> dosage can restore the performance (trial date September 1<sup>st</sup> 2005).

Figure 5-29 to Figure 5-32 show that particle size was greater for higher dose and lower when protein was added. While treatment of a fluid without protein was effective at 3 A (L min<sup>-1</sup>)<sup>-1</sup>, the addition of protein caused the outflow to remain turbid at the same dose. Raising the dose to 4 A (L min<sup>-1</sup>)<sup>-1</sup> was effective in restoring the clarity of the supernatant. While the analyte was generally more readily filterable than the whole outflow when undisturbed, ultra-sonication

generally caused more disruption of the anolyte than the whole outflow. This is related to the pH, with the floc being weaker when formed at lower pH.

## **5.6 Modification of pH and effective conductivity by catholyte modification**

### **5.6.1 The need to improve effective conductivity**

A test of the Flume for processing pulp mill effluent (see §4.3) found that the conductivity of  $1600 \mu\text{S cm}^{-1}$  was too low. The test of landfill leachate (see §4.2) found that the pH was too low to permit electroflocculation. This led to a novel solution: modify the salinity and pH of the catholyte to improve the effective conductivity of the electrolyte and condition the outflow pH without altering the anolyte salinity significantly.

The first trial used inflow fluid with conductivity of  $0.48 \text{ S m}^{-1}$ . This was less than half of the minimum salinity measured in the DAF outflow at the tannery. The active catholyte flow was 1.2% of the anolyte flow rate, which was more than ten times the passive catholyte seepage flow. At 25 minutes after the power was switched on, an acid saline solution ( $17800 \mu\text{S cm}^{-1}$ , pH 0.8) was delivered to catholyte compartment at the top of the flume. The active catholyte flow was stopped at 67 minutes. At 147 minutes a catholyte flow of acidic concentrated saline ( $255000 \mu\text{S cm}^{-1}$ , pH 0.89) was started. This flow was stopped at 172 minutes. At 202 minutes catholyte flow of alkaline saline ( $257000 \mu\text{S cm}^{-1}$ , pH 11.5) was started. This was changed to neutral from 240 minutes ( $254000 \mu\text{S cm}^{-1}$ , pH 7.6) and acid again ( $260000 \mu\text{S cm}^{-1}$ , pH 0.7) from 260 minutes. The results are shown in Figure 5-33.

Figure 5-33 shows that addition of saline to the catholyte lowered both the pH of the anolyte outflow, shown in graph 1, and cell resistance as shown by lowered cell voltage plot in graph 2, even when the added catholyte was of higher pH than the anolyte. Acidic catholyte flow had the most effect. Graph 4 shows that the anolyte conductivity was not significantly different to that of the inflow. The catholyte outflow remained above pH 12 throughout the trial.

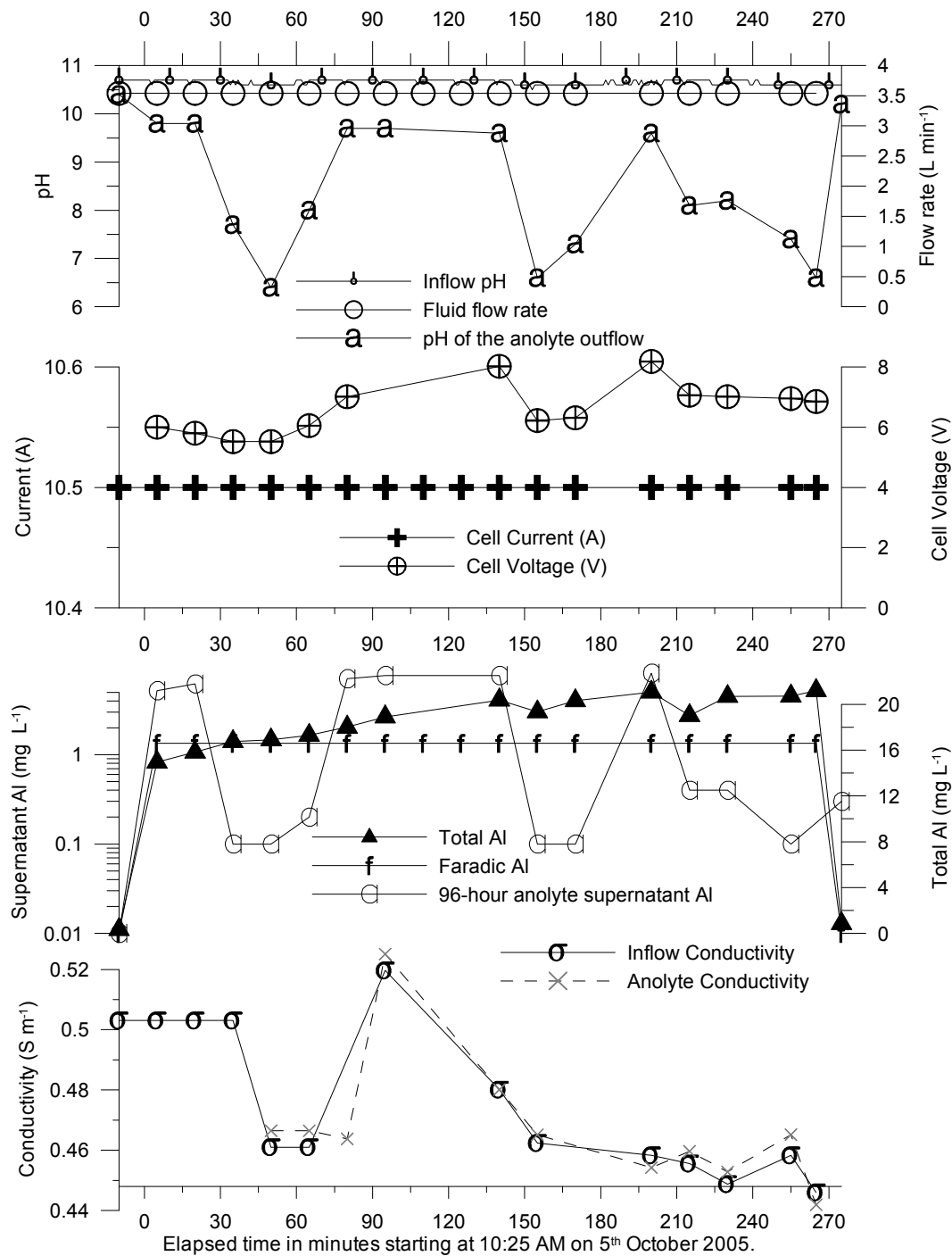


Figure 5-33 The effect of adding a small concentrated flow to the catholyte. The first and last samples are inflows (October 5<sup>th</sup> 2005).

Tap water of much lower conductivity and near neutral pH was used to increase the difficulty. A constant voltage supply was used. Alkaline catholyte addition ( $232000 \mu\text{S cm}^{-1}$  pH 11.2) was started at 30 minutes, stopped at 55 minutes then re-started at 85 minutes ( $235000 \mu\text{S cm}^{-1}$  pH 11.8). The results are shown in Figure 5-34.

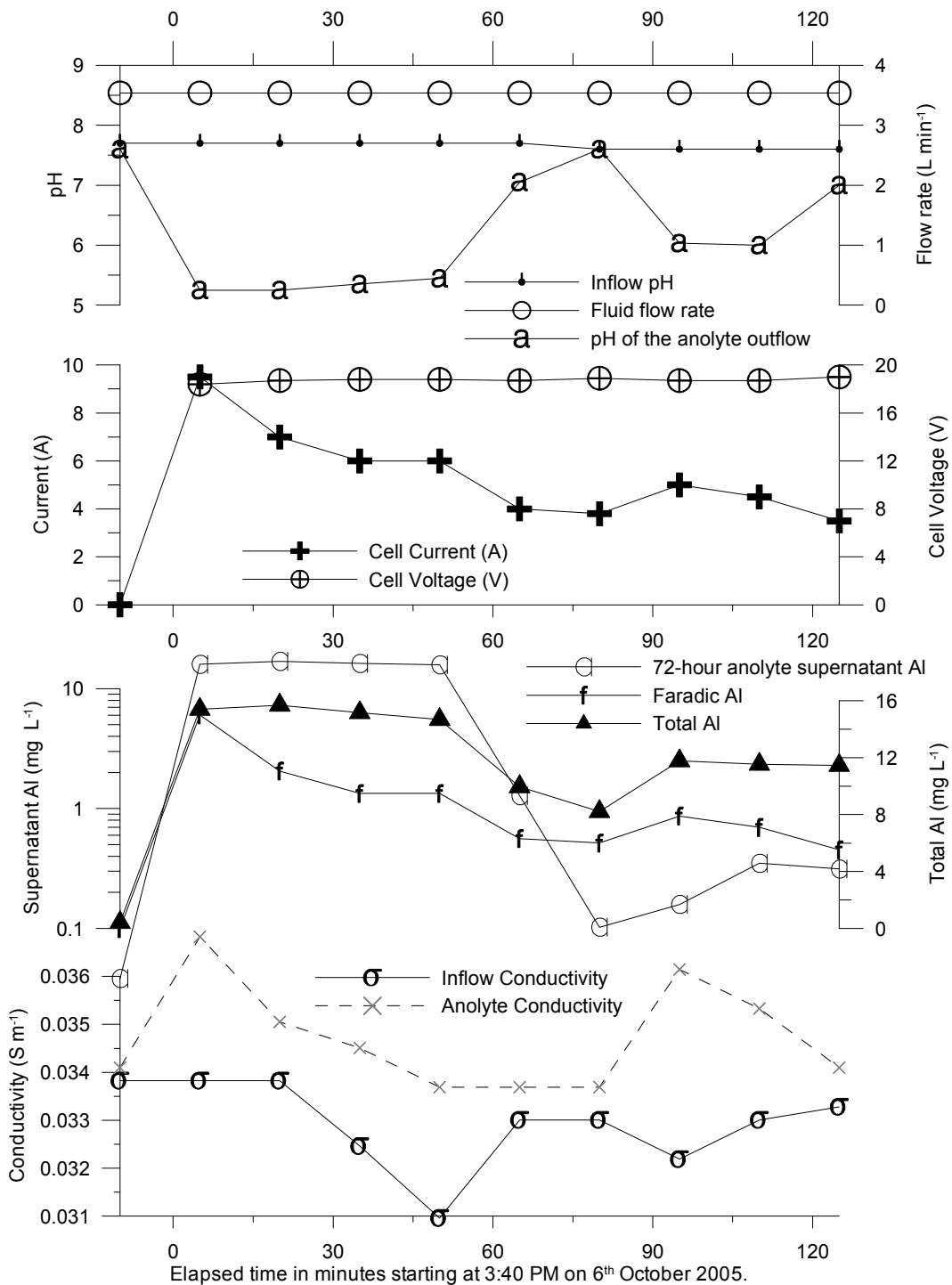


Figure 5-34 Electrolytic treatment of very low conductivity neutral pH water by modification of the catholyte.

Figure 5-34 shows that alkaline catholyte flow negated the usual acidification of the anolyte to produce a neutral outflow (pH of the anolyte outflow plot in graph 1) with low aluminium residual (72-hour anolyte supernatant aluminium plot of graph 3). However, there was a time delay in the response of 30 minutes due to the slow flow of the catholyte. The anolyte conductivity (in graph 4) was slightly



higher than the inflow conductivity but could still be considered fresh water. The latter analyte samples contained a floc that was floated to the surface by electrolytically produced bubbles. The cell current plot, shown in graph 2, was reduced by addition of alkaline saline.

## **5.6.2 Discussion**

For near-neutral inflow, the pH of analytes was altered readily by modifying the pH of a relatively small catholyte flow. The pH of the analyte outflow was manipulated to achieve low residual aluminium. By adding a small flow of high conductance fluid to the catholyte, the effective conductance of the electrolyser was increased by more than 10% without significantly increasing the analyte conductivity. Even very low conductivity neutral pH tap water could be electro-flocculated effectively by adding concentrated alkaline saline to the catholyte, though the cell resistance was increased.

The results showed that it is possible to extend the range of conductivities treatable by electroflocculation down to  $0.1 \text{ S m}^{-1}$ .

## **5.7 Pulse modulation of the current or voltage**

### **5.7.1 Capacitance of the processor**

The capacitance of the Flume was measured. A 25 kHz square wave voltage of 5 V amplitude was applied to the wet flume, shown in the Channel 2 plot in Figure 5-35, and the current was sensed across a small shunt resistance. The invert of the current signal was Channel 1, which decayed to 37% of its peak value in 400 ns, allowing for the 100 ns switch-off time for the voltage. The total series resistance was  $17 \Omega$ . The capacitance of the Flume, determined experimentally by time constant, was 24 nF. By comparison, if considered as a parallel plate capacitor with area  $0.16 \text{ m}^2$  and gap through water of 0.001 m, the calculated capacitance by geometry is 100 nF. The discrepancy depends greatly on the estimate of the gap and area when the shavings do not contact the membrane uniformly.

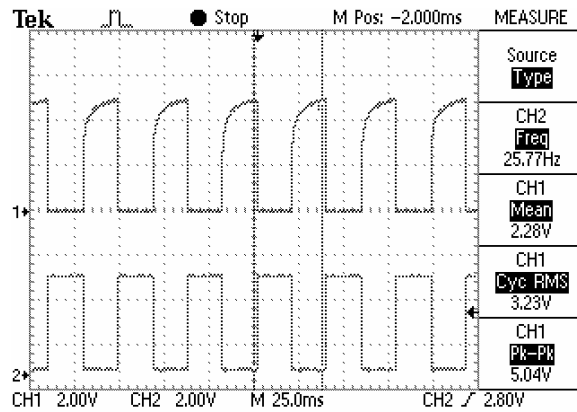


Figure 5-35 The current decay (Channel 1) for a 25 kHz square wave input voltage.

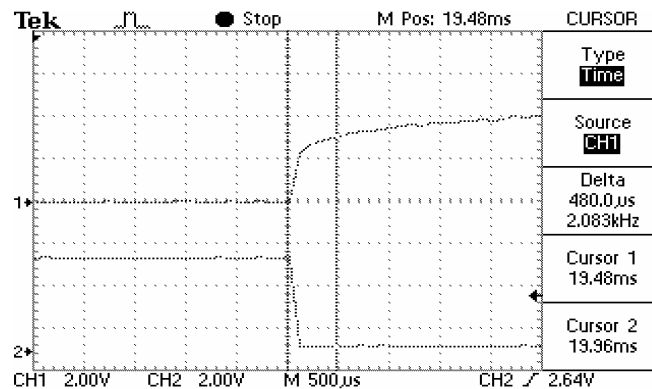


Figure 5-36 A time-expanded view of the (inverted) current decay with 400 µs time constant.

### 5.7.2 Pulse modulation of the power

The main goal of pulse modulation of the power supply was to improve both the clearance of corrosion products and enable non-mechanical control of pH drop with some independence from total aluminium addition.

#### High frequency pulsing

Variable duty cycle square waves of current with constant RMS current were applied to the electrolyser while processing saline. Results are shown in Figure

5-37. The frequency axis in graph 3 is logarithmic but DC is set at 0.01 Hz on this axis.

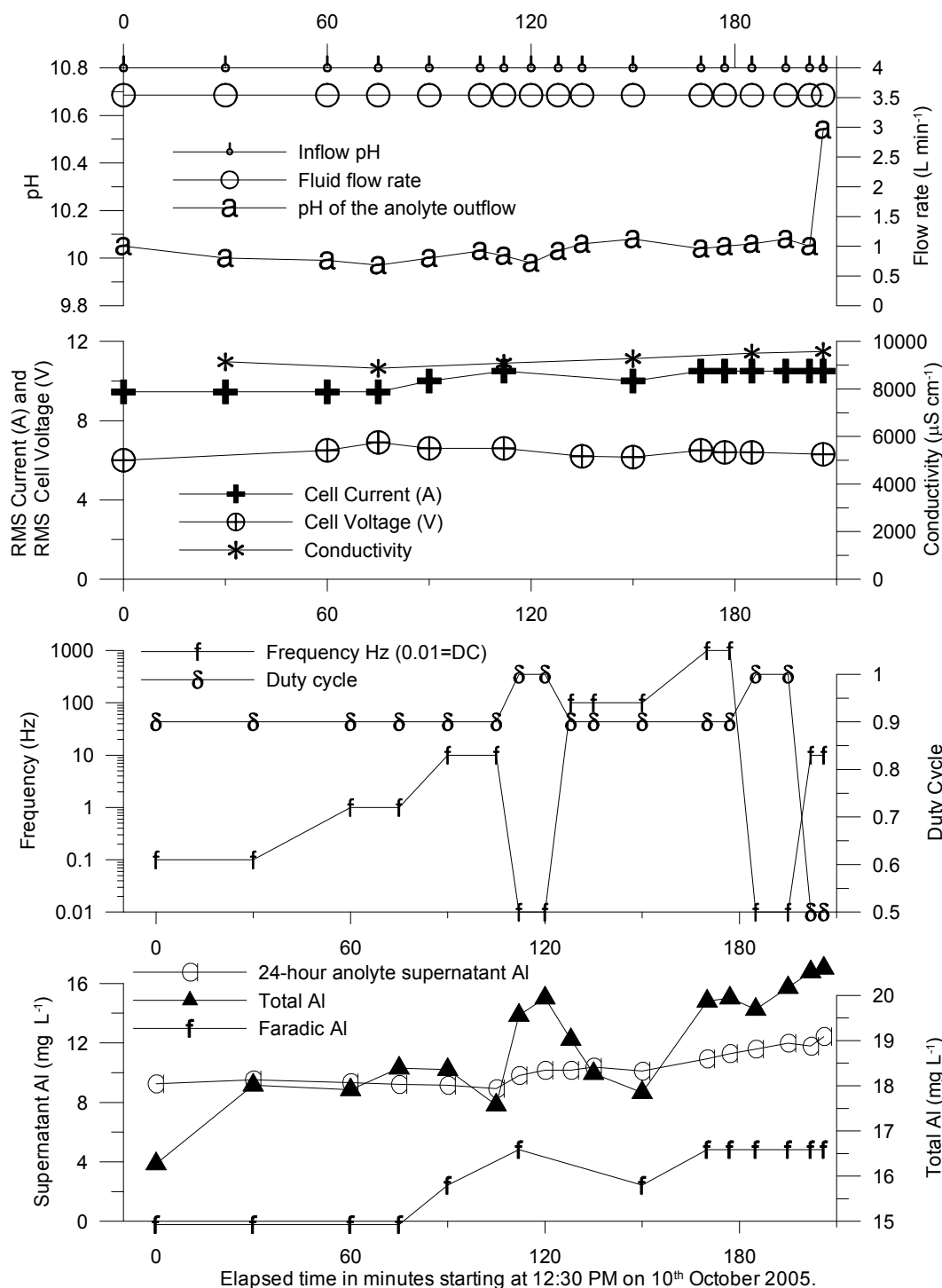


Figure 5-37 The effect of varying frequency and duty cycle at constant RMS current on the electrolytic processing. The actual waveforms used are shown in Figure 5-38.

Figure 5-37 shows that the effect of lower duty cycle (graph 3) on outflow pH (the pH of the anolyte outflow plot of graph 1) was not significant.

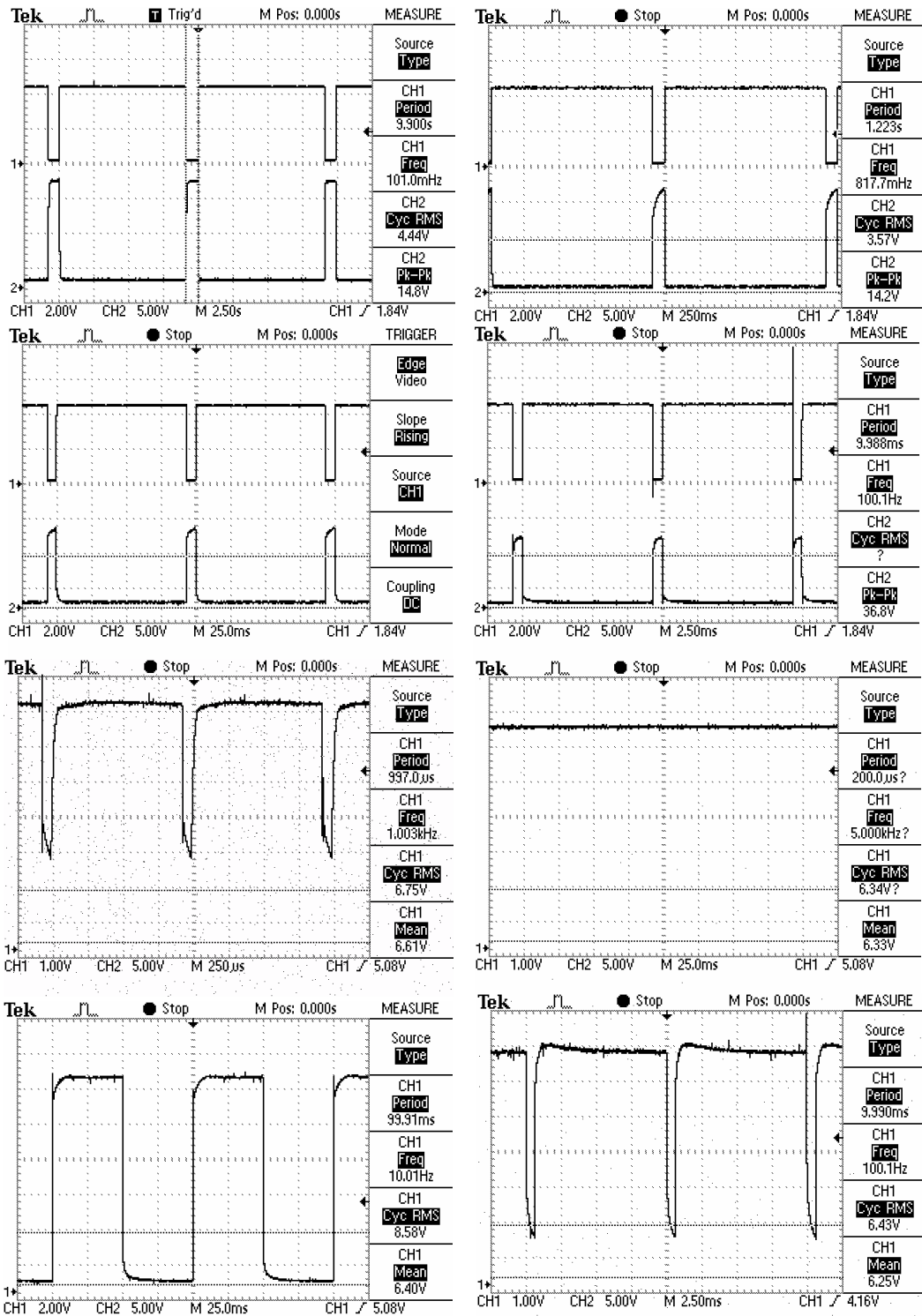


Figure 5-38 Waveforms used for results shown in Figure 5-37.

The results shown in Figure 5-36 were not conclusive. It is likely that the high pH and high conductivity were not conducive to achieving a substantial pH drop that would vary clearly with duty cycle and frequency. While a high peak-current low duty-cycle modulation (for example, 100 A peak by 20 V at 10% duty) could have an appropriate affect, this requires more expensive power electronic circuitry.

## **Low frequency pulsing**

When the period of the current modulation was adjusted to be twice the passage time for fluid in the Flume (a modulation frequency of 0.05 Hz) and a duty cycle of 0.5 was maintained, the observed amount of floc in the outflow of treatment of saline oscillated slightly at the same period as the modulation. This indicated that stored corrosion products were at least partly removed during the zero current part of the modulated waveform by alkaline fluid flushing.

Faster modulations of between 0.1 Hz and 1 Hz with consistent duty cycle of 0.9 were also trialed. Strong flocculation was observed in all cases.

## **5.8 Discussion**

### **5.8.1 Dissolution of hydroxide to form aluminate**

The pH drop due to dissolution of amorphous  $\text{Al}(\text{OH})_3$  to  $\text{Al}(\text{OH})_4^-$  at high pH is calculated by application the Henderson equation to Equation 1-41. The pH will drop from 10 to 8.09 after equilibrating with  $\text{Al}(\text{OH})_3$  because at that terminal pH the  $\text{Al}(\text{OH})_4^-$  level saturates. Similarly for water of pH 9 the terminal pH would be 6.9. If the actual solubility is smaller, because of slight crystallinity of the  $\text{Al}(\text{OH})_3$ , then the pH change will be reduced.

### **5.8.2 pH modification control by cell voltage**

Reduction of pH during treatment of alkaline saline was proportional to the amount of extra-faradic corrosion. The level of extra-faradic corrosion could be controlled by adjustment of the cell voltage. Two strategies to achieve separate control of the total aluminium corroded and the pH reduction are available:

- Alteration of the reaction surface area. For example, reduction of the reaction surface area when both the pH and conductivity are high so that the cell voltage is high enough that a significant fraction of the corrosion is extra-faradic. If the pH increased from 9 to 10 while the conductivity was  $1 \text{ S m}^{-1}$ , the reaction area should be reduced to 33% of the original and the

cell voltage doubled to 12 V from 6 V (noting that the total corrosion per area would be approximately tripled, according to Equation 5-2). This would give the same total aluminium dose with a greater proportion being extra-faradic, and hence more pH drop. Because the rate of corrosion is also pH dependent, a corrosion density function based on both cell voltage and pH should be developed to make control more accurate over a broader range of conditions.

- Pulse modulation of the power supply with duty cycle variation so that the peak voltage could be varied independently of the RMS current. This achieves the same as the area system but by dividing the time instead. For example, a duty cycle of 33% could be used with a doubled peak voltage as in the above example.

### **5.8.3 Crystallinity and co-floc of aluminium and chromium**

The low solubility of the aluminium floc produced in the laboratory was explained by the slight crystallinity seen in Figure 5-21. Floc composed of very small crystals which would have solubility between that of true amorphous  $\text{Al}(\text{OH})_3$  and gibbsite. Mixed aluminium-chromium floc was found to be strongly crystalline (with a new XRD spectrum).

## **5.9 Discussion of Technical Applications**

### **5.9.1 Trials summary**

Pre-filtration of organic matter from the water prior to the electrolytic processing is essential in order to prevent clogging of the electrolyser's narrow flow channels by suspended solids. It also assists in reducing the required charge dose. The coarse filter's output should supply the electrolytic processor, with post-processing filtration of metals.

Faradic corrosion is based on the current but drops slightly from linearity with current density due to a drop in effective aluminium current fraction at higher cell voltage to favour oxygen production. The small oxygen bubbles were utilised to float out flocculated material.

## **5.9.2 Variable pH and salinity of tannery effluent**

### **Self regulation**

Electrolytic processing of tannery effluent at a constant cell voltage is partially self-regulating in the face of rapid variation of the inflow pH between 8 and 10 due to the greater rate of passive dissolution of aluminium at higher pH in anodic conditions. If the salinity and alkalinity correlate with the levels of dissolved chromium and suspended solids, the current drawn from a voltage source power supply will change appropriately. Setting the cell voltage based on either inflow or outflow pH with current limiting and an out-of-range alarm would be the simplest control system. Greater control was achieved by using a current source regulated to deliver an appropriate charge dose, according to the level of contaminants, independent of the salinity-based conductivity.

### **Independent control of flocculation and pH adjustment**

There were difficult periods when the pH of the water to be treated was very high, leaving a high level of residual aluminium in the water; or too low, causing the same as well as poor flocculation. There are several means to combat this. The most convenient in the circumstances is to use the H&S pond as the inflow source because the variation in composition will be greatly moderated compared to the DAF outflow (the inflow to the H&S pond) due to the relatively large volume of the pond. Even if this is possible there will still be some variation to contend with. If the salinity is low when the pH is high, a current source directed to give a high current dose will have to increase the cell voltage. This will increase the extra-faradic corrosion and the pH will be lowered more, albeit with additional energy consumption. To cope with a worst case situation where the salinity and pH combinations are unrestricted and wide-ranging, independent control of the faradic and extra-faradic corrosion is useful. This can be achieved by two means: changing the surface area of the reactor which will inversely change the current density; or by operating the power supply at less than 100% duty cycle but with higher peak current. The latter option has the advantage of not requiring moving parts.

A further means of pH manipulation is to separate the flows into anolyte and catholyte. By putting the main flow through the anode compartment and collecting a very low rate caustic (pH > 12) catholyte flow separately, the anolyte pH was lowered beyond the effect of the extra-faradic corrosion. Recycling the caustic flow to the tannery would be a direct benefit.

### **pH modification by modifying the catholyte**

Adding concentrated saline to the usual seepage that forms the catholyte flow is another means of manipulating the anolyte pH and has the additional benefit of increasing the effective conductivity of the electrolytic system without increasing the conductivity of the anolyte much. An active catholyte flow of 1% of the anolyte flow, even if it has higher pH than the anolyte at the inflow to the process, causes additional pH drop and is able to lower the voltage required for a moderate charge dose significantly. As a last resort, supplying a strongly acidic catholyte flow at the inflow to the process, of 1% of the anolyte flow, would greatly reduce the anolyte pH if necessary. The small active catholyte flow will be diluted slightly and will certainly become more alkaline by the time it exits the cathode compartment. If the water to be treated is at an extremely low (below 8) pH or low alkalinity, the flocculation will be poor and all pH decreasing effects should be minimised, otherwise the outflow will be acidic and contain colloidal aluminium. Minimisation of the pH drop could be achieved by lowering the cell voltage and using high duty cycle and high area to compensate.

### **Pulsed power**

High frequency pulsing is of marginal utility, as the low duty cycles required to enable full recovery of the diffusion gradients offset the gain during the on-time. However, this approach is worthy of further investigation. Very low frequency pulsing, say 100 s on and 10 s off, has a place in preventing blockage by allowing an off-time that will allow a slug of high pH water to remove corrosion products adhered to the anode surface. While the power is off the active acidification is off and the bound corrosion products are freed. The key is to time the off period to be greater than the transit period of the water, but not so great that the cleaning is completed to the extent that a portion of the water leaves without being flocculated. The flocculation is liable to be less effective for the water that passes



through during the off period and insoluble corrosion products will also be carried out during this time but they will be mixed with flocculated water shortly thereafter anyway.

### 5.9.3 Proposed larger scale processing systems

A scheme for an initial pilot plant to treat 10% of the tannery effluent flow is shown in Figure 5-39. The extension could be achieved by either adding another flume or splitting the existing flume in half lengthways with a partition. The partitioning would be achieved by electrically switched sections in the anode current distribution grid. A high cell voltage, which will give rise to more extra-faradic corrosion and greater pH reduction, would be used to treat high pH effluent.

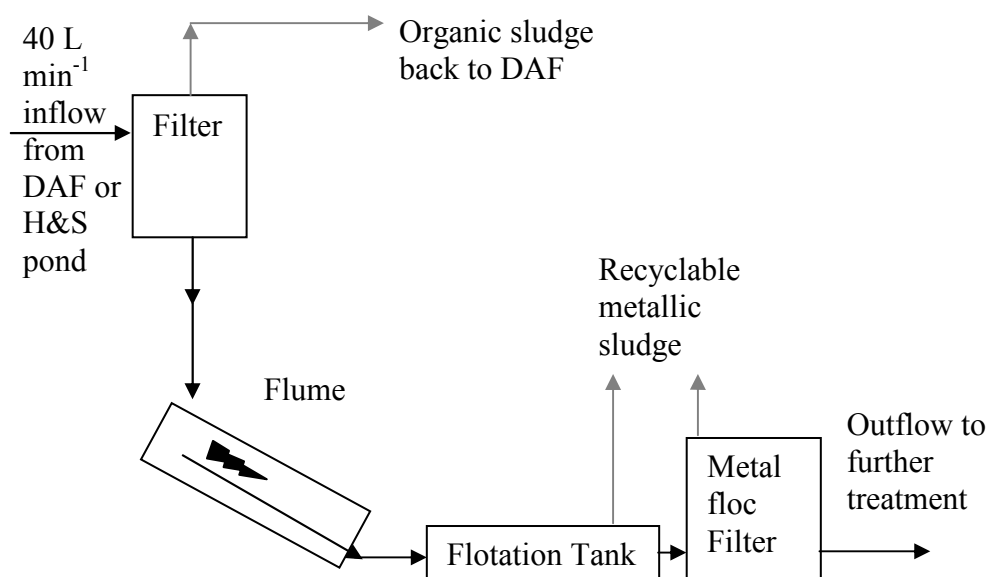


Figure 5-39 Basic scheme for treatment of 10% of the tannery effluent, making use of the existing DAF to collect the organic sludge.

Figure 5-40 shows a schematic of a proposed treatment system for the entire effluent flow. While most of the chromium is dissolved in the effluent some is bound to the solid organic matter. Separation of the organic contaminants from the metallic contaminants is a key feature which enables chromium recycling. Electroflotation and settling of electro-flocculated effluent is shown as means of reducing the load on a filter. The system is designed to partly recycle aluminium, thereby lowering the amount of aluminium that must be supplied or disposed.

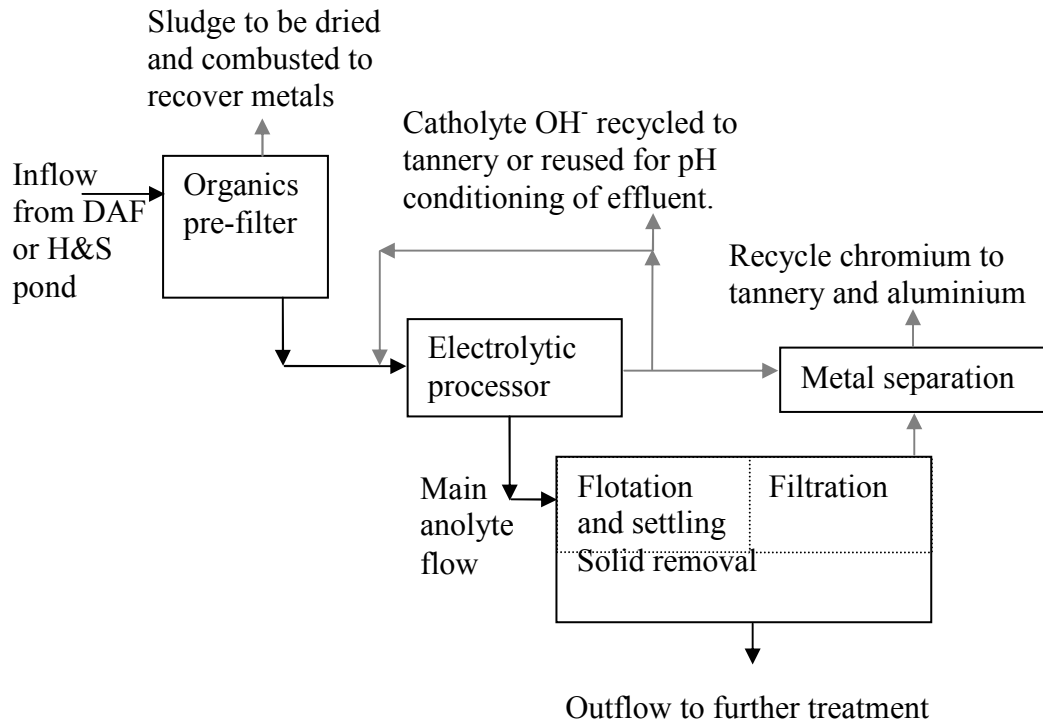


Figure 5-40 Proposed scheme for processing the entire tannery effluent flow. Chromium could be recycled at  $10 \text{ kg day}^{-1}$ . Recycling of aluminium coagulant is also shown.

The function of pH adjustment is crucial. For alkaline tannery effluent, the ideal catholyte for producing low residual aluminium anolyte is acidic highly concentrated saline. However, since this catholyte becomes alkaline at the outflow anyway and alkaline saline is also effective, it would be much more practical to recycle the alkaline catholyte, topping up with neutral saline as necessary. A minimalist method is to pass 1% of the filtered outflow as catholyte without any attempt to condition the salinity. The catholyte outflow will be available as recycled alkali for the tannery, although it will have significant aluminium in it. The tannery effluent already has  $1 \text{ mg L}^{-1}$  aluminium in it, mainly from the impure materials used to raise the pH, and additionally from the impure Solar 23 grade salt.

It is worth considering the benefits to the entire effluent treatment process of removing as much chromium as possible with a PPP and recycling it instead of contaminating the oxidation-settling ponds with chromium.

Figure 5-41 shows a longitudinal cross section of a possible flume in more detail.

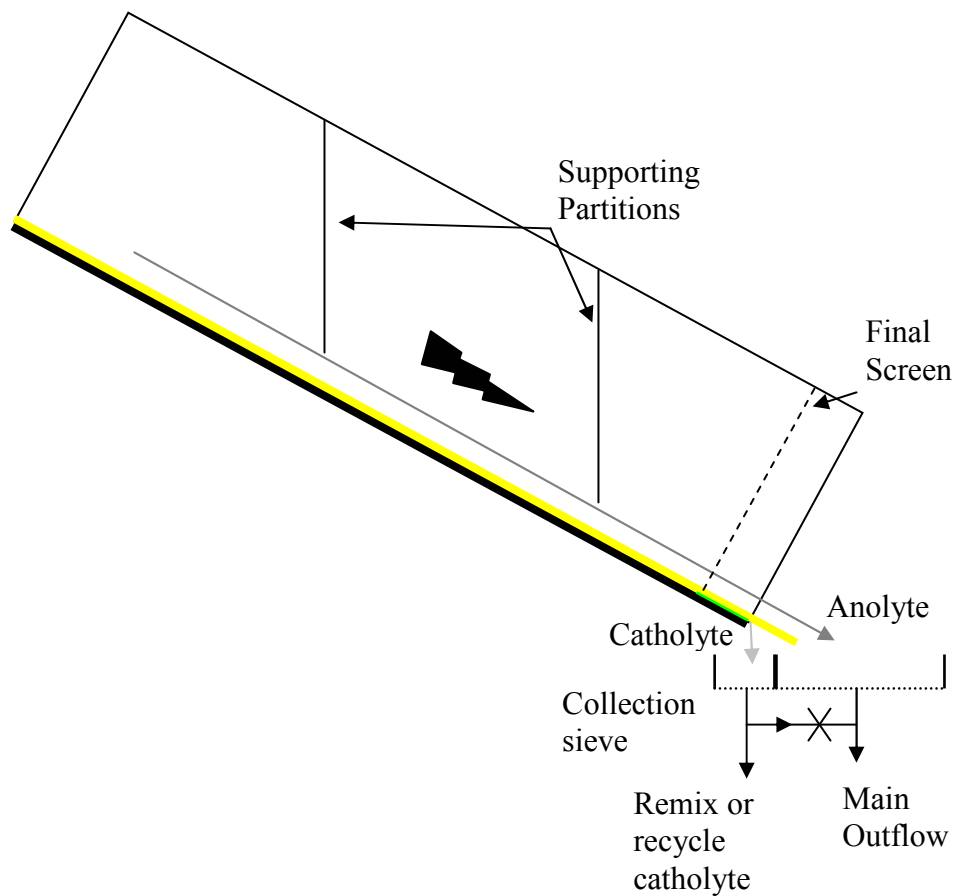
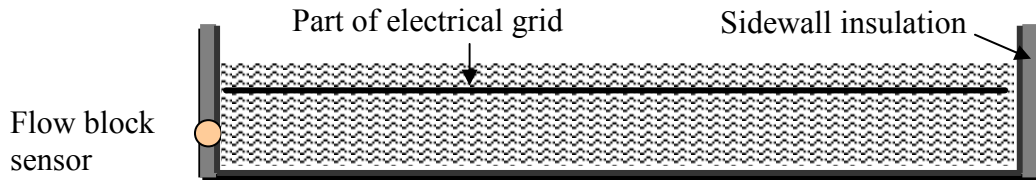


Figure 5-41 A longitudinal section of a flume system that could be used for continuous treatment of tannery effluent.

The outflow end should have a coarse mesh plastic filter to stop release of shavings. A further deck-plate style filter should be used to allow the main flow to drop through but capture fine pieces of partly oxidised metal. To prevent clogging at the outflow by self-made floc, the slope should be high enough to keep the flow speed above  $0.2 \text{ m s}^{-1}$ . To stop the shavings sliding down the slope, a series of cross wires or thin partitions down the length of the Flume should be used. This also protects against jamming of the shavings against the bottom filter. While the shavings were actively compressed in the trial flumes, self-compression of a thick layer of shavings occurred. Options to prevent bottom-end blockage include either narrowing the Flume at the lower end or increasing the slope of the Flume at the lower end. Regularly spaced grommets in the separating membrane will allow upward release of the hydrogen.

Figure 5-42 shows a cross section of the proposed Flume featuring sidewall insulation, an electrical distribution grid and a flow block sensor. The sidewall should be plastic coated or otherwise insulated so that corrosion products don't build up there.



*Figure 5-42 Idealised Flume cross-section featuring moveable electrical distribution grid (just one cross-member shown) made of aluminium rod fitted to the partitions and able to be picked up for clearing floc deposits in the shavings matrix. A flow block warning sensor is placed below the level of the distribution grid. The shavings are replaced by gravity.*

If a mid-section of a single shaving corrodes first then smaller wet pieces of partly corroded aluminium will be formed. These will not make good electrical contact with the dry part of the shavings body and therefore will slowly corrode at any wet junctions, which includes zones of low fluid flow speed. These fragments will either leave the Flume in partly metallic form or cause blockage. Hence, a suggested improvement is flat straight ribbons of aluminium. These are arranged vertically in the Flume as illustrated in Figure 5-43. In this case the aluminium will corrode from the bottom up. The wide dimension of the ribbon should be longitudinal with the flow so as not to impede the fluid flow. The maximum or ideal thickness of the anode pieces is unknown but a layer of corrosion products that would significantly impede the current should not be allowed to form. The ideal situation is where the entire piece of anode corrodes from the bottom (which is closest to the cathode) at a faster rate upwards than through the thickness so that no metal pieces break off. If the metal is less than 0.1 mm thick it would be prone to mechanical breakage (tearing) especially as the pieces are liable to settle at different rates according to the local current density.

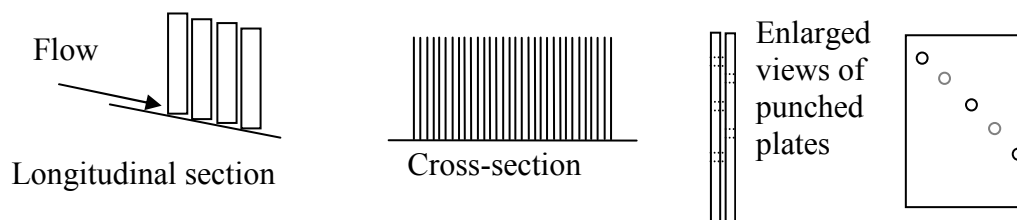


Figure 5-43 Proposed use of straight vertical ribbons or punched plates to improve upon curly shavings. The punched holes in the plates will have a rough edge that ensures a gap between the plates. The staggering of holes precludes catching on another hole if different plates corrode at different rates.

Neither the optimal downward compression nor the optimal packing density for ribbons has been established. The two extremes are: a single block clamped to the membrane which would have the highest initial current density but also the quickest failure due to buildup of corrosion products and a single isolated ribbon dangled above the membrane which would have a poor usage of the area and high resistance. Between these two extremes there is a point where both the corrosion density and clearance rate of corrosion product are both high and well matched. This point of balance may be determined by trials that vary the packing density of the ribbons and the slope of the flume.

#### 5.9.4 Sensitivity to electricity and aluminium price increases

A cost function (Equation 5-4) was formed, based on the feasibility of treatment of  $10 \text{ L min}^{-1}$  of tannery effluent at 5 V and 20 A, where X is the cost of aluminium in dollars per kilogram and Y is the cost of electricity in dollars per kWh. Triple-faradic corrosion is assumed. The cost function is shown in

$$\text{Equation 5-4} \quad \text{Total operating cost } (\$ \text{ m}^{-3}) = 0.03355X + 0.16667Y$$

Equation 5-4 shows that the present-day costs of  $\$0.03 \text{ m}^{-3}$  for both electricity and aluminium add to a total cost of  $\$0.06 \text{ m}^{-3}$ . Increasing the price of the solid aluminium source by a factor of 2 to  $\$2 \text{ kg}^{-1}$ , which is realistic in the medium term if scrap aluminium is not sufficient to meet demand, raises the total cost to  $\$0.09 \text{ m}^{-3}$ . If instead the price of electricity doubled to  $\$0.30 \text{ kWh}^{-1}$  the total cost would rise to  $\$0.08 \text{ m}^{-3}$ . Even if both prices tripled, treatment would still cost less than

$\$0.20 \text{ m}^{-3}$  which is lower than the approximately  $\$1 \text{ m}^{-3}$  present-day cost of effective treatment by PACl (which will also rise in price with time). In this context, extra-faradic corrosion is a bonus, giving more flocculent per coulomb. However, this apparently free corrosion comes at the cost of higher voltage and power input. The cost advantage in using solid aluminium as the source of flocculent is likely to remain and offers some margin for making a profit from sale of solid flocculent.

## **5.10 Conclusions**

### **5.10.1 Verification in laboratory conditions**

The laboratory flume system was found to have similar function to the field version. The phenomenon of pH adjustment was replicated. Lack of either polymer coagulant or complex organic mixtures in the effluent detracted from the performance at very high pH.

### **5.10.2 Mechanism of treatment**

At high anodic voltage in a fast flowing high pH electrolyte both passive and active corrosion of the aluminium anode can occur continuously. The effect of faradic dose was magnified by extra-faradic corrosion. Comparisons with chemical flocculants must specify whether the electrolytic dose is based on measured outflow aluminium, faradic corrosion, or total corrosion including extra-faradic corrosion.

Electrolytic processing has a major advantage over chemical means for treatment of buffered high pH effluent. Controlled pH reduction was achieved. The aluminium species in chemical flocculants are supplied in partially neutralised form (requiring 2.5  $\text{OH}^-$  to be fully neutralised) whereas the aluminium produced electrolytically requires 3 hydroxides to be neutralised. If the alkalised catholyte is separated in a low flow then the anolyte pH will be reduced. The amount of extra-faradic corrosion depends on the cell voltage and is a greater fraction of the total corrosion at higher voltages. The amount of pH adjustment also depends on the cell voltage. The cell voltage changes could be driving changes in the anodic

over-potential, but being able to alter the pH easily without the need for a potentiostat-controlled cell is very convenient.

Alkaline water would decrease in pH along the length of the Flume. Hence, a robust aluminium floc could form in the first section at high pH and then collect other contaminants, including colloidal aluminium, as the pH dropped.

While cell voltage is a very convenient means of control of pH modification, the link between cell voltage and pH modification is not clear, nor has the exact control function of cell voltage on pH modification been established. It is postulated that the  $\text{Al}(\text{OH})_3$  that is formed by extra-faradic corrosion is initially less crystalline, and therefore more soluble, than the  $\text{Al}(\text{OH})_3$  formed by faradic corrosion. This would explain the greater pH drop when the proportion of extra-faradic corrosion increases.

### **5.10.3 Extending operating time**

Blockage was found to occur even without coarse suspended solid in the inflow and means to prevent it are necessary. The system fails if solid blocks the lower part of the Flume because the flow is then forced further up the matrix over wider cross-section, slowing the flow speed and causing flocculent production in the low flow speed region, lowering the clearance in a feedback loop until even a very high flow will not completely flush the Flume. Measures that should be taken to avoid the blockage failure include pre-filtering the influent so the blocking solid does not reach the matrix, limiting the compression of the shavings against the membrane and using a steeper slope that optimises the components of gravitational force to direct the flow along the bottom of the conduit in minimum cross-section. In order to maintain operation for as long as possible, the flow down the Flume should be fast, moving at a minimum speed of  $0.2 \text{ m s}^{-1}$ , and thin.

## 6 Conclusions

### 6.1 Evolutionary design to address historical problems

Electrolytic water purification has a long history but has not been fully exploited. Problems with electrolysis include: low conductivity of the water to be purified; poor clearance of corrosion products from the anode; fouling of the electrodes and the high cost of corrosion resistant anode materials.

Evolutionary design addressed these problems. Distinct strategies, corroding anode and non-corroding anode, lead to two final designs (see §4.1). The final corroding anode design was called the Flume, with an aluminium shavings anode insulated from a steel cathode by porous fabric (Mathieson et al. 2005; Mathieson et al. 2006). The final non-corroding anode design was bipolar stacks. The poor conductivity of wastewater and potable water was overcome by reducing the gap between the electrodes and catholyte salination.

### 6.2 The Flume - an advance in electrolytic water purification

#### 6.2.1 Structure of the Flume

A steel flume was used as the cathode and aluminium shavings were used at the anode. The fluid to be treated flowed down the Flume in a thin layer at the bottom of the shavings. A water permeable nylon mesh insulated the shavings anode from the steel cathode. The high fluid flow speed in the zone of anodic corrosion increased the clearance of anodic corrosion products and limited electrode fouling. Good performance was achieved with normalised space velocity in the order of  $10 \text{ m}^3 \text{ m}^{-3} \text{ h}^{-1}$  and normalised space energy consumption in the order of  $40 \text{ kWh m}^{-3} \text{ m}^{-3}$ . A cross-section of the Flume is shown in Figure 6-1 (see also Figure 4-5 in §4.1.4).



Figure 6-1 Cross section of the Flume.



### **6.2.2 Increasing conductance with an inert membrane**

The Flume used a thin parka nylon fabric mesh membrane. This was 0.1 mm thick, so the gap between the electrodes was low, yet strong enough to prevent direct electrode contact. The open area fraction of the mesh was 0.4 while the fabric fibres were 0.01 mm thick, so the size of the pores was smaller than the smallest dimension of the anode pieces. Because the mesh was sufficiently open the improvement in conductance due to reduced electrode gap was greater than the reduction due to loss of area. This made it possible to improve the efficiency of water treatment while maintaining electrical insulation. Open gaps of less than a millimetre with no membrane are unreliable whereas the nylon mesh membrane used in the Flume resulted in an equivalent gap of 0.25 mm and performed satisfactorily. The uses of mesh membranes, or their possible function in electrolyzers, are not described in prior literature.

### **6.2.3 Electro-flocculator**

The function of an electro-flocculator is best served by an electrolyzer that has a readily corrodible anode. This type of electro-flocculator could also be adapted for use with iron ribbons. Chapters 4 and 5 describe the design and use of the Flume. Fluids of pH 8 to pH 10 are the most promising candidates for electroflocculation using aluminium anodes because they are easily conditioned to produce a strong floc with low residual aluminium.

### **6.2.4 Turning waste into a resource at the point of production**

Removal of the vast majority of chromium in the effluent from a tannery by the Flume, using extremely cheap materials, has been shown to be technically feasible (see §4.4). The extracted chromium was concentrated in a floc and could be returned to the tannery, after further concentration, saving of the order of 10 kg of chromium per day and preventing it from entering and contaminating other waste streams and waterways. Furthermore, concentrated alkali was manufactured and extracted from electrolyte (see §6.2.7). Neutralisation of fluid pH is assisted and the alkali is recyclable. By this example, a point of production processor (PPP) has been shown to be useful as a means of improving an existing treatment process and could be implemented.

### **6.2.5 Control of flocculation and pH adjustment**

The rate of corrosion of aluminium in the Flume was increased by either applying an anodic potential or immersing the aluminium in fluid that is acidic or alkaline. A combination of the two effects has been found to be synergistic, in that the rate of corrosion was several times than that predicted faradically. The extra-faradic corrosion rate is larger, and a greater proportion of the total corrosion rate, when the cell voltage is higher. Where extra-faradic corrosion of aluminium occurred it moderated the pH and the moderation was greater when the extra-faradic corrosion is greater.

The Flume was able to manipulate fluid pH toward neutral independent of total flocculent addition. This is useful to both improve the function of downstream biological oxidation processes and to lower the solubility of dissolved contaminants including the flocculent. Moderation of the outflow pH was beneficial to subsequent discharge quality.

### **6.2.6 Modification of the pH of either split or whole flows**

An electrolytic processor generates acid at the anode and alkali at the cathode. By separating the fluid flows into anolyte and catholyte using a membrane the fluid is split into an acidified portion and an alkalisied portion. By adjusting the flow ratios it was possible to create a larger pH change in the portion with lower flow.

The pH of whole outflow from an electrolyser with a corroding aluminium anode, such as the Flume, was moderated toward the isoelectric point of  $\text{Al}(\text{OH})_3$ . Extra-faradic corrosion arose due to passive hydrolysis of aluminium but was accelerated by higher cell voltage. Lower conductivity electrolytes had greater proportions of extra-faradic corrosion compared to total corrosion. Total corrosion was a quadratic function of either cell current or cell voltage. The degree of pH moderation could be controlled by the cell voltage or cell current.

### **6.2.7 Extraction of useable alkali from effluent**

When the anolyte and catholyte flows were separated, and the catholyte flow was minimised, the hydroxide generated at the cathode produced a catholyte outflow with  $\text{pH} > 13$  for a wide range of inflow pH.  $\text{OH}^-$  is produced at the cathode at 6.22

$\times 10^{-4} \text{ mol A}^{-1} \text{ min}^{-1}$ , which is twice the molar rate of production of hydrogen. Where an industrial process uses neutral water as an input and requires net addition of alkali, the hydroxide in the effluent of the industrial process could be, in effect, recovered from the moderately alkaline effluent stream by an electrolytic processor and reused (see Figure 6-2). At a current dose of  $3 \text{ A (L min}^{-1})^{-1}$ , which is a level of treatment appropriate for treatment of typical effluent, the  $\text{OH}^-$  production per volume of fluid treated is  $1.87 \times 10^{-3} \text{ mol L}^{-1}$ , sufficient to raise the pH of the neutral fluid of equal volume to that treated in the electrolyser to 11.3.

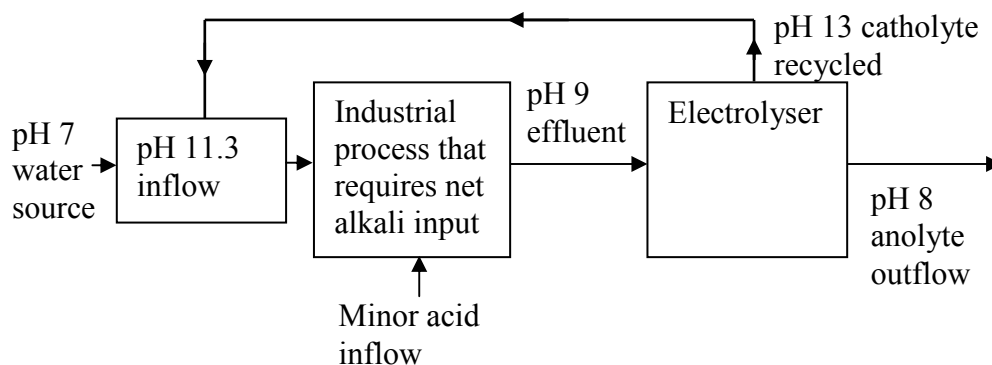


Figure 6-2 Proposed alkali recycling scheme for an industrial process requiring net alkali input.

### 6.2.8 Increasing the effective conductivity of the electrolyte

The energy efficiency of electrolytic processing of low conductivity waters was improved by splitting the flow into anolyte and catholyte. The vast majority of the fluid to be treated was passed through the anolyte compartment while a very low flow passed through the other compartment. The low flow compartment was salinated to increase the current at a given cell voltage without significantly increasing the salinity of the main flow.

### 6.2.9 Using acidic catholyte and alkaline anolyte

Where waste streams such as pulp and paper effluent are already split into two streams with strongly opposing pH, they could be used to improve the energy efficiency of electrolytic processors with separate anolyte and catholyte compartments by off-setting both the extreme acidification at the anode and extreme alkalisation at the cathode.

### **6.2.10 Continuously replaced corrodible aluminium anode**

The anode was composed of loosely packed ribbons that dipped into the fluid. Passive corrosion in anodic conditions, described as extra-faradic corrosion, was significant. The fluid flow speed was high. The corrosion products were cleared in the fluid flow rather than building up on the electrodes. Improved long-term performance compensated for the reduction in effective anode surface area. As the lower part of the anode corrode and was cleared from the Flume, dry parts of the anode material dropped into the fluid, by force of gravity, replacing the corroded parts and thereby minimising anode maintenance. This was the basis of NZ Provisional Patent 537700, applied for in 2005.

### **6.2.11 Crystalline co-flocculation of aluminium and chromium**

Electrolytic corrosion of aluminium into an alkaline saline electrolyte containing chromium results in a floc that, upon freeze drying, shows a crystalline X-ray diffraction spectrum that is not readily recognisable as a previously catalogued phase. The spectral peaks partly match both known phases of aluminium species and known phases of chromium species, but some peaks were unique. This indicated that co-flocculation of aluminium (III) and chromium (III) had occurred, producing a previously unknown phase. A crystalline co-floc could have a much lower solubility than amorphous aluminium which partly explains why the measured residual aluminium levels were lower in both field and laboratory trials than the theoretically estimated amorphous aluminium solubility levels predicted. It is not known whether crystalline co-flocculation is unique to electrolytic processing. While there are many possible ratios of aluminium to chromium in co-flocs, it is proposed that the generic name for crystalline phases of aluminium-chromium co-flocs be Alexandrite.

## **6.3 Bipolar stack structure and functions**

### **6.3.1 Bipolar stack structure**

Bipolar stacks of electrolytic cells in series are used to overcome the difficulties of both large area electrode construction and heavy current power supplies. However, the resistance of the electrolyte still limits energy efficiency.

A design proposed for a bipolar stack structure that maximises electrolyte conductance when the electrolyte conductivity is low is shown in Figure 6-3 (see also Figure 3-17). Current leakage is minimised by a narrow intracell gap, based on a nylon mesh membrane, and a wide intercell gap, based on a conductive link.

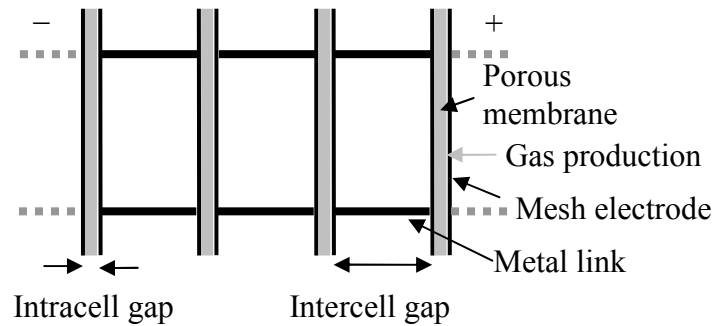


Figure 6-3 Proposed bipolar stack structure, showing narrow intracell gap and wide intercell gap that minimises current leakage.

The design shown in Figure 6-3 enables release of the fine gas bubbles produced by electrolysis. A low rate of corrosion of stainless steel electrodes can be achieved by using a cell voltage below 5 V. The design has yet to be tested.

### 6.3.2 Electroflotation

An electrolytic module specialised for flotation of suspended solid should be made of a stack of stainless steel or graphitic carbon electrodes. The ability to recover energy in the form of hydrogen is a definite advantage but to make best use of it, the capital cost of achieving cell voltages less than 5 V by use of large area electrodes will be significant.

Up-flow through the electrolyser would be of most benefit to production and use of fine bubbles. A down-flow scheme has the advantage of re-direction of the suspended solid away from the outflow. Cross-flow is a compromise between the other extremes that relies on gas pumping and convection to stir the electrode surfaces and clear the bubbles. By using a downward fluid-flow system, it has been found that 90% of the gas produced by the electrolysis is contained in bubbles that are able to rise against clear water travelling at a flow speed of 0.003

$\text{m s}^{-1}$  ( $11 \text{ m h}^{-1}$ ). Because this rate of rise is greater than the usual flow speed of gravity filters, electroflotation was achieved in a smaller area.

### **6.3.3 Rapid electrolytic oxidation and self-flocculation of iron**

An intermediate electrolyser design (see Figure 3-8) for rapid oxidation of  $\text{Fe}^{2+}$  in bore water to  $\text{Fe}^{3+}$  created a readily filterable floc that first floated then settled, leaving very low residual iron in the water. The current efficiency for direct oxidation of the  $\text{Fe}^{2+}$ , as opposed to that chemically oxidised by species produced at the anode was not found. This method was named electrolytic floxidation of iron. This method has the potential to produce better quality water in commercial application than spray oxidation and filtration.

### **6.3.4 Electro-steriliser**

The current efficiency for production of aggressive oxidizing agents should be raised and the current efficiency of oxygen production should be lowered. Very dilute solutions of chloride ions were used as the source of electrolytically generated chlorine. The cell voltage had to be greater than 5 V to raise current efficiency ahead of the competing oxygen production reaction. Low cell voltages did not improve the energy efficiency of sterilisation.

## **6.4 Combined functions**

### **6.4.1 The value of combining functions**

Combining functions in a single cell or group of cells exploits the synergies between functions and reduces the capital cost. Separate cells with specialised electrolytic functions can be assembled into complete systems that use a common power supply thereby saving duplication of this expensive electrical component. Manipulation of cell voltages and current density is an effective function control mechanism.

#### **6.4.2 Electroflocculation and electroflotation**

Electroflocculation and electroflotation are synergistic functions. Electro-oxidation and electroflotation are also synergistic functions if the product of oxidation is a flocculent. Each pair of functions was achieved with a common anode material. Flocculation-flotation, using a corroding anode, relies on setting the cell voltage to enable sharing of the anodic current between simultaneous production of flocculent and fine gas bubbles. Electro-oxidation and electroflotation, using a non-corroding anode, relies on current sharing between oxidisation and production of gas. In both cases rapid development of the floc which can then entrain gas bubbles is crucial.

In the Flume, anodic current was shared between corrosion and bubble production to enable combined flocculation and flotation. This required both that the flocculation occurred rapidly, so that the gas bubbles were still in the fluid when floc particles were of the right size to enmesh them, and that there are sufficient gas bubbles to raise the floc. By simultaneously performing the functions of a dissolved air flotation plant (DAF) and flocculator, the electrolytic treatment can reduce the load on filtration components, so that the time between filter backwashes is increased. The flocculated suspended solid can be floated or settled out prior to filtration. Because the catholyte flow was separated from the anolyte, the hydrogen gas produced at the cathode was not useful for flotation. Rapid flocculation occurred when the inflow pH was 8 to 9 and sufficient oxygen bubbles for flotation were produced when the cell voltage was above 7 V.

Combined electroflocculation and electroflotation was also observed when water containing  $\text{Fe}^{2+}$  was electro-oxidised using a bipolar stack electrolyser. Hydrogen produced at the cathode supplemented the oxygen produced at the anode. Flocculation was effective at neutral pH and sufficient gas for flotation was produced at cell voltages above 5 V.

#### **6.4.3 Combination with sterilisation**

Electrosterilisation is best done subsequent to removal of as much oxidisable impurity as possible, because electrosterilisation is achieved mainly by oxidation processes ranging from electro-oxidation through production of short-lived

aggressive radicals to production of persistent disinfectants. It could be claimed that flocculation is a form of sterilisation because microbes are removed from the fluid by capture in floc. However, an anode that corrodes readily cannot effectively produce oxidising agents so flocculation cannot complete the sterilisation. An anode that does not corrode readily is required for effective production of oxidising agents. This anode could be part of a set of electrolyzers with a common power supply. When all the readily oxidisable material has been exhausted, production of residual oxidants begins.

#### **6.4.4 Combination with electrowinning**

Electrowinning of a metal occurs at the cathode whenever the cathodic voltage exceeds the potential for reduction of that metal. The rate will be enhanced by having a high proportion of the flow pass close to the cathode surface.

Recirculation will enable a larger proportion of the metal to be plated. By periodically reversing the polarity of the cell, the functions of electrowinning and electroflocculation could be applied in sequence to first remove a metal from solution then capture it in floc.

#### **6.4.5 Combination of more than two functions**

The ideal anode properties for electroflocculation are mutually exclusive with those for electrosterilisation, because a corrodible anode will produce metal cations for flocculation rather than more directly effective disinfectants. Even if such agents are produced they are liable to be consumed locally by the anode. Bore-water, with an inorganic contaminant like trace  $\text{Fe}^{2+}$ , was both flocculated and sterilised using a single anode, as the oxidised and flocculated form did not consume additional residual disinfection agent. A system that performs electroflotation, electroflocculation and electrosterilisation with a single electrical power supply could be made by using a series or parallel arrangement of cells with two types of anodes, corroding and non-corroding.



## **6.5 Enhancing or surpassing chemical water treatment**

### **6.5.1 Electro-flocculants**

Flocculants produced by corrosion of a metal anode in dilute electrolytes are more cost-effective than traditional chemical flocculants (partially hydrolysed metal salts) for the treatment of alkaline fluids (see §4.4). This is because a solid electrode material is a more concentrated source of flocculent than a liquid solution. The total amount of metal required to be added is slightly lower because the trivalent ions produced by the anodic corrosion have greater acidity than partially hydrolysed flocculants. The cost of transporting a pure solid metal sourced from a recycler to a water or waste water processing facility plus the electrical cost of electrolysis of the same metal in alkaline solution is lower than the cost of transporting a liquid solution that is 5% active metal by weight. In electrolytic treatment pH adjustment can be controlled partly independently of metal dosage whereas for chemical dosing the pH drop is directly related to metal dosage. By adjusting the pH to a point of low solubility for metal-containing species, electrolytic treatment produced a lower residual metal content in the outflow than chemical dosing.

### **6.5.2 Overcoming low conductivity electrolyte**

The conductance of an electrolyser was increased by reducing the electrolyte gap to a practical minimum by using a membrane as in the Flume (see §3.2.6). The effective conductance of an electrolyte was increased by separating the flow into anolyte and catholyte, making one of the flows much smaller than the other and adding salt to the low flow compartment. The salinity of the main flow was not affected significantly (see §5.6). By a combination of gap reduction and catholyte salination it was possible to lower the minimum conductivity of fluid that could be treated economically.

### **6.5.3 Benign anodes**

Anode materials that have extremely low corrosion rates at acceptable current density, over-potential and current efficiency are available. However, they are not economic due to the inclusion of various combinations of platinum, ruthenium and iridium in specially prepared coatings.

Cheap anodes that have a low corrosion rate are not available. Either the anode material's corrosion products must be entirely benign and easily removed from the water or the current density must be lowered to achieve an acceptably low corrosion rate. The aluminium shavings anode in the Flume corroded rapidly and caused flocculation so the corrosion products were removed along with other contaminants. Electroflotation by bipolar stacks used very large area electrodes at low current density. Lower cell voltage both reduces the life-cycle cost and raises the fraction of energy input energy recoverable as hydrogen.

If a stainless steel anode is used it should have the optimum proportion of nickel and chromium to minimise the rate of leaching of these toxic elements. Coating metals with thin layers of poorly or slightly conducting oxides that are selective for different reactions is a last resort, even if the coatings are initially effective. The coating will deteriorate over time. Anode materials that are already largely oxidised, and not prone to further oxidation, yet electrically conductive are a possible solution to the dilemma of optimising between conductivity and corrosion resistance.

#### **6.5.4 Energy recovery by production of hydrogen**

Hydrogen recovery is favoured when the cell voltage is low. Large area electrodes made of a cheap material are the best option. Where passage of the flow through the electrode gap is not necessary, and gas separation is required, a thin ion-porous membrane between the electrodes is sufficient. If the vast majority of the water flow is vertical and perpendicular to the membrane there is very little driving force to push the gas bubbles through the membrane. The electrodes can also be very close together without risk of electrical contact.

In cases where the cell voltage has to be raised to achieve a treatment function, such as pH reduction by enhanced passive anodic corrosion of aluminium, energy recovery as hydrogen is not likely to be economic. Where additional infrastructure for use of the hydrogen is already in place, such as bio-gas driven electrical generators at a waste water plant, use of the hydrogen could be achieved with very little additional investment. However, the scale of the operation must be large to

recover significant energy. Applications where electroflotation is emphasised are the most likely candidates for implementation of energy recovery.

#### **6.5.5 Flexibility and control**

An electrolytic system would be connected directly to an electronic controller via electrical inputs and outputs. For example the resistance of a cell is monitored directly by voltage and current measurements. Likewise an electrical power supply for an electrolyser is controlled directly by electrical control signals. By switching sections of an electrolyser in or out of power circuits it is possible to change dosage or pH modification instantly. Finer control of the amplitude and shape of voltage or current waveforms is straightforward. A processing system can therefore respond rapidly to changing inflow conditions. It is possible to construct entire systems with few or no moving parts by using electronic sensing and control and electrical actuators.

#### **6.5.6 Feasible scale of operation**

Flows of between  $1 \text{ m}^3 \text{ day}^{-1}$  and  $1000 \text{ m}^3 \text{ day}^{-1}$  can be treated economically by electrolytic means. Below the lower limit the cost of setting up an electrolyser would outweigh any benefit in operating cost compared to standard treatment. The fixed cost of installation would be significant even for a  $0.01 \text{ m}^3 \text{ day}^{-1}$  system and would have to be justified by performance advantages. The collection of hydrogen for the purpose of energy recovery is not worth the effort for energy-equivalent hydrogen production rates below  $10 \text{ kWh day}^{-1}$  which would arise from fluid treatment rate of 1 to  $10 \text{ m}^3 \text{ day}^{-1}$ . A single phase mains power supply can supply a maximum of 2.4 kW. This would, at best, treat a fluid flow of up to  $500 \text{ m}^3 \text{ day}^{-1}$  and as little as  $50 \text{ m}^3 \text{ day}^{-1}$  of heavily polluted water. A three phase mains power supply, which is more likely to be available for industrial scale operations, is sufficient to power the processing. Above the maximum size it is difficult to engineer small electrode gaps while still maintaining good clearance of products.

## **6.6 Suggestions for further work**

### **6.6.1 Resolve the anodic potential experimentally**

Establishing the relationship between anodic potential and the rate of passive hydrolysis for an aluminium anode in dilute solutions will allow better control of pH modification. This can be achieved by experiments using a potentiostat. Better quantification of the connection between cell voltage and pH drop is essential so that control functions can be implemented.

### **6.6.2 Microscopic observation of anodic corrosion of aluminium**

The destruction of the protective oxide layer on aluminium and subsequent corrosion should be observed by microscopy. By observing differences at different pH, cell voltage and anodic over-potential it may be possible to clarify the mechanisms of both corrosion and corrosion product clearance.

### **6.6.3 Application**

The designs developed for both the Flume and bipolar stacks should be built and tested. Crucial parts of this work include determination of both the mass transport co-efficient and the hydraulic conductivity of a packed bed of shavings.

### **6.6.4 Make non-porous Magnéli phase anodes**

Reduce  $\text{TiO}_2$  to a low order Magnéli phase and then compact it severely in a mould to form a non-porous material. This could be a useful corrosion-resistant anode.

### **6.6.5 Accounting for pH changes**

Examine more closely why the pH of whole outflow from an aluminium corroder is much lower than the pH of the inflow.



## 7 Appendices

### 7.1 Appendix A

#### Inductively coupled plasma techniques

Figure 7-1 and Figure 7-2 show inductively coupled plasma optical emission spectroscopy (ICP-OES) analysis method details that enabled resolution of sub- $\text{mg L}^{-1}$  levels of chromium and aluminium. These methods could not be used when iron was in the standards or samples due to interfering iron peaks. Both methods used a high nebuliser flow and moderate plasma gas flow to improve the sensitivity.

Figure 7-3 shows an example from a similar method for measurement of a  $0.1 \text{ mg L}^{-1}$  aluminium standard.

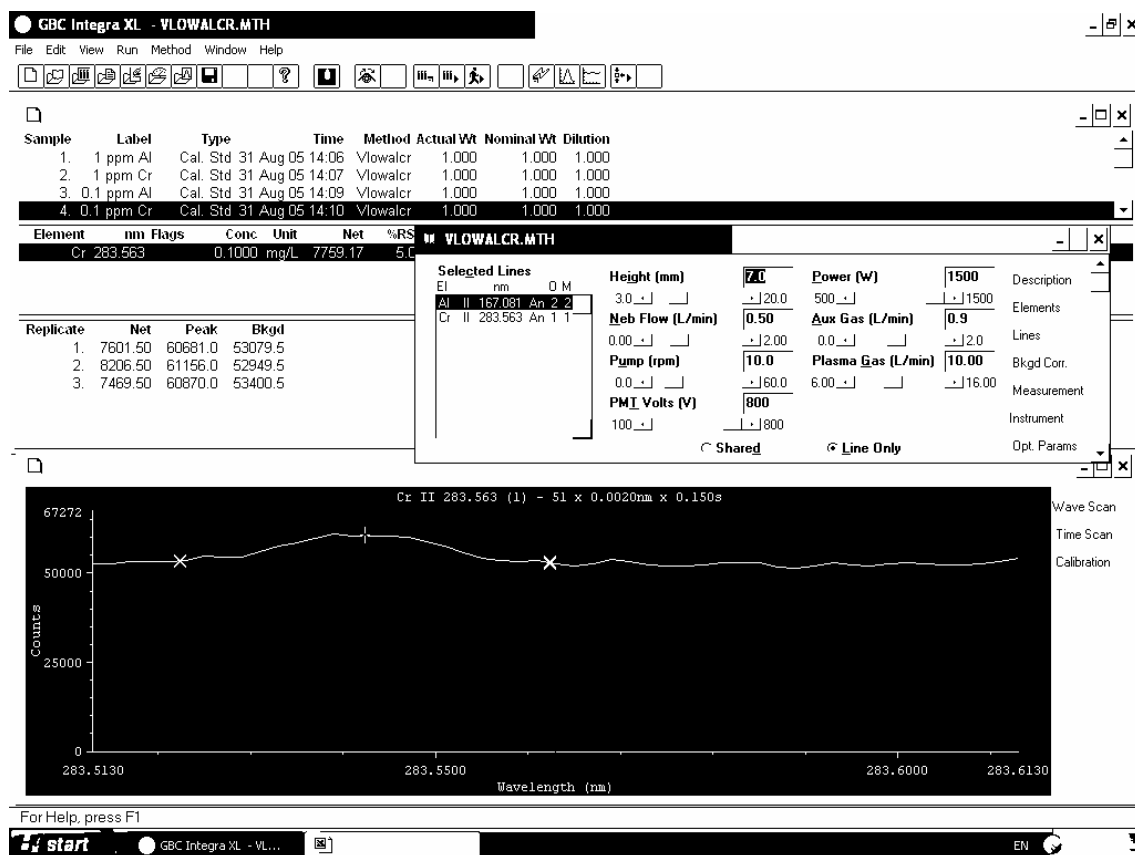


Figure 7-1 The basic method settings for low aluminium measurement by ICP and low level chromium signal.

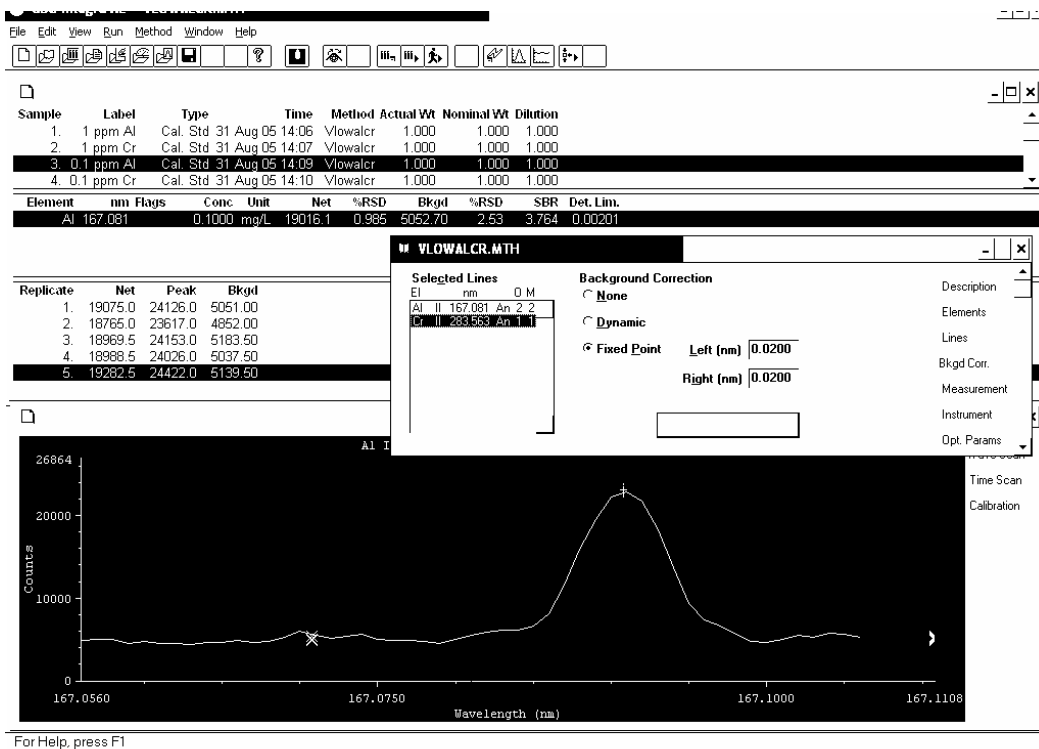


Figure 7-2 The background settings for low chromium measurement by ICP and a low level aluminium signal

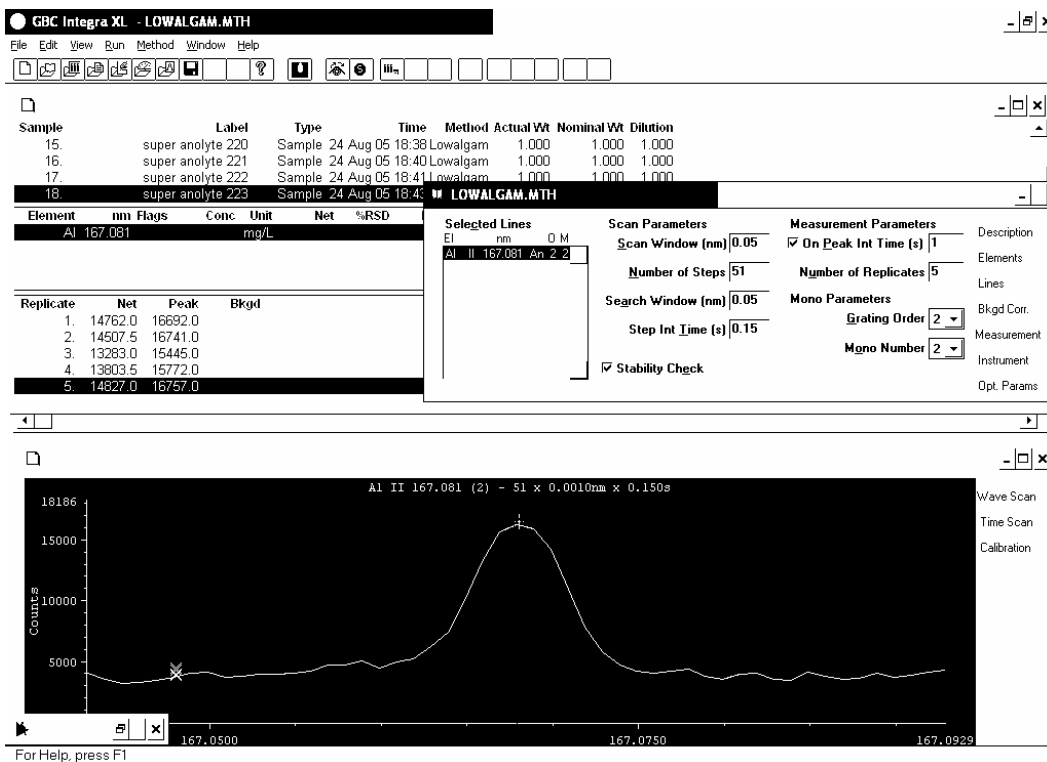
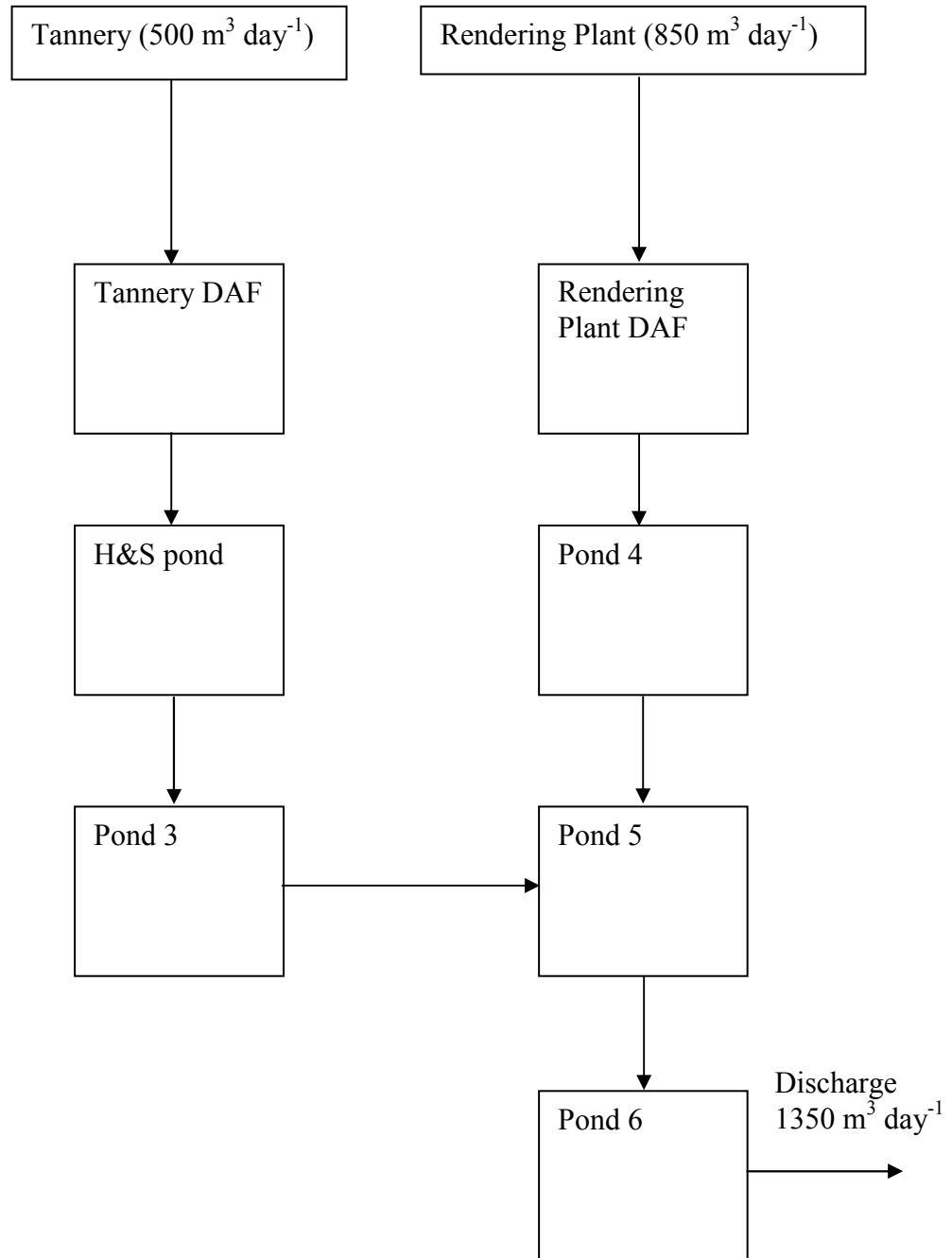


Figure 7-3 The grating settings for low aluminium measurement and a sample trace.

## 7.2 Appendix B

### Site process diagram for the tannery and rendering plant





## References

- Abu-Orf, M., C. D. Muller, C. Park and J. Novak (2004). "Innovative technologies to reduce water content of dewatered municipal residuals." Journal of Residuals Science & Technology **1**(2): 83-91.
- Adin, A. and N. Vescan (2002). "Electrofloculation for particle destabilization and aggregation for municipal water and wastewater treatment." Preprints of Extended Abstracts presented at the ACS National Meeting, American Chemical Society, Division of Environmental Chemistry **42**(2): 537-541.
- Ahmed, O., P. Biswas and M. Mollah (2004). "Removal of Cr<sup>6+</sup> from wastewater by electroreduction and coagulation." Dhaka University Journal of Science **52**(2): 249-252.
- Alekseev, A. D. (1988). "Effect of current density on gas-bubble concentration in electroflotation." Vestnik L'vovskogo Politekhniceskogo Instituta **227**: 3-4.
- Alpha Knife Supply. (2004). "Titanium Sheet." Retrieved 16 January 2006, from <http://www.alphaknifesupply.com/ti-small.htm>.
- Anon (1995). "Pollution control by electrocoagulation electroflotation: the Ecolysis process." Galvano-Organo **64**(658): 703-5.
- Archakova, G. A. (1969). "Purification of wastewaters by an electrochemical method." Vodootvedenie Ochistka Vod: 82-90.
- Backhurst, J. R., J. M. Coulson, F. Goodridge, R. Plimley and M. Fleischmann (1969). "A preliminary investigation of fluidised bed electrodes." Journal of the Electrochemical Society **116**: 1600-1607.
- Baes, C. F. J. and R. E. Mesmer (1976). The hydrolysis of cations. New York, Wiley.
- Bard, A. J., R. Parsons and J. Jordan, Eds. (1985). Standard potentials in aqueous solution. Monographs in electroanalytical chemistry and electrochemistry. New York, Marcel Dekker.
- Barnitz, H. L. (1920). "Electrolytic production of hydrogen." Chemical and Metallurgical Engineering **22**: 201-6.
- Barradas, R. G., O. Kutowy and D. Shoemith (1974). "Electrochemical reduction of benzoic acid at mercury and lead electrodes." Electrochimica Acta **19**(2): 49-56.
- Barrett, F. (1975). "Electroflotation. Development and application." Water Pollution Control (Maidstone, England) **74**(1): 59-62.
- Barteneva, O. I., V. V. Bartenev and V. Grigor'ev (1999). "Electrode reactions of aluminum anodic dissolution in chloride-containing electrolytes." Russian Journal of Electrochemistry (Translation of Elektrokimiya) **35**(11): 1177-1181.
- Bayramoglu, M., M. Kobyas, O. Can and M. Sozibir (2004). "Operating cost analysis of electrocoagulation of textile dye wastewater." Separation and Purification Technology **37**(2): 117-125.
- Beck, E. C., A. P. Giannini and E. Ramirez (1974). "Electrocoagulation clarifies food wastewater." Food Technology (Chicago, IL, United States) **28**(2): 18-19, 22.
- Bellakhal, N., J. L. Brisset and M. Dachraoui (2004). "Electrocoagulation treatment of tannery wastewater." Journal de la Societe Chimique de Tunisie **6**(1): 61-66.

- Bellakhal, N., M. Dachraoui, H. Gannoun, M. Hamdi (2004). "Examples of water treatment. Some experiences in treatment of industrial wastewater by electroflocculation." Le Bup **98**(867): 1441-1446.
- Bennett, J. E. (1980). "Electrodes for Generation of Hydrogen and Oxygen from Seawater." International Journal of Hydrogen Energy **5**(4): 401-408.
- Berg, N., P. Marais (1977). "The use of polyelectrolytes in a closed system of tannery effluents." Journal of the Society of Leather Technologists and Chemists **61**(6): 129-31.
- Berl, E. (1937). Electrolytic production of hydrogen peroxide. US, (Mathieson Alkali Works).
- Berl, E. (1939). "A New Cathodic Process for the Production of H<sub>2</sub>O<sub>2</sub>." Transactions of the Electrochemical Society **139**: 359.
- Bertay, A., J. L'Hermitte, and F. Bichon (1981). "Compact installation for electrocoagulation and electroflotation of aqueous effluents". French patent application 79-15914 2459078 assigned to Electricite de France.
- Bestetti, M., U. Ducati, G. Kelsall, G. Li, E. Guerra and R. Allen (2001). "Zinc electrowinning with gas diffusion anodes: State of the art and future developments." Canadian Metallurgical Quarterly **40**(4): 459-469.
- Bockris, J. O. M., A. K. N. Reddy (1970). Modern electrochemistry; an introduction to an interdisciplinary area. New York, Plenum Press.
- Bonilla, C. F. (1947). "Possibilities of the electronic coagulation for water treatment." Water and Sanitation **85**(No. 3): 21-2,44-5.
- Briner, E., R. Haefeli and H. Paillard (1937). "Production of ozone by electrolysis. Electrolysis at low temperature." Helvetica Chimica Acta **20**: 1510-23.
- Briner, E. and A. Yalda (1941). "Electrolytic production of ozone and anodic overvoltage." Helvetica Chimica Acta **24**: 1328-45.
- Bryan, A. M. (2003). "Conductivity of Dilute Aqueous Solutions." Retrieved 28 December, 2005, from [http://www.campbell.edu/faculty/bryan/CHEM334/CHEM334L%20Handouts/CHEM334L%20Conductivity\\_2005.pdf](http://www.campbell.edu/faculty/bryan/CHEM334/CHEM334L%20Handouts/CHEM334L%20Conductivity_2005.pdf).
- Burns, S. E., S. Yiacoumi and C. Tsouris (1997). "Microbubble generation for environmental and industrial separations." Separation and Purification Technology **11**(3): 221-232.
- Buso, A., L. Balbo, M. Giomo, G. Farnia and G. Sandona (2000). "Electrochemical Removal of Tannins from Aqueous Solutions." Industrial & Engineering Chemistry Research **39**(2): 494-499.
- Busse, B. and S. Kotowski (1985). "Polarity-reversible electrodes for seawater electrolysis and other processes." DECHEMA Monographien **98**(Tech. Elektrolysen): 357-66.
- Calder, V. (2003, September 2005). "Conductivity of Concentrated Brine." from <http://www.newton.dep.anl.gov/askasci/gen01/gen01755.htm>.
- Canizares, P., M. Carmona, J. Lobato, F. Martinez and M. Rodrigo (2005). "Electrodissolution of Aluminum Electrodes in Electrocoagulation Processes." Industrial & Engineering Chemistry Research **44**(12): 4178-4185.
- Carrara, G. (1918). "The Zorzi system for the electrolytic production of hydrogen and oxygen." Electrotecnica **5**: 86-90.
- Chebanov, V. B., A. A. Mamakov and L. Fainshtein (1972). "Continuous electroflotation purification of waste waters from tanneries." Elektronnaya Obrabotka Materialov(5): 88-91.
- Chen, G. (2004). "Electrochemical technologies in wastewater treatment." Separation and Purification Technology **38**(1): 11.

- Chen, X., Z. Wang, C. Huang and M. Cai (2003). "Treatment of paper-mill wastewater by electroflocculation using Fe anode." Guangxi Daxue Xuebao, Ziran Kexueban **28**(2): 87-90.
- Chen, X. (2002). "High-performance electrodes for wastewater treatment." A dissertation written at Hong Kong University of Science and Technology, Hong Kong, Peop. Rep. China.
- Chen, X. and G. Chen (2005). "Stable Ti/RuO<sub>2</sub>-Sb<sub>2</sub>O<sub>5</sub>-SnO<sub>2</sub> electrodes for O<sub>2</sub> evolution." Electrochimica Acta **50**(20): 4155.
- Chen, X., P. L. Yue and G. Chen (2002). "Investigation on the electrolysis voltage of electrocoagulation." Chemical Engineering Science **57**(13): 2449-2455.
- Chen, X., P. L. Yue and G. Chen (2002). "Novel Electrode System for Electroflotation of Wastewater." Environmental Science and Technology **36**(4): 778-783.
- Chipcatalog. (2005). "Datasheet for STP60NE06-16." Retrieved July, 2005, from <http://www.chipcatalog.com/Datasheet/9854C4013FD17871097D39AA16A01703.htm>
- Chou, T. C. and A. C. Lee (1995). Quinone synthesized from an aromatic compound in an undivided electrochemical cell. United States patent application assigned to National Science Council, Taiwan.
- Christoforetti, C. and G. Pratolongo (1986). "Wastewater treatment and recycling by electroflotation." Inquinamento **28**(7-8): 88-92.
- Collier, W. R. (1912). "Description of Plants at Oklahoma City, Oklahoma and Santa Monica, California." Engng. Rec. **66**: 55.
- Costaz, P., J. Miquel and M. Reinbold (1983). "Simultaneous electroflotation and disinfection of sewage." Water Research **17**(3): 255-62.
- Coup, M. R. and A. G. Campbell (1964). "The Effect of Excessive Iron Intake upon the Health and Production of Dairy Cows." NZ Journal of Agricultural Research **7**(4): 624-638.
- da Rosa, J. J. and J. Rubio (2005). "The FF (flocculation-flotation) process." Minerals Engineering **18**(7): 701-707.
- Damien, A. (1992). "Electrocoagulation and electroflocculation." Revue Generale de l'Electricite(3): 24-7.
- de Lima Leite, R. H., P. Cognet, A. Wilhelm and H. Delmas (2002). "Anodic oxidation of 2,4-dihydroxybenzoic acid for wastewater treatment: study of ultrasound activation." Chemical Engineering Science **57**(5): 767-778.
- Debillmont, P. (1996). "Electroflocculation for purification of industrial waters." Recents Progres en Genie des Procedes **10**(47): 129-137.
- Delplancke, J. L., R. Winand, J. De Mussy and A. Pagliero (1999). "New anode compositions for copper electrowinning and copper electrodeposition at high current density." Proceedings of the COPPER 99-COBRE 99 International Conference, 4th, Phoenix, Oct. 10-13, 1999 **3**: 603-608.
- Demmerle, C. (2002). "Use of electrolytically produced ozone for disinfection of ultrapure water." F&S, Filtrieren und Separieren **16**(5): 237-240.
- DiBari, G. A. (1970). Electrochemical and corrosion behavior of aluminum, Ordnance Res. Lab., Pennsylvania State Univ., University Park, PA, USA.: 92 pp.
- DiBari, G. A. and H. J. Read (1971). "Electrochemical behavior of high-purity aluminum in chloride-containing solutions." Corrosion (Houston, TX, United States) **27**(11): 483-93.
- Diegner, A. (2003). "Germ-free water." Wasserwirtschaft, Wassertechnik, Abwassertechnik(1-2): 43-44.

- Donini, J. C., C. W. Angle, T. Hassan, K. Kasperski, J. Kan, K. Kar and S. Thind (1993). "Electrocoagulation." Emerging Sep. Technol. Met. Fuels, Proc. Symp.: 409-24.
- Donini, J. C., C. W. Angle, K. Kasperski, C. Preston, K. Kar, T. Hassan and S. Thind (1992). "The effect of different parameters on the optimization of electrocoagulation." Waste Process. Recycl. Min. Metall. Ind., Proc. Int. Symp.: 119-24.
- Donini, J. C., J. Kan, J. Szykarczuk, T. Hassan and K. Kar (1994). "The operating cost of electrocoagulation." Canadian Journal of Chemical Engineering **72**(6): 1007-12.
- Dorokhina, L. N. (1976). "Use of a combined system for electrochemical purification of cyanide-containing waste waters with simultaneous additional extraction of heavy metals by electroflotation." Fiz.-tekhn. Probl. Razrabotki i Obogashch. Polezn. Iskopaemykh: 132-6.
- Douglas, J. (1975). Bacteriophage. New York: , John Wiley and Sons, Inc.
- Drazic, D. M. and J. P. Popic (1997). "Corrosion rates and negative difference effects for Al measured by the disk-ring technique." ATB Metallurgie **37**(2-3-4): 307-310.
- Drazic, D. M. and J. P. Popic (1999a). "The negative difference effect and stress corrosion cracking." Institution of Chemical Engineers Symposium Series **145**(Electrochemical Engineering): 111-120.
- Drazic, D. M. and J. P. Popic (1999b). "Corrosion rates and negative difference effects for Al and some Al alloys." Journal of Applied Electrochemistry **29**(1): 43-50.
- Drogui, P., S. Elmaleh, M. Rumeau, C. Bernard and A. Rambaud (2001). "Hydrogen peroxide production by water electrolysis: application to disinfection." Journal of Applied Electrochemistry **31**(8): 877-882.
- Drogui, P., M. Rumeau, S. Elmaleh, C. Bernard and A. Rambaud (2001). "Oxidising and disinfecting by hydrogen peroxide produced in a two-electrode cell." Water Research **35**(13): 3235-3241.
- DuPont. (2005). "DuPont Corporation Website." Retrieved October 2005, 2005, from [www2.dupont.com](http://www2.dupont.com).
- Dylewski, R., A. Korczynski and J. Dylewska (1996). "Principles of usability assessment of brines containing organic substances for electrolytic chlorine production." Polish Journal of Applied Chemistry **40**(1-2): 33-41.
- Elmore, F. E. (1904). A process for separating certain constituents of subdivided ores and like substances, and apparatus therefor. B. P. Office. United Kingdom. British Patent 13578 (1905).
- Em, S. (2003). BTEch 430 Project for Biotechnology. Auckland, University of Auckland.
- Evans, B. R. (1974). "Treatment of scouring liquor by electroflotation." Effluent & Water Treatment Journal **14**(2): 85-8.
- Fassina, L. (1938). "Purification of tannery effluents." Journal of the American Leather Chemists Association **33**: 380.
- Feng, C., K. Suzuki, S. Zhao, N. Sugiura, S. Shimada and T. Maekawa (2004). "Water disinfection by electrochemical treatment." Bioresource Technology **94**(1): 21-25.
- Feng, Z., B. Yang and Y. Xu (2001). "Mechanism of electrochemical corrosion of Al-foil in aluminium capacitor anode." Dianzi Yuanjian Yu Cailiao **20**(6): 1001-1028.

- Filippov, E. L., T. G. Vyal'tseva, L. Smirnova, L. Afanas'eva and S. Nefedkin (1983). "Electrolytic production of hydrogen in compact electrolyzer." Tr. Mosk. Energ. In-t(604): 53-60.
- Fischer, F. (1905). Ozone by the electrolysis of aqueous fluids. German patent.
- Fischer, F. and K. Massenez (1907). "On the Production of Ozone by Electrolysis. (Second Part)." Z. anorg. Chem. **52**: 229-55.
- Foller, P. C. (1982). "Status of research on ozone generation by electrolysis." Handb. Ozone Technol. Appl. **1**: 85-102.
- Foller, P. C., M. L. Goodwin and C. Tobias (1981). Electrolytic process for ozone production. United States patent application assigned to University of California, Berkeley.
- Forstmeier, M., G. Wozny, K. Buss, J. Toelle (2005). "Legionella control in cooling towers by electrolytic disinfection." Chemical Engineering & Technology **28**(7): 761-765.
- Franz, J. A., R. J. Williams, J. Flora, M. Meadows and W. Irwin (2002). "Electrolytic oxygen generation for subsurface delivery: effects of precipitation at the cathode and an assessment of side reactions." Water Research **36**(9): 2243-2254.
- Furuta, T., H. Tanaka, Y. Nishiki, L. Pupunat, W. Haenni and P Rychen (2004). "Legionella inactivation with diamond electrodes." Diamond and Related Materials **13**(11-12): 2016-2019.
- Gao, H., A. Scheeline and A. Pearlstein (2000). "Early stages of pattern evolution in anodic porous oxide film on Al 6061." Proceedings - Electrochemical Society **99-33**(Fundamental Aspects of Electrochemical Deposition and Dissolution): 101-109.
- Gao, P., X. Chen, F. Shen and G. Chen (2005). "Removal of chromium(VI) from wastewater by combined electrocoagulation-electroflotation without a filter." Separation and Purification Technology **43**(2): 117-123.
- Ge, J., J. Qu, P. Lei and H. Liu (2004). "New bipolar electrocoagulation-electroflotation process for the treatment of laundry wastewater." Separation and Purification Technology **36**(1): 33-39.
- Gerasimov, I. V., M. G. Ivleva and M. Malyavko (1962). "Electroflotation purification of emulsified sewage from oil refineries." Novosti Neft. i Gaz. Tekhn., Neftepererabotka i Neftekhim.(12): 18-20.
- Gleick, P. H. (1993). Water in Crisis: A Guide to the World's Freshwater Resources. New York, Oxford University Press.
- Glembotskii, V. A., A. A. Mamakov and V. Sorokina (1973). "Size of gas bubbles formed under electroflotation conditions." Elektronnaya Obrabotka Materialov(5): 66-8.
- Gomella, C. (1974). Clarification avant Filtration, Ses Progrès Recents (Rapport General 1). International Water Supply Association, International Conference.
- Gordon, G. and B. Bubnis (2001). "Why chlorine solutions appear to behave differently: a comparison of electrolyzed salt brine and FAC." Proceedings - Annual Conference, American Water Works Association: 1210-1221.
- Gordon, G., G. Emmert, R. Gauw and B. Bubnis (1998). "Can ozone and ozone oxidative byproducts be formed during the electrolysis of salt brine?" Ozone: Science & Engineering **20**(3): 239-249.
- Gottard, W. (2001). Determination of chlorine dioxide, chlorite, and chlorous acid in aqueous solutions. Ger. Offen. De. (Gottard, Waldemar, Austria). 8 pp.
- Hagiya, J. and M. Yonemura (1974). "Polyaluminum chloride". Japanese patent application 72-115567 49084991 assigned to Showa Tansan Co., Ltd.

- Herrington, R. E. and W. L. Bradford (1997). "Pilot-study report, mixed oxidant disinfection system at Greenfield, Iowa." Proceedings - Water Quality Technology Conference: P6J/1-P6J/17.
- Hill, T. A. and A. Langdon (1991). "Porous ceramic dual media filtration." Water and Wastes in New Zealand **1**: 19.
- Hine, F., M. Yasuda and T. Tanaka (1977). "Mass transfer through the deposited asbestos diaphragm in chlor-alkali cells." Electrochimica Acta **22**(4): 429-437.
- Hjulstrom, F. (1935). Studies of the morphological activities of rivers as illustrated by the River Fyris, Uppsala University. PhD Thesis.
- Holt, P. K., G. W. Barton and C. Mitchell (2005). "The future for electrocoagulation as a localized water treatment technology." Chemosphere **59**(3): 355-367.
- Houghton, R. W. (1985). "Degassing/brine tank for pool chlorinating system". US patent application 83-505928 4508687.
- Hu, C. Y., S. L. Lo, C. Li and W. Kuan (2005). "Treating chemical mechanical polishing (CMP) wastewater by electrocoagulation-flotation process with surfactant." Journal of Hazardous Materials **120**(1-3): 15-20.
- Huang, C. P., M. C. Hsu and P. Miller (2000). "Recovery of EDTA from power plant boiler chemical cleaning wastewater." Journal of Environmental Engineering-Asce **126**(10): 919-924.
- Hurst, C. J. (2000). Viral Ecology. San Diego, Attarcourt Science and Technology Company.
- ICDD (2005). International Centre for Diffraction Data from [www.icdd.com](http://www.icdd.com), accessed 17 August 2006.
- Ichimaru, O., M. Kato and N. Ishii (2005). Electrolytic water purification apparatus for providing purified acidic water and alkaline water. Japanese patent application.
- Innovative Energies. (2004). "SMPS JWS 50 - 150 Series." from <http://www.innovative.co.nz/PDF/DS-JWS50-150.pdf>
- Jiang, J.-Q., N. Graham, C. Andre, G. Kelsall and N. Brandon (2002). "Laboratory study of electrocoagulation-flotation for water treatment." Water Research **36**(16): 4064-4078.
- Johnsen, S. (1938). "Electrosterilization of water. Oligodynamics and the catadyn process." Teknisk Ukeblad **85**: 114-17.
- Juttner, K., U. Galla and H. Schmieder (2000). "Electrochemical approaches to environmental problems in the process industry." Electrochimica Acta **45**(15-16): 2575-2594.
- Kanso, S., A. C. Greene and B. Patel (2002). "Bacillus subterraneus sp. nov., an iron- and manganese-reducing bacterium from a deep subsurface Australian thermal aquifer." International Journal of Systematic and Evolutionary Microbiology **52**(3): 869-874.
- Karpuzcu, M., A. Dimoglo and H. Akbulut (2002). "Purification of agro-industrial wastewater from the grease-protein mixture by means of electroflotocoagulation." Water Science and Technology **45**(12): 233-240.
- Kasai, H., K. Watanabe and M. Yoshimizu (2001). "Disinfectant effects of hypochlorite produced by batch electrolytic system on fish pathogenic bacteria and virus." Suisan Zoshoku **49**(2): 237-241.
- Kaspar, V. and J. Dvorak (1988). Treatment of wastewaters from production of synthetic rubber. Czechoslovakian patent application.

- Ketkar, D. R., R. Mallikarjunan and S. Venkatachalam (1988). "Size determination of electrogenerated gas bubbles." Journal of the Electrochemical Society of India **37**(4): 313-18.
- Khaydarov, R. A., R. L. Olsen, S. Rogers and R. Khaydarov (2004). "Water disinfection using electrolytically generated silver, copper and gold ions." Journal of Water Supply: Research and Technology--AQUA **53**(8): 567-572.
- Khosla, K., S. Venkatachalam, P. Somasundaran and N. Khosla (1995). "Flotation of alumina with electrogenerated gas bubbles." Minerals & Metallurgical Processing **12**(3): 132-7.
- Khosla, N. K., S. Venkatachalam and P. Somasundaran (1991). "Pulsed electrogeneration of bubbles for electroflotation." Journal of Applied Electrochemistry **21**(11): 986-90.
- Kim, B. H., I. S. Chang, H. Moon, J. Jang, J. Lee, T. Pham and T. Phung (2004). "Microbial fuel cells and beyond." Preprints of Extended Abstracts presented at the ACS National Meeting, American Chemical Society, Division of Environmental Chemistry **44**(2): 1502-1506.
- Kimbrough, D. E. and I. H. Suffet (2002). "Electrochemical removal of bromide and reduction of THM formation potential in drinking water." Water Research **36**(19): 4902-4906.
- Kitco Bullion Dealers. (2006). "Platinum World Spot Price." Retrieved 16 January, 2006, from <http://www.kitco.com/market/>.
- Klein, K.-J. (2003). Method and device for disinfecting water. German patent application.
- Kobayashi, S., H. Hayashi, H. Yamada, K. Osamura, T. Yamaguchi (2004). "Units for electrolytic treatment of water". Japanese patent application assigned to Tobishima Corporation.
- Kobayashi, T. (1985). "Electroflocculation and magnetic separation of wastewater". Japanese patent application 77-47019 60044036.
- Koga, O. and Y. Hori (1993). "Reduction of adsorbed Co on a Ni electrode in connection with the electrochemical reduction of CO<sub>2</sub>." Electrochimica Acta **38**(10): 1391-1394.
- Kolibaba, S. K. (1970). "Determination of hydrogen bubble sizes during electroflotation." Sb. Tr. Molodykh Uch. Kishinev. Politekh. Inst. No. 2: 159-61.
- Kondo, Y., H. Umezawa and T. Koizumi (2003). Sterilizing method and electrolysis water purification apparatus. United States patent application.
- Koparal, A. S. and U. B. Ogutveren (2002). "Removal of nitrate from water by electroreduction and electrocoagulation." Journal of Hazardous Materials **89**(1): 83.
- Kraft, A. (2004). "Electrochemical water treatment processes." Vom Wasser **102**(3): 12-19.
- Krasnobryzhii, A. V., A. I. Rusin, V. Varypaev, V. Nikol'skii and S. Alekseev (2004). "A study of the kinetics of electrochemical dissolution of aluminum alloys in alkaline electrolytes." Russian Journal of Applied Chemistry **77**(10): 1642-1645.
- Krofta, M. W. L. (1984). "Development of an Innovative Flotation-Filtration System for Water Treatment, Part C: An Electroflotation Plant for Single Families and Institutions." Proceedings of the Water Reuse Symposium August 26-31, 1984 San Diego, California **3**.

- Kruger, P. (2001). "Electric power requirement for large-scale production of hydrogen fuel for the world vehicle fleet." International Journal of Hydrogen Energy **26**(11): 1137-1147.
- Kul'skii, L. A., Y. V. Epifanov and E. Matskevich (1989). "Modern state of technology for regeneration of aluminum-containing coagulants from hydroxide water treatment slurries." Khimiya i Tekhnologiya Vody **11**(2): 123-37.
- Kul'skii, L. A., P. P. Strokach, V. Slipchenko and E. Saigak (1978). Water Purification by Electrocoagulation. Kiev, Budivel'nik.
- Kunugi, Y., T. Nonaka, Y. Chong, N. Watanabe (1993). "Preparation of hydrophobic zinc and lead electrodes and their application to electroreduction of organic compounds electro-organic reactions on organic electrodes. Part 20: Electrolysis using composite-plated electrodes. Part IX." Journal of Electroanalytical Chemistry **356**(1-2): 163-169.
- Lambert, L., J. Halldorson and S. Kresnyak (2001). Waste water treatment method and apparatus. Patent application assigned to Applied Oxidation Technologies (2000) Inc.
- Landreth, C. P. (1914). "Electrolysis of sewage". Great British patent application 1418564.
- Langdon, A., P. Smyth and T. Hill (1995). Titanomagnetite ceramic nozzles for water and wastewater filter systems. IPENZ Annual Conference, Dunedin.
- Langdon, A. G., T. A. Hill, and P. Smyth (1995). "Porous Ceramic Dual Media Filtration: Commercial Benefits." Water and Wastes in New Zealand **1**: 26.
- Lanza, M. R. V. and R. Bertazzoli (2002). "Selection of a commercial anode oxide coating for electro-oxidation of cyanide." Journal of the Brazilian Chemical Society **13**(3): 345-351.
- Latutz, N., J. A. Jacobs and J. Guertin (2005). "Treatment for chromium(VI) containing waste water using electrocoagulation and electrooxidation." Chromium (VI) Handbook: 477-489.
- Leite, R. H. D., P. Cagnet, A. Wilhelm and H. Delmas (2002). "Anodic oxidation of 2,4-dihydroxybenzoic acid for wastewater treatment: study of ultrasound activation." Chemical Engineering Science **57**(5): 767-778.
- Leitzau, P. (2004a). General Product Specification. Product: PAC23 Chem Spec, Aluminates Chemical Industries.
- Leitzau, P. (2004b). General Product Specification. Product: PAC Chem Spec, Aluminates Chemical Industries.
- Leitzau, P. (2004c). General Product Specification. Product: PFS Chem Spec, Aluminates Chemical Industries.
- Lessene, G., M. Bordeau, C. Biran, D. de Montauzon and J. Gerval (2000). "Towards the electroreduction of very weak acids." Journal of Electroanalytical Chemistry **490**(1-2): 79-84.
- Liao, L. and A. van Sandwijk (2002). "Electro-oxidation of hydrogen chloride to chlorine in a membrane equipped cell." Chloride Metallurgy 2002: Practice and Theory of Chloride/Metal Interaction, Annual Hydrometallurgy Meeting, 32nd, Montreal, QC, Canada, Oct. 19-23, 2002 **1**: 155-172.
- Lin, C.-J., S.-L. Lo, C. Kuo, C. Wu (2005). "Pilot-Scale Electrocoagulation with Bipolar Aluminum Electrodes for On-Site Domestic Greywater Reuse." Journal of Environmental Engineering (Reston, VA, United States) **131**(3): 491-495.
- Llerena, C., J. C. K. Ho and D. Piron (1997). "Effects of pH on electroflotation of sphalerite." Chemical Engineering Communications **155**: 217-228.



- Logan, B. E. (2004). "Extracting hydrogen and electricity from renewable resources." Environmental Science and Technology **38**(9): 160A-167A.
- Lu, C., S. Lu, W. Qu and Q. Liu (1999). "Electroreduction of nitrate to ammonia in alkaline solutions using hydrogen storage alloy cathodes." Electrochimica Acta **44**(13): 2193-2197.
- Lu, G., J. Qu and H. Tang (1999). "The electrochemical production of highly effective polyaluminium chloride." Water Research **33**(3): 807-813.
- Maddock, J. L. (1977). Research experience in the thickening of activated sludge by dissolved-air flotation. Conference on flotation for water and waste treatment, Water Research Centre, Medenham, United Kingdom.
- Malik, M. A., A. Ghaffar and S. Malik (2001). "Water purification by electrical discharges." Plasma Sources Science and Technology **10**: 82-91.
- Mamakov, A. A., V. I. Zelentsov and N. Filimonov (1976). "Effect of electrolytic gases on the flotation of gold-containing ores." Izvestiya Akademii Nauk Moldavskoi SSR, Seriya Fiziko-Tekhnicheskikh i Matematicheskikh Nauk(1): 44-7.
- Marceta Kaninski, M. P., A. D. Maksic, D. Stojic and S. Miljanic (2004). "Ionic activators in the electrolytic production of hydrogen-cost reduction-analysis of the cathode." Journal of Power Sources **131**(1-2): 107-111.
- Marceta, M. P., D. L. Stojic, S. Sovilj and S. Miljanic (2002). "Electrolytic production of hydrogen; possibility of energy saving." Physical Chemistry 2002, Proceedings of the International Conference on Fundamental and Applied Aspects of Physical Chemistry, 6th, Belgrade, Yugoslavia, Sept. 26-28, 2002 **1**: 296-298.
- Marconato, J. C., E. D. Bidoia and R. Rocha (1998). "Electrolytic treatment of wastewater from a fowl slaughterhouse using cast-iron electrodes." Bulletin of Electrochemistry **14**(6-7): 228-230.
- Marson, H. W. (1965). "Electrolytic Sewage Treatment." The Engineer **4**: 591.
- Marti, M. C., M. Roeckel, E. Aspe and M. Novoa (1994). "Fat removal from process waters of the fish meal industry. A study of three flotation methods." Environmental Technology **15**(1): 29-39.
- Maslennikov, N. A. and T. M. Zhdanova (1961). "Concentration of excess activated sludge by electroflotation." Sb. Nauchn. Rabot Akad Kommun. Khoz.(No. 6): 230-53.
- Mathieson, G., A. Langdon and G. Jamieson. (2005). Purification of Tannery Effluent by Electrolytic Corrosion of Aluminum. Electrochemical Society 208, Los Angeles, Electrochemical Society.
- Mathieson, G. A., A. G. Langdon and G. Jamieson (2006). "Production of Hydrogen by Electrolytic Purification of Water." Dev. Chem. Eng. Mineral Process **14**(1/2): 71-84.
- Matis, K. A. (1980). "Bubble measurements in electrolytic flotation." Chimika Chronika **9**(1): 71-6.
- Matis, K. A. and N. K. Lazaridis (2002). "Flotation techniques in water technology for metals recovery: dispersed-air vs. dissolved-air flotation." Journal of Mining and Metallurgy, Section A: Mining **38**(1-4): 1-27.
- Matov, B. M. (1967). "Application of electrolysis in coagulation and flotation." Izvestiya Vysshikh Uchebnykh Zavedenii, Pishchevaya Tekhnologiya(2): 84-6.
- Matter Project, T. U. o. L. (2001). "Alloy Composition Details." Retrieved 14 June, 2003, from [http://aluminium.matter.org.uk/aluselect/06\\_composition\\_browse.asp](http://aluminium.matter.org.uk/aluselect/06_composition_browse.asp)

- Matteson, M. J., R. L. Dobson, R. Glenn Jr., N. Kukunoor, W. Waits III and E. Clayfield (1995). "Electrocoagulation and separation of aqueous suspensions of ultrafine particles." Colloids and Surfaces, A: Physicochemical and Engineering Aspects **104**(1): 101-9.
- MatWeb. (1996). "MatWeb - The Online Materials Information Resource." Retrieved June 20, 2004, from <http://www.matweb.com/>
- Mayer, J., L. Zhang and H. Hahn (1990). "Liquid-solid separation by electroflotation: an attractive alternative to dissolved air flotation." Chem. Water Wastewater Treat., Proc. Gothenburg Symp., 4th: 151-67.
- Mazur, S., C. E. Jackson and G. Foggin (2005) "Membrane Mediated Electro-polishing of Damascene Copper." DuPont Central Research & Development. 2005 IEEE Interconnect Technology Conference 6/6/05.
- Mazzone, R. and E. Nyvold (1969). "Effect of pH on the corrosion rate of aluminum in sodium chloride solutions." Scand. Corros. Congr., Proc., 5th **1**: 4, 15 pp.
- Meixner, A. J. (2005). "Reaction of Aluminum with Water and Sodium Hydroxide." Retrieved 2005/07/25, from <http://www.pc.chemie.uni-siegen.de/pci/versuche/english/v44-10.html>
- MEPS International. (2006). "MEPS - WORLD STAINLESS STEEL PRODUCT PRICES " Retrieved 16 January, 2006, from <http://www.meps.co.uk/Stainless%20Prices.htm>.
- Meunier, N., P. Drogui, C. Gourvenec, G. Mercier, R. Hausler and J. Blais (2004). "Removal of metals in leachate from sewage sludge using electrochemical technology." Environmental Technology **25**(2): 235-245.
- Miller, H. C. and W. Knipe (1963). Electrochemical Treatment of Municipal Wastewater. Final Report., US Public Health Service, Division of Water Supply and Pollution Control.
- Millet, J. M. M. and A. Sebaoun (1993). "Influence of various electrolysis parameters and electrode characteristics on corrosion behavior of titanium supported RuO<sub>2</sub>-TiO<sub>2</sub> anodes." Materials Science and Technology **9**(9): 820-6.
- Minerals Council of Australia. (2005). "Groundwater Conductivity." Retrieved September 2005, 2005, from <http://www.ga.gov.au/education/minerals/electmeth.html>.
- Ministry of Health, N. Z. (2005). Drinking-water Standards for New Zealand 2005.
- Mollah, M. Y. A., P. Morkovsky, J. Gomes, M. Kesmez, J. Parga and D. Cocke (2004). "Fundamentals, present and future perspectives of electrocoagulation." Journal of Hazardous Materials **114**(1-3): 199.
- Mollah, M. Y. A., S. R. Pathak, P. Patil, M. Vayuvegula, T. Agrawal, J. Gomes, Jewel, M. Kesmez and D. Cocke (2004). "Treatment of Orange II azo-dye by electrocoagulation (EC) technique in a continuous flow cell using sacrificial iron electrodes." Journal of Hazardous Materials **109**(1-3): 165-171.
- Moriizumi, M., A. Fukumoto, K. Fujimoto, Y. Yamamoto and S. Okumura (2000). "Studies on the electrolytic conditions for the electrochemical elution of iron as applied to phosphorus removal technology." Mizu Kankyo Gakkaishi **23**(5): 279-284.
- Mouli, P. C., S. V. Mohan and S. Reddy (2004). "Electrochemical processes for the remediation of wastewater and contaminated soil: emerging technology." Journal of Scientific & Industrial Research **63**(1): 11-19.

- Mraz, R. and J. Krysa (1993). "Dimensionally stable anodes with a long lifetime for electroflotation." Precis. Process Technol. [Int. Conf.], 1st: 681-8.
- Muller, K.-J. (2002). "Electroflocculation - wastewater purification in the nonferrous metallurgy." Schriftenreihe der GDMB 95(Prozesswasser/Abwasser/Kuehlwasser): 167-176.
- Mumm, O. (1907). "On the Action of Oxygen upon Aqueous Solutions and on the Processes Attending the Electrolytic Decomposition of Water and the Operation of the Hydrogen-Oxygen Cell." Z. physik. Chem. 59: 459-91.
- Murugananthan, M., G. Bhaskar Raju and S. Prabhakar (2004). "Separation of pollutants from tannery effluents by electroflotation." Separation and Purification Technology 40(1): 69-75.
- Murugananthan, M., G. B. Raju, S. Prabhakar (2004). "Removal of sulfide, sulfate and sulfite ions by electro coagulation." Journal of Hazardous Materials 109(1-3): 37.
- Musquere, P. (1983). "Electricity in the treatment of potable water and town sewage." Water Supply 1(2-3, World Water Supply): SS8/1-SS8/12.
- Musquere, P., F. Ellingsen and E. Vik (1983). "Electrotechnics in drinking and wastewater." Water Supply 8 pp. Special Subject 8-1 to Special Subject 8-25.
- Nagai, M., I. Toyota, M. Tabata, M. Asano and M. Sakimura (2004). Apparatus and method for wastewater treatment by electrolysis to recover fuel gas used in fuel cell. Japanese patent application assigned to Mitsubishi Heavy Industries, Ltd., Japan.
- Nagai, N., M. Takeuchi, T. Kimura and T. Oka (2003). "Existence of optimum space between electrodes on hydrogen production by water electrolysis." International Journal of Hydrogen Energy 28(1): 35-41.
- Nakajima, N., T. Nakano, F. Harada, H. Taniguchi, I. Yokoyama, J. Hirose and E. Daikoku
- Sano, Kouichi (2004). "Evaluation of disinfective potential of reactivated free chlorine in pooled tap water by electrolysis." Journal of Microbiological Methods 57(2): 163-173.
- Napper, D. H. (1983). "Polymeric Stabilisation of Colloidal Dispersions." Academic Press, ISBN 0-12-513980-2.
- Neti Nageswara, R. and N. Kaul Santosh (2003). "Electrochemical treatment of wastewater from a phosphoric acid manufacturing plant." Annali di chimica 93(9-10): 777-82.
- Neti, N. R. and S. N. Kaul (2003). "Electrochemical treatment of wastewater from a phosphoric acid manufacturing plant." Annali di Chimica (Rome, Italy) 93(9-10): 777-782.
- Nielson, K. and D. W. Smith (2005). "Ozone-enhanced electroflocculation in municipal wastewater treatment." Journal of Environmental Engineering and Science 4(1): 65-76.
- Nikolaev, N. V., A. S. Kozlovskii and I. Utkin (1982). "Treating natural waters in small water systems by filtration with electrocoagulation." Soviet Journal of Water Chemistry and Technology 4 (No. 3): pp. 244-247.
- Norsk Hydro (1928). Electrolytic production of hydrogen and oxygen. NO, (Norsk Hydro-Elektrisk Kvaestofaktieselskab).
- Onda, K., T. Ohba, H. Kusunoki, S. Takezawa, D. Sunakawa and T. Araki (2005). "Improving Characteristics of Ozone Water Production with Multilayer Electrodes and Operating Conditions in a Polymer Electrolyte Water Electrolysis Cell." Journal of the Electrochemical Society 152(10): D177-D183.

- Ordóñez, G. A. (1997). "In situ electrolytic disinfection." Proceedings - Water Quality Technology Conference: P6C/1-P6C/15.
- Osaka, T. and M. Uno (2000). "Electrode for hydrogen peroxide production and its fabrication." Jpn. Kokai Tokkyo Koho. Jp, (Permelec Electrode Ltd., Japan): 6.
- Osasa, K., H. Itemoto and H. Tanaka (1995). "Performance of continuous electroflotation by using bipolar-type sacrificial electrodes fitted with rotating disks." Kagaku Kogaku Ronbunshu **21**(3): 617-21.
- Osasa, K., H. Nakakura and H. Tanaka (1993). "Treatment of colloidal waste material by electroflotation using sacrificial electrodes." Kagaku Kogaku Ronbunshu **19**(2): 317-24.
- Osipenko, V. D. and P. I. Pogorelyi (1977). "Electrocoagulation detoxification of chromium-containing waste waters." Metallurg (Moscow, Russian Federation)(9): 44-5.
- Paidar, M., I. Rousar and K. Bouzek (1999). "Electrochemical removal of nitrate ions in waste solutions after regeneration of ion exchange columns." Journal of Applied Electrochemistry **29**(5): 611-617.
- Parga, J. R., D. L. Cocke, V. Valverde, J. Gomes, M. Kesmez, H. Moreno, M. Weir and D. Mencer (2005). "Characterization of electrocoagulation for removal of chromium and arsenic." Chemical Engineering & Technology **28**(5): 605-612.
- Park, J., Y. Jung, M. Han and S. Lee (2002). "Simultaneous removal of cadmium and turbidity in contaminated soil-washing water by DAF and electroflotation." Water Science and Technology **46**(11-12, Water Quality and Environmental Management in Asia): 225-230.
- Paschoal, F. M. M. and G. Tremiliosi-Filho (2005). "Application of the electroflocculation technology for the recovery of indigo blue from industrial effluents." Quimica Nova **28**(5): 766-772.
- Pekmez, K., M. Can and A. Yildiz (1993). "Electrochemistry in aprotic solvents containing anhydrous perchloric acid: Electroreduction behavior of quinones." Electrochimica Acta **38**(4): 607-611.
- Pelegri, R. T., R. S. Freire, N. Duran and R. Bertazzoli (2001). "Photoassisted Electrochemical Degradation of Organic Pollutants on a DSA Type Oxide Electrode: Process Test for a Phenol Synthetic Solution and Its Application for the E1 Bleach Kraft Mill Effluent." Environmental Science and Technology **35**(13): 2849-2853.
- Pensaert, S. and A. P. Van Peteghem (1995). "Removal of heavy metals from groundwater by bipolar electrolysis." Soil & Environment **5**(Contaminated Soil 95, Vol. 2): 1323-1324.
- Peters, R. W., W. L. Oresik, C. Engelder, V. Gopalratnam and J. Greenfield (1987). "Physical and chemical methods [of wastewater treatment]." Journal - Water Pollution Control Federation **59**(6): 364-88.
- Plantes, W. J., R. P. Goldstein and J. Wolfe (1982). Simplified maintenance electrocoagulator. US patent application assigned to Westinghouse Electric Corp., USA.
- Pletcher, D. (1984). Industrial electrochemistry. London ; New York, Chapman and Hall.
- Pletcher, D. and F. C. Walsh (1990). Industrial Electrochemistry. Cambridge, University Press.
- Pontius, F. W. (1990). Water Quality and Treatment - A handbook of community water supplies, McGraw-Hill.

- Prokhorov, A. V. (1963). "Analysis of oxidation-reduction equilibria in bleaching solutions during the processing of sulfate pulp with hypochlorite or chlorine water." Tr. Karel'sk. Filiala Akad. Nauk SSSR **No. 38**: 53-78.
- Public Health Commission (1995). Guidelines for the control of Legionellosis, Public Health Commission (New Zealand).
- Purenovic, M. M., A. R. Despic and D. Drazic (1976). "Anodic properties of alloys of aluminum with indium and gallium." Elektrokhimiya **12(2)**: 296-9.
- Qu, J., J. Ge and P. Lei (2002). Method and apparatus for electrochemical rapid treatment of laundry wastewater. Application: CN  
CN, (Eco-Engineering Research Center, Chinese Academy of Sciences, Peop. Rep. China). 5 pp.
- Qu, J. and H. Liu (2004). "Optimum conditions for Al13 polymer formation in PACl preparation by electrolysis process." Chemosphere **55(1)**: 51-6.
- Ramanathan, G. (2003). Electrochemical Synthesis of Hydrogen Peroxide. Patent PCT/US02/23327.
- Ramirez, E. R., L. K. Barber and O. Clemens. (1978). "Physiochemical treatment of tannery wastewater by electrocoagulation." Proceedings of the Industrial Waste Conference **32**: 183-8.
- Rav-Acha, C. (1998). "Transformation of aqueous pollutants by chlorine dioxide: reactions, mechanisms and products." Handbook of Environmental Chemistry **5(Pt. C)**: 143-175.
- Rembar. (2005). "Titanium." Retrieved December 12, 2005, from <http://www.rembar.com/Titanium.htm>.
- Rengakuji, S., Y. Nakamura and A. Yamada (1998). "Fundamentals of separation methods: electrochemical separation." Bunseki(5): 328-336.
- Rengarajan, V., R. Palanisamy and K. Narasimham (1985). "Electrolytic preparation of ozone." Transactions of the SAEST **20(4)**: 195-200.
- Rimpler, M., F. Kueke and M. Rimpler (1997). Preparation of aqueous chlorine dioxide solutions. Ger. Offen. De, (Rimpler, Manfred, Germany). 8 pp.
- Rios, G. B., F. Almeraya and M. Herrera (2005). "Electrode passivation in the electrocoagulation process." Portugaliae Electrochimica Acta **23(1)**: 17-34.
- Rodrigo, M. A., P. A. Michaud, I. Duo, M. Panizza, G. Cerisola and C. Cominellis (2001). "Oxidation of 4-chlorophenol at boron-doped diamond electrode for wastewater treatment." Journal of the Electrochemical Society **148(5)**: D60-D64.
- Rogov, V. M., V. L. Filipchuk, V. Anopol'skii and E. Shmat'ko (1978). "Use of electrocoagulation-flotation in the technology of water treatment." Elektronnaya Obrabotka Materialov(6): 80-3.
- Rounds, S. A. and F. D. Wilde. (2001, 9/2001). "Alkalinity and Acid Neutralizing Capacity: U.S. Geological Survey Techniques of Water-Resources Investigations, book 9, chap. 6.6." 2nd Edition. Retrieved 18 January, 2006, from <http://water.usgs.gov/owq/FieldManual/Chapter6/section6.6/>.
- Rovel, J. M. (1975). "New electroflocculation process for the treatment of industrial waste water." Quaderni - Istituto di Ricerca sulle Acque **31**: 251-61.
- Sakakibara, Y. and H. Nakajima (2002). "Phosphate removal and recovery by a novel electrolytic process." Water Science and Technology **46(11-12, Water Quality and Environmental Management in Asia)**: 147-152.
- Sakakibara, Y. and T. Nakayama (2001). "A novel multi-electrode system for electrolytic and biological water treatments: electric charge transfer and application to denitrification." Water Research **35(3)**: 768-778.

- Salama, A. (2001). Device and method for treating water with ozone generated by water electrolysis. United States patent application.
- Sasaki, S. (2004). Method for low-cost treatment of wastewater. Japanese patent application assigned to Toyo Riken K. K.
- Semchenko, D. P., V. I. Lyubushkin and E. Lyubushkina (1973). "Electrolytic production of ozone." Elektrokhimiya **9**(11): 1744.
- Sharma, S. K., B. Petrusovski and J. Schippers (2005). "Biological iron removal from groundwater: A review." Journal of Water Supply: Research and Technology--AQUA **54**(4): 239-247.
- Sherif, S. A., F. Barbir and T. Veziroglu (2003). "Principles of hydrogen energy production, storage and utilization." Journal of Scientific & Industrial Research **62**(1-2): 46-63.
- Shiklomanov, I. (1999). "World Water Resources: Modern Assessment and Outlook for the 21st Century (Summary of World Water Resources at the Beginning of the 21st Century, prepared in the framework of the IHP UNESCO)."
- Shin, S.-H., Y.-H. Kim, S. Jung, K. Suh, S. Kang, S. Jeong and H. Kim (2004). "Combined performance of electrocoagulation and magnetic separation processes for treatment of dye wastewater." Korean Journal of Chemical Engineering **21**(4): 806-810.
- Sides, P. J. (1981). "Bubble dynamics at gas evolving electrodes." PhD Thesis(University of California, Berkeley): 153.
- Sides, P. J. (1986). "Phenomena and Effects of Electrolytic Gas Evolution." Modern Aspects of Electrochemistry **18**(Butterworths): 303-354.
- Smith, J. R., F. C. Walsh and R. Clarke (1998). "Electrodes Based on Magneli Phase Titanium Oxides: the properties and applications of Ebonex (R) Materials." Journal of Applied Electrochemistry **28**: 1021-1033.
- Smith, R. W. and J. D. Hem (1972). Effect of Aging of Aluminum Hydroxide Complexes in Dilute Aqueous Solutions. U. G. Survey, US Government Printing Office.
- Society of Automotive Engineering. (2005). "42 V Efforts." Retrieved 28 December, 2005, from <http://www.sae.org/42volt/other/>.
- Spagnoletto, G. (2005). "Innovation in food grade hypochlorination generation and injection plant at Al Taweelah site." Desalination **182**(1-3): 259-265.
- Stoica, L. and A. Razvan (2005). "Removal of Cd(II) ions from aqueous solutions by flotation." Revista de Chimie (Bucharest, Romania) **56**(4): 349-354.
- Stojic, D. L., N. D. Simic and B. Sekic (2004). "Intermetallics-advanced cathode materials in the electrolytic production of hydrogen." Physical Chemistry 2004, Proceedings of the International Conference on Fundamental and Applied Aspects of Physical Chemistry, 7th, Belgrade, Serbia and Montenegro, Sept. 21-23, 2004 **1**: 299-301.
- Stoyanov, V. K. and L. D. Ushakov (1987). "Effect of high level of iron in drinking water on the quality of bull semen." Zhivotnovodstvo **9**: 50-2.
- Strokach, P. P. (1975). Electrochem. Ind. Process Biol. **55**: 375.
- Stuart, F. E. (1946). "Electronic water purification; Progress report on the electronic coagulator - a new device which gives promise of unusually speedy and effective results." Water and Sewage **84**(May): 24-26.
- Stuart, F. E., Jr. (1947). "Electronic coagulation." Public Works **78**(No. 4): 27,36.
- Stuckart, R., W. Zust, A. Le Talludec, R. Shahani and H. Sigurdsson (1998). "Coated aluminum and the filiform corrosion phenomenon." Berichtsband - Deutsche Forschungsgesellschaft fuer Oberflaechenbehandlung **36**(Aluminium-Anwendungen): 97-101.

- Szpyrkowicz, L., C. Juzzolino, S. Kaul, S. Daniele and M. De Faveri (2000). "Electrochemical oxidation of dyeing baths bearing disperse dyes." Industrial & Engineering Chemistry Research **39**(9): 3241-3248.
- Tabakov, D. (1982). "Electrochemical purification of effluents by means of soluble anode materials." Prace Naukowe Instytutu Technologii Nieorganicznej i Nawozow Mineralnych Politechniki Wroclawskiej **24**: 105-11.
- Tabakov, D. and R. Dimitrov (1982). "Influence of material of electrode system on the effect of treatment of dairy sewage by electrocoagulation and flotation." Gaz, Woda i Technika Sanitarna **56**(9-10): 197-8.
- Takahashi, M. (1986). "Energetics of ozone production by discharge or electrolysis." Soda to Enso **37**(437): 225-34.
- Tanaka, T., T. Sugawara, J. Akisawa, M. Kenmotsu and K. Kimura (2005). "Fundamental studies of acidic electrolyzed water on the bactericidal activity and its mechanism." Hokkaido Kogyo Daigaku Kenkyu Kiyo **33**: 283-287.
- Tanji, H., T. Sasaki, C. Shiki, Y. Horita (1975). Aqueous polyaluminum chloride. Japanese patent application assigned to Nippon Steel Chemical Industry Co., Ltd., Japan.
- Tao, Y., X. Zhang and Z. Gu (1999). "Electropurification of sulfur-containing sewage by electro-oxidizing desulfurization." Electrochemical and Solid-State Letters **2**(3): 133-134.
- Targetti, G. (1899). "Electrolytic production of ozone." Nuovo Cimento **10**: 360.
- Tax Free Gold. (2006). "Iridium Spot Prices." Retrieved 16 January, 2006, from <http://www.taxfreegold.co.uk/iridiumpricesusdollars.html>.
- Tender, L. M. and D. A. Lowy (2004). "Harvesting energy from marine and river sediment." Abstracts of Papers, 228th ACS National Meeting, Philadelphia, PA, United States, August 22-26, 2004: ENVR-293.
- Terryn, H. (2002). "Reactivity of the Aluminium Surface in Aqueous Solutions." Retrieved 2005/05/15, from [http://www.aluminium.org/education/TALAT/lectures/5102.pdf#search='P ourbaix%20diagram%20of%20aluminium'](http://www.aluminium.org/education/TALAT/lectures/5102.pdf#search='P%20ourbaix%20diagram%20of%20aluminium')
- Tetrault, A. (2003). "Electrocoagulation Treatment of Low Temperature Rendering Plant Wastewater at an Australian Abattoir." New Zealand Water and Waste Conference, Auckland, New Zealand.
- Tiemann, W. (2003). "Purifying highly polluted wastewater. Operational experiences with Morselt electroflotation." Chemie-Anlagen + Verfahren **36**(3): 92.
- Tokai Carbon Co. (2005). "Tokai Carbon Announces Graphite Electrode Price Increase." Retrieved 16 January, 2006, from [http://www.tokaicarbon.co.jp/en/information/news\\_20050107.shtml](http://www.tokaicarbon.co.jp/en/information/news_20050107.shtml).
- Torem, M. L., F. Oliveira da Cunha and R. Casqueira (2005). "Removal of heavy metal from liquid effluents using the electroflotation technique." Tecnologia em Metalurgia e Materiais **1**(4): 40-46.
- Troester, I., L. Schaefer, M. Fryda, T. Matthee (2004). "Electrochemical advanced oxidation process using DiaChem electrodes." Water Science and Technology **49**(4, Oxidation Technologies for Water and Wastewater Treatment III): 207-212.
- Tsai, L. S., B. Hernlem and C. Huxsoll (2002). "Disinfection and solids removal of poultry chiller water by electroflotation." Journal of Food Science **67**(6): 2160-2164.

- Tsouris, C., D. W. DePaoli, J. Shor, M. Hu and T. Ying (2001). "Electrocoagulation for magnetic seeding of colloidal particles." Colloids and Surfaces, A: Physicochemical and Engineering Aspects **177**(2-3): 223-233.
- Turner, M. T. (1975). "The use of dissolved air flotation for the thickening of waste activated sludge." Effluent Water Treatment Journal **15**: 243-251.
- Turner, R. C. and G. J. Ross (1970). Canadian Journal Of Chemistry **48**: 723.
- UNEP. (2002). "Vital Water Graphics : Freshwater Resources." Retrieved June 25, 2005, from <http://www.unep.org/vitalwater/01.htm>
- UNESCO. (2000). "Water use in the world: present situation / future needs." Retrieved 25 June, 2005, from [http://www.unesco.org/science/waterday2000/water\\_use\\_in\\_the\\_world.htm](http://www.unesco.org/science/waterday2000/water_use_in_the_world.htm)
- Vennekens, G. and W. Stinissen (2001). Zetek plc ZASI guide, Zetek Power bvba.
- Vertes, G. and K. Kovacs (1983). Electroflocculation treatment of emulsion-and suspension-type wastewaters. Hungarian patent application.
- Veze, M. and J. Labatut (1902). "Apparatus for preparing pure hydrogen." Zeitschrift fuer Anorganische Chemie **32**: 464.
- Vijayaraghavan, K., T. K. Ramanujam and N. Balasubramanian (1999). "In situ hypochlorous acid generation for the treatment of syntan wastewater." Waste Management **19**(5): 319-323.
- Vik, E. A., D. A. Carlson, A. Eikum, E. Gjessing (1984). "Electrocoagulation of potable water." Water Research **18**(11): 1355.
- Vlyssides, A. G. and C. J. Israilides (1997). "Detoxification of tannery waste liquors with an electrolysis system." Environmental Pollution **97**(1-2): 147-152.
- Walde, H. (1937). "Processes and equipment for alkali-chlorine electrolysis; electrolytic production of hydrogen and oxygen; and the purification of water by electro.ovrddot.osmosis." Siemens-Zeitschrift **17**: 322-6.
- Wendt, H. and G. Kreysa (1999). Electrochemical Engineering: Science and Technology in Chemical and Other Industries.
- Wilk, I. J., R. S. Altmann and J. Berg. (1987). "Antimicrobial activity of electrolyzed saline solutions." Science of the total environment **63**: 191-7.
- Wilson, G. E. (1980). "Teacup pretreatment of wastewaters." Natl. Conf. Environ. Eng., Proc. ASCE Environ. Eng. Div. Spec. Conf.: 651-6.
- Wilson, H. W. (1995). "An alternative to gas chlorination." Public Works [ - AST] **126**: F34.
- Wright, M. R. (1988). The Nature of Electrolyte Solutions. London, MacMillan Education.
- Wu, X. and T. Gao (2002). "Iron removal by electrochemical method for water supply system of buildings." Zhongguo Jishui Paishui **18**(6): 10-13.
- Xiong, Y., P. J. Strunk, H. Xia, X. Zhu and H. Karlsson (2001). "Treatment of dye wastewater containing acid orange II using a cell with three-phase three-dimensional electrode." Water Research **35**(17): 4226-4230.
- Yamamoto, O. (2005). "Hydrogen production device with gasification of biomass and electrolysis of water". Japanese patent application assigned to Fuji Electric Holding Co., Ltd., Japan
- Yiasoumi, B. (2003). "Removal of Iron from Groundwater." Agfact AC.2 (part) Edition: ninth edition Retrieved 23 December, 2005, from <http://www.agric.nsw.gov.au/reader/financial-recovery/ac2-solubleiron.htm>.



- Zaroual, Z., M. Azzi, N. Saib, Y. Karhat, M. Zertoubi (2005). "Treatment of tannery effluent by an electrocoagulation process." Journal of the American Leather Chemists Association **100**(1): 16-21.
- Zekel, R. M., A. G. Nedosekin, A. Morozov, V. Makarenko (1975). "Effect of bubble size during the electroflotation of hydrated sediments of heavy metals without collecting reagents." v sb., Tekhnol. Razrabotki i Obogashch. Polezn. Iskop.: 92-6.
- Zhang, Q., F. B. Song, D. Li, X. Ding (2002). "Study of the intergranular corrosion mechanism of the aluminum alloys with electrochemical method." Materials Science Forum **396-402**(Pt. 3, Aluminium Alloys 2002): 1479-1484.
- Zhurkov, V. S., Z. I. Ponomarenko and A. Kozyura (1977). "Removal of suspension polystyrene from waste waters". Soviet Union patent application assigned to the All-Union Scientific-Research Institute for Water Supply, Sewage Systems, and Hydraulic Installations, Kharkov, USSR.